SH
11
.A2
F53
FISH

U.S. Department
of Commerce

Volume 116
Numbers 3–4
July–October 2018

Fishery Bulletin

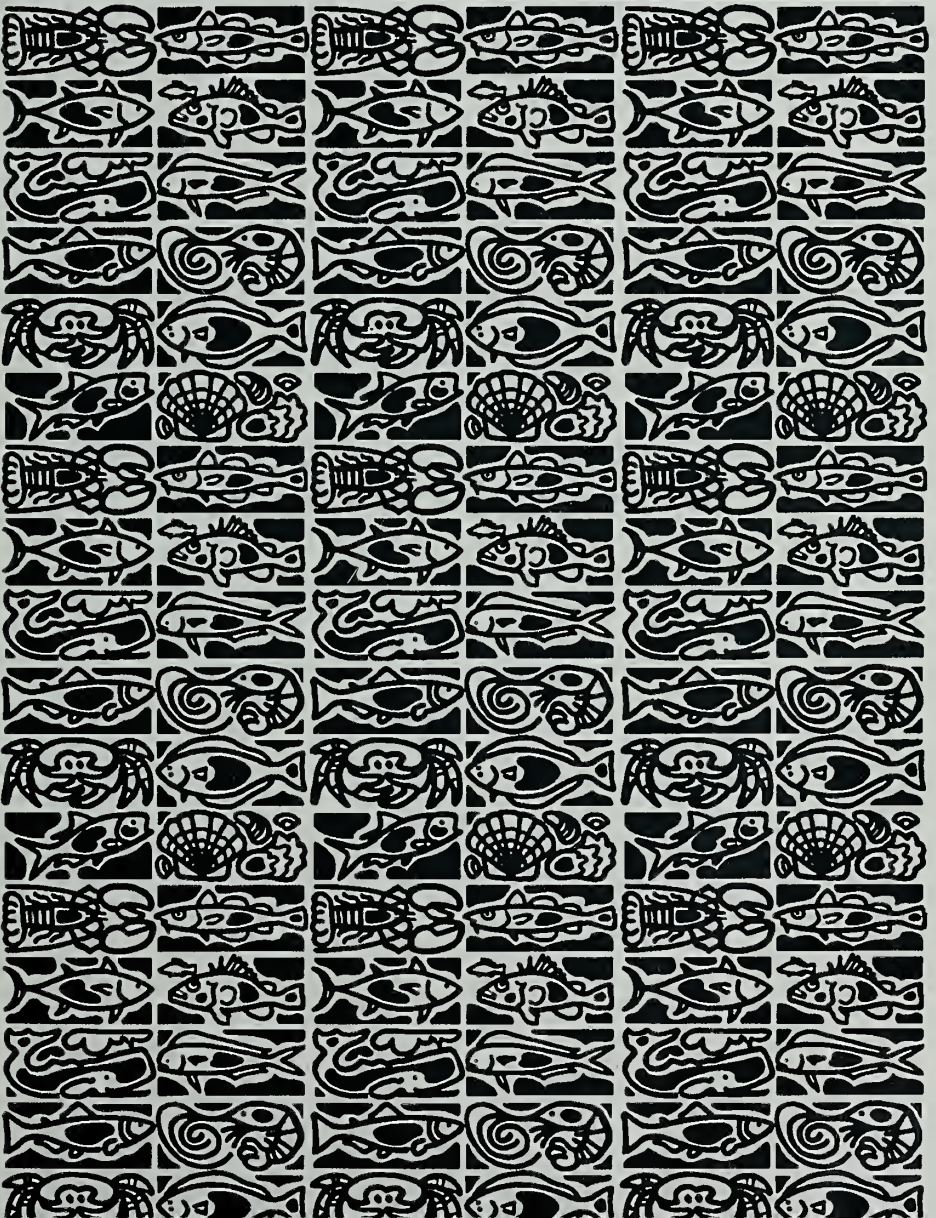

SHOUT
SHARE
IT

Fishery Bulletin

U.S. Department of Commerce

Wilbur L. Ross Jr.
Secretary

National Oceanic and Atmospheric Administration

Timothy Gallaudet
Deputy Administrator
of NOAA

National Marine Fisheries Service

Chris Oliver
Assistant Administrator
for Fisheries

The *Fishery Bulletin* (ISSN 0090-0656) is published quarterly by the Scientific Publications Office, National Marine Fisheries Service, NOAA, 7600 Sand Point Way NE, Seattle, WA 98115-0070.

Although the contents of this publication have not been copyrighted and may be reprinted entirely, reference to source is appreciated.

The Secretary of Commerce has determined that the publication of this periodical is necessary according to law for the transaction of public business of this Department. Use of funds for printing of this periodical has been approved by the Director of the Office of Management and Budget.

For Sale by the Superintendent of Documents, U.S. Government Printing Office, Washington, DC 20402. Subscription price per year: $32.00 domestic and $44.80 foreign. Cost per single issue: $19.00 domestic and $26.60 foreign. **See back for order form.**

Scientific Editor
José I. Castro

National Marine Fisheries Service, NOAA
263 13th Avenue South
Saint Petersburg, Florida 33701

Managing Editor
Sharyn Matriotti

National Marine Fisheries Service, NOAA
Scientific Publications Office
7600 Sand Point Way NE
Seattle, Washington 98115-0070

Associate Editor
Kathryn Dennis

National Marine Fisheries Service, NOAA
Scientific Publications Office
1845 Wasp Blvd., Bldg. 176
Honolulu, Hawaii 96818

Editorial Board

Henry L. Bart Jr.	Tulane University, New Orleans, Louisiana
Richard D. Brodeur	National Marine Fisheries Service, Newport, Oregon
Shannon L. Cass-Calay	National Marine Fisheries Service, Miami, Florida
William B. Driggers III	National Marine Fisheries Service, Pascagoula, Mississippi
Gretchen L. Grammer	South Australian Research and Development Institute, Adelaide, Australia
Richard Langton	National Marine Fisheries Service, Walpole, Maine
Richard S. McBride	National Marine Fisheries Service, Woods Hole, Massachusetts
Richard D. Methot	National Marine Fisheries Service, Seattle, Washington
Joseph M. Quattro	University of South Carolina, Columbia, South Carolina
Mark S. Peterson	University of Southern Mississippi, Ocean Springs, Mississippi
John F. Walter III	National Marine Fisheries Service, Miami, Florida
Bruce Wright	Aleutian Pribilof Island Association, Anchorage, Alaska

***Fishery Bulletin* web site: https://spo.nmfs.noaa.gov/fb.htm**

The *Fishery Bulletin* carries original research reports on investigations in fishery science, engineering, and economics. It began as the Bulletin of the United States Fish Commission in 1881; it became the Bulletin of the Bureau of Fisheries in 1904 and the *Fishery Bulletin* of the Fish and Wildlife Service in 1941. Separates were issued as documents through volume 46; the last document was no. 1103. Beginning with volume 47 in 1931 and continuing through volume 62 in 1963, each separate appeared as a numbered bulletin. A new system began in 1963 with volume 63 in which papers are bound together in a single issue. Beginning with volume 70, number 1, January 1972, *Fishery Bulletin* became a periodical, issued quarterly. In this form, it is available by subscription from the Superintendent of Documents, U.S. Government Printing Office, Washington, DC 20402. It is also available free in limited numbers to libraries, research institutions, state and federal agencies, and in exchange for other scientific publications.

U.S. Department
of Commerce
Seattle, Washington

Volume 116
Numbers 3–4
July–October 2018

Fishery Bulletin

SMITHSONIAN
NOV 16 2018
LIBRARIES

Contents

Short contribution

219–227 Adam G. Fox, Edward S. Stowe, Keith J. Dunton, and Douglas L. Peterson

Seasonal occurrence of Atlantic sturgeon (*Acipenser oxyrinchus oxyrinchus*) in the St. Johns River, Florida

Articles

228–239 Phoebe A. Woodworth-Jefcoats, Jeffrey J. Polovina, and Jeffrey C. Drazen

Synergy among oceanographic variability, fishery expansion, and longline catch composition in the central North Pacific Ocean

240–253 Christina M. Schobernd, M. Conor McManus, Joanne Lyczkowski-Shultz, Nathan M. Bacheler, and Denice M. Drass

Extrusion of fish larvae from SEAMAP plankton sampling nets: a comparison between 0.333-mm and 0.202-mm mesh nets

254–265 Bryce N. Oldemeyer, Timothy Copeland, and Brian P. Kennedy

A multiyear hierarchical Bayesian mark-recapture model incorporating data on recurring salmonid behavior to account for sparse or missing data

266–280 Mattias L. Johansson, Marisa N. C. Litz, Richard D. Brodeur, Tristan A. Britt, Camilo A. Vanegas, John R. Hyde, and Michael A. Banks

Seasonal distribution of late larval and juvenile rockfish (*Sebastes* spp.) and associated environmental conditions off Oregon and Washington: new insights based on genetics

281–290 George A. Maynard, Lisa K. Izzo, and Joseph D. Zydlewski

Movement and mortality of Atlantic salmon kelts (*Salmo salar*) released into the Penobscot River, Maine

---

The National Marine Fisheries Service (NMFS) does not approve, recommend, or endorse any proprietary product or proprietary material mentioned in this publication. No reference shall be made to NMFS, or to this publication furnished by NMFS, in any advertising or sales promotion which would indicate or imply that NMFS approves, recommends, or endorses any proprietary product or proprietary material mentioned herein, or which has as its purpose an intent to cause directly or indirectly the advertised product to be used or purchased because of this NMFS publication.

The NMFS Scientific Publications Office is not responsible for the contents of the articles.

291–301 Diana L. Watters and E. J. Dick

A comparison of length distributions of rockfishes (*Sebastes* spp.) from submersible and trawl surveys off central California

Short contribution

302–309 Dariusz P. Fey, Adam M. Lejk, and Martyna Greszkiewicz

Daily deposition of growth increments in sagittae and lapilli of laboratory-reared northern pike (*Esox lucius*)

Articles

310–322 Francisco Córdova-Zavaleta, Jaime Mendo, Sergio A. Briones-Hernández, Nicolas Acuña-Perales, Adriana Gonzalez-Pestana, Joanna Alfaro-Shigueto, and Jeffrey C. Mangel

Food habits of the blue shark, *Prionace glauca* (Linnaeus, 1758), in waters off northern Peru

323–336 Richard S. McBride, Matthew K. Tweedie, and Kenneth Oliveira

Reproduction, first-year growth, and expansion of spawning and nursery grounds of black sea bass (*Centropristis striata*) into a warming Gulf of Maine

Short contribution

337–347 William B. Driggers III, Matthew D. Campbell, David S. Hanisko, Kristin M. Hannan, Eric R. Hoffmayer, Christian M. Jones, Adam G. Pollack, and David S. Portnoy

Distribution of angel sharks (Squatinidae) in United States waters of the North Atlantic Ocean

Article

348–359 Constantina Karlou-Riga, Dimitra Petza, and Konstantinos Ganias

Sex change and oscillating growth pattern of the picarel (*Spicara smaris*) in the Saronikos Gulf (Greece)

360 Acknowledgment of reviewers

361–364 Guidelines for authors

National Marine
Fisheries Service
NOAA

Fishery Bulletin
established in 1881

Spencer F. Baird
First U.S. Commissioner
of Fisheries and founder
of *Fishery Bulletin*

Seasonal occurrence of Atlantic sturgeon (*Acipenser oxyrinchus oxyrinchus*) in the St. Johns River, Florida

Adam G. Fox[1]
Edward S. Stowe[2]
Keith J. Dunton[3]
Douglas L. Peterson (contact author)[1]

Email address for contact author: sturgeon@uga.edu

[1] Warnell School of Forestry and Natural Resources
University of Georgia
180 East Green Street
Athens, Georgia 30602-2152

[2] Odum School of Ecology
University of Georgia
140 East Green Street
Athens, Georgia 30602-2202

[3] Department of Biology
School of Science
Monmouth University
400 Cedar Avenue
West Long Branch, New Jersey 07764

Abstract—The Atlantic sturgeon (*Acipenser oxyrinchus oxyrinchus*) is an anadromous species that historically occurred in the Atlantic Ocean along the North American coast from maritime Canada to the St. Johns River, Florida. A century of overharvesting and habitat loss has resulted in range-wide population declines, and in 2012 the species was listed under the U.S. Endangered Species Act. The extirpation of several individual populations—especially in the southeastern United States—was an important consideration in the final determination to list the species as endangered. Although historical data confirm the presence of Atlantic sturgeon in the St. Johns River, no recent evidence of a viable population exists for that river system. The primary objective of our study was to document the presence or absence of Atlantic sturgeon in the St. Johns River. During 2014–2015, we conducted nearly 200 hours of directed sampling with gill nets of different mesh sizes in the St. Johns River estuary but found no evidence of an extant population within the St. Johns River system. We did document the seasonal presence of several adult and subadult individuals that had been acoustically tagged by researchers working in other coastal systems, and that finding indicates that nonnatal individuals still use this estuary.

Manuscript submitted 10 October 2017.
Manuscript accepted 27 April 2018.
Fish. Bull 116:219–227 (2018).
Online publication date: 15 May 2018.
doi: 10.7755/FB.116.3-4.1

The views and opinions expressed or implied in this article are those of the author (or authors) and do not necessarily reflect the position of the National Marine Fisheries Service, NOAA.

The Atlantic sturgeon (*Acipenser oxyrinchus oxyrinchus*) is an anadromous species characterized by a long life span and late age at maturity. Historically, this species occurred in the rivers and estuaries of the Atlantic Ocean along the North American coast from the St. Lawrence River, Canada, to the St. Johns River, Florida, United States (ASSRT, 2007). Commercial fisheries of both the United States and Canada exploited populations of Atlantic sturgeon throughout much of the 19th and 20th centuries (Smith and Clugston, 1997); however, most of these fisheries collapsed during the early 20th century because of gross overharvesting, industrial development, and damming and pollution of Atlantic coast rivers (Smith and Clugston, 1997; ASSRT, 1998; Secor, 2002; ASSRT, 2007).

In response to the rapid population declines of Atlantic sturgeon that resulted from commercial overexploitation, federal management agencies in the United States and Canada implemented several regulatory protections for this species during the late 20th century. Commercial fisheries for Atlantic sturgeon were closed in U.S. waters with the issuance of a 1998 federal moratorium, and in 2012 the species was listed under the U.S. Endangered Species Act. Under this listing, distinct population segments (DPSs) were designated for 5 regions within U.S. waters: Gulf of Maine, New York Bight, Chesapeake Bay, North and South Carolina, and the southeastern United States (ASSRT, 2007). All DPSs were listed as endangered except the Gulf of Maine DPS, which was listed as threatened (Federal Register, 2012a, 2012b).

Although several northern populations of Atlantic sturgeon have had at least some level of recovery in recent decades, many populations within the DPS for the southeastern United States remain severely depressed or possibly extirpated (ASSRT, 1998; ASSRT, 2007). Despite federal protections, many of these populations continue to suffer from degraded habitats in natal river systems, and from incidental bycatch in commercial fisheries that target other coastal or estuarine species (ASSRT, 1998; Collins et al., 2000; ASSRT, 2007). The implementation of modern environmental regulations has helped reduce point sources of pollution in many river systems in the southeastern United States, but nonpoint sources continue to degrade water quality, particularly in the lower rivers and estuarine habitats that were historically inhabited by juvenile Atlantic sturgeon (ASSRT, 2007).

As an anadromous fish, Atlantic sturgeon adults typically reside in marine environments but migrate into freshwater rivers to spawn (Vladykov and Greeley, 1963). In northern populations, spawning occurs in the spring (Bain, 1997), whereas the results of recent studies indicate that at least some central and southern populations spawn in the fall (Hager et al., 2014; Smith et al., 2015; Ingram and Peterson, 2016). During the first several years of life, the young fish, known as river-resident juveniles (RRJs), occupy estuarine habitats near the freshwater–saltwater interface. The period of river residency varies depending on latitude, but in southern populations the RRJs typically remain in their natal system for 2–4 years before transitioning to nearshore marine habitats as marine-migratory juveniles (MMJs) (Bain, 1997). Consequently, the presence of RRJs within a river system is considered strong evidence of an extant population, especially in depressed populations in which adult spawners may be rare (Schueller and Peterson, 2010).

The St. Johns River in Florida is considered the southernmost river system historically occupied by Atlantic sturgeon (ASMFC[1]; ASSRT, 2007). Throughout the 20th century, sturgeon were commonly reported as bycatch in commercial fisheries that operate on the St. Johns River (Cox and Moody[2]); however, reports of small juveniles are rare and spawning has never been confirmed there (McLane, 1955; Gilbert, 1992a). Furthermore, the construction of Rodman Dam (now called Kirkpatrick Dam) in 1968 blocked adults from accessing some of the best potential spawning habitats in the Ocklawaha tributary (Gilbert, 1992a; ASMFC[1]; ASSRT, 2007). The current status of Atlantic sturgeon, however, remains unknown within the St. Johns River system. The most recent survey of this population, conducted from 2002 to 2003 by the Florida Fish and Wildlife Commission, yielded zero Atlantic sturgeon despite hundreds of hours of directed sampling effort (Holder et al.[3]). The results of that study indicate that Atlantic sturgeon likely have been extirpated from St. Johns River, although rare but recurring captures of adult and subadult individuals by local anglers indicate that a small population could be present or that migrants from other systems are regularly occupying the estuary.

Extirpation of any fish population is difficult to establish conclusively, but it is especially difficult with sturgeons because of their cryptic nature, complex migratory life history, and periodic reproductive strategy. Given the uncertain status of Atlantic sturgeon within the St. Johns River, the objectives of this study were 1) to document seasonal occurrence of Atlantic sturgeon in the lower estuary and 2) to sample for RRJs as evidence of an extant population of Atlantic sturgeon in the St. Johns River.

Materials and methods

Study site

The St. Johns River is a large, blackwater river in northeast Florida, characterized by tannic waters and a very low mean gradient (~2.0 cm/km) (Whitney et al., 2004). It flows for 500 km to the Atlantic Ocean, draining several subbasins and associated tributaries that have in total a combined watershed area of approximately 22,900 km^2. Nontidal flow at the mouth averages 420 cm/s, but the rate may exceed 4220 cm/s after heavy rains. Much of the St. Johns River basin is urbanized and developed, and the river itself has been modified by dam construction and dredging (EPB[4]).

Sampling of sturgeon

All sampling was conducted in the lower St. Johns River estuary below the head of tide, between river kilometer (rkm) 25 and rkm 115. Sampling occurred during summer months because this season is the most effective time to capture RRJ Atlantic sturgeon (Schueller and Peterson, 2010; Bahr and Peterson, 2016). Specific netting locations within this zone (Fig. 1) were selected by using navigational charts and preliminary sonar surveys to find areas with depths of at least 2.5 m and

---

[1] ASMFC (Atlantic States Marine Fisheries Commission). 1998. Amendment 1 to the interstate fishery management plan for Atlantic sturgeon. Fish. Manage. Rep. 31, 42 p. ASMFC, Washington, DC. [Available from website.]

[2] Cox, D. T., and H. L. Moody. 1981. St. Johns River fisheries resources. Completion report. Study I. Ecological aspects of the fishery. Florida Game Fresh Water Fish Comm., Tallahassee, FL. [Available from Florida Fish Wildl. Conserv. Comm., Farris Bryant Bldg., 620 S. Meridian St., Tallahassee, FL 32399-1600.]

[3] Holder, J. C., R. E. Lundy, A. R. Hyle, and L. West. 2005. Completion report: St. Johns River fisheries resources, Lower St. Johns River resource development. Florida Fish Wildl. Conserv. Comm., Tallahassee, FL. [Available from Florida Fish Wildl. Conserv. Comm., Farris Bryant Bldg., 620 S. Meridian St., Tallahassee, FL 32399-1600.]

[4] EPB (Environmental Protection Board). 2014. State of the river report for the lower St. Johns River basin, Florida: water quality, fisheries, aquatic life, and contaminants 2014. State River Rep. 7, 301 p. EPB, City of Jacksonville; Univ. North Florida; and Jacksonville Univ., Jacksonville, FL. [Available from website.]

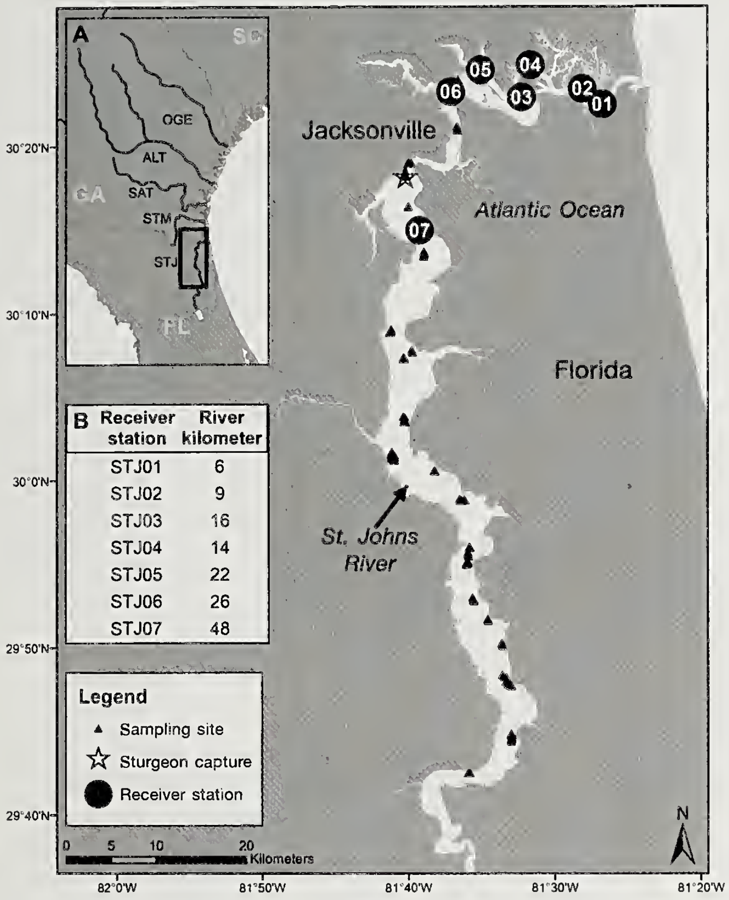

Figure 1

Map of sites where sampling was conducted during 2014–2015, the location where an Atlantic sturgeon (*Acipenser oxyrinchus oxyrinchus*) was captured in July 2015 (☆), and the stations (01–07) where acoustic receivers were deployed in the St. Johns River (STJ) in Florida. Inset A depicts the rivers of the southeastern United States, including several rivers nearby the St. Johns River with documented populations of Atlantic sturgeon: Ogeechee (OGE), Altamaha (ALT), and Satilla (SAT) in Georgia and St. Marys (STM) along the border of Georgia and Florida. Approximate river kilometers (rkm) of the locations of the receivers from the mouth of the estuary are listed in inset B.

obstruction-free bottoms. On sampling days, crews set 5–12 anchored gill and trammel nets perpendicular to the channel and soaked them for approximately 30–90 min, depending on conditions. Gill nets 91.4 m in length and 3.1 m deep, were composed of panels of 7.6-, 10.2-, and 15.3-cm monofilament mesh (stretch measure). Trammel nets were of similar dimensions and material and were composed of one 7.6-cm inner panel and three 30.5-cm outer panels. As nets were retrieved, entangled sturgeons were quickly removed and placed in a floating net pen.

Once all nets had been recovered, each captured sturgeon was measured to the nearest millimeter (total length [TL] and fork length [FL]) and was inspected for tags. If no tag was present, a passive integrated transponder tag was injected under the 4th dorsal scute and a small tissue sample was taken from the dorsal fin for genetic analysis. The fish was then placed on a custom-made, v-shaped surgical board that held the fish in lateral recumbency. A small bilge pump (473.2 L/h) was used to maintain a gentle flow of river water over the gills. A sterile scalpel was then used to make a 1-cm incision along the midline of the ventrum for insertion of a 69-kHz Vemco V7-4x[5] sonic transmitter (Vemco, Bedford, Canada). The incision was closed by using a 2/0 absorbable monocryl suture (Monoswif L943, CP Medical, Inc., Norcross, GA) as a simple suture with interrupted stiches as described by Boone et al. (2013). Once the incision was closed, the fish was allowed to recover and returned to the river at its original capture site.

Fish ages were estimated by using a length-frequency histogram based on Schueller and Peterson (2010); individuals with TL<550 mm were considered to be age-1 RRJs.

Acoustic telemetry

A passive array of 7 stationary acoustic receivers (Vemco VR2W) were distributed in June 2014 throughout the St. Johns River estuary to monitor the spatial and temporal movements of acoustically tagged Atlantic sturgeon. The submerged acoustic receivers were attached to channel markers and other stationary structures by using aluminum u-channel or stainless steel cables and hardware. All acoustic receivers were affixed in an upright position, 2–3 m below the surface to ensure that they remained completely submerged throughout the tidal cycle. Range testing conducted at receiver locations indicated an average tag detection radius of approximately 400 m (range: 200–800 m). Once the receivers were deployed, data from these acoustic receivers were downloaded every 3–5 months throughout the duration of this study.

Water-quality

To monitor variations in water quality throughout the sampling period, we collected measurements of water temperature (degrees Celsius), dissolved oxygen (milligrams per liter), and salinity at each fish sampling site during June–July in 2015 and 2016. These measurements were obtained at the surface and at 0.5 m from the bottom at each netting site by using a portable YSI Pro2030 multiprobe (YSI, Inc., Yellow Springs, OH).

---

[5] Mention of trade names or commercial companies is for identification purposes only and does not imply endorsement by the National Marine Fisheries Service, NOAA.

Table 1

Sampling effort by net type within the St. Johns River, Florida, during the summers of 2014 and 2015 in our study of the seasonal occurrence of Atlantic sturgeon (*Acipenser oxyrinchus oxyrinchus*).

	Gill nets		Trammel nets		Annual totals	
Year	No. of sets	Soak time (h)	No. of sets	Soak time (h)	No. of sets	Soak time (h)
2014	30	24	1	1	31	25
2015	105	127	14	22	119	149
Combined totals	135	151	15	23	150	174

Results

Sampling of sturgeon

Initial sampling was conducted from 25 June through 2 July 2014 to identify suitable sampling sites within the estuary where anchored nets could be safely fished without impeding commercial or recreational vessels. During this period, we set 31 nets for a total of 24.3 h of soak time (Table 1). Between 23 June and 10 July 2015, we set 119 nets for a total of 149.4 h of soak time. Only one MMJ Atlantic sturgeon (786 mm FL, 920 mm TL) was captured during this study, and subsequent genetic analysis assigned this individual to the population of the Altamaha River, Georgia, with 98% probability (Wirgin[6]).

Acoustic telemetry

The single Atlantic sturgeon captured at rkm 40 in July 2015 was was tagged with an acoustic tag, but it was never detected on the acoustic array. The array did, however, detect 8 previously tagged Atlantic sturgeon that had been captured and released by other researchers working outside St. Johns River (Table 2, Fig. 1). At the time of tagging, these individuals were either MMJs (n=3) or adults (n=5). We examined data recorded by the acoustic receivers from June 2014 through June 2016. All detections of Atlantic sturgeon obtained during the period of this study occurred in winter or early spring (Figs. 2 and 3)—a temporal pattern that was consistent in both 2014 and 2015. Most of these migrant Atlantic sturgeon (n=5, 62.5%) were never detected upriver from receiver STJ02 (rkm 9), and only one individual (12.5%) was detected as far upstream as receiver STJ06 (rkm 48).

Water quality

During the summer sampling period, mean daily water temperatures in the St. Johns River estuary were comparable to those obtained in other nearby rivers where populations of Atlantic sturgeon have been well documented (Table 3, Fig. 4). Dissolved oxygen levels in the St. Johns River were also well within the range of those observed in other rivers of the southeastern United States with extant populations of Atlantic sturgeon (Table 3, Fig. 5).

Discussion

After expending 174 net hours of sampling effort dispersed over 150 individual net-sets, we could not confirm the presence of a juvenile cohort of Atlantic sturgeon within the St. Johns River estuary. Our sampling efforts included many of the same sampling sites used in previous surveys of sturgeon in the St. Johns River (Holder et al.[3]), and these sites were primarily established on the basis of incidental captures of sturgeon in commercial and recreational fisheries that target other species. Although salinities at specific sampling sites varied depending on tidal cycle and seasonal precipitation, the range of salinities that we observed within our sampling area was similar to those documented in other nearby rivers (e.g., Altamaha and Satilla rivers in Georgia) where several RRJ cohorts have been documented in recent years (Schueller and Peterson, 2010; Bahr and Peterson, 2016; Fritts et al., 2016). Likewise, water temperatures and levels of dissolved oxygen at sampling sites in this study were well within the known tolerances of juvenile Atlantic sturgeon and, again, were comparable to those in other nearby rivers with extant populations of Atlantic sturgeon. Genetic analysis of the tissue sample obtained from the single Atlantic sturgeon captured indicates that this fish was almost certainly a subadult migrant from the Altamaha River.

During 2 summers of sampling in the St. Johns River, we captured no RRJ Atlantic sturgeon. Concurrent sampling was conducted in several nearby estuaries, including the Ogeechee and Altamaha rivers in Georgia and St. Marys River on the border of Georgia and Florida; the same methods and gear successfully captured RRJ Atlantic sturgeon in those rivers (senior author and D. Peterson, unpubl. data). Furthermore, the catch rate for Atlantic sturgeon (at all life stages)

---

[6] Wirgin, I. 2017. Personal commun. Sch. Med., New York Univ., 57 Old Forge Rd., 2nd Fl., Tuxedo, NY 10987.

Table 2

Details for tagged Atlantic sturgeon (*Acipenser oxyrinchus oxyrinchus*) detected by acoustic receivers in the St. Johns River (STJ), Florida, from June 2014 through June 2016. Each fish was assigned to a distinct population segment (DPS) based on genetic analyses provided by the U.S. Geological Survey Leetown Science Center, which maintains a comprehensive genetic database for all known populations of Atlantic sturgeon.

Life stage when tagged	Total length (mm) when tagged	Tagging location	Tagging year	Tagging organization	Number of days detected in the STJ	Region of origin of DPS
Subadult	1380	Coastal NY/NJ	2011	Stony Brook University	1	Southeastern United States
Adult	2290	Coastal Mid-Atlantic	2012	Delaware State University[a]	1	Southeastern United States
Adult	2040	Altamaha River, GA	2012	University of Georgia	2	Southeastern United States[d]
Adult	1466	Altamaha River, GA	2013	University of Georgia	2	Not available
Adult	1870	Altamaha River, GA	2013	University of Georgia	2	Not available
Subadult	893	Cape Fear River, NC	2013	NC DMF[b]	4	Southeastern United States
Adult	1093	Santee Bay, SC	2014	SC DNR[c]	1	Southeastern United States
Adult	1490	Cooper River, SC	2015	SC DNR[c]	1	Not available

[a] Fox, D. 2017. Personal commun. Dep. Agric. Nat. Resour., Coll. Agric. Relat. Sci., Delaware State Univ, Agric. Annex Rm. 123, 1200 N. DuPont Hwy., Dover, DE 19901.

[b] Loeffler, M. 2017. Personal commun. North Carolina Div. Mar. Fish., 3441 Arendell St., Morehead City, NC 28557.

[c] Post, W. 2017. Personal commun. South Carolina Dep. Nat. Resour., P.O. Box 12559, Charleston, SC 29422-2559.

[d] Stock assignment was based on telemetry data from Ingram and Peterson (2016) that indicated that this fish made a putative spawning run in the Altamaha River, Georgia, in 2014.

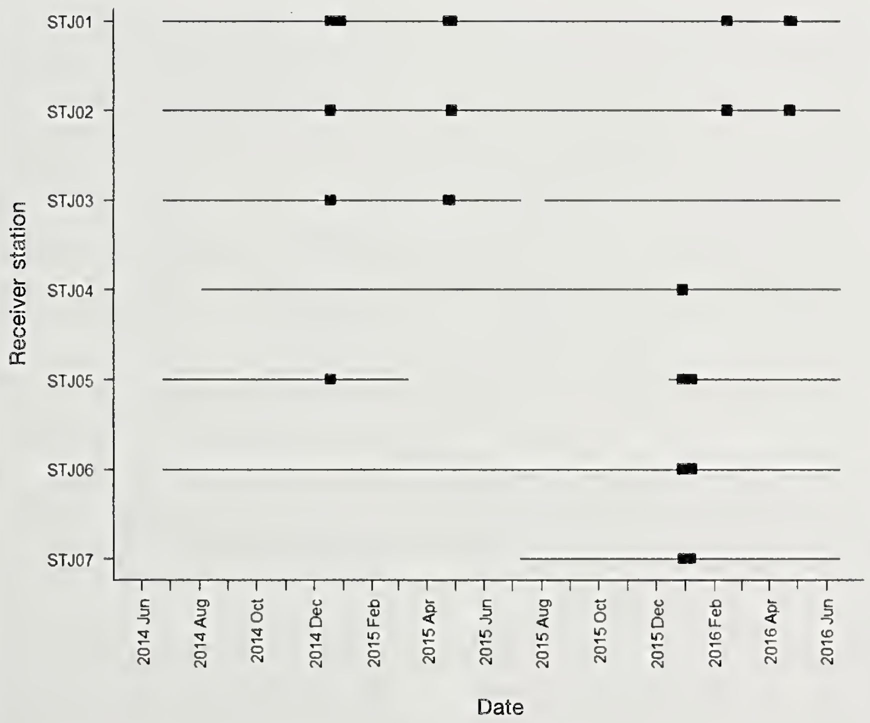

Figure 2

Temporal distribution of acoustic receivers (horizontal lines) and days with detection of individual tagged Atlantic sturgeon (*Acipenser oxyrinchus oxyrinchus*) (black rectangles) in the St. Johns River estuary in Florida from June 2014 through June 2016.

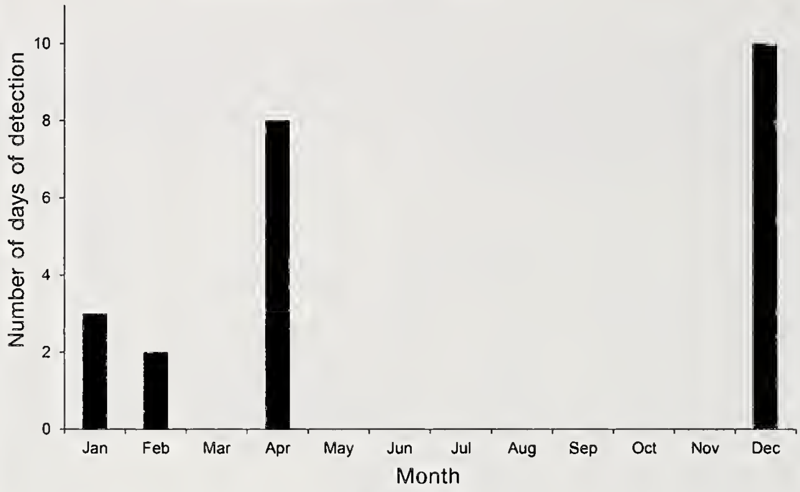

Figure 3

Number of days of detection per month of tagged Atlantic sturgeon (*Acipenser oxyrinchus oxyrinchus*) by acoustic receivers in the St. Johns River in Florida during 2014–2016. The number of days of detection (one detection per individual per day) were combined by month across all years of the study.

Table 3

Water temperatures and dissolved oxygen levels in the Altamaha and Satilla rivers in Georgia and the St. Johns River in Florida during June–July 2015.

	Temperature (°C)		Dissolved oxygen (mg/L)	
River	Mean	Standard deviation	Mean	Standard deviation
Altamaha	30.30	0.73	5.70	0.47
Satilla	29.96	0.67	3.39	0.61
St. Johns	29.50	0.47	4.70	0.82

Table 4

Concurrent sampling efforts in 2015 with the use of similar entanglement gear and the resulting catch of Atlantic sturgeon (*Acipenser oxyrinchus oxyrinchus*) measured as the number of individual fish caught per hour, in several rivers in the southeastern United States.

River	Soak time (h) of nets	Number of individuals captured	Catch (individuals/h)
Ogeechee	175	154	0.880
Altamaha	50	76	1.520
Satilla	176	76	0.432
St. Marys	122	10	0.082
St. Johns	149	1	0.007

for our study in the St. Johns River was far below the rates typically observed for sampling for studies in other rivers of the southeastern United States where populations have been documented (Table 4). Even in St. Marys River, which hosts the smallest known extant population of Atlantic sturgeon (ASSRT, 2007; senior author and D. Peterson, unpubl. data), catch rates were an order of magnitude greater than those we observed in our study of the St. Johns River. In rivers with extant populations of Atlantic sturgeon, the methods employed in our study generally produce dozens to hundreds of RRJ sturgeon annually (Schueller and Peterson, 2010; Bahr and Peterson, 2016; senior author and D. Peterson, unpubl. data). The complete absence of RRJs captured over the 2 consecutive summers of sampling in the St. Johns River indicates that a natal RRJ cohort was not likely present in either year of the study.

The observed absence of RRJs during this study, though not conclusive, indicates that a viable population of Atlantic sturgeon is not currently present within the St. Johns River, as was suggested by Holder et al.[3]. Although a historical status of this population has never been confirmed, Gilbert (1992b) suggests that access to potential spawning habitat for a natal population likely was eliminated by the construction of the Kirkpatrick Dam in 1968. Still, we emphasize caution in designating Atlantic sturgeon as extirpated

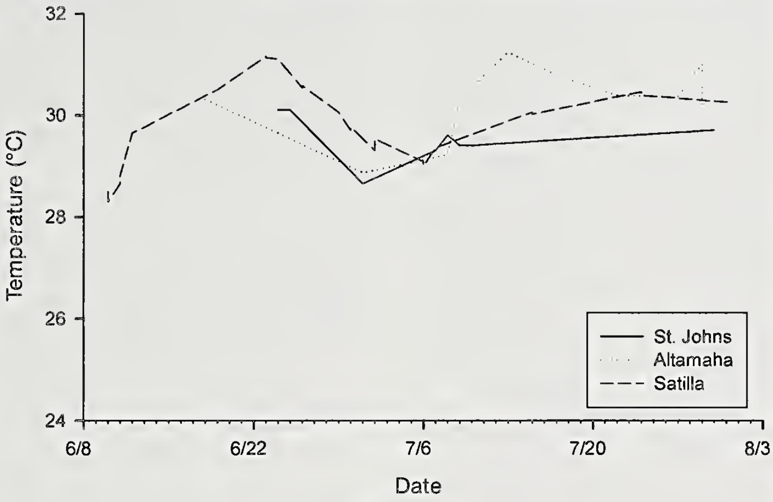

Figure 4

Mean daily water temperature (°C) measured at sampling sites in the St. Johns River in Florida and in the Altamaha and Satilla rivers in Georgia during June–July 2015.

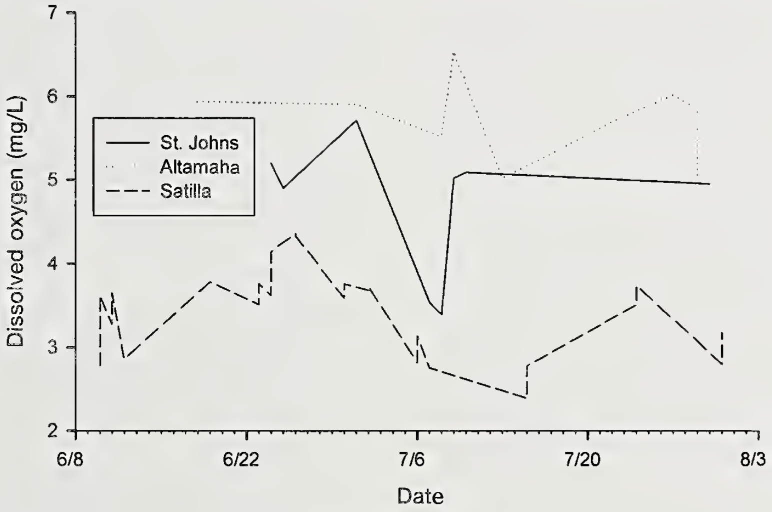

Figure 5

Mean daily levels of dissolved oxygen (mg/L) measured at sampling sites in the St. Johns River in Florida and in the Altamaha and Satilla rivers in Georgia during June–July 2015.

from the St. Johns River—the absence of evidence is, by no means, conclusive evidence of absence. Atlantic sturgeon are long-lived, intermittent spawners, and several previous studies have shown that remnant populations can be extremely difficult to detect even with intensive sampling efforts. For example, populations of Atlantic sturgeon were, until recently, thought to be extirpated from the St. Marys River, an adjacent river located only 34 km north of the St. Johns River (Blair et al.[7]). Recent sampling in that river system, however, has documented the presence of an RRJ cohort in that system, confirming the presence of an extant population (senior author and D. Peterson, unpubl. data). Despite the limited sample size obtained there, preliminary genetic analyses of tissue samples from those juveniles indicate that they represent a unique population within the DPS for the southeastern United States, one likely produced from a remnant population of subadults that survived the era of commercial fishing (Wirgin[6]).

---

[7] Blair, S., M. Ezell, H. Hall, and J. November. 2009. St. Marys River watershed. Prepared for the St. Marys River Management Committee in collaboration with the University of Florida Conservation Clinic and the University of Georgia Environmental Law Practicum. [Available from website.]

Although the St. Johns River channel has been dammed and dramatically altered, the river still potentially could support a population of Atlantic sturgeon. Water temperatures and levels of dissolved oxygen measured during this study were quite comparable to those in nearby rivers with extant populations. Consequently, we emphasize that additional assessments are needed in the future (every 2–3 years) to definitively ascertain the status of Atlantic sturgeon within the St. Johns River system. If neither RRJs nor spawning adults can be captured in future studies, the use of modern environmental DNA (eDNA) methods could be used to help establish the presence of spawning adults within the upper reaches of the St. Johns River. A similar approach was used recently by Pfleger et al. (2016) to document the presence of the Alabama sturgeon (*Scaphirhynchus suttkusi*) in the Mobile River basin, Alabama.

The data collected in this study confirm the seasonal presence of both adult and MMJ Atlantic sturgeon in the lower St. Johns River estuary during the late winter and early spring months. The seasonal presence of adult and MMJ individuals was detected on all acoustic receivers within our array. All 8 migrants originally had been tagged in either the mid-Atlantic or southeastern United States, indicating that the St. Johns River may still provide important wintering habitat for nonresident Atlantic sturgeon. Similar movement patterns have been documented in several other river systems of the southeastern United States (senior author and D. Peterson, unpubl. data); however, more information is needed to better understand the seasonal importance of nonspawning migrations. Regardless, the results of this study indicate that adult fish are most abundant in the St. Johns River estuary during the late winter and early spring. As range-wide recovery of Atlantic sturgeon continues, seasonal abundance within the lower St. Johns River will likely increase even in the absence of a natal population. Consequently, we emphasize the need for future studies with sample sizes larger than those in our study because the use of larger sample sizes will help to better define seasonal patterns of habitat use by migrating Atlantic sturgeon within the St. Johns River estuary.

Acknowledgments

This work was funded by the Naval Facilities Engineering Command Southeast, U.S. Department of the Navy; the National Marine Fisheries Service (NMFS); and the National Institute of Food and Agriculture, U.S. Department of Agriculture. Our thanks to C. Watterson, D. Fox, M. Loeffler, J., W. Post, J. Galvez, C. Williams, I. Wirgin, D. Kazyak, T. King, and D. Higginbotham. This study was conducted under NMFS Permits 16482, 16507, 16442, 16422, and 16375, and the University of Georgia Animal Use and Care Permit A2013 01-012-Y3-A1.

Literature cited

ASSRT (Atlantic Sturgeon Status Review Team).
1998. Status review of Atlantic sturgeon (*Acipenser oxyrinchusoxyrinchus*), 126 p. Report prepared for Natl. Mar. Fish. Serv., Silver Springs, MD. [Available from website.]
2007. Status review of Atlantic sturgeon (*Acipenser oxyrinchus oxyrinchus*), 174 p. Report to Northeast Reg. Off., Natl. Mar. Fish. Serv., Gloucester, MA. [Available from website.]

Bahr, D. L., and D. L. Peterson.
2016. Recruitment of juvenile Atlantic sturgeon in the Savannah River, Georgia. Trans. Am. Fish. Soc. 145:1171–1178.

Bain, M. B.
1997. Atlantic and shortnose sturgeons of the Hudson River: common and divergent life history attributes. Environ. Biol. Fish. 48:347–358.

Boone, S. S., S. J. Divers, A. C. Camus, D. L. Peterson, C. A. Jennings, J. L. Shelton, and S. M. Hernandez.
2013. Pathologic and physiologic effects associated with long-term intracoelomic transmitters in captive Siberian sturgeon. North Am. J. Fish. Manage. 33:869–877.

Collins, M. R., S. G. Rogers, T. I. J. Smith, and M. L. Moser.
2000. Primary factors affecting sturgeon populations in the southeastern United States: fishing mortality and degradation of essential habitats. Bull. Mar. Sci. 66:917–928.

Federal Register.
2012a. Endangered and threatened wildlife and plants; threatened and endangered status for distinct population segments of Atlantic sturgeon in the northeast region. Fed. Register 77:5880–5912. [Available from website.]
2012b. Endangered and threatened wildlife and plants; final listing determinations for two distinct population segments of Atlantic sturgeon (*Acipenser oxyrinchus oxyrinchus*) in the southeast. Fed. Register 77:5914–5982. [Available from website.]

Fritts, M. W., C. Grunwald, I. Wirgin, T. L. King, and D. L. Peterson.
2016. Status and genetic character of Atlantic sturgeon in the Satilla River, Georgia. Trans. Am. Fish. Soc. 145:69–82.

Gilbert, C. R.
1992a. Atlantic sturgeon, *Acipenser oxyrinchus*. *In* Rare and endangered biota of Florida. Vol. 2: fishes (C. R. Gilbert, ed.), p. 31–39. Univ. Press Florida, Gainesville, FL.
1992b. Shortnose sturgeon, *Acipenser brevirostrum*. *In* Rare and endangered biota of Florida. Vol. 2: fishes (C. R. Gilbert, ed.), p. 15–22. Univ. Press Florida, Gainesville, FL.

Hager, C., J. Kahn, C. Watterson, J. Russo, and K. Hartman.
2014. Evidence of Atlantic sturgeon spawning in the York River system. Trans. Am. Fish. Soc. 143:1217–1219.

Ingram, E. C., and D. L. Peterson.
2016. Annual spawning migrations of adult Atlantic sturgeon in the Altamaha River, Georgia. Mar. Coast. Fish. 8:595–606.

McLane, W. M.
1955. Fishes of the St. Johns River system. Ph. D. diss., 361 p. Univ. Florida, Gainesville, FL.

Pfleger, M. O., S. J. Rider., C. E. Johnston, and A. M. Janosik.
2016. Saving the doomed: using eDNA to aid in detection of rare sturgeon for conservation (Acipenseridae). Global Ecol. Conserv. 8:99–107.

Schueller, P. and D. L. Peterson.
2010. Abundance and recruitment of juvenile Atlantic sturgeon in the Altamaha River, Georgia. Trans. Am. Fish. Soc. 139:1526–1535.

Secor, D. H.
2002. Atlantic sturgeon fisheries and stock abundances during the late nineteenth century. Am. Fish. Soc. Symp. 28:89–98.

Smith, T. I. J., and J. P. Clugston.
1997. Status and management of Atlantic sturgeon, *Acipenser oxyrinchus*, in North America. Environ. Biol. Fish. 48:335–346.

Smith, J. A., H. J. Flowers, and J. E. Hightower.
2015. Fall spawning of Atlantic sturgeon in the Roanoke River, North Carolina. Trans. Am. Fish. Soc. 144:48–54.

Vladykov, V. D., and J. R. Greeley.
1963. Order Acipenseroidei. *In* Fishes of the western North Atlantic, part 3 (Y. H. Olsen, ed.), p. 24–60. Sears Foundation for Marine Research, Yale University, New Haven, CT.

Whitney, E., D. B. Means, and A. Rudloe.
2004. Priceless Florida: Natural ecosystems and native species, 423 p. Pineapple Press, Inc., Sarasota, FL.

National Marine
Fisheries Service
NOAA

Fishery Bulletin
established in 1881

Spencer F. Baird
First U.S. Commissioner
of Fisheries and founder
of *Fishery Bulletin*

Synergy among oceanographic variability, fishery expansion, and longline catch composition in the central North Pacific Ocean

Phoebe A. Woodworth-Jefcoats (contact author)[1,2]
Jeffrey J. Polovina[1]
Jeffrey C. Drazen[2]

Email address for contact author: phoebe.woodworth-jefcoats@noaa.gov

[1] Ecosystem Sciences Division
Pacific Islands Fisheries Science Center
National Marine Fisheries Service, NOAA
1845 Wasp Boulevard, Building 176
Honolulu, Hawaii 96818

[2] Department of Oceanography
School of Ocean and Earth Science and Technology
University of Hawaii at Manoa
1000 Pope Road
Marine Science Building
Honolulu, Hawaii 96822

Abstract—The fishing grounds of the Hawaii-based longline fleet span over 13 million km^2 in the central North Pacific Ocean. We investigated over 20 years of commercial fishery logbook data and independent observer data to gain an understanding of the variation in magnitude and composition of the fleet's catch on both intra- and interannual scales. We found that the fishery follows a quarterly geographic migration and that the fishery has expanded over time with a 5-fold increase in effort and a spatial expansion primarily to the northeast of Hawaii during the third quarter of the year. The World Ocean Atlas and ocean reanalysis data indicate that waters to the northeast of Hawaii are a particularly effective fishing ground because of the vertical overlap of preferred thermal habitat and fishing gear. Furthermore, we found that the Hawaii-based fleet faced little international competition in this region. The expansion of the fishery has also affected catch composition, resulting in discard rates that exceed target catch rates. Understanding how catch varies as a result of oceanographic variability and fleet movement can lead to a more efficient, resilient, and cost-effective fishery.

Manuscript submitted 6 July 2017.
Manuscript accepted 12 April 2018.
Fish. Bull. 116:228–239 (2018).
Online publication date: 24 May 2018.
doi: 10.7755/FB.116.3-4.2.

The views and opinions expressed or implied in this article are those of the author (or authors) and do not necessarily reflect the position of the National Marine Fisheries Service, NOAA.

The Hawaii-based longline fishery is among the most economically valuable fisheries in the United States, ranked 6th in 2015 (NMFS[1]). Its footprint spans over 13 million km^2 in the central North Pacific Ocean, ranging from the dateline to 120°W and from equatorial waters to roughly 40°N. The Hawaii-based longline fleet includes 2 fisheries: a shallow-set fishery targeting swordfish (*Xiphias gladius*) and a deep-set fishery targeting bigeye tuna (*Thunnus obesus*). The deep-set fishery is the dominant fishery; both effort and catch (magnitude and value) are an order of magnitude greater than that of the shallow-set fishery (NMFS[2]). For this reason, we focused on the deep-set fishery in our study.

The deep-set fishery operates largely during the day (Bigelow et al., 2006). Hooks are primarily set between 100 and 400 m below the surface, and the median hook depth is 250 m (Boggs, 1992; Bigelow et al., 2006). This depth range coincides with the daytime vertical habitat of bigeye tuna; tagging data indicate that fish of this species spend much of the day 200–400 m below the surface (Boggs, 1992; Ward and Myers, 2005a; Howell et al., 2010) in waters with a temperature range of 8–14°C (Howell et al., 2010) and oxygen concentrations over 1.0 mL/L (Boggs, 1992; Lehodey et al., 2010).

Although bigeye tuna are the target of the deep-set fishery, the catch also includes a number of other species, some of which are also of commercial value. These commercially valuable, nontarget species include dolphinfish (*Coryphaena hippurus*), also known as mahi mahi; yellowfin tuna (*Thunnus albacares*); striped marlin (*Kajikia audax*); sickle pomfret (*Taractichthys steindachneri*); and opah (*Lampris guttatus*). This fishery also catches but discards several noncommercial species, such as the longnose lancetfish (*Alepisaurus ferox*) and snake mackerel (*Gempylus serpens*). Recent studies have noted increased catch rates of these noncommercial species concurrent with declines in the catch rate for target species. These changes have been attributed to increasing fishing effort (Ward and Myers, 2005b; Polovina et al., 2009) and prey release of the often smaller, noncommercial fish as larger target species are removed (Polovina and Woodworth-Jefcoats, 2013). These studies support the previous finding that longline fisheries function as a keystone predator in the central North Pacific Ocean (Kitchell et al., 2002).

---

[1] NMFS (National Marine Fisheries Service). 2016. Total commercial fishery landings at major U.S. ports summarized by year and ranked by dollar value. Fisheries Statistics Division, NMFS. [Data available at w ebsite, accessed October 2016.]

[2] NMFS (National Marine Fisheries Service). 2016. Annual commercial landing statistics. Fisheries Statistics Division, NMFS. [Data available from website, accessed October 2016.]

Despite spanning millions of square kilometers, pelagic fisheries have often been examined as a spatial aggregate (e.g., Cox et al., 2002; Kitchell et al., 2002; Sibert et al., 2006). Previous studies of the Hawaii-based longline fishery, for example, have used spatially averaged trends focused on the core region of the fishery's operating area (12–27°N; Polovina et al., 2009; Polovina and Woodworth-Jefcoats, 2013). Shifting spatial patterns in fishing effort and the influence these changes may have on catch in the central North Pacific Ocean are under-explored in the primary literature (although see Gilman et al., 2012; Walsh and Brodziak, 2015). Additionally, the effect that international competition has had on the movement of the Hawaii-based fleet has not been explored. In this study, we aimed to determine how both the changing spatial footprint of the fishery and oceanographic variability have influenced catch magnitude and composition, the understanding of which is essential for ensuring a sustainable and cost-effective fishery.

Materials and method

Materials

We used both logbook and observer records in this study. Logbook data are reported by fishing vessel masters and contain records of all hooks set (time, date, and location), as well as all commercially valuable catch. Observer data cover an average of roughly 17% of the fishing effort in the study period and contain records of all hooks set (time, date, and location), as well as all catch, regardless of commercial value. The distribution of observer data correlates well with that of the logbook data (Suppl. Fig. 1) (online only), and taken together the 2 data sets provide a robust measure of both fishing effort and catch from 1995 through 2015. Logbook data are complete through 2015 and observer data through 2014. We used all deep-set fishery data, which span the area of 16°S–42°N and 179–120°W. We defined deep sets as those with ≥10 hooks/float (Polovina et al., 2009; Polovina and Woodworth-Jefcoats, 2013). Logbook data are collected by the Pacific Islands Fisheries Science Center. Observer data are collected by the Pacific Islands Regional Office.

We used publicly available data for longline effort from the Western and Central Pacific Fisheries Commission (WCPFC, data available at website) and the Inter-American Tropical Tuna Commission (IATTC, data available at website) to place Hawaii-based effort in an international context. These data are available at a 5°×5° horizontal and a monthly temporal resolution through 2014. The WCPFC provides data for areas west of 150°W, and the IATTC provides data for areas east of 150°W. This 150°W boundary divides the 2 fishing convention areas of the Hawaii-based fishery.

Global Ocean Data Assimilation System (GODAS) reanalysis data (Saha et al., 2006) provided modeled monthly temperature at depth across the fishing grounds for the entire period studied. The GODAS data used in this study were provided by the Physical Sciences Division of the NOAA Earth System Research Laboratory in Boulder, Colorado, and were downloaded from the Asia Pacific Data Research Center's OPeNDAP server (website). World Ocean Atlas 2013 (WOA13) data (Garcia et al., 2013) provided a 3-dimensional climatological reference of oxygen concentration. The WOA13 oxygen data were downloaded from the National Centers for Environmental Information's OPeNDAP server (website). Both the GODAS and WOA13 data sets are based on in situ observations such as those from Argo floats (Saha et al., 2006) and discrete water samples (Garcia et al., 2013).

Methods

All data (fishery and environmental), except those from the WCPFC and IATTC, were transformed into a common 1°×1° grid matching that of the WOA13 data. The GODAS data were changed from their native 0.33°×1.00° resolution by using nearest coordinate regridding. In this study, we examined data at regional and quarterly resolutions (e.g., quarter 1 represents January, February, and March). The Ferret program (NOAA's Pacific Marine Environmental Laboratory, Seattle, WA, website) was used for regridding data.

We assessed several measures of catch magnitude and composition, all in terms of numbers of fish caught as opposed to weight of fish. Catch rates were measured as catch per unit of effort (CPUE), which we defined as the number of fish caught per 1000 hooks set. We focused primarily on catch rates of the target species, bigeye tuna, and on the primary bycatch species, longnose lancetfish. For our assessment of catch composition, we used the 21 most commonly caught species identified by Polovina and Woodworth-Jefcoats (2013). We also followed their method for measuring discard rate (measured as the ratio of catch of longnose lancetfish, snake mackerel, pelagic stingray (*Pteroplatytrygon violacea*), and 95% of sharks to total catch).

We defined preferred thermal habitat for bigeye tuna as waters with temperatures of 8–14°C. Tagging data from Howell et al. (2010) indicate that when bigeye tuna are at depth during the daytime, which is when the fishery for bigeye tuna operates, they are primarily in waters within this thermal range. The GODAS data were used to determine the minimum, maximum, and median depths of preferred thermal habitat of bigeye tuna in 2 ways: 1) these depths were determined for all grid cells (each 1°×1°) with fishing effort at any point in the time series; 2) quarterly GODAS data were weighted by the number of hooks set in each grid cell during each quarter. We then used standard linear regression to evaluate whether there were significant ($P<0.05$) linear trends in both unweighted and weighted median depths of preferred thermal habitat. Where significant trends were found, we used linear regression to determine how the depth of preferred thermal habitat changed over the years studied.

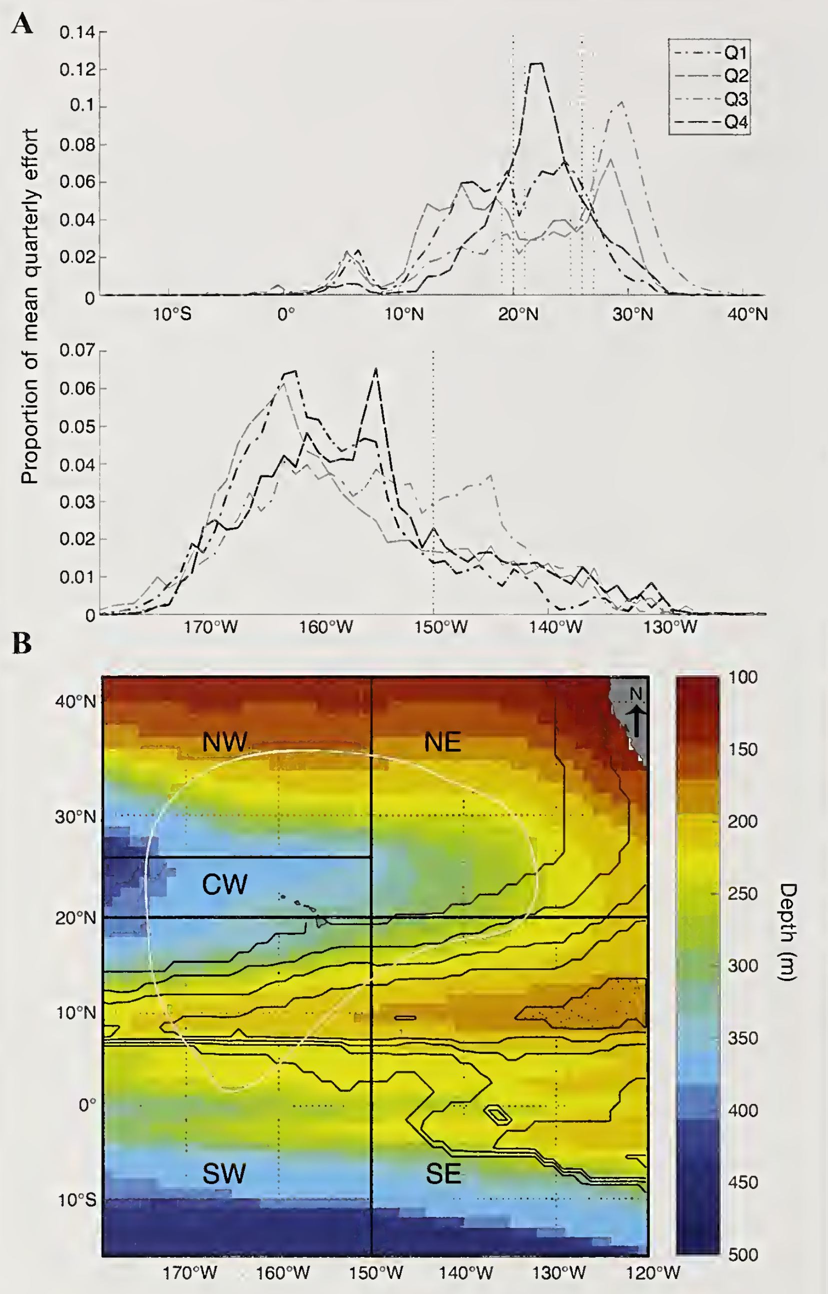

Figure 1

(**A**) The meridional (top) and zonal (bottom) distributions of quarterly effort of the Hawaii-based longline fishery, averaged across the full time series (1995–2015). Dashed black vertical lines are drawn at 20°N and 26°N (top) and at 150°W (bottom) and delineate the divides between the SE and NE regions and the SW, CW, and NW regions, and dashed gray lines are drawn at ±1° for comparison of alternate options (top). (**B**) Map depicting the 5 regions by which the Hawaii-based longline fishery was examined overlaid on the climatological (1995–2015) median depth of preferred thermal habitat of bigeye tuna (*Thunnus obesus*) (8–14°C) obtained from Global Ocean Data Assimilation System (shaded) and the depth of the 1.0 mL/L oxygen-concentration threshold from World Ocean Atlas 2013 data (contoured every 100 m from 100 to 500 m, with stippling where the depth is less than 100 m). The white line in panel B encompasses grid cells with fishing effort from at least 3 vessels over the full time series. Effort in panel A is from logbook data.

Results

Fishing effort

Seasonal variability The Hawaii-based longline fishery exhibited strong seasonal movement during the period studied, 1995–2015. Figure 1A shows the temporally averaged meridional and zonal distribution of effort (number of hooks set) each quarter. On the basis of this distribution, as well as the 150°W boundary between the 2 fishing convention areas of the Hawaii-based fishing grounds, we divided the fishery into the 5 regions shown in Figure 1B: northeast (NE); northwest (NW); central west (CW); southwest (SW); and southeast (SE). Together, Figures 1A and 2 show the movement of the fishery by quarter throughout the year. In the first quarter of the year, most of the effort took place in the SW region north of 10°N and in the CW region. During the second quarter, effort was concentrated in the SW and NW regions. The fishery then underwent a large geographic shift in the third quarter, and most of its effort was directed within the NE region. Effort occurred closest to Hawaii in the CW region during the fourth quarter.

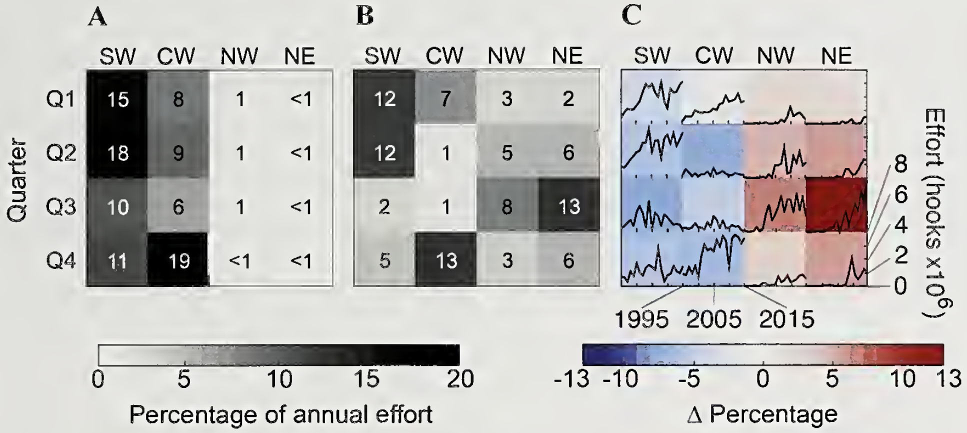

Figure 2

The mean percentages of total annual effort that occurred in each quarter and region at the (**A**) beginning (1995–1997) and (**B**) end (2013–2015) of the time series from logbook data examined in this study of the Hawaii-based longline fishery. (**C**) The change in the percentage of total annual effort that occurred in each quarter and region is shaded in color and overlaid with the total annual effort set in each region and quarter in black. Four regions were used in these analyses: southwest (SW); central west (CW); northwest (NW); and northeast (NE).

There was virtually no fishing effort in the SE region; therefore, it was not included in our analysis.

Interannual variability In 1995, nearly all (97.1%) of the Hawaii-based longline effort occurred west of 150°W and south of 26°N in the CW and SW regions. Over time, the fishery expanded, and in 2015, 41.3% of the longline fishing effort occurred either north of 26°N or east of 150°W in the NW and NE regions. Total effort also increased; the total number of hooks set increased steadily from nearly 8.4 million in 1995 to over 47 million in 2015. This increase in fishing effort was greatest in the NE region (Fig. 2). Time series of total effort in each region and quarter (Fig. 2) show that effort increased in the CW and SW regions until about 2004. After this time, and with the exception of the CW region in the first quarter, effort in these regions has remained roughly stable, whereas effort in the NW and NE regions increased steadily.

Fishery expansion is detailed in Figure 2. It shows that, over the past 21 years, the geographic focus of the fishery changed substantially. Across all quarters, the proportion of total annual effort in the SW and CW regions declined by about 1–8%. At the same time, the proportion of total annual effort in both northern regions increased by 2–13%, with a strong maximum in the NE region during the third quarter (13% versus 7%, the next closest value).

International competition The ratio of Hawaii-based effort to international effort varied by region (Suppl. Fig. 2) (online only). Hawaii-based effort accounted for nearly all effort recorded in the CW region; there was little to no competition from international fisheries. For the grid cells in the SW region with Hawaii-based fishing effort, international fisheries' effort was roughly equal to the effort of the Hawaii-based fishery. However, the ratio of Hawaii-based effort to international effort has increased steadily in the first quarter of each year over the years studied. For grid cells in the NW region with Hawaii-based fishing effort, there was little competition from international fisheries during the second and third quarters. In the first and fourth quarters, the ratio of Hawaii-based fishing effort to international effort has increased over the past decade, and the efforts of the 2 groups are now roughly equal. With the exception of the first and fourth quarters during the first 5 years of the time series, there was virtually no international fishing effort in the NE region.

Oceanographic variability

Spatial variability A great deal of spatial variability across the fishing grounds was observed in the median depth and vertical extent of the preferred thermal habitat of bigeye tuna (8–14°C) (Fig. 1B). Median thermal habitat depth was at its maximum in the CW region, about 350–400 m below the surface, and it was shallowest in the NE region where it occurred within about 300 m of the surface. In the SW and NW regions, median thermal habitat depth ranged from 400 m to the surface at the northernmost latitudes. The full vertical extent of preferred thermal habitat of bigeye tuna also varied by region (Suppl. Fig. 3) (online only). The extent of this habitat was greatest in the SW and NW regions (depth: 200–450 m), least in the CW region (depth:

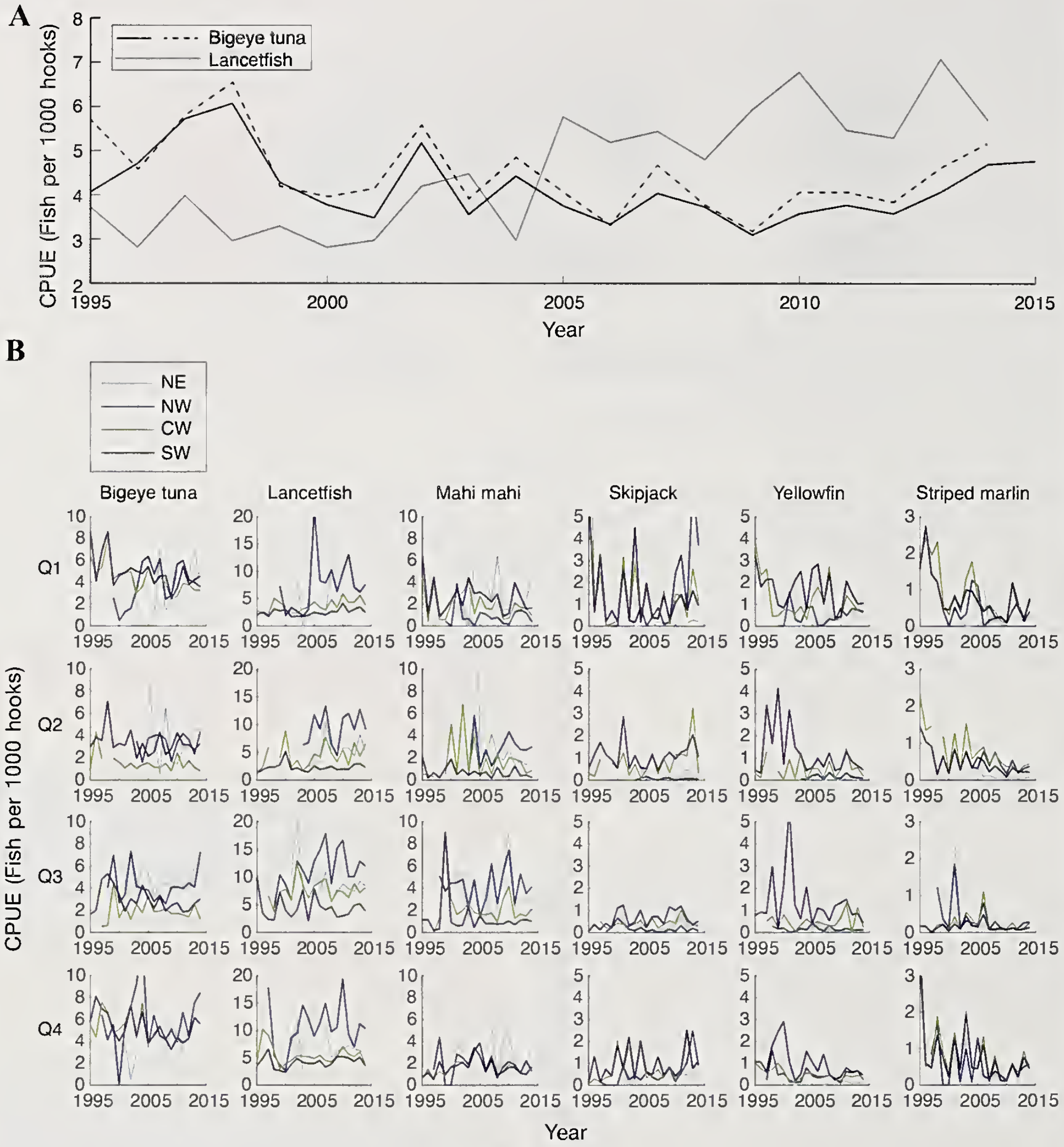

Figure 3

(**A**) Annual catch per unit of effort (CPUE) for bigeye tuna (*Thunnus obesus*; black lines) and longnose lancetfish (*Alepisaurus ferox*; gray line) for the Hawaii-based longline fishery from 1995 through 2015. The CPUE for bigeye tuna was calculated from both logbook records (solid black line), which are complete through 2015, and observer records (dashed black line), which are complete through 2014. The CPUE of longnose lancetfish was calculated from observer records. (**B**) Quarterly and regional CPUE, based on observer data, of bigeye tuna; longnose lancetfish; dolphinfish (*Coryphaena hippurus*), also known as mahi mahi; skipjack tuna (*Katsuwonus pelamis*); yellowfin tuna (*Thunnus albacares*); and striped marlin (*Kajikia audax*). Note that the scales of the y-axes vary by species.

300–425 m), and shallowest in the NE region (depth: 200–350 m).

Across the CW and NW regions, as well as much of the NE region, the depth of the oxygen-concentration threshold (1.0 mL/L) for bigeye tuna was below 500 m. In the SW region, this threshold was shallowest along 10°N (depth: 100–200 m) and progressed to depths below 500 m at the meridional extremes of the region. The oxygen-concentration threshold for bigeye tuna was shallowest in the SE region, generally above 500 m and above 100 m along 10°N (Fig. 1B).

Temporal variability Across all grid cells where fishing occurred at some point during the time series, the median depth of preferred thermal habitat for bigeye tuna shoaled at a rate of 0.55–0.71 m/year, or by 12–15 m

Table 1

Significant linear trends ($P<0.05$) in the median depth of the preferred thermal habitat of bigeye tuna (*Thunnus obesus*) (8–14 °C) based on logbook records of the Hawaii-based longline fishery and ocean temperatures obtained from the Global Ocean Data Assimilation System for 1995 through 2015. These records were transformed into a grid, and the values in this table were determined by using all grid cells with fishing effort at any time (any effort) and by weighting grid cells by total quarterly effort (effort-weighted). A dash denotes the lack of a significant trend. Each trend value is followed by the depth for 2005 from the linear regression or, in the absence of a significant trend, by the mean depth of the time series. Results are presented for the full fishing ground, as well as for the northeast (NE), northwest (NW), central west (CW), and southwest (SW) regions individually.

		Any effort		Effort-weighted	
Region	Quarter	Trend (m/y)	Depth (m)	Trend (m/y)	Depth (m)
NE	Q1	−1.36	255.46	–	302.59
	Q2	−1.38	256.66	–	301.29
	Q3	−1.17	254.00	−2.64	291.71
	Q4	−0.96	251.55	–	292.45
NW	Q1	–	264.21	–	346.42
	Q2	–	263.20	−3.49	328.70
	Q3	–	262.85	−3.69	290.24
	Q4	–	262.92	−1.71	336.40
CW	Q1	−1.52	367.35	−0.85	358.42
	Q2	−1.64	369.48	−1.15	357.56
	Q3	−1.76	365.06	−1.63	352.98
	Q4	−1.75	361.89	−2.07	348.46
SW	Q1	–	265.83	–	292.62
	Q2	–	265.43	−1.47	292.82
	Q3	−0.48	266.78	–	302.72
	Q4	−0.69	264.76	−2.14	320.98
Full fishing ground	Q1	−0.55	272.21	–	319.58
	Q2	−0.71	272.67	−1.78	303.25
	Q3	−0.63	271.92	−3.11	300.54
	Q4	−0.70	269.91	−2.23	336.08

overall, shoaling from roughly 280 to 265 m between 1995 and 2015 (Table 1). Shoaling was significant and greater when the depths of these temperatures were weighted by total quarterly effort (1.78–3.11 m/year or 37–65 m overall in the second–fourth quarters, shoaling from depths of 320–340 m to depths of 270–315 m over the course of the study period; Table 1). Significant shoaling within each region is presented in Table 1.

We lack sufficient data to examine variability in oxygen concentration over time. However, given that the oxygen-concentration threshold of bigeye tuna was found below 500 m across much of the area where the fishery operates, it is unlikely that low oxygen concentrations affected bigeye tuna in the study area.

Catch variability

Catch rates The annual catch rates of bigeye tuna declined until 2009, but have increased in subsequent years (Fig. 3A). Catch rates of longnose lancetfish, on the other hand, have increased over the past 2 decades, especially after 2004. For the past decade, catch rates of longnose lancetfish have exceeded those of bigeye tuna (Fig. 3A).

Quarterly catch rates of bigeye tuna and longnose lancetfish were considerably variable across the 4 regions of the fishery included in our analysis (Fig. 3B). The variability in catch rates of bigeye tuna was most striking in the third quarter, when the rates were notably higher in the NW and NE regions than in the SW and CW regions. Catch rates of longnose lancetfish were highest in the NW region and lowest in the SW region throughout the year. The quarterly and regional catch rates of mahi mahi, skipjack tuna (*Katsuwonus pelamis*), yellowfin tuna, and striped marlin are also presented in Figure 3B. The highest catch rates for these species, with the exception of mahi mahi, generally occurred in the SW and CW regions.

Catch composition The contribution of bigeye tuna to total catch varied by both quarter and region as did

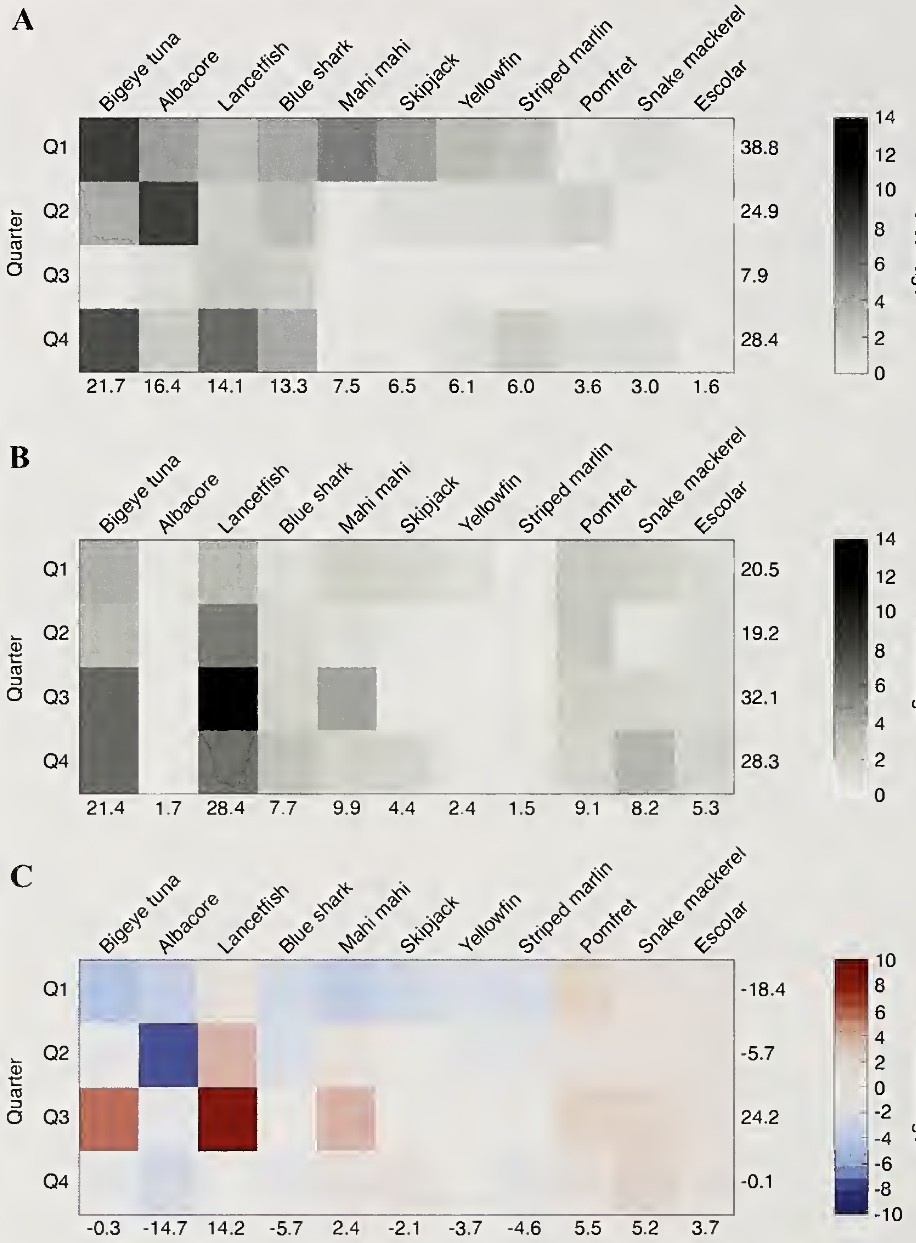

Figure 4

The mean percentages of total annual catch of the Hawaii-based longline fishery to which 11 species contributed each quarter, shaded for (**A**) the beginning (1995–1997) and (**B**) the end (2012–2014) of the time series of observer data, and (**C**) the differences between these percentages. The species were the following: bigeye tuna (*Thunnus obesus*); albacore (*Thunnus alalunga*); longnose lancetfish (*Alepisaurus ferox*); blue shark (*Prionace glauca*); dolphinfish (*Coryphaena hippurus*), also known as mahi mahi; skipjack tuna (*Katsuwonus pelamis*); yellowfin tuna (*Thunnus albacares*); striped marlin (*Kajikia audax*); sickle pomfret (*Taractichthys steindachneri*); snake mackerel (*Gempylus serpens*); and escolar (*Lepidocybium flavobrunneum*). In graphs A and B, the total annual contribution of each species is listed below each column, and the total annual contribution from each quarter is listed along the right-hand side of each row. In graph C, the difference in total annual contribution is listed below each column and along each row.

the proportion of catch that was discarded (Suppl. Fig. 4) (online only). In general, bigeye tuna composed nearly 20% of the total catch, although their contribution ranged from as low as 8% (CW region, second and third quarter averages) to over 21% (CW and SW regions, fourth quarter averages). Discard rates had more variability; the lowest rates occurred in the SW region in the first and second quarters (<30% on average), and the highest rates in the third and fourth quarters across all regions (40–55% on average).

In looking at catch composition, we found that each of the 11 species in Figure 4 accounted for at least 5% of the total annual catch at some point in the time series. Their contribution to total catch is broken down in that figure by quarter for the beginning (Fig. 4A) and end (Fig. 4B) of the time series. These distributions indicate that the seasonal timing of catch of bigeye tuna shifted from the first and fourth quarters to the third and fourth quarters, but that the overall contribution of this species to the annual catch changed little. Conversely, the contribution of longnose lancetfish to total annual catch increased by about 14%, primarily in the third quarter. The proportion of blue shark (*Prionace glauca*), yellowfin tuna, and striped marlin in total annual catch declined by 4–6%, whereas the proportion of sickle pomfret, snake mackerel, and escolar (*Lepidocybium flavobrunneum*) rose by 4–6% over the time series.

Discussion

Over the 21-year period examined in this study, the fishing effort of the Hawaii-based longline fishery increased more than 5-fold. A growing proportion of this effort occurred in the NE region of the fishing grounds, particularly during the third quarter of the year. The GODAS reanalysis and WOA13 data indicate that oceanographic conditions are favorable for bigeye tuna across much of the fishery's footprint. Although increasing effort should correlate with the desire of fishermen to catch more fish, the shift in the seasonal and spatial deployment of effort raises several biologically pertinent questions. Why did the fishery expand its spatial footprint, as opposed to it simply setting more hooks across the CW and SW regions? Why did it expand, primarily, into the NE region and only during the third quarter of the year?

The expansion of the fishery into the NE region during the third quarter is likely the result of several factors. One possibility is that the CW and SW regions were already supporting maximum effort. Effort was rather stable in these regions after about 2004 (Fig. 2), and previous work has documented that the catch rates of large, high-trophic-level, commercially valuable fish were declining in these waters as a result of increased fishing effort (Polovina et al., 2009; Polovina and Woodworth-Jefcoats, 2013). Furthermore, competition from international fisheries may have precluded additional Hawaii-based effort in the SW region. In the NW and NE regions, on the other hand, there was comparably little Hawaii-based effort and little to no competition from international fisheries.

Less than 10% of the total annual catch was caught during the third quarter of the year at the beginning of the time series (Fig. 4). Furthermore, in the CW and SW regions, target catch rates were lowest (9% and 14% on average, respectively) and discard rates highest (56% and 44% on average, respectively; Suppl. Fig. 4) (online only) during the third quarter, possibly explaining why fishermen have been willing to change fishing locations. These low target catch rates may also explain why effort was lowest in the third quarter at the beginning of the time series, and why, unlike in other quarters, effort was not concentrated in a specific region (before the focus of the fishery on the NE region).

Considering the distribution of fishing effort together with catch rates, we found that trends in catch rates are strongly correlated with the shift in the location of effort. Comparison of quarterly CPUE of bigeye tuna with the proportion of annual effort in each region and quarter indicates that the third-quarter CPUE of bigeye tuna was strongly correlated with the proportion of effort in the NE region (coefficient of correlation [r]=0.66) and negatively correlated with third quarter effort in the CW and SW regions (r=−0.56 and −0.46, respectively). No other significant correlations were found (P<0.5). Given the above correlations and the trends in catch composition, we conclude that the fishery reaction was a response to low catch rates for the target species in the CW and SW regions during the third quarter. The NE region proved to be a particularly effective fishing ground with high catch rates of target species, relatively low discard rates, and with little competition from international fishing fleets. As a result, a large portion of annual catch of bigeye tuna occurred in the third quarter by the end of the time series (Fig. 4).

Although the movement of the fishery toward the NE region was greatest in the third quarter, the fishery does occur in this region throughout the year, although to a lesser degree (Fig. 2). As discussed above, catch rates of target species in the SW and CW regions were generally higher during the rest of the year, possibly explaining why there was less fleet movement outside the third quarter.

The role of oceanographic variability in fishery expansion

The enhanced fishery yield in the NE region can be explained by the oceanographic conditions of the region. It has the largest area in which preferred thermal habitat of bigeye tuna closely overlaps vertically with both deep-set hooks (100–400 m) and with waters that have suitable oxygen concentrations (>1.0 mL/L; Fig. 1B). The time series of the depths of preferred thermal habitat shows that in the NE region, the preferred daytime habitat of bigeye tuna was consistently and completely within the depth range of deep-set hooks (Suppl. Fig. 3) (online only). Oceanographic variability also explains why the fishery did not expand into the SE region. This region encompasses the oxygen minimum zone of the eastern tropical Pacific Ocean. Across much of the SE region, the oxygen-concentration threshold of 1.0 mL/L occurred at depths shallower than the depths of both the preferred thermal habitat of bigeye tuna and the depths of deep-set gear (Fig. 1B), rendering it poor habitat for bigeye tuna and poor longline fishing grounds.

Effort-weighted trends in the depth of preferred habitat of bigeye tuna indicate that the fishery has moved into the more favorable oceanographic conditions of the NE region. At the beginning of the time series, the fishery was operating largely in waters where the median depth of preferred thermal habitat for bigeye tuna was roughly 320–340 m below the surface. However, by the end of the time series, the fishery was operating in waters where the median depth of preferred thermal habitat was 270–315 m below the surface and more closely aligned with the median depth of deep-set gear (250 m; Boggs, 1992; Bigelow et al., 2006). These trends in depth weighted by total quarterly effort indicate that fishermen were targeting regions where either preferred thermal habitat was more closely aligned with their gear or thermal habitat shoaling was greatest or possibly employing a combination of these 2 tactics. Across the entire fishing ground, the preferred thermal habitat of bigeye tuna shoaled by only about 12–15 m. Yet, when weighted by quarterly effort, the shoaling increased to roughly 37–65 m. Without information on depth of capture, it is difficult to determine the degree to which this shoaling actually influenced the fishery yield. However, given the vertical distributions of both deep-set gear and preferred daytime thermal habitat of bigeye tuna, shoaling could increase the degree to which these distributions overlap and could compress the total vertical habitat that bigeye tuna occupy. Both scenarios should increase the catchability of bigeye tuna, and in turn, fishery yield.

Effects of fishery expansion on catch composition

During the period studied, the spatial expansion and seasonal shift of the fishery influenced the seasonal timing of both the catch and catch composition. Although the primary target species, bigeye tuna, consistently was about 20% of the total annual catch, the bulk of the annual catch shifted from the first and fourth quarters to the third and fourth quarters. A combination of factors could have contributed to this shift. The foremost factor was the increase during the third quarter in effort deployed in the NE region (Fig. 2), where catch rates of bigeye tuna were consistently high over time (Fig. 3B). Additionally, by the end of the period examined, less effort was deployed in the SW region in the first quarter than in the CW region during the fourth quarter (Fig. 2). First quarter catch rates of bigeye tuna in the SW region declined over the past 2 decades (Fig. 3B), whereas fourth quarter catch rates of bigeye tuna in the CW region remained consistently high. In summary, by 2015, the fishery deployed most of its effort in the regions and during the quarters when catch rates of bigeye tuna were highest. It is interesting to note that these regions are also those where preferred thermal habitat for bigeye tuna completely overlaps with deep-set gear (NE region) and where preferred thermal habitat for bigeye tuna is most compressed (CW region) (Suppl. Fig. 3) (online only).

It is possible that the shift in time and place of the bulk of bigeye tuna catch each year can be attributed to changes in fishing gear, although we found no evidence that this shift was the cause. Using the number of hooks per float as a proxy for hook depth, we found no significant differences between gear set in the SW region during the first quarter, in the NE region during the third quarter, and in the CW region during the fourth quarter (5% significance level, Wilcoxon–Mann–Whitney rank-sum tests).

The shift in the annual timing of catch of bigeye tuna could also be attributed to fish movement or changes in population dynamics. Stock assessments from both fishing convention areas (west of 150°W, WCPFC, Harley et al., 2014; east of 150°W, IATTC, Aires-da-Silva and Maunder, 2015), along with tagging data (Schaefer et al., 2015), indicate that there is extensive zonal movement by bigeye tuna. At low latitudes (e.g., 15°S–15°N), there is more eastward movement than westward movement (Aires-da-Silva and Maunder, 2015; Schaefer et al., 2015). However, a lack of tagging data for areas farther north makes it difficult to determine whether bigeye tuna make the same directional movement in our study area. If they do, the high catch rates in the NE region noted in our study may have been fueled in part by fish moving into the region. The role of population dynamics is also unclear. Although it is likely that large-scale population dynamics affect interannual changes in CPUE of bigeye tuna (Harley et al., 2014; Aires-da-Silva and Maunder, 2015), size structure (and presumably age structure) of bigeye tuna was fairly consistent across the fishing ground (Suppl. Fig. 5) (online only), echoing earlier work (Kume, 1969).

For other commercially valuable species, such as yellowfin tuna and striped marlin, the spatial shift in effort exacerbated declining catch rates. Although CPUEs for both species declined across the fishing grounds, catch rates for these species were greatest in the SW and CW regions despite the movement of the fishery away from these regions (Fig. 3B). Catch rates for skipjack tuna, although not declining, were generally highest in the SW and CW regions (Fig. 3B). Therefore, the fishery's changing footprint likely contributed to an overall decline in the contribution of skipjack tuna to total annual catch (Fig. 4).

Discard rates also were influenced by the spatiotemporal shift in effort. In the core region of the fishery (12–27°N), rising discard rates were linked to increased fishing effort (Polovina and Woodworth-Jefcoats, 2013). At the same time, catch rates of longnose lancetfish in particular rose as a result of the fishery's northward expansion and increased focus on the third quarter. Catch rates of longnose lancetfish were not only highest in the NW region but were also highest within-region in the third quarter (Fig. 3B). Therefore, the fishery deployed more effort in a region where longnose lancetfish were more commonly caught and during the season when catch rates were highest. As a result, catch of longnose lancetfish, all of which was discarded, exceeded the catch of target species for the last decade of the study period (Fig. 3A). The same spatiotemporal shift in effort also explains the change in the contribution of mahi mahi to annual catch (Figs. 3B and 4), although mahi mahi are retained by the fishery and sold.

As with bigeye tuna, it is possible that both fish movement and population dynamics could have influenced changes in total composition of the catch. Tagging data and stock assessments are lacking for many of the species caught by the Hawaii-based longline fishery, especially the noncommercial species. Future research on the seasonal timing, location, and size structure of this catch may provide insight into such changes.

When using observer data to determine catch composition, as we did, there is a possibility that observer error could influence results. Such errors in the reporting of rare or cryptic species have been noted for individual longline sets and can influence results at fine spatiotemporal resolutions (e.g., months and single geographic degrees) and when observer coverage is low (Walsh et al., 2002; Walsh et al., 2005). However, it is not clear that such errors would be distinguishable when observer data are aggregated more broadly, such as on a quarterly and regional basis. Additionally, our results indicate strong agreement between data collected from independent scientific observers and data reported in commercial vessel logbooks for catch rates of bigeye tuna (Fig. 3A) and, therefore, consistent species identification of target species. The observed increase in catch of longnose lancetfish is corroborated by the regional expansion of the fishery: catch rates of longnose lancetfish were much higher in the NW region than elsewhere (Fig. 3B), and, in the early years of our study, the fishery was not operating in the NW region (Fig. 2A). Therefore, we conclude that the impacts of fishery expansion on catch composition are robust.

A look ahead

We have detailed how both fishery expansion and oceanographic variability have influenced catch of the Hawaii-based longline fishery. In particular, we found that the fishery has expanded into a region that has proven to be an efficient fishing ground by virtue of its local oceanography. With this perspective on past catch, can CPUEs continue to rise into the future? The results of previous work indicate that sustained increases in fishing effort drive down the abundance of large, high-trophic-level fish, such as those targeted by the Hawaii-based longline fishery (Ward and Myers, 2005b; Polovina et al., 2009; Polovina and Woodworth-Jefcoats, 2013). We also note that, although bigeye tuna are not considered to be subject to overfishing in the NE region (Aires-da-Silva and Maunder, 2015), overfishing of bigeye tuna has been documented to be occurring in the 3 western regions (Harley et al., 2014). This disparity creates the potential for further eastward displacement of fishing effort (both Hawaii-based and international) and for hastening removals of bigeye tuna. Therefore, it is possible that catch rates in the NE region eventually will diminish as have the catch rates in the SW and CW regions over the past 20 years.

Another change that will affect the fishery in coming years is the recent expansion of the Papahānaumokuākea Marine National Monument. In August 2016, the monument boundaries were expanded to encompass the full U. S. Exclusive Economic Zone west of 163°W, moving the boundaries an additional 150 nm from land (Federal Register, 2016). This expansion bars commercial fishing over a portion of the fishing grounds and has the greatest effect on the CW region. On average, 21% of the effort in the CW region in the fourth quarter (when fishing effort in this region is the greatest) and 25% of the bigeye tuna caught in the CW region during the fourth quarter are from waters that will now be off limits to the fishery. It is uncertain how the fishery will adjust, possibly by simply relocating fourth quarter effort outside the monument area or by shifting the allocation of that effort to another quarter or region.

Finally, climate change can be expected to affect the Hawaii-based longline fishery in a number of ways, potentially driving productive fishing grounds even farther from Hawaii. As ocean temperatures continue to rise, the preferred thermal habitat of bigeye tuna will be displaced northward (Lehodey et al., 2010; Bopp et al., 2013; Woodworth-Jefcoats et al., 2017). Additionally, the oxygen minimum zone that covers much of the SE region (Fig. 1B) has expanded over the past 50 years (Stramma et al., 2008). Although climate projections of further expansion are mixed (Stramma et al., 2008; Bopp et al., 2013; Cabré et al., 2015), continued expansion potentially would encroach on the NE region and render a larger portion of the SW region inhospitable to bigeye tuna.

We have shown how movement of the Hawaii-based longline fishery, particularly its seasonally focused expansion to the NE region, has helped shape the composition, magnitude, and seasonal timing of its catch. This information, together with previous studies of the effect of the Hawaii-based fishery on the ecosystem, as well as future climate projections and socioeconomic data (such as trip cost and catch value), has the potential to help guide future fishery management actions. For example, recent increases in CPUE of bigeye tuna can be placed in the context of the high catch rates the fishery saw in the late 1990s. Climate models could be used to project future changes in habitat of bigeye tuna. Additionally, the effect of the continued expansion of the fishery away from Hawaii can be assessed in relation to other factors, such as future fuel prices for fishing vessels. Such context and analyses can help fishery managers ensure that the Hawaii-based longline fishery remains both ecologically and financially sustainable.

Acknowledgments

The authors are grateful for insight from E. Portner, C. Boggs, M. Donahue, A. Timmermann, and K. Edwards that greatly improved this manuscript. We thank the scientific observers of the Pacific Islands Region for their ongoing collection of longline fishery data. We also thank A. Tomita for help in formatting international fisheries data. This article is contribution 10356 of the School of Ocean and Earth Science and Technology, University of Hawaii at Manoa.

Literature cited

Aires-da-Silva, A., and M. N. Maunder.
2015. Status of bigeye tuna in the eastern Pacific Ocean in 2014 and outlook for the future. Inter-American Tropical Tuna Commission Stock Assess. Rep. 16, 13 p. [Available from website, accessed October 2016.]

Bigelow, K., M. K. Musyl, F. Poisson, and P. Kleiber.
2006. Pelagic longline gear depth and shoaling. Fish. Res. 77:173–183.

Boggs, C. H.
1992 Depth, capture time, and hooked longevity of longline-caught pelagic fish: timing bites of fish with chips. Fish. Bull. 90:642–658.

Bopp, L., L. Resplandy, J. C. Orr, S. C. Doney, J. P. Dunne, M. Gehlen, P. Halloran, C. Heinze, T. Ilyina, R. Séférian, et al.
2013. Multiple stressors of ocean ecosystems in the 21st century: projections with CMIP5 models. Biogeosciences 10:6225–6245.

Cabré, A., I. Marinov, R. Bernardello, and D. Bianchi.
2015. Oxygen minimum zones in the tropical Pacific across CMIP5 models: mean state differences and climate change trends. Biogeosciences 12:5429–5454.

Cox, S. P., T. E. Essington, J. F. Kitchell, S. J. D. Martell, C. J. Walters, C. Boggs, and I. Kaplan.
2002. Reconstructing ecosystem dynamics in the central Pacific Ocean, 1952–1998. II. A preliminary assessment of the trophic impacts of fishing and effects on tuna dynamics. Can. J. Fish. Aquat. Sci. 59:1736–1747.

Federal Register.
2016 Papahānaumokuākea Marine National Monument expansion. Fed. Reg. 81:60227–60234. GPO, Washington, D.C. Available at website

Garcia, H. E., R. A. Locarnini, T. P. Boyer, J. I. Antonov, A. V. Mishonov, O. K. Baranova, M. M. Zweng, J. R. Reagan, and D. R. Johnson.
2013. World ocean atlas 2013. Volume 3: dissolved oxygen, apparent oxygen utilization, and oxygen saturation. NOAA Atlas NESDIS 75, 27 p.

Gilman, E., M. Chaloupka, A. Read, P. Dalzell, J. Holetschek, and C. Curtice.
2012. Hawaii longline tuna fishery temporal trends in standardized catch rates and length distributions and effects on pelagic and seamount ecosystems. Aquat. Conserv. 22:446–488.

Harley, S., N. Davies, J. Hampton, and S. McKechnie.
2014. Stock assessment of bigeye tuna in the western and central Pacific Ocean. West. Cent. Pac. Fish. Comm. WCPFC-SC10-2014/SA-WP-01, 115 p. [Available from website, accessed October 2016.]

Howell, E. A., D. R. Hawn, and J. J. Polovina.
2010. Spatiotemporal variability in bigeye tuna (*Thunnus obesus*) dive behavior in the central North Pacific Ocean. Prog. Oceanogr. 86:81–93.

Kitchell, J. F., T. E. Essington, C. H. Boggs, D. E. Schindler, and C. J. Walters.
2002. The role of sharks and longline fisheries in a pelagic ecosystem of the central Pacific. Ecosystems 5:202–216.

Kume, S.
1969. Ecological studies on bigeye tuna—V: A critical review on distribution, size composition and stock structure of bigeye tuna in the North Pacific Ocean (north of 16°N). Bull. Far Seas Fish. Res. Lab. 1:57–75.

Lehodey, P., I. Senina, J. Sibert, L. Bopp, B. Calmettes, J. Hampton, and R. Murtugudde.
2010. Preliminary forecasts of Pacific bigeye tuna population trends under the A2 IPCC scenario. Prog. Oceanogr. 86:302–315.

Polovina, J. J., and P. A. Woodworth-Jefcoats.
2013. Fishery-induced changes in the subtropical Pacific pelagic Ecosystem size structure: observations and theory. PLoS ONE 8(4):e62341.

Polovina, J. J., M. Abecassis, E. A. Howell, and P. Woodworth.
2009. Increases in the relative abundance of mid-trophic level fishes concurrent with declines in apex predators in the subtropical North Pacific, 1996–2006. Fish. Bull. 107:523–531.

Saha, S., S. Nadiga, C. Thiaw, J. Wang, W. Wang, Q. Zhang, H. M. Van den Dool, H.-L. Pan, S. Moorthi, D. Behringer, et al.
2006. The NCEP Climate Forecast System. J. Clim. 19:3483–3517.

Schaefer, K., D. Fuller, J. Hampton, S. Caillot, B. Leroy, and D. Itano.
2015 Movements, dispersion, and mixing of bigeye tuna (*Thunnus obesus*) tagged and released in the equatorial Central Pacific Ocean, with conventional and archival tags. Fish. Res. 161:336–355.

Sibert, J., J. Hampton, P. Kleiber, and M. Maunder.
2006. Biomass, size, and trophic status of top predators in the Pacific Ocean. Science 314:1773–1776.

Stramma, L., G. C. Johnson, J. Sprintall, and V. Mohrholz.
2008. Expanding oxygen-minimum zones in the tropical oceans. Science 320:655–658. Article

Walsh, W. A., and J. Brodziak.
2015. Billfish CPUE standardization in the Hawaii longline fishery: model selection and multimodel inference. Fish. Res. 166:151–162.

Walsh, W. A., P. Kleiber, and M. McCracken.
2002. Comparison of logbook reports of incidental blue shark catch rates by Hawaii-based longline vessels to fishery observer data by application of a generalized additive model. Fish. Res. 58:79–94.

Walsh, W. A., R. Y. Ito, K. E. Kawamoto, and M. McCracken.
2005. Analysis of logbook accuracy for blue marlin (*Mak-*

aira nigricans) in the Hawaii-based longline fishery with a generalized additive model and commercial sales data. Fish. Res. 75:175–192.

Ward, P., and R. A. Myers.

2005a. Inferring the depth distribution of catchability for pelagic fishes and correcting for variations in the depth of longline fishing gear. Can. J. Fish. Aquat. Sci. 62:1130–1142.

2005b. Shifts in open-ocean fish communities coinciding with the commencement of commercial fishing. Ecology 86:835–847.

Woodworth-Jefcoats, P. A., J. J. Polovina, and J. C. Drazen.

2017. Climate change is projected to reduce carrying capacity and redistribute species richness in North Pacific pelagic marine ecosystems. Global Change Biol. 23:1000–1008.

National Marine
Fisheries Service
NOAA

Fishery Bulletin
established in 1881

Spencer F. Baird
First U.S. Commissioner
of Fisheries and founder
of *Fishery Bulletin*

Extrusion of fish larvae from SEAMAP plankton sampling nets: a comparison between 0.333-mm and 0.202-mm mesh nets

Christina M. Schobernd (contact author)[1]
M. Conor McManus[2]
Joanne Lyczkowski-Shultz[3]
Nathan M. Bacheler[1]
Denice M. Drass[3]

Email address for contact author: christina.schobernd@noaa.gov

[1] Southeast Fisheries Science Center
National Marine Fisheries Service, NOAA
101 Pivers Island Road
Beaufort, North Carolina 28516

[2] Graduate School of Oceanography
University of Rhode Island
215 South Ferry Road
Narragansett, Rhode Island 02882

[3] Southeast Fisheries Science Center
National Marine Fisheries Service, NOAA
3209 Frederic Street
Pascagoula, Mississippi 39567

Abstract—To assess larval fish and egg extrusion through the standard-size mesh plankton net used during resource surveys of the Southeast Area Monitoring and Assessment Program (SEAMAP), 81 bongo tows with side-by-side nets, each constructed with a different mesh size (0.333 mm and 0.202 mm), were taken during 5 SEAMAP surveys conducted in the Gulf of Mexico during 2005–2007. Retention by length class for the larvae of 6 taxa and an unidentified group was evaluated by using 2 deterministic functions to estimate the number of larvae missed when sampling with the net with standard-size mesh (0.333 mm) compared with sampling with the smaller mesh net (0.202 mm). Smaller larvae, particularly those between 1.5 and 3 mm in body length, were retained in greater numbers in the 0.202-mm-mesh net than in the 0.333-mm-mesh net. Extrusion was most pronounced for small, undeveloped larvae that could be identified only to the suborder Percoidei or that could not be identified. Extrusion was evident also among larvae of taxa in the families Engraulidae, Sciaenidae, and Scombridae, but less so for Clupeidae and Lutjanidae; the latter result was most likely attributable to a mismatch between the timing of sampling and spawning seasons. The functional relationships presented here, based on larval abundance ratios and body lengths, represent the first empirically derived estimates of extrusion and size bias in SEAMAP ichthyoplankton samples.

Planktonic, early-life-stage fish (ichthyoplankton) have been monitored for over a century worldwide to assess the abundance and distribution of fish stocks (Hjort, 1914; McClatchie et al., 2014). Ichthyoplankton surveys have been used to estimate changes in spawning stock biomass, to identify spawning habitats and seasonality, and to quantify survival through the larval stage (Richardson et al., 2010). Arguably, the greatest value of these surveys is that they provide a method for measuring changes in the trends of larval assemblages over time. Such trends are particularly valuable during a changing climate, since alterations in sea temperature, carbonate chemistry, and ocean circulation influence larval growth, mortality, dispersal, and assemblage connectivity (Llopiz et al., 2014).

In the southeastern United States, larval fish abundances are monitored under the Southeast Area Monitoring and Assessment Program (SEAMAP; Stuntz et al.[1]; Lyczkowski-Shultz and Hanisko, 2007). As part of SEAMAP protocol, plankton samples are collected during annual surveys in the Gulf of Mexico by the National Marine Fisheries Service (NMFS) and agencies of 4 states: Alabama, Florida, Louisiana, and Mississippi. Data from these surveys are used in stock assessments for many managed, commercially significant species, including the bluefin tuna (*Thunnus thynnus*; Scott et al., 1993), king mackerel (*Scomberomorus cavalla*; Gledhill and Lyczkowski-Shultz, 2000), red snapper (*Lutjanus campechanus*;

Manuscript submitted 30 November 2017.
Manuscript accepted 8 May 2018.
Fish. Bull. 116:240–253 (2018)
Online publication date: 31 May 2018.
doi: 10.7755/FB.116.3-4.3

The views and opinions expressed or implied in this article are those of the author (or authors) and do not necessarily reflect the position of the National Marine Fisheries Service, NOAA.

---

[1] Stuntz, W. E., C. E. Bryan, K. Savastano, R. S. Waller, and P. A. Thompson. 1983. SEAMAP environmental and biological atlas of the Gulf of Mexico, 1982, 145 p. Gulf States Mar. Fish. Comm., Ocean Springs, MS. [Available from website.]

Hanisko et al., 2007), and vermilion snapper (*Rhomboplites aurorubens*; Hanisko et al.[2]). Ichthyoplankton data from the SEAMAP surveys have also been used to describe larval transport, decadal changes in fish habitat, and annual variations in egg densities in the Gulf of Mexico (Johnson et al., 2009; Marancik et al., 2012; Hernandez et al.[3]; Lyczkowski-Shultz et al., 2013). Additionally, SEAMAP samples have been used to assess the potential impacts of 1) entrainment of larvae in offshore liquefied natural gas facilities (Gallaway et al., 2007) and 2) larval mortality from the 2010 Deepwater Horizon oil spill (Muhling et al., 2012) to Gulf of Mexico fisheries.

Application of such abundance-at-size data is predicated on the assumption that larvae caught and retained in plankton nets consistently and accurately represent the assemblage being sampled (Tranter, 1968; Smith and Richardson, 1977). Inherent catchability issues with plankton nets, however, result in underrepresentation of larger, more developed larvae that are able to detect and avoid the net (Morse, 1989; Somerton and Kobayashi, 1989) and in underrepresentation of the smallest larvae in catches because they are extruded through net meshes (Colton et al., 1980; Lo, 1983; Houde and Lovdal, 1984; Johnson and Morse, 1994). The effect of these sources of bias on larval abundance data have been widely investigated in studies outside the Gulf of Mexico but have never been addressed specifically for data generated from SEAMAP ichthyoplankton surveys. Only 2 previous studies with gear other than SEAMAP plankton nets investigated the extrusion of larval fish from plankton nets in northern Gulf of Mexico waters (Comyns, 1997; Hernandez et al., 2011).

Ideally both of these biases should be evaluated before abundance data are interpreted and used in resource monitoring and environmental and fisheries assessments (Smith and Richardson, 1977). In recent stock assessments, the effect of avoidance was mitigated by including in analyses only the largest size class of larvae that are consistently captured in the net—a decision based on examination of size frequency distributions (Hanisko et al., 2007; Hanisko et al.[2]). Despite the importance of the earliest life stages in estimating absolute abundance or mortality, the underrepresentation of these values due to extrusion of the smallest larvae in SEAMAP samples has not been considered in the development of SEAMAP indices of larval abundance.

Table 1

Cruise number, start and end dates, and number of tows conducted with bongo nets with different mesh sizes during Southeast Area Monitoring and Assessment Program surveys in the northern Gulf of Mexico between October 2005 and August 2007.

Cruise	Start date	End date	No. of tows
04266	22-Oct-2005	01-Nov-2005	45
63062	23-March-2006	29-May-2006	15
63064	31-Aug-2006	27-Sep-2006	7
63075	29-Aug-2007	28-Sep-2007	14

The use of standard gear and towing methods during plankton surveys has ensured consistent sampling within and among SEAMAP cruises and surveys (McClatchie et al., 2014; GSMFC[4]). However, the specific characteristics of the SEAMAP bongo net in relation to loss of eggs and larvae though the meshes of the standard SEAMAP sampling gear have yet to be investigated. Our objective was to evaluate the degree of extrusion of fish eggs and larvae through the standard SEAMAP bongo net, which has a 0.333-mm mesh, by comparing numbers of larvae from that net with larval numbers from a bongo net with a finer, 0.202-mm mesh.

Materials and methods

Field and laboratory methods

Between October 2005 and August 2007, 81 bongo tows with side-by-side nets, each with a different mesh size, were performed during 5 SEAMAP surveys conducted in the Gulf of Mexico (Table 1, Fig. 1). Given the primary objectives for these surveys, samples were taken as time permitted after standard sampling was completed. The 61-cm bongo net frame with a mouth opening of 0.29 m^2 that is used during standard SEAMAP sampling was used in the tows of our study. However, unlike the standard SEAMAP bongo net configuration, which consists of 2 nets with a mesh size of 0.333 mm, the configuration consisted of a net with 0.202-mm mesh on one side of the frame and a net with 0.333-mm mesh on the other side. Although no side-by-side effect was evaluated, it is thought to be minimal because of the short distance between the mouth openings of the 2 nets on the bongo frame. Sampling was conducted

---

[2] Hanisko, D. S., A. Pollack, and G. Zapfe. 2015. Vermilion snapper (*Rhomboplites aurorubens*) larval indices of relative abundance from SEAMAP Fall Plankton Surveys, 1986 to 2012. Southeast Data, Assessment and Review SEDAR45-WP-05, 34 p. [Available from: website.]

[3] Hernandez, F. J., W. M. Graham, and K. Bayha. 2013. Spatial distribution and abundance of red snapper (*Lutjanus campechanus*), vermilion snapper (*Rhomboplites aurorubens*), and red drum (*Sciaenops ocellatus*) eggs across the northern Gulf of Mexico based on SEAMAP continuous underway fish egg sampler (CUFES) surveys, 52 p. Final Report NOAA/MARFIN Award Number NA09NMF4330153. [Available from Grants Branch, Southeast Reg. Off., Natl. Mar. Fish. Serv., NOAA, 263 13th Ave. S., St. Petersburg, FL 337101.]

[4] GSMFC (Gulf States Marine Fisheries Commission). 2016. SEAMAP operations manual for trawl and plankton surveys, 61 p. GSMFC, Ocean Springs, MS. [Available from website.]

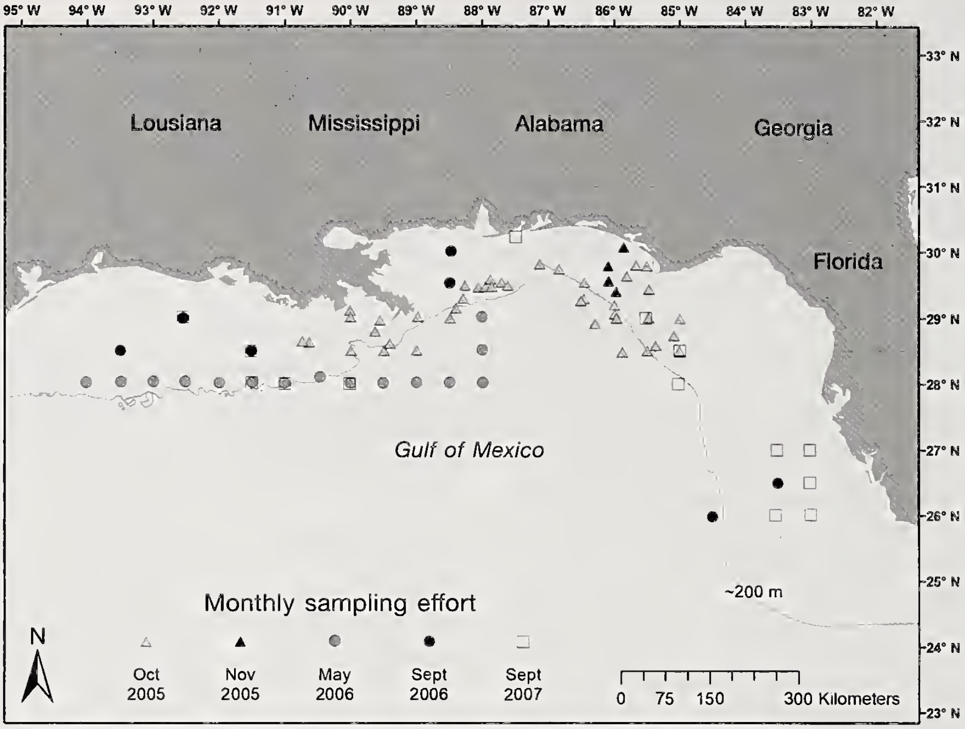

Figure 1

Locations of the 81 tows conducted with bongo nets with different mesh sizes during 5 Southeast Area Monitoring and Assessment Program surveys of ichthyoplankton conducted in the Gulf of Mexico between October 2005 and August 2007. Month and year of sampling are denoted by symbols at each location. The bathymetric contour represents the edge of the continental shelf (~200 m).

irrespective of time of day during 24-h survey operations and resulted in the collection of 35 daytime and 46 nighttime samples with nets of different mesh size. Shipboard handling of the concentration and preservation of samples taken from the nets with different mesh size followed standard SEAMAP protocols (Lyczkowski-Shultz and Hanisko, 2007). Samples were preserved initially in either 5–10% formalin or 95% ethanol. Formalin-fixed samples were later transferred to 95% ethanol after 48 h; samples initially preserved in ethanol were transferred to fresh ethanol after 24–36 h. All tows were made in a double-oblique pattern from the surface to a maximum depth of 200 m (or to within 2 m of the bottom at station depths <200 m) and then back to the surface. Tows were made at ~0.8 m/s (~1.5 kt) and maintained a targeted towing wire angle of ~ 45° (Smith and Richardson, 1977). Tow speeds ranged from 0.64 to 1.47 m/s (1.24–2.85 kt) and an average speed of 0.87 m/s (1.69 kt [standard error 0.03]). Tow durations ranged from 1.7 to 26.3 min depending on station depth and the consequent tow (sampling) depth prescribed by SEAMAP protocols. The volume of water filtered by each net was measured with a flow meter attached within the net mouth.

Larval fish abundances were standardized to account for sampling effort by using volume of filtered sea water and maximum depth at which the nets sampled and were expressed as 'number of larvae under 10 m^2 of sea surface' (Smith and Richardson, 1977; GSMFC[3]). This standardization was accomplished by dividing the number of larvae of each taxon caught in a sample by the volume of water filtered during the tow, and then multiplying the resultant by the maximum depth of the tow in meters and the factor 10. Larval abundances were also standardized by volume of water filtered alone, and are expressed as 'number of larvae per 1000 m^3 of filtered sea water'. This was accomplished simply by dividing the number of larvae of each taxon caught in a sample by the volume of water filtered during the tow, and then multiplying the resultant by the factor of 1000 (number of larvae per 1000 m^3).

Fish larvae from the 162 samples collected during the 81 tows of paired bongo nets were removed and identified to the lowest possible taxon (most often to family) at the Plankton Sorting and Identification Center of the Sea Fisheries Institute in Gdynia and Szczecin, Poland. Fish eggs were also removed and enumerated but were not measured or identified. Wet plankton volumes were measured by displacement ('displacement volume') to estimate net-caught zooplankton biomass (Smith and Richardson, 1977). Following established SEAMAP identification and measurement protocols, body length (BL) was measured as either notochord or standard length depending on caudal fin development of the specimen, to the nearest 0.1 mm. This is the length reported throughout this article. The actual number of specimens measured depended on the taxonomic group and level of identification. To increase the number of observations available for analysis, up to 50 randomly chosen specimens in the 5 families targeted for analysis (Engraulidae, Clupeidae, Scombridae, Sciaenidae, and Lutjanidae) and unidentified and Percoidei larvae were measured at the NMFS laboratory in Pascagoula, Mississippi. These families were examined because they contain either ecologically or economically important species, many of which are federally managed. Additionally, larvae within these families represent the 2 body shapes of larval fish, clupeiform (slender) and perciform (robust) that have been shown to influence susceptibility to extrusion (Smith and Richardson, 1977). Unidentified larvae (with mixed body shapes) and those identifiable only to the suborder Percoidei (perciform) were measured because larvae in these 2 categories were among the smallest specimens in the samples and were, therefore, most likely to be extruded from the coarser mesh net. Although larval size can shrink as much as 22% to 33% because of tissue damage during capture and preservation (Miller and Sumida, 1974; Theilacker, 1980), this potential damage was not accounted for in our length measurements. This factor may explain why nominal lengths of the smallest larvae in the samples collected with the nets of 2 different mesh sizes were smaller than reported larval sizes at hatching. Larval shrinkage rates, however, were not expected to differ between samples from the nets with fine and coarse mesh sizes.

Species-level identification based on published larval descriptions for the Gulf of Mexico region requires the morphological presence of characters not generally present in larvae <3 mm BL (Richards, 2006). As such, many small specimens in early stages of development from the samples taken with the 2 nets were identifiable only to family. To use data over all sizes represented in the study collections while maintaining taxonomic groups of distinct body shapes, specimens of the 5 targeted families identified to genus or species were combined with specimens at the family level for subsequent analysis (i.e., analysis occurred at the family level).

Statistical analyses

Paired Wilcoxon signed-rank tests were used to determine significant differences in means between samples from nets with the 2 mesh sizes, 0.202 mm and 0.333 mm. Means were examined for the following values: volume filtered, total sample displacement volume, total fish eggs (raw counts), total fish larvae (raw counts), and standardized larval abundance (the number of larvae under 10 m^2 sea surface, and number of larvae per 1000 m^3). To reduce the chance of type-I errors, α values were adjusted by using a sequential Bonferroni adjustment (Rice, 1989). Analyses were not stratified by time of day because the samples from each plankton net attached to the bongo frame were taken at the same time (paired tows) so that any diel influence would be the same for both samples. Plots of volume filtered versus tow depth, by mesh size, were examined to determine whether clogging between the meshes of the 2 nets over the entire range of sampling depths had occurred in our study. Plots of tow duration (related to depth) by larval abundance for each mesh size were also examined to determine whether shorter tows at shallower, inshore stations collected abundances similar to those of longer tows at deeper, offshore stations. Paired *t*-tests were used to test for significant differences in mean larval abundances between the 2 mesh sizes for the groups of interest: unidentified larvae and larvae of Percoidei, Engraulidae, Clupeidae, Scombridae, Sciaenidae, and Lutjanidae. The Kolmogorov–Smirnov test (K–S test) was used to determine whether length-frequency distributions varied significantly for larvae under 10 mm BL for samples from the nets with 0.202-mm and 0.333-mm meshes.

Functional relationships were constructed by comparing the ratio of the numbers of larvae collected with the 0.202 mesh net to the numbers of larvae collected with the standard 0.333 mesh net to assess the numbers of larvae extruded through the coarser mesh. Models were constructed for unidentified larvae, percoidei larvae, and larvae from the 5 targeted families. Ratios of mean standardized abundance (number under 10 m^2 sea surface) from the nets with 0.202-mm mesh to the mean standardized abundance from the nets with 0.333-mm meshes were calculated for each taxon by 0.1-mm size classes. Only size classes where both nets had positive catches of the target taxa were used as data for fitting the models. All functions were fitted with maximum likelihood estimation and log-normally distributed error structures by using the 'bbmle' package in the software R, vers. 3.3.1 (Bolker, 2008; R Core Team, 2016). Power (Eq. 1) and exponential (Eq. 2) models were used to describe the relationship between the larval abundance ratios:

$$P_r = aL^b \text{ and} \tag{1}$$

$$P_r = de^{-Lf}, \tag{2}$$

where P_r = the predicted ratio of abundances in samples collected with nets of the 2 mesh sizes (0.202-mm:0.333-mm); and

L = the size class (in millimeters).

Parameters a, b, d, and f are constants estimated during the fitting process.

Akaike information criterion (AIC) was used to determine which model was the best fit for a given taxon (Burnham and Anderson, 2002). In this study, ΔAIC scores are presented as the relative difference between the AIC score of each model from that of the best fitting model within a taxonomic group.

Results

Fish eggs and larvae were collected in all 162 samples from 81 tows of paired bongo nets. Samples included

Table 2

Mean values, with standard errors (SEs), for sample displacement volume (mL), total number of larvae caught (raw counts), standardized larval abundances, volume filtered (m^3), and total number of eggs (raw counts) of samples collected with bongo nets that had different mesh sizes, 0.202 mm (n=81) and 0.333 mm (n=81), during Southeast Area Monitoring and Assessment Program surveys in the northern Gulf of Mexico during 2005–2007. The standardized larval abundances were calculated as the number of larvae per 1000 m^3 of filtered sea water and as the number of larvae caught in a sample by the volume of water filtered during the tow, multiplied by the maximum depth of the tow in meters and the factor 10 (abundance under 10 m^2 of sea surface). P-values and adjusted α levels are listed for paired Wilcoxon signed-rank tests. Asterisks denote significant differences between samples from the nets with the 2 mesh sizes.

	Mean (SE)			
	0.202 mm	0.333 mm	P-value	Adj. α
Displacement volume	32 (2.7)	19 (1.3)	<0.0001	0.0083*
Total number of larvae	465 (102.1)	299 (73.5)	<0.0001	0.01*
Abundance per 1000 m^3	4665 (1340.7)	2660 (797.3)	<0.0001	0.0125*
Abundance under 10 m^2	2455 (557.3)	1537 (342)	<0.0001	0.0167*
Volume filtered	171 (9.3)	170 (9.5)	0.1888	0.025
Total number of eggs	778 (591.6)	596 (390.4)	0.9498	–

Table 3

Summary of total number of larvae caught and standardized total and mean larval abundances in samples collected with nets of 2 different mesh sizes in the northern Gulf of Mexico during 2005–2007. Values are given for unidentified larvae and larvae of 6 taxa of interest: Percoidei, Engraulidae, Clupeidae, Scombridae, Sciaenidae, and Lutjanidae. Asterisks represent significant statistical differences in mean larval abundances (paired t-tests) and length-frequency distributions (K–S test) between paired samples from the nets with 2 different mesh sizes, 0.202 mm and 0.333 mm. Larval abundance was calculated as the number of larvae caught in a sample per the volume of water filtered during the tow multiplied by the maximum depth of the tow in meters and the factor 10 (number under 10 m^2 of sea surface).

		Total larvae		Total abundance		Mean abundance (SE)			
Taxa	Body shape	0.202 mm	0.333 mm	0.202 mm	0.333 mm	0.202 mm	0.333 mm	P-value	K–S test
Unidentified	Undetermined	3808	430	22,141	2335	273 (125)	29 (9)	0.02*	*
Percoidei	Perciform	1227	180	4614	699	58 (28)	9 (3)	0.03*	*
Engraulidae	Clupeiform	1261	1306	5246	5642	65 (22)	69 (26)	0.31	*
Clupeidae	Clupeiform	8283	7102	36,207	31,290	447 (373)	386 (330)	0.09	*
Scombridae	Perciform	432	256	2447	1404	30 (10)	17 (4)	0.06	*
Sciaenidae	Perciform	4674	1901	32,874	10,582	406 (297)	131 (66)	0.18	*
Lutjanidae	Perciform	307	292	1525	1448	19 (4)	19 (4)	0.33	*

a total of 111,283 eggs and 61,950 fish larvae representing 252 taxa. Samples collected from nets with the finer mesh (0.202 mm) contained more larvae than samples from nets with the larger mesh (0.333 mm)—37,696 versus 24,254 larvae—an increase of 55.4%. For all tows combined by mesh size, samples from nets with a 0.202-mm mesh had significantly higher mean displacement volumes (68.4% difference), number of larvae (55.5%), larvae per 1000 m^3 (75.4%), and larvae under 10 m^2 (59.7%) than samples from nets with a 0.333-mm mesh (Table 2). Mean number of eggs did not vary significantly between mesh sizes (0.6% difference). Volume of water filtered, by mesh size, ranged from 27 to 382 m^3 for the samples from nets with a 0.202-mm mesh and from 40 to 380 m^3 for the samples from nets with a 0.333-mm mesh. Mean volume filtered did not vary significantly between the mesh sizes (30.5% difference; Table 2). Additionally, regressions of volume filtered by tow depth revealed similar filtering efficiencies for both mesh sizes over the range of sampling depths, tow durations, and the broad spatial extent of our study (y=1.1003x+55.036, coefficient of determina-

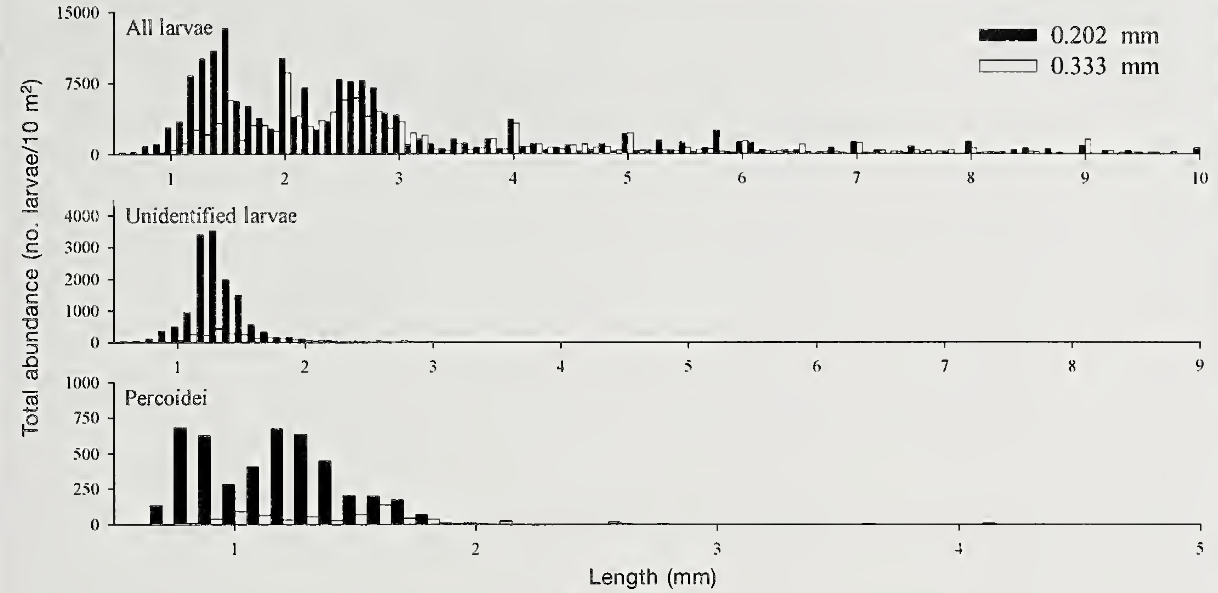

Figure 2

Length-frequency histograms of body length by total larval abundance in samples collected in the Gulf of Mexico during 2005–2007 with nets of 2 different mesh sizes (0.202 and 0.333 mm) for all larvae, unidentified larvae, and larvae of the suborder Percoidei. Larval abundance was measured as the total number of larvae caught in a sample per the volume of water filtered during the tow multiplied by the maximum depth of the tow in meters and the factor 10 (total number of larvae under 10 m^2 of sea surface). Only body lengths up to 10 mm are displayed in this figure. Note the different range in body length for each category of larvae.

tion (r^2)=0.841; y=1.0615x+57.643, r^2=0.8076, for the samples collected with nets with 0.202-mm and those collected with 0.333-mm mesh, respectively). Plots of tow duration by larval abundance for each mesh size revealed that higher levels of abundance occurred in shorter tows at shallower, inshore stations where larvae are more concentrated than in longer tows at deeper, offshore stations.

Larval abundance in samples collected with the different mesh sizes varied widely among the 6 taxa and the unidentified group chosen for analysis (Table 3). Overall, clupeid larvae were captured in the greatest numbers followed by sciaenids and the category for unidentified larvae. Lutjanid larvae were the least numerous taxon collected. Disparities between samples from nets with the 2 mesh sizes were greatest for sciaenid, unidentified, and percoid larvae, and least for lutjanid, engraulid, and clupeid larvae. These disparities were especially evident for unidentified and percoid larvae for which total larval abundance in samples from nets with 0.202-mm mesh was an order of magnitude greater than in samples from nets with 0.333-mm mesh (Table 3). Although mean abundance varied significantly only for 2 of the groups examined (unidentified larvae and Percoidei), K–S tests revealed significant differences in length-frequency distribution for larvae under 10 mm for all taxa examined (Table 3).

Larvae of taxa that spawn during late summer and early fall predominated in collections from the nets of different mesh size because of the preponderance of sampling in the months of September and October (Table 4). This temporal coverage resulted in greater availability of the smallest, least developed sciaenid larvae in samples taken with both mesh sizes. Scombrid larvae were equally prevalent in spring (May) and late summer (September) samples. The presence of both spring-spawning taxa (*Auxis* spp. and *Thunnus* spp.) and protracted-spawning taxa, including the little tunny (*Euthynnus alletteratus*), king mackerel, and Spanish mackerel (*S. maculatus*), increased the availability of the smallest size category of scombrid larvae.

Standardized abundances (number of larvae under 10 m^2) of all fish larvae taken in the nets with 2 different mesh sizes during this study, combined and grouped by 0.1-mm size classes, indicate that larvae ≤3 mm were consistently found in greater numbers in the nets with 0.202-mm mesh than in the nets with 0.333-mm mesh (Fig. 2). This was also the case for the categories of unidentified larvae and larvae identified to the suborder Percoidei, for which most specimens were <2 mm in length (Fig. 2). Among the smallest larvae identifiable to 1 of the 5 target families, all but clupeid larvae were abundant at sizes ≤2 mm, and larvae in that size category were found in greater numbers in the finer-mesh net than in the coarser-mesh net (Fig. 3). The smallest, most abundant size classes of clupeid larvae present in study samples ranged from 2 to 3 mm, and those larvae were also found in greater num-

Table 4

Summary of mean body length (mm), number of larvae measured, and total number of samples by month for taxa within the 5 target families as originally identified in samples collected with 0.202-mm and 0.333-mm-mesh nets in the northern Gulf of Mexico during 2005–2007. The total number of samples is the total number of samples in which a taxon was collected. The total number of samples collected in a month is provided in parenthesis next to name of the month. Months of peak spawning as inferred from larval abundance or occurrence were obtained primarily from Hernandez et al.[1] and the following additional studies: Ditty et al.[2]; Scott et al. (1993)[3]; Lyczkowski-Shultz and Hanisko (2007)[4]; Domeier et al.[5]; Lyczkowski-Shultz and Hanisko.[6]

		Mean length (mm)		Number measured		Total no. of samples	May (*n*=15)		Sept (*n*=21)		Oct (*n*=41)		Nov (*n*=4)		Peak spawning
Family	Taxon	0.202	0.333	0.202	0.333		0.202	0.333	0.202	0.333	0.202	0.333	0.202	0.333	
Engraulidae	Engraulidae	4.6	5.0	227	206	57	2	2	7	6	19	18	1	2	-
Clupeidae	*Brevoortia patronus*	3.6	3.9	125	98	30	1	1	-	-	14	13	1	-	[1] Nov/Jan
Clupeidae	Clupeidae	2.4	1.9	64	52	11	-	-	3	3	3	1	-	1	-
Clupeidae	*Etrumeus teres*	3.4	4.4	10	10	9	2	3	-	-	2	-	1	1	[1]Mar
Clupeidae	*Harengula jaguana*	-	5.6	-	12	7	-	-	-	7	-	-	-	-	[1] June/Aug
Clupeidae	*Opisthonema oglinum*	4.6	4.0	120	126	16	1	-	9	6	-	-	-	-	[1]May
Clupeidae	*Sardinella aurita*	4.6	6.1	21	22	6	-	-	3	3	-	-	-	-	[1] June/Aug/Oct
Scombridae	*Acanthocybium solandri*	-	5.1	-	1	1	-	-	-	1	-	-	-	-	?
Scombridae	*Auxis* spp.	3.1	3.6	47	51	33	8	11	3	6	2	2	-	1	-
Scombridae	*Euthynnus alletteratus*	3.6	3.6	69	86	19	1	-	9	9	-	-	-	-	[1] June/Aug
Scombridae	*Katsuwonus pelamis*	3.2	3.0	12	8	14	3	2	4	2	2	1	-	-	?
Scombridae	*Sarda sarda*	-	6.1	-	1	1	-	-	-	1	-	-	-	-	?
Scombridae	*Scomber scombrus*	-	2.2	-	1	1	-	-	-	-	-	1	-	-	?
Scombridae	*Scomberomorus* spp.	2.0	-	5	-	3	1	-	2	-	-	-	-	-	-
Scombridae	*Scomberomorus cavalla*	3.0	2.7	19	25	18	-	-	7	9	2	-	-	-	[2] Aug/Sept
Scombridae	*Scomberomorus maculatus*	1.9	3.4	7	8	7	-	-	3	4	-	-	-	-	[2] Aug/Sept
Scombridae	Scombridae	1.9	2.2	136	12	30	8	-	9	11	2	-	-	-	-
Scombridae	*Thunnus* spp.	2.6	3.0	59	46	33	10	9	6	8	-	-	-	-	-
Scombridae	*Thunnus thynnus*	4.5	5.9	3	3	5	3	2	-	-	-	-	-	-	[3] May
Sciaenidae	*Bairdiella chrysoura*	1.6	-	1	-	1	-	-	1	-	-	-	-	-	[2] Apr-Aug
Sciaenidae	*Cynoscion* spp.	2.2	3.0	2	15	6	-	-	-	2	1	2	-	1	-
Sciaenidae	*Cynoscion arenarius*	1.9	3.6	34	19	17	-	-	4	4	5	3	-	1	[1] Aug
Sciaenidae	*Cynoscion nothus*	3.7	5.3	39	26	26	-	-	4	4	10	6	1	1	[1] Sept/Oct
Sciaenidae	*Larimus fasciatus*	2.5	2.6	52	41	38	1	-	4	4	15	12	2	-	[1]Oct
Sciaenidae	*Leiostomus xanthurus*	1.7	1.8	172	147	44	-	-	-	2	19	15	4	4	[1]Nov
Sciaenidae	*Menticirrhus* spp.	2.8	2.4	12	19	20	-	-	3	6	4	6	1	-	-
Sciaenidae	*Micropogonias undulatus*	2.6	2.7	365	368	68	-	-	-	1	29	31	3	4	[1] Oct-Dec
Sciaenidae	*Pareques* spp.	-	2.2	-	1	1	-	1	-	-	-	-	-	-	-
Sciaenidae	*Pogonias cromis*	1.9	-	3	-	2	2	-	-	-	-	-	-	-	[2] Feb-Apr
Sciaenidae	Sciaenidae	1.7	2.3	36	17	25	-	-	4	-	11	7	-	3	-
Sciaenidae	*Sciaenops ocellatus*	1.7	2.5	9	14	7	-	-	2	2	2	1	-	-	[2] Sept/Oct
Sciaenidae	*Stellifer lanceolatus*	3.6	3.7	11	14	6	-	-	1	1	1	2	-	1	?
Lutjanidae	Lutjanidae	2.3	2.2	144	151	57	9	6	19	14	1	7	1	-	-
Lutjanidae	*Lutjanus* spp.	3.2	3.0	28	24	17	1	1	7	8	-	-	-	-	-
Lutjanidae	*Lutjanus campechanus*	3.7	4.3	10	20	18	1	2	6	6	-	3	-	-	[4] July/Sept
Lutjanidae	*Lutjanus griseus*	3.5	4.4	4	8	8	-	1	2	5	-	-	-	-	[5] July/Aug
Lutjanidae	*Pristipomoides aquilonaris*	2.6	2.9	50	37	31	4	7	6	6	3	5	-	-	?
Lutjanidae	*Rhomboplites aurorubens*	4.5	4.8	29	35	32	-	3	7	10	7	2	1	2	[6] Aug/Sept

Table 4 notes on following page

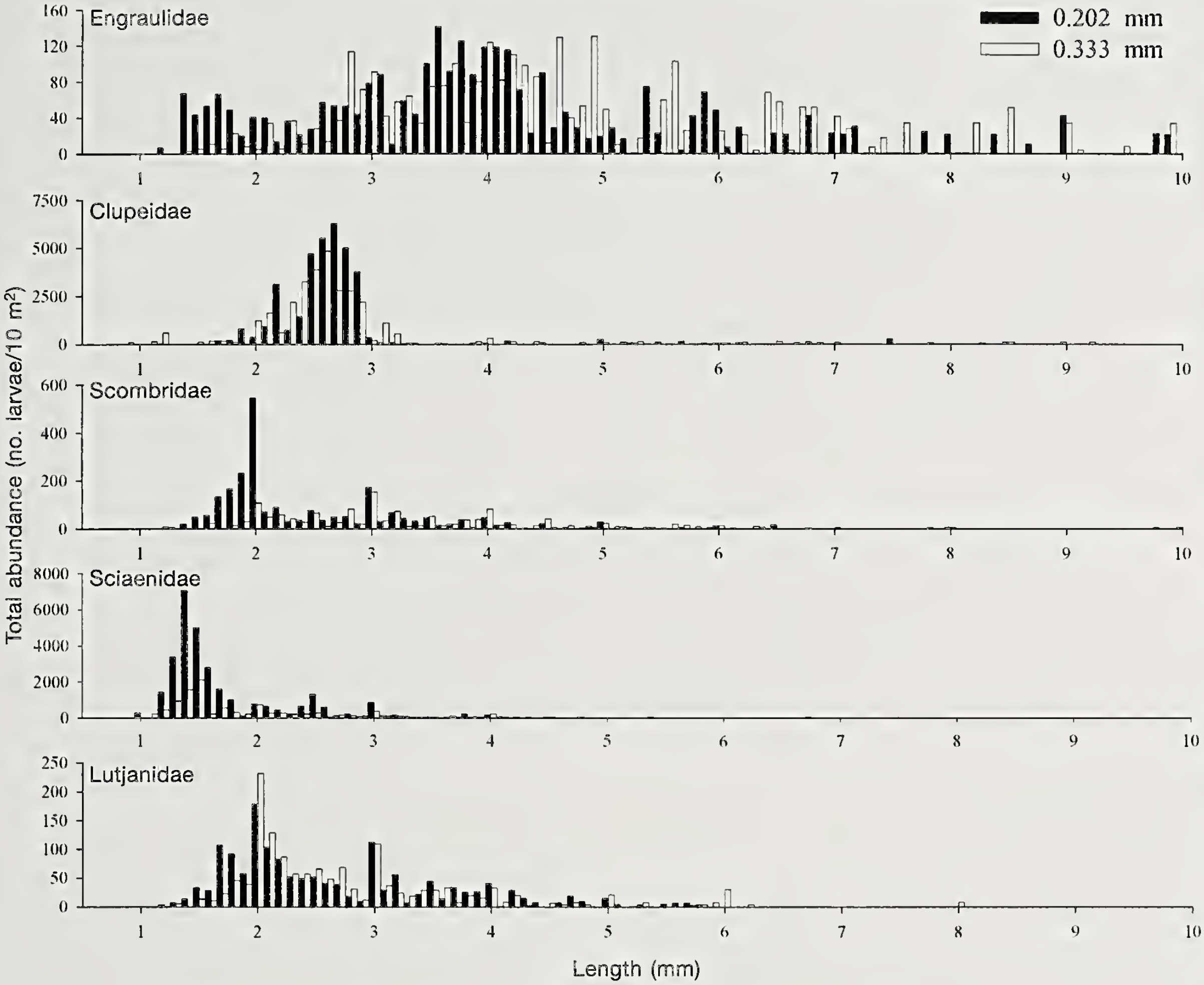

Figure 3

Length-frequency histograms of body length by total larval abundance in samples collected in the Gulf of Mexico during 2005–2007 with nets of 2 different mesh sizes (0.202 and 0.333 mm) for larvae of the 5 families targeted in this study: Engraulidae, Clupeidae, Scombridae, Sciaenidae, and Lutjanidae. Larval abundance was measured as the total number of larvae caught in a sample per the volume of water filtered during the tow multiplied by the maximum depth of the tow in meters and the factor 10 (total number of larvae under 10 m^2 of sea surface). Only larval lengths up to 10 mm are displayed in this figure.

Table 4 notes

---

[1] Hernandez, F. J., Jr., S. P. Powers, and W. M. Graham. 2010. Detailed examination of ichthyoplankton seasonality from a high-resolution time series in the northern Gulf of Mexico during 2004–2006. Trans. Am. Fish. Soc. 139:1511–1525. [Available from website.]

[2] Ditty, J. G., G. G. Zieske, and R. F. Shaw. 1988. Seasonality and depth distribution of larval fishes in the northern Gulf of Mexico above latitude 26°00′N. Fish. Bull. 86:811–823.

[3] Scott, G. P., S. C. Turner, B. Grimes, W. J. Richards, and E. B. Brothers. 1993. Indices of larval bluefin tuna, *Thunnus thynnus* , abundance in the Gulf of Mexico: modelling variability in growth, mortality, and gear selectivity. Bull. Mar. Sci. 53:912–929.

[4] Lyczkowski-Shultz, J., and D. S. Hanisko. 2007. A time series of observations on red snapper larvae from SEAMAP surveys 1982–2003: seasonal occurrence, distribution, abundance, and size. Am. Fish. Soc. Symp. 60:3–23.

[5] Domeier, M. L., C. Koenig, and F. Coleman. 1996. Reproductive biology of the gray snapper (*Lutjanus griseus*), with notes on spawning for other Western Atlantic snapper (Lutjanidae). *In* Biology, fisheries and culture of tropical groupers and snappers (F. Arreguín-Sánchez, J. L. Munro, M. C. Balgos, and D. Pauly, eds.), p. 189–201. ICLARM Conf. Proc. 48. [Available from website.]

[6] Lyczkowski-Shultz, J., and D. S. Hanisko. 2005. Review of the early life history of vermilion snapper, *Rhomboplites aurorubens*, with a summary of data from SEAMAP plankton surveys in the Gulf of Mexico: 1982–2002. Southeast Data, Assessment and Review SEDAR9-DW24, 42 p. [Available from website.]

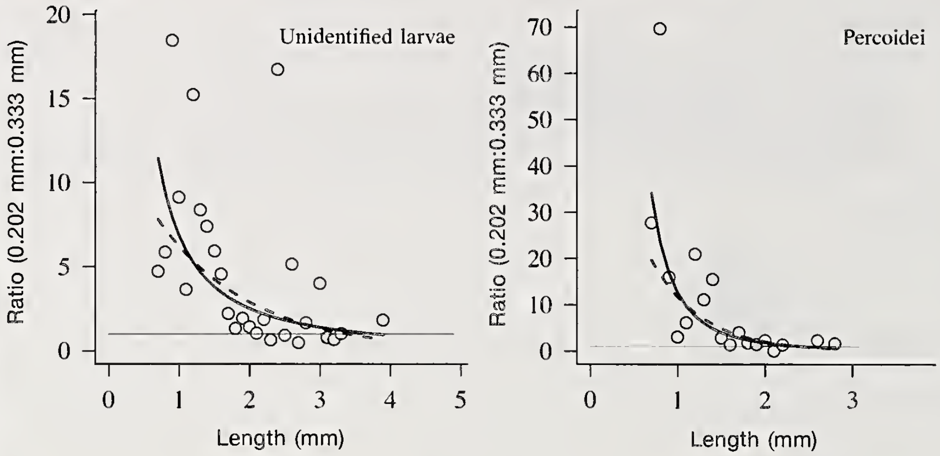

Figure 4

Ratios of larval abundance observed in nets with 0.202-mm mesh to larval abundance observed in nets with 0.333-mm mesh, by body length, for unidentified larvae and larvae of the suborder Percoidei. The solid and dashed lines represent modeled ratios of larval abundance that represent how many larvae were extruded from the coarser-mesh net (power and exponential functional relationships, respectively). The thin, horizontal line represents 1:1 ratios of total larval abundance or the point at which the finer- and coarser-mesh nets retained the same number of larvae at subsequent size classes.

bers in the net with 0.202-mm mesh than in the net with 0.333-mm mesh (Fig. 3).

The ratios of larval abundance collected with the finer net to larval abundance collected with the coarser net varied among the 6 taxa and unidentified group that were analyzed (Figs. 4 and 5). Although no pattern was seen regarding extrusion rates and body shape (perciform versus clupeiform), greater extrusion was suggested by the somewhat higher predicted abundance ratio of engraulid (clupeiform) larvae 1–2 mm in length compared with that of similar-size scombrid (perciform) and sciaenid (perciform) larvae. Extrusion for the categories of unidentified larvae and Percoidei was greater than for larvae identified to the family level. All abundance ratios for unidentified larvae, both observed and modeled, were greater than 1, indicating greater retention in the samples from the nets with a 0.202-mm mesh (Fig. 4). The greatest modeled abundance ratio for unidentified larvae was 11.4 for the 0.7-mm size class with the use of the power function. Modeled abundance ratios for the suborder Percoidei were above 1.0 for all sizes under 2.4 mm, and abundance ratios were as high as 34.0 and 17.0 for 0.7-mm larvae, with the power and exponential functions, respectively (Fig. 4). Modeled engraulid abundances were 4.0 and 1.9 times greater (power and exponential models, respectively) in samples from nets with 0.202-mm mesh than in samples from nets with 0.333-mm mesh for larvae at 1.2 mm (Fig. 5). Abundances of engraulid larvae in samples from nets with the different mesh sizes were equal for larvae at 4.7 mm for the power model and at 6.1 mm for the exponential model. Contrary to expectations, both the power and exponential models for Clupeidae indicated slight increases in abundance ratios with increasing size (Fig. 5). Abundance ratios were greatest at 10 mm, reaching 1.2 and 1.1 for the power and exponential models, respectively. Scombrid larvae at 1.2 mm were retained 3.1 (power model) to 2.2 (exponential model) times more in the samples from nets with a 0.202-mm mesh than in the samples from nets with a 0.333-mm mesh (Fig. 5). Larval abundances in both mesh sizes were higher at sizes between 4.1 and 4.5 mm. Sciaenid larvae appear to be extruded from 0.333-mm-mesh nets at sizes less than 5.5 mm (power model) and 5.1 mm (exponential model; Fig. 5). Sciaenid extrusion was greatest at the 1.0-mm size, and power and exponential models indicated that abundances were 3.1 and 2.5 greater in samples from nets with 0.202-mm mesh were than in samples from nets with 0.333-mm mesh, respectively (Fig. 5). Despite the high variability of abundance ratios for Lutjanidae (Fig. 5), both models projected greater abundances of larvae in the samples from nets with 0.202-mm mesh over all lengths. The power model for Lutjanidae reflected little overall change in abundance ratios by lengths, whereas the exponential model indicated slightly greater abundances in finer-mesh nets as larval lengths increased.

Coefficients derived from the models for both power and exponential functions are presented for use in future comparisons of sampling with bongo nets of differ-

Table 5

Parameters and the relative difference between the Akaike information criterion (ΔAIC) score from each model and that of the best fitting model within a group for unidentified larvae and larvae of 6 taxa: Percoidei, Engraulidae, Clupeidae, Scombridae, Sciaenidae, and Lutjanidae. The 2 models used were the power (*a*, *b*) and exponential (*d*, *f*) model.

	Parameters					
	Power		Exponential		ΔAIC	
Taxa	*a*	*b*	*d*	*f*	Power	Exponential
Unidentified	6.83	−1.44	13.29	−0.76	0	1
Percoidei	12.59	−2.80	66.26	−1.74	0	2.46
Engraulidae	4.79	−1.00	2.21	−0.13	0	8.04
Clupeidae	0.75	0.21	0.92	0.02	0	0.3
Scombridae	3.64	−0.90	2.96	−0.24	0	1.51
Sciaenidae	3.10	−0.66	3.15	−0.22	0	0.22
Lutjanidae	1.27	0.00	1.13	0.03	0.13	0

ent mesh sizes, 0.202 and 0.333 mm (Table 5). Among the 6 taxa and the unidentified group, extrusion was better described by using the power rather than the exponential model (Table 5). The difference between power and exponential model performance was greatest for Engraulidae, with the power model having the best fit. Differences in AIC scores obtained from the models, however, were relatively small for the unidentified group and all other taxa that were analyzed (ΔAIC<2.5), indicating that both functions are suitable for predicting extrusion rates for those taxa (Burnham and Anderson, 2002).

Discussion

Despite the wide range in observed larval abundance ratios among samples collected with the nets of different mesh sizes, functional relationships between predicted larval abundance and size indicated that small larvae were underrepresented in samples collected with a standard SEAMAP survey bongo net (0.333 mm). For smaller body lengths, predicted abundance ratios indicated that samples from the finer-mesh net contained up to 3–4 times the numbers of larval fish for 3 of 5 Gulf of Mexico fish families than samples from the coarser-mesh net. Observed abundance ratios indicated extrusion could be even higher, depending on the taxa. Underestimation of the smallest size category of sampled larvae was greatest for larvae that could not be identified to any taxonomic level or could be identified only to a suborder because the smallest larvae in the samples had not yet developed enough morphological characteristics that could be used for identifications to family level. Fish egg densities, however, did not differ significantly between the nets with 2 mesh types, suggesting that the standard SEAMAP survey net adequately samples fish eggs. This finding is not surprising because egg sizes of the analyzed taxa all exceeded the mesh size of the standard SEAMAP plankton net.

Differences in larval fish retention between 0.333-mm-mesh and 0.202-mm-mesh plankton nets were previously investigated in northern Gulf of Mexico waters by Comyns (1997) and Hernandez et al. (2011). Comyns (1997) found that red drum larvae in the smallest size group, 1.5–1.9 mm, were 5 to 8 times more abundant in the finer than in coarser mesh samples. Hernandez et al. (2011) found few to no significant differences among the taxa between the samples from nets with the 2 mesh sizes in either larval abundances or length frequencies. Mean size of larvae, however, was smaller in samples from the finer-mesh nets than in samples from the coarser-mesh nets for 4 groups: total fish larvae (all taxa combined, excluding unidentified larvae), Leptocephali and Syngnathidae (combined), Sciaenidae (the family that includes the red drum), and unidentified larvae. In the current study, mean standardized abundances varied significantly between samples from nets with the different mesh sizes for only 2 groups examined (unidentified larvae and Percoidei), whereas length-frequency distributions for all 6 taxa and the unidentified group that were examined were significantly different in samples taken with nets of the 2 mesh sizes.

Study design, sampling gear, and collection protocols used in these prior studies differed from each other and from the current study, as did results, making direct comparisons of the 3 studies problematic. Despite these differences, some useful inferences can be drawn regarding the influence of study design, sampling gear, and protocols on larval fish retention in comparisons of mesh sizes of nets. In the Comyns study, sampling was conducted only during the peak month of red drum spawning and consisted of collections taken in association with a subsurface current drogue, which

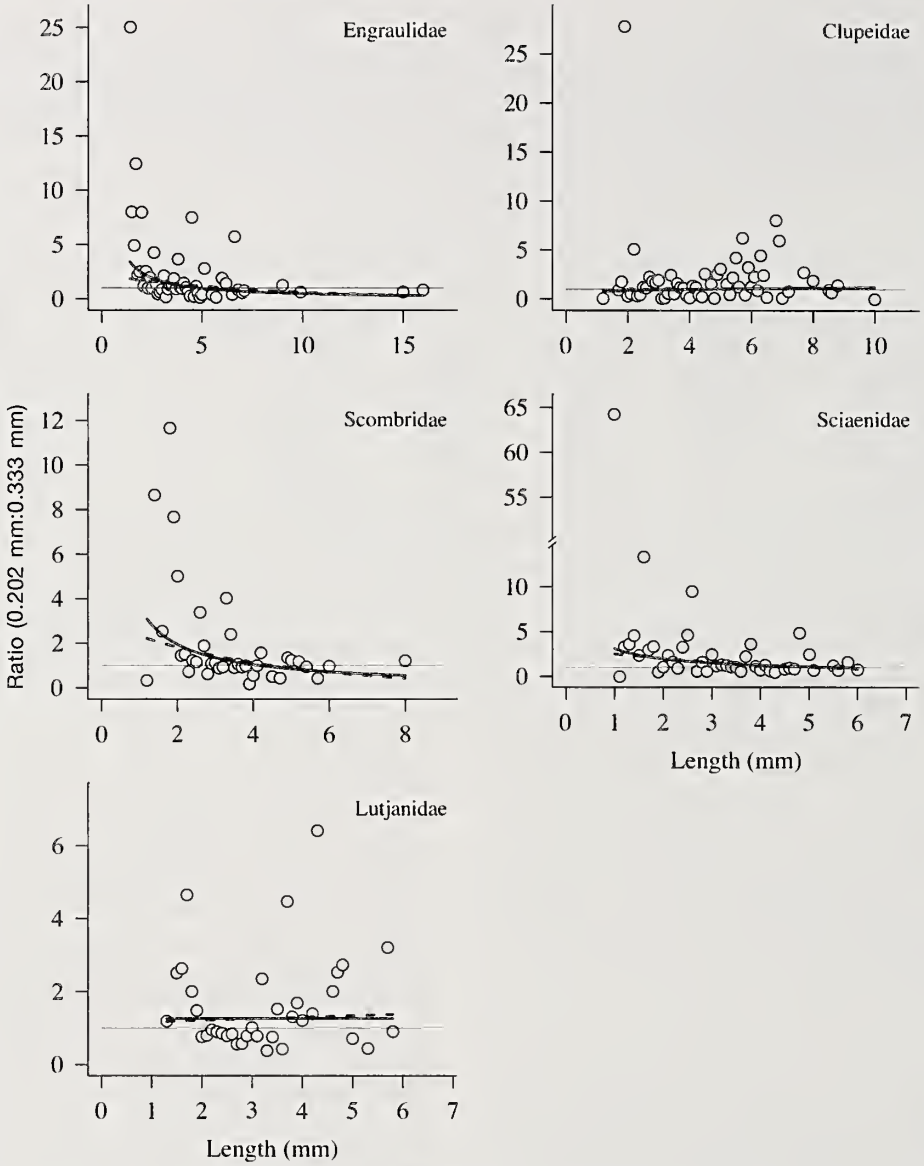

Figure 5

Ratios of larval abundance observed in nets with 0.202-mm mesh to larval abundance observed in nets with 0.333-mm mesh, by body length, for larvae of Engraulidae, Clupeidae, Scombridae, Sciaenidae, and Lutjanidae. The solid and dashed lines represent modeled ratios of larval abundance that represent how many larvae were extruded from the coarser-mesh net (power and exponential functional relationships, respectively). The thin, horizontal line represents 1:1 ratios of total larval abundance or the point at which the finer- and coarser-mesh nets retained the same number of larvae at subsequent size classes.

maximized sampling in the same patch of larvae over a period of hours (Lyczkowski-Shultz et al.[5]). However, in the Hernandez et al. (2011) and the current study, samples were collected without consideration of taxon-specific spawning seasons, and no attempt was made to remain in a defined water mass. The discrepancy in the findings for Sciaenidae between Comyns (1997) and Hernandez et al. (2011) was attributed by Hernandez et al. (2011) to gear differences—the larger mouth opening of the net and longer tow durations used by Comyns (1997) resulted in higher volumes of water filtered and subsequent greater numbers of larvae captured than in the Hernandez et al. (2011) study. Similarly, mean volume filtered in our study was less than that in the Comyns (1997) study, 170 m^3 and 256 m^3, respectively. Additionally, of the different gear used in the 3 studies, only the SEAMAP bongo frame allowed side-by-side towing and paired sample collection. These 'true' paired tows ensured that the nets sampled at the same location in the water column, at the same tow speed and ambient light level, and would, presumably, encounter the same assemblage of larvae. The arrangement of the nets used to gather plankton samples by Comyns (1997) and Hernandez et al. (2011) did not allow simultaneous sampling with different mesh sizes.

---

[5] Lyczkowski-Shultz, J., J. P. Steen Jr., and B. H. Comyns. 1988. Early life history of red drum (*Sciaenops ocellatus*) in the northcentral Gulf of Mexico. Miss.-Ala. Sea Grant Consort., Tech. Rep. MASGP-88-013, 126 p. [Available from website.]

Although the opportunistic nature of this study allowed the sampling of various regions and species in the Gulf of Mexico, directed sampling in months and locations of peak spawning for species of interest would have improved the probabilities of capturing greater numbers of smaller larvae, and increased the number of taxa within the target families that would have been 'available' for evaluating mesh retention. The importance of sampling with nets of different size during times of peak spawning when earliest stage larvae are most abundant was exemplified by the observed size distributions among sciaenid and scombrid larvae. Sampling with different mesh sizes coincided with reported months of peak spawning for 4 species of Sciaenidae and 5 species of Scombridae. A clear relationship between abundance ratios of the smallest sampled larvae and the mesh size of sampling nets was evident for those 2 families. This was the case even though scombrid larvae were the second least abundant of the target families. Although retention of small clupeid and lutjanid larvae was observed to differ between the paired samples collected with the nets with both mesh sizes and was supported by the significant difference in the length-frequency distributions of the 2 taxa, the modeled results for those taxa failed to indicate a substantial difference in abundance-at-size between the samples collected with the finer- and coarser-mesh nets. The lack of apparent difference between the nets with the 2 mesh sizes in size-related retention for those 2 families most likely resulted from the smallest larvae being unavailable to our plankton samplers because of a mismatch between sampling with these nets and the times, locations, and seasons of clupeid and lutjanid spawning (Fitzhugh et al.,[6]; Ditty et al., 2005; Hanisko et al., 2007).

Species-specific correction factors for larval abundance by body length in coarser mesh nets, generated from comparison studies of net meshes have been used to adjust larval abundances in order to mitigate bias caused by extrusion of the smallest size category of larvae in sampled assemblages (Lo, 1983; Houde and Lovdal, 1984; Somerton and Kobayashi, 1989). However, our study did not result in species-level comparisons of retention between the nets with different mesh sizes because of the problematic nature of morphology-based identification of fish larvae in waters of the U.S. Southeast (Richards, 2006; Fahay, 2007). Large abundance ratios for unidentified and percoid larvae in our samples highlight the effect of extrusion at the smallest sizes. Those 2 categories can represent a large portion of ichthyoplankton survey catches. In our study alone, the unidentified and percoid categories accounted for 9.1% of all specimens. Improved identification of smaller larvae with genetic procedures (Marancik et al., 2010) would provide more accurate estimates of total abundances of both eggs and larvae and aid in identifying true larval retention patterns by species. Although not at species-level, these models represent the first empirically derived approach to evaluating the degree of extrusion in SEAMAP ichthyoplankton samples.

Currently, SEAMAP larval indices are used as indicators of spawning stock biomass, not as direct estimates of biomass. Furthermore, these indices are calculated from the abundance of larger larvae that can be reliably identified to species by using established morphological features and that are of a size indicating full recruitment to the sampling gear. Including the size fraction of larvae that are underrepresented in SEAMAP samples collected in bongo nets with a 0.333-mm mesh could eventually lead to more realistic estimates of larval mortality and therefore more precise larval indices than those currently in use. Such an improvement in the reliability of a SEAMAP larval index was recently demonstrated when data on the abundance of small, genetically identified, early stage red snapper larvae were, for the first time, incorporated into the SEAMAP index (Pollack[7]).

Corrections for larval extrusion will also aid in better estimation of larval fish injuries and mortalities in future Gulf of Mexico damage assessments. Previously larval fish mortalities and subsequent production have been estimated in preparation of offshore liquefied natural gas developments (Gallaway et al., 2007) and as a result of the 2010 Deep Water Horizon oil spill (Muhling et al., 2012). Such estimates have been based on SEAMAP data for constructing baseline larval conditions for injury calculations (French McCay et al.[8]), however net efficiency issues with larval retention in the standard SEAMAP nets were simply noted.

---

[6] Fitzhugh, G. R., M. S. Duncan, L. A. Collins, W. T. Walling, and D. W. Oliver. 2004. Characterization of red snapper (*Lutjanus campechanus*) reproduction: for the 2004 Gulf of Mexico SEDAR. Southeast Data, Assessment and Review SEDAR7-DW-35, 27 p. [Available from website.]

[7] Pollack, A. G. 2015. Personal commun. Riverside Technology, Inc. Southeast Fish. Sci. Cent., Natl. Mar. Fish. Serv., NOAA, 3209 Frederic St., Pascagoula, MS 39568.

[8] French McCay, D., M. C. McManus, R. Balouskus, J. J. Rowe, M. Schroeder, A. Morandi, E. Bohaboy, and E. Graham. 2015. Technical Reports for Deepwater Horizon Water Column Injury Assessment—WC_TR.10: Evaluation of baseline densities for calculating direct injuries of aquatic biota dur-

The lack of taxa-specific information on extrusion has inhibited correcting larval abundances for previous damage claims (French McCay et al.[6]). Other injury assessments have assumed a single multiplier for all fish larvae abundances to correct for extrusion (Nielsen et al.[9])—an approach that our results indicate is an inadequate simplification.

Despite its shortcomings, our comparison study with nets of different mesh size provides the first estimates of size bias in SEAMAP ichthyoplankton sampling. Where previously the effect of extrusion on the smallest larvae in sampled assemblages was either ignored or approximated, the functional models presented here can be used to provide more accurate estimates of true larval fish abundances, and assessments of biological injuries due to industrial disasters. Extrusion-corrected larval abundance estimates could be used to improve the reliability of SEAMAP indices only after species-specific identification of the earliest and smallest larvae of species are attained. These species-level identifications could be achieved with more complete, traditional morphological descriptions of larval development and/or by incorporation of genetic identification methods in SEAMAP protocols that explicitly target problematic species.

Acknowledgments

For significant contributions to this work, we thank the Ichthyoplankton Group, Sea Fisheries Institute, Plankton Sorting and Identification Center, Szczecin and Gdynia, Poland; K. Williams and T. Cullins, collection managers at the SEAMAP Archiving Center, St. Petersburg, Florida; P. Bond, C. Cowan, G. Zapfe, D. Hanisko, NMFS Mississippi Laboratories, Pascagoula, Mississippi; and crews of the NOAA Ships *Oregon II* and *Gordon Gunter*. The manuscript benefited from discussion with A. Pollack, NMFS Mississippi Laboratories, Pascagoula.

Literature cited

Bolker, B. M.
2008. Ecological models and data in R, 396 p. Princeton Univ. Press, Princeton, NJ.

Burnham, K. P., and D. R. Anderson.
2002. Model selection and multimodel inference: a practical information-theoretic approach, 2nd ed., 488 p. Springer-Verlag, New York.

Colton, J. B., Jr., J. R. Green, R. R. Byron, and J. L. Frisella.
1980. Bongo net retention rates as effected by towing speed and mesh size. Can. J. Fish. Aquat. Sci. 37:606–623.

Comyns, B. H.
1997. Growth and mortality of fish larvae in the north-central Gulf of Mexico and implications to recruitment. Ph.D. diss., 150 p. Louisiana State Univ., Baton Rouge, LA.

Ditty, J. G., T. W. Farooqi, and R. F. Shaw.
2005. Clupeidae: sardines and herrings. *In* Early stages of Atlantic fishes: an identification guide for the western central Atlantic, vol. 1 (W. J. Richards, ed.), p. 73–99. Taylor & Francis Group, Boca Raton, FL.

Fahay, M. P.
2007. Early stages of fishes in the western north Atlantic Ocean (Davis Strait, southern Greenland and Flemish Cap to Cape Hatteras), vol. 1, 931 p. Northwest Atlantic Fish. Org., Dartmouth, Canada.

Gallaway, B. J., W. J. Gazey, J. G. Cole, and R. G. Fechhelm.
2007. Estimation of potential impacts from offshore liquefied natural gas terminals on red snapper and red drum fisheries in the Gulf of Mexico: an alternative approach. Trans. Am. Fish. Soc. 137:655–677.

Gledhill, C. T., and J. Lyczkowski-Shultz.
2000. Indices of larval kind mackerel (*Scomberomorus cavalla*) abundance in the Gulf of Mexico for use in population assessments. Fish. Bull. 98:684–691.

Hanisko, D. S., J. Lyczkowski-Shultz, and G. W. Ingram.
2007. Indices of larval red snapper occurrence and abundance for use in stock assessment. Am. Fish. Soc. Symp. 60:285–300.

Hernandez, F. J., Jr., L. Carassou, S. Muffleman, S. P. Powers, and W. M. Graham.
2011. Comparison of two plankton net mesh sizes for ichthyoplankton collection in the northern Gulf of Mexico. Fish. Res. 108:327–335.

Hjort, J.
1914. Fluctuations in the great fisheries of northern Europe viewed in the light of biological research. Rapp. p.-v. Reun. 20:1–228.

Houde, E. D., and J. A. Lovdal.
1984. Seasonality of occurrence, foods and food preferences of ichthyoplankton in Biscayne Bay, Florida. Est. Coast. Shelf Sci. 18:403–419.

Johnson, D. L., and W. W. Morse.
1994. Net extrusion of larval fish: correction factors for 0.333 mm versus 0.505 mm mesh bongo nets. NAFO Sci. Coun. Stud. 20:85–92.

Johnson, D. R., H. M. Perry, J. Lyczkowski-Shultz, and D. Hanisko.
2009. Red snapper larval transport in the northern Gulf of Mexico. Trans. Am. Fish. Soc. 138:458–470.

Llopiz, J. K., R. K. Cowen, M. J. Hauff, R. Ji, P. L. Munday, B. A. Muhling, M. A. Peck, D. E. Richardson, S. Sogard, and S. Sponaugle.
2014. Early life history and fisheries oceanography: new questions in a changing world. Oceanography 27(4):26–41.

Lo, N. C. H.
1983. Re-estimation of three parameters associated with anchovy egg and larval abundance: temperature dependent incubation time, yolk-sac growth rate and egg and larval retention in mesh nets. NOAA Tech. Memo. NMFS-TM-SWFC-31, 33 p.

---

ing the Deepwater Horizon oil spill, 122 p. RPS ASA, South Kingstown, RI.

[9] Nielsen, R. D., T. C. Ginn, L. M. Ziccardi, and P. D. Boehm. 2005. An evaluation of the approaches used to predict potential impacts of open loop LNG vaporization systems on fishery resources of the Gulf of Mexico, 62 p. Report prepared for The Center for Liquefied Natural Gas Seawater Usage Technology Committee. Exponent, Menlo Park, CA. [Available from website.]

Lyczkowski-Shultz, J., and D. S. Hanisko.
2007. A time series of observations on red snapper larvae from SEAMAP surveys 1982–2003: seasonal occurrence, distribution, abundance, and size. Am. Fish. Soc. Symp. 60:3–23.

Lyczkowski-Shultz, J., D. S. Hanisko, K. J. Sulak, M. Konieczna, and P. J. Bond.
2013. Characterization of ichthyoplankton in the northeastern Gulf of Mexico from SEAMAP plankton surveys, 1982–1999. Gulf Caribb. Res. 25:43–98.

Marancik, K. E., D. E. Richardson, J. Lyczkowski-Shultz, M. Konieczna, and R. K. Cowen.
2010. Evaluation of morphological characters to identify grouper (Serrandiae: Epinephelini) larvae in the Gulf of Mexico using genetically identified specimens. Bull. Mar. Sci. 86:571–624.

Marancik, K. E., D. E. Richardson, J. Lyczkowski-Shultz, R. K. Cowen, and M. Konieczna.
2012. Spatial and temporal distribution of grouper larvae (Serranidae: Epinephelinae: Epinephelini) in the Gulf of Mexico and Straits of Florida. Fish. Bull. 110:1–20.

McClatchie, S., J. Duffy-Anderson, J. C. Field, R. Goericke, D. Griffith, D. S. Hanisko, J. A. Hare, J. Lyczkowski-Shultz, W. T. Peterson, W. Watson, et al.
2014. Long time series in US fisheries oceanography. Oceanography 27(4):48–67.

Miller, J. M., and B. Y. Sumida.
1974. Development of eggs and larvae of *Caranx mate* (Carangidae). Fish. Bull. 72:497–514.

Morse, W. W.
1989. Catchability, growth, and mortality of larval fishes. Fish Bull. 87:417–446.

Muhling, B. A., M. A. Roffer, J. T. Lamkin, G. W. Ingram, Jr., M. A. Upton, G. Gawlikowski, F. Muller-Karger, S. Habtes, and W. J. Richards.
2012. Overlap between Atlantic bluefin tuna spawning grounds and observed Deepwater Horizon surface oil in the northern Gulf of Mexico. Mar. Pollut. Bull. 64:679–687.

R Core Team.
2016. R: a language and environment for statistical computing. R Foundation for Statistical Computing, Vienna, Austria. [Available from website, accessed July 2016.]

Rice, W. R.
1989. Analyzing tables of statistical tests. Evolution 43:223–225.

Richards, W. J. (ed.).
2006. Early stages of Atlantic fishes: an identification guide for the western central Atlantic, 2 vols. (set), 2591 p. Taylor & Francis Group, Boca Raton, FL.

Richardson, D. E., J. A. Hare, W. J. Overholtz, and D. L. Johnson.
2010. Development of long-term larval indices for Atlantic herring (*Clupea harengus*) on the northeast US continental shelf. ICES J. Mar. Sci. 67:617–627.

Scott, G. P., S. C. Turner, B. Grimes, W. J. Richards, and E. B. Brothers.
1993. Indices of larval bluefin tuna, *Thunnus thynnus*, abundance in the Gulf of Mexico; modelling variability in growth, mortality, and gear selectivity. Bull. Mar. Sci. 53:912–929.

Smith, P. E., and S. L. Richardson.
1977. Standard techniques for pelagic fish egg and larval surveys. FAO Fish. Tech. Pap. 175, 100 p. FAO, Rome.

Somerton, D. A., and D. R. Kobayashi.
1989. A method for correcting catches of fish larvae for the size selection of plankton nets. Fish. Bull. 87:447–455.

Theilacker, G. H.
1980. Changes in body measurements of larval northern anchovy, *Engraulis mordax*, and other fishes due to handling and preservation. Fish. Bull. 78:685–692.

Tranter, D. J. (ed.).
1968. Zooplankton sampling. Monogr. Oceanogr. Method. 2, 174 p. UNESCO, Paris.

National Marine
Fisheries Service
NOAA

Fishery Bulletin
established in 1881

Spencer F. Baird
First U.S. Commissioner
of Fisheries and founder
of Fishery Bulletin

A multiyear hierarchical Bayesian mark-recapture model incorporating data on recurring salmonid behavior to account for sparse or missing data

Bryce N. Oldemeyer (contact author)[1]
Timothy Copeland[2]
Brian P. Kennedy[3]

Email address for contact author: bryce@henrysfork.org

[1] Henry's Fork Foundation
801 Main Street
Ashton, Idaho 83420

[2] Idaho Department of Fish and Game
600 South Walnut Street
Boise, Idaho 83686

[3] Department of Fish and Wildlife Resources
University of Idaho
875 Perimeter Drive
Moscow, Idaho 83844

Abstract—Mark-recapture studies using data collected at rotary screw traps (RSTs) are used to estimate abundances of migrating juvenile salmonids exiting natal rearing habitats. Frequently, environmental conditions and mechanical failures decrease RST efficiencies, or completely halt operations, leading to sparse and missing data. In this study, we show how a time-stratified hierarchical Bayesian model framework can incorporate prior information to increase the accuracy and precision of estimates made with sparse and missing data. To do this, we incorporated annually recurring salmonid emigration characteristics into the model using multiple years of data. We compared abundance estimates of the hierarchical multiyear model with 3 single-year Bayesian models, using simulated and real RST data. The hierarchical multiyear model was as accurate and precise as the best model when data were complete and abundant, but outperformed other models when data were sparse and missing for multiweek blocks. For species with low abundances or low detection efficiencies, the hierarchical multiyear model used data from all years and recurring emigration characteristics to increase the accuracy and precision of estimates. This model is a valuable tool for fish and wildlife biologists who repeat mark-recapture studies annually and encounter sparse and missing data.

Manuscript submitted 5 January 2018.
Manuscript accepted: 10 May 2018.
Fish. Bull. 116:254–265 (2018)
Online publication date: 7 June 2018.
doi: 10.7755/FB.116.3-4.4

The views and opinions expressed or implied in this article are those of the author (or authors) and do not necessarily reflect the position of the National Marine Fisheries Service, NOAA.

To effectively manage free-ranging animals, information on survival rate, population growth rate, and recruitment are needed to understand factors influencing populations (Fryxell et al., 2014). It is often necessary to know abundances during various life stages to calculate this information but obtaining censuses of natural populations is difficult (Seber, 2002). Studies structured around sighting, capturing, or counting individuals and expanding these counts based on detection or sampling efficiencies are regularly implemented to estimate abundances when a census is not feasible (Nichols, 1992; Mill, 2007). These types of mark-recapture studies have broad application and have been used to estimate abundances of blue whales (*Balaenoptera musculus*) and humpback whales (*Megaptera novaeangliae*) (Calambokidis and Barlow, 2004), grizzly bears (Ursus *arctos*) (Mowat and Strobeck, 2000), herbivorous insects (Kareiva, 1983), and numerous other species so that marked individuals in the population can be detected during later sampling periods.

The Lincoln-Petersen model is foundational for estimating abundances using mark-recapture data where unmarked abundance, U, is estimated using the number of marked individuals in the population, n, the number of unmarked individuals counted or captured at a sampling event, u, and the number of marked individuals counted or captured at a sampling event, m:

$$U = n \cdot u \cdot m^{-1}. \qquad (1)$$

Lincoln–Petersen model assumptions can be difficult to satisfy, primarily the assumption of equal capture probability throughout a sampling period, necessitating modifications to the model. Commonly, mark-recapture studies occur continuously over time where individuals are marked, captured, and recaptured for several weeks or months. The accuracy of an abundance estimate obtained from pooling data relies on the assumption that capture probabilities are homogenous throughout the sampling period. Changes in the environment, species behavior, or sampling equipment can alter capture efficiencies, violating the assumption of homogenous capture probabilities and lead to biased abundance estimates. Sampling periods are often stratified temporally into smaller, more homogenous stratum for computation and later summed to minimize the violation of the capture probability assumption (Otis et al., 1978; Schwarz and Taylor, 1998). This stratification approach can be effective when sufficient data are available, but stratifying sparse data can lead to wide confidence intervals or estimation failure resulting from division by zero when individuals are not recaptured during a stratum (Seber, 2002).

When mark-recapture data are sparse or missing, hierarchical Bayesian models have proven to be an effective approach for obtaining abundance estimates (Mackey et al., 2008; Royle et al., 2011; Sethi and Tanner, 2013). The Bayesian paradigm provides a framework to incorporate prior biological knowledge into models by using hierarchal structures between parameters and by specifying informative prior distributions (Ellison, 2004). When prior biological information is available, structuring models to incorporate this information can produce more accurate and precise estimates (Royle and Dorazio, 2008). Mäntyniemi and Romakkaniemi (2002) implemented a hierarchical Bayesian model to estimate Atlantic salmon (*Salmo salar*) smolt abundances in the Conne River, Canada, and River Tornionjoki, in northern Scandinavia, while accounting for overdispersion associated with the species schooling behavior. Bonner and Schwarz (2011) increased the precision and accuracy of abundance estimates of Conne River Atlantic salmon smolts by parameterizing the expected abundances of smolts as a smooth function of time, using penalized Bayesian splines (P-splines) to address sparse data. These single-year models are effective with sparse data and short periods of missing data but fail to use or incorporate all the information available in long term monitoring data sets.

The goal of our study was to illustrate how a time-stratified hierarchical Bayesian model framework can incorporate prior years of information to increase the accuracy and precision of estimates made using sparse and missing data. To achieve this goal, we took a 2-step approach. First, we compared the performance of 3 Bayesian models that had within-year structures and 1 Bayesian model with a between-year hierarchical structure by using a simplified data set exhibiting various degrees of sparse and missing information roughly similar to real data. By using a simplified data set constructed from known parameters, we were able to quantify model performance by comparing the approximate posterior distributions produced by each model to the known parameters used to create the simplified data set. To illustrate how the concept works with real data, we then compare abundance estimates of the 4 models to 2 data sets, one set with complete and abundant data and another set with sparse and missing data. Covariates that were suspected to influence migration characteristics and juvenile abundances between years, e.g., seasonal hydrographic fluctuations and previous year counts of redds (nests dug by salmon in river beds), were excluded from both the data sets and model formulas in order to illustrate the basic concept and functionality of the competing models. After we compared the use and functionality of competing models, we discuss the various ways covariates could be included and how models could be extended to address more specific scenarios.

The model that used multiple years of data via the between-year hierarchical structure was able to bridge large periods of missing data (upwards of several weeks in some years) and sparse data by using the annually recurring emigration characteristics expressed by the species in the study, juvenile Chinook salmon (*Oncorhynchus tshawytscha*) in Idaho, to produce the most accurate and precise estimates. To our knowledge, this is the first time multiple years of data have been used to increase the robustness of abundance estimates calculated from sparse and missing mark-recapture data based on annually recurring behavioral characteristics.

Materials and methods

There are 2 primary components to our study. First, we compare estimates produced from 3 single-year Bayesian models and 1 hierarchical multiyear Bayesian model, using simulated scenarios reflective of missing and sparse data typical for monitoring with rotary screw traps (RSTs) in Idaho. To illustrate a proof of concept on how the structures of the Bayesian models function, models where simple (e.g., did not include environmental covariates or individual movement parameters) and data for simulated scenarios were not stochastic. Parameter estimates produced for the simplistic simulated data scenarios were compared with the known parameters used to create the simulated data to evaluate bias and precision for each of the models. Next, we demonstrate how models performed with real juvenile Chinook salmon data collected at Marsh Creek and Big Creek, Idaho, which reflect good and poor quality data sets. We used the full data record from the initial year of trap operation to 2014 to inform the estimates for the 2014 emigration.

Field sampling and data collections

Mark-recapture studies have been widely implemented to calculate anadromous juvenile salmonid abundances at RSTs (Zabel et al., 2005; Venditti et al.[1]; Copeland et al.[2]). Since 1990, over 150 RSTs have been deployed in the Columbia River basin. Many RSTs operating for more than 20 years (Pacific States Marine Fisheries Commission, Columbia Basin PIT Tag Information System, database available from website, accessed July 2015). Abundance estimates obtained from RST data are used to assess population productivity from the freshwater habitat and as the foundation for other life-cycle performance metrics (e.g., Venditti et al.[1]; Copeland et al., 2014). This demographic information is central for monitoring salmonid populations and is often used to inform conservation actions (Venditti et al.[1]; Copeland et al.[2]).

---

[1] Venditti, D. A., J. Flinders, R. Kinzer, C. Bretz, M. Corsi, B. Barnett, K. A. Apperson, and A. Teton. 2012. Idaho supplementation studies: brood year 2009 synthesis report, August 1, 2009–July 31, 2011. Idaho Dep. Fish Game Rep. 12-13, 24 p. [Available from website.]

Rotary screw traps are passively operating traps constructed of a partially submerged cone mounted to 2 pontoons (Johnson et al., 2007). The pontoons enable a RST to float while the cone funnels fish into a holding box located at the stern of the RST. Once fish are in the holding box, a helical twist within the cone prevents individuals from swimming upstream and out of the trap. When a RST is in operation, a trap tender removes captured fish from the holding box. Targeted individuals are anesthetized, inspected for tags, and length and weight data are recorded (Johnson et al., 2007). An allotted number of individuals are marked and released upstream of the RST (for a single trap design) or downstream (for a double-trap design) to be recaptured during proceeding days.

Rotary screw traps in Idaho typically operate from early March until freezing temperatures and frazil ice make them inoperable in November. The exact dates of RST installation and removal are dependent on yearly environmental conditions and sampling duration can vary by 1 or 2 weeks among years. Unexpected ice, high water, and RST mechanical failures can reduce trap efficiency or halt RST operations for several days to several weeks within a year. During these outages, it is assumed fish continue to pass the RST because this migratory behavior was observed during previous years. Most stream-type Chinook salmon in Idaho follow a recurring bimodal migratory pattern where the majority of a cohort begins emigration out of headwater rearing habitat in the fall and the remainder of the cohort emigrates in the spring (Bjornn, 1971, 1978).

Parameterization of time-stratified mark-recapture models

Data collection at RSTs consists of the daily number of unmarked and marked fish captured, and the number of marked fish released the day prior. Schwarz and Bonner[3] found that weekly stratification of RST mark-recapture data provided a sufficient balance between maintaining run characteristics while avoiding unnecessary data sparsity issues under the assumption that daily capture probabilities were similar within the week. Therefore, we opted to stratify year ($j=1,\ldots,t$) by ordinal week ($i=1,\ldots,s$). If capture probabilities were subject to high variability within a weekly stratum, stratum size could be decreased. For our model that used multiple years of data, the weekly stratification of the number of unmarked fish captured in the ith stratum in the jth year was denoted as u_{ij}, the number of marked fish released in the ith stratum in the jth year as n_{ij}, and the number of recaptured fish captured in the ith stratum in the jth year as m_{ij}. For the 3 models that used data from 1 year, symbol designation remained the same but the subscript denoting year, j, was removed.

The likelihood function of time-stratified mark-recapture models implemented in the Bayesian framework consisted of 2 primary components: the probability an individual was captured at the RST and the estimated number of unmarked individuals passing the RST. The numbers of individuals recaptured in a stratum, m_{ij}, were assumed to be binomially distributed by the number of marked individuals released upstream of the RST within the stratum, n_{ij}, and the probability that an individual passing the RST was captured, p_{ij}:

$$m_{ij} \sim Binomial(n_{ij}, p_{ij}). \tag{2}$$

Previous studies have modeled m_{ij} as a multinomial distribution incorporating an additional parameter describing the process of an individual's probability of being available for recapture during a later stratum (Mäntyniemi and Romakkaniemi, 2002; Bonner and Schwarz, 2011). We chose to exclude this parameter to simplify our models because >96% of juvenile Chinook salmon recaptured at RSTs in our study did so within the proceeding day of release. The likelihood of the model is complete when the number of unmarked individuals captured within a stratum, u_{ij}, is incorporated by using the binomial distribution:

$$u_{ij} \sim Binomial(U_{ij}, p_{ij}), \tag{3}$$

where U_{ij} = the estimated number of unmarked fish passing the RST during the stratum.

The assumptions of the time-stratified Lincoln–Petersen model are (Otis et al., 1978) as follows:

1 Individuals do not emigrate or die between marking and recapture;
2 Marks or tags are not shed;
3 Marks or tags are detected if present at recapture;
4 Marked and unmarked individuals within a stratum have the same probability of capture;
5 Individual movements within a stratum are independent; and
6 Individuals passing or being released below the RST are emigrating downstream and remain below the RST.

---

[2] Copeland, T., R. V. Roberts, B. N. Oldemeyer, and K. A. Apperson. 2013. Idaho steelhead monitoring and evaluation studies: annual progress report, January 1, 2012–December 31, 2012. Idaho Dep. Fish Game Rep. 13-07, 47 p. [Available from website.]

[3] Schwarz, C. J., and S. J. Bonner. 2012. An application of a Bayesian stratified-Petersen model to estimate the number of outgoing fish on the Cheakamus River, British Columbia. Simon Fraser Univ. Rep. 2012-02-22 . [Available from website.]

Model set

We compared 4 models by using the constructed likelihood components outlined above with different parameter structures. The most basic model, M_{PS} (pooled capture probability and simple abundance parameters), analyzed 1 year of data with a simple prior for U where $\log(U_i)$ shared identical normal priors with fixed mean and variance and where capture probability (p) was pooled, $p_i=p$ for $i=1,\ldots,s$ across all strata. The M_{PS} model structures are functionally similar to a pooled Lincoln-Petersen model in that p are structured to be pooled and constant across strata within the year and U is independent between strata.

The second model was similar to models used by Mäntyniemi and Romakkaniemi (2002), which allowed information about U and p to be shared among strata within the year, and is denoted M_{HW} (hierarchical within-year parameter structure). This model contained a hierarchical structure that assigned both U and p, $\log(U_i)$ and $\text{logit}(p_i)$, normal priors with common mean and variance within the year. The M_{HW} hierarchical structures allow information about U and p to be shared across all strata within a single year.

The third model is structured from Bonner and Schwarz (2011) and uses the P-spline hierarchical prior for U to smooth estimates between adjacent strata, localizing the sharing of information between adjacent strata within the year, and is denoted M_{SPLINE}. A hierarchical structure for p assigned $\text{logit}(p_i)$ normal priors, with common but unknown mean and variance within the year, was used for the M_{SPLINE} model. The M_{SPLINE} hierarchical structures allows information about p to be shared among strata throughout the year but uses the temporal ordering of strata within the year to give greater weight to adjacent strata for sharing information in regards to U. Following the recommendations of Lang and Brezger (2004) and Schwarz and Bonner,[3] we placed knot points evenly across strata at 4-week intervals. These authors found that this spacing was a suitable compromise between spline overfitting and sharing information among strata. We chose to exclude the additional parameter used to model the probability that an individual is available for recapture in proceeding strata as explained above.

The hierarchical multiyear (between-year) model, M_{HB}, allows information from the same temporal period among years to be shared in regard to p and U. M_{HB} contains a hierarchical structure for U and p, where $\log(U_{ij})$ and $\text{logit}(p_{ij})$ have a common mean within strata of the same ordinal time period between years. By structuring the hierarchy between years, recurring run characteristics specific to each stratum (ordinal week for this study) were integrated into the model.

Selection of prior distributions for the highest level of the model hierarchies was chosen to be vague and weakly informative in regard to their parameters and to be identical to prior distributions used in previous research when applicable. Prior distributions selected also aligned with expert knowledge of and experience with RSTs. For instance, capture probabilities at RSTs rarely exceed 0.5 and often average 0.1–0.2 depending on the trap location and time of year. The prior distributions selected for the hyperparameters of each capture probability for each model had a median of roughly 0.1 and 95th percentiles from 0.0 to 0.5. Additionally, prior distributions for the hyperparameters of each abundance parameter have a median abundance of roughly 22,000 with 95th percentiles from 814 to 583,381, with the exception of the M_{SPLINE} model that uses hyperparameters implemented by Bonner and Schwarz (2011). Complete structures for all models can be found in Supplementary Table 1 and Supplementary Figures 1–4 (online only).

Test data sets

A simplified data set roughly similar to RST data found in Idaho was created with known U and p parameters. The simulated data set used for the scenarios spanned 10 years ($j=10$) with 35 strata per year ($i=35$). This scheme roughly corresponds to the early spring transition in mid-March and the late fall transition in mid-November. The migration of juvenile Chinook salmon in Idaho typically has 2 pulses, one in the spring and one in the fall; therefore, parameters U_{ij} followed a smooth bimodal run with a small peak at strata 6 (mid-May) and the majority of the individuals centered on a peak at stratum 29 (late September). Parameters p_{ij} were constant at 0.333 for strata 1–4 and 13–35, and constant at 0.111 for strata 5–12. As discharge increases in the spring, RSTs are often relocated out of the thalweg to slower portions of the river transect to avoid woody debris and decrease mechanical stress on the sampling equipment. In addition, as discharge increases, the relative amount of water sampled by RSTs decreases. These conditions often decrease trap efficiencies and are the justification for the decreased capture efficiencies for strata 5–12 in our simulated data. The number of marked individuals, n_{ij}, released in each stratum was equivalent to the number of unmarked individuals captured, u_{ij}, up to 50 individuals. The restriction to 50 individual was implemented to mimic tag and handling permit constraints that are common when dealing with threatened or fragile species at RSTs. Total yearly abundance summed over all 35 stratum was 23,477.

This data set was modified to simulate realistic occurrence of sparse and missing data. The scenario using data produced from the parameters listed above was denoted as “full” owing to the completeness across strata and years and was the initial scenario in our simulation study used for subsequent modification. The second scenario is identical to the full scenario with the exception of information from strata 5–8 in the first year being removed. This 4-stratum exclusion mimicked RST conditions when spring flows halt RST operations for several weeks. The third scenario had information from strata 5–8 removed from the first year in addition to reducing the number of marked and recaptured individuals by 60% across all strata and years. The 60% reduction typifies data for several RSTs that have low numbers of marked and recaptured fish because of site limitations or low abundances. The fourth scenario had information from 8 strata, strata 12–19, removed from the first year of the data set and had a 60% reduction across all marked and recaptured individuals across all strata and years. This modification emulates several RSTs that did not operate during summer months initially because it was thought that salmonid migration had ceased during this time period (see history of the Marsh Creek data set below). It was later realized that small, but significant, numbers of individuals did migrate throughout the summer and RSTs now operate during this time period. Simulated scenarios and known parameters used to create the data are presented in Supplementary Table 2 and Supplementary Figures 5–8 (online only). Each model was tested with these 4 scenarios.

We illustrate the relative performance of the 4 competing models, using 2 RST data sets. Marsh Creek and Big Creek are tributaries to the Middle Fork of the Salmon River located in central Idaho, have comparable salmon populations, but have “good” and “poor” quality data sets, respectively.

Marsh Creek is a third-order tributary with a RST located at a river transect that has geographic and hydrographic features conducive to continuous operation throughout the majority of the migratory season with high capture efficiencies (Venditti et al.[1]). In addition, the RST has been operating for 21 years. Median day of installation is March 20 and removal is November 3. Within this period, the RST operates a median of 97% of the days. Gaps in operations are typically short for reasons such as icing and passing thunderstorms. During the first few years of operations, the RST was removed during the summer for 2.5 months until it was discovered that fish emigrated in that time period, too. This gap in the record motivated the fourth scenario in the simulations described above. Annual total catch of Chinook salmon has fluctuated more than 2 orders of magnitude from 846 to 91,719 fish. The high capture efficiencies, abundant amount of juvenile salmonids captured, and longevity of RST operation present a nearly ideal RST mark-recapture data set (Suppl. Fig. 9) (online only).

Big Creek, in comparison, is a fourth-order tributary located in the Frank Church River of No Return Wilderness. The RST was first installed in 2007 in a reach with widths from 30 to 40 m, resulting in low capture efficiencies (Copeland et al.[2]). Trap efficiencies are much lower than those seen in Marsh Creek and can be quite variable (Suppl. Fig. 10) (online only). Annual total catch of Chinook salmon has fluctuated from 5167 to 33,308 fish. Median day of installation is March 11 and removal is November 10. Within this period, the RST operates a median of 80% of the days. There are frequent short gaps in operations for reasons such as icing and thunderstorms that produce concomitant turbidity and debris. In addition, there are substantial gaps in operations during snowmelt. For example, adding up gaps in service >7 days, the RST missed a median of 55 days in mid to late spring, ranging from 20 to 75 days. The exception was 2007, the first year of operation, but the RST was not installed until May 21. The Big Creek RST data exemplifies nearly all potential pitfalls possible at RSTs in terms of sparse and missing data. Scenarios like those at the Big Creek RST are what motivated this study.

We focused on the results for the 2014 emigration year. During 2014, the Marsh Creek RST was deployed on March 22, 1 week later than the earliest date the trap had been deployed in its 21 years of operation. In 2014, the Marsh Creek RST ran continuously with high capture and recapture efficiencies throughout the trapping season and was removed on October 31 when snow and ice prevented operation. In total during 2014, the Marsh Creek RST missed 3 weeks of the trapping season at the tail ends when few fish were suspected to be migrating. In 2014, the Big Creek RST was deployed on March 13 and operated for roughly 5 weeks before high water prevented the RST from operating from April 11 to June 13. On June 14, the trap was redeployed and ran continuously until snow and ice prevented operation on November 9. During the 8-week outage, it was known that age-1 Chinook salmon overwintering in upper portions of Big Creek migrated out of the system during this time because this behavior had been observed in past years and at other RSTs in Idaho. In addition, when the Big Creek RST was operating, RST capture and recapture efficiencies where low owing to the site limitations described above. The Marsh Creek and Big Creek RST operations in 2014 exemplify the 1) complete and abundant mark-recapture data and 2) sparse and missing mark-recapture data.

Model implementation

All models were implemented with the statistical program JAGS (vers. 4.0.0; Plummer, 2003) run through the program R interface, vers. 3.2.2 (R Core Team, 2015) with the R2jags package vers. 0.5-7 (Su and Yajima, 2015). The complexity of the models inhibited calculating an exact posterior distribution. As such, Markov chain Monte Carlo (MCMC) simulations were implemented in JAGS to sample from the joint posterior distributions of all parameters to approximate a posterior distribution. Three parallel chains initiated at random values were run for each model. Chains were run for a total of 500,000 iterations and the first 100,000 iterations were discarded and the remaining iterations were thinned by a factor of 100. The final sample size for each chain comprised 4000 values. MCMC posterior distributions were visually inspected for multiple peaks and Gelman–Rubin test statistics were calculated to ensure chain convergence. Multiple peaks in the posterior distribution or Gelman–Rubin test statistics >1.1 were subject to nonconvergence and chains were run for additional iterations to try to achieve convergence.

Model performance was evaluated by comparing the median parameter estimates produced for the first year of each scenario to the known parameters used to simulate the data. Estimated median values and credible interval characteristics of posterior parameter distributions were examined to assess strata-specific and total yearly abundance estimates. Total yearly abundance estimates and corresponding credible intervals were calculated by randomly sampling one value from the posterior abundance distribution each unique stratum for the first year of the scenario. The number of unique values is dependent on how many strata are in the year—35 for this simulation. Summing these values and reiterating the random sampling procedure 50,000 times creates a total yearly abundance distribution, $\hat{U}_{\mathrm{Tot}}$. Yearly model bias was measured by the difference of $\hat{U}_{\mathrm{Tot}}$ from the known U_{Tot}. Strata-specific accuracy was judged on the number of strata that included the known abundance parameter within the predicted 95% credible intervals. For abundance estimates produced for the 2 real data sets, point estimates and credible interval widths were used to evaluate relative performance among the models. To imitate a naive Lincoln–Peterson estimator, the M_{PS} posterior parameter distributions had portions removed that corresponded to strata missing data.

Results

Simulation and scenarios

Markov chains converged for all models and produced representative posterior distributions for parameters with the exception of the M_{PS} model. The M_{PS} model had Gelman-Rubin test statistics >1.1 and density plots with multiple peaks for posterior distributions when strata were missing data. The M_{PS} model relied primarily on the vague prior U parameter distributions to construct posterior distributions when data were missing and MCMC required additional iterations (100,000) to converge around the highest density sample space and achieve Gelman–Rubin test statistics <1.1. The posterior U distributions obtained from missing strata by using the M_{PS} model were largely the product of the prior U distribution and added little relevant biological information to the study, and therefore these strata were removed from the analysis. This exclusion of strata is also illustrative of typical Lincoln–Petersen model performance in that strata without data are excluded from total abundance estimates even if fish are known to be migrating.

The pooled probability model, M_{PS}, produced the most precise yearly abundance estimates from the simulated scenarios with credible interval widths between 5–9% of the $\hat{U}_{\mathrm{Tot}}$ (Table 1). The M_{PS} precision is misleading in that the uncertainty associated with the stratum missing data was excluded from the total yearly abundance estimate. In addition, the precision of the MPS model is dependent on the assumption that capture probabilities are constant across all strata, which was not true. The inflated precision of the M_{PS} model also caused known parameters to be excluded from strata-specific 95% credible intervals and to result in M_{PS} having the worst strata-specific coverage. The M_{PS} model overestimated $\hat{U}_{\mathrm{Tot}}$ by 2467 individuals (10.4%) for the full scenario. In subsequent scenarios, total yearly abundance estimates became less biased as strata were removed and data were reduced. By removing strata missing data, the M_{PS} model $\hat{U}_{\mathrm{Tot}}$ should theoretically become negatively biased by 2093 individuals (8.9%) when missing 4 strata in the spring and by 1200 individuals (5.1%) when missing 8 strata in the summer. In these scenarios, the nature of the pooled capture probabilities overestimating $\hat{U}_{\mathrm{Tot}}$ offset the negative bias incurred from removing strata with missing data.

The M_{HW} and $\mathrm{M}_{\mathrm{SPLINE}}$ models performed better than M_{PS} when addressing sparse and missing data (Table 1). The M_{HW} model had a credible interval width of 13% for the full data scenario with a bias of 543 individuals (2.3%). As data were reduced and removed, bias increased up to 7064 individuals (30.0%) and the percent credible interval width increased up to 63%. The hierarchical structure of the M_{HW} model integrated information from the entirety of the year, causing additional variability to be incorporated into the posterior distributions, particularly for strata missing data. Similar to the M_{HW} model, the $\mathrm{M}_{\mathrm{SPLINE}}$ model used information from throughout the year to inform strata with sparse and missing data but implemented a P-spline function to localize interpolation of abundance estimates to adjacent strata. This process reduced the variability of posterior parameter distributions for strata with sparse and missing data and produced abundance estimates that were biased from −818 individuals (−3.5%) to 516 individuals (2.2%) with credible interval widths that were 18–23% that of $\hat{U}_{\mathrm{Tot}}$. The predetermined spline characteristics prevented the $\mathrm{M}_{\mathrm{SPLINE}}$ model from producing estimates for periods missing >4 consecutive strata. The M_{HW} and $\mathrm{M}_{\mathrm{SPLINE}}$ model had comparable numbers of strata-specific 95% credible interval bounds that included known abundance parameters but the credible interval bounds with the $\mathrm{M}_{\mathrm{SPLINE}}$ model were more precise.

The M_{HB} model had the most accurate U_{Tot} estimates in 3 scenarios and the second smallest credible interval widths (Table 1). Strata-specific credible intervals produced by the M_{HB} model where the only credible intervals to encompass the known parameters for each strata in every scenario. As the quality of simulated data sets decreased, the hierarchical multiyear structure was able to draw inferences from previous years to supplement the missing and sparse data. This procedure allowed model M_{HB} to produce the most accurate estimates with missing data.

Application of models to Marsh Creek and Big Creek data

Total population estimates for Marsh Creek during 2014 were similar among the models, although confi-

Table 1

For the simulated data scenario produced by 4 competing models, total yearly abundance estimates ($\hat{U}_{Tot}$) for juvenile Chinook salmon (*Oncorhynchus tshawytscha*) in Idaho, bias from true U_{Tot} (23,527 individuals), 95% credible intervals (CIs), credible interval width in relation to the total yearly abundance estimate as a percentage (% CI width), and the percentages of temporal strata with 95% CI bounds that covered the true value of unmarked abundance (Strata coverage %). The M_{PS} model structure includes pooled capture probability and simple abundance parameters, the M_{HW} model has a hierarchical within-year parameter structure, and the M_{SPLINE} model uses a P-spline hierarchical prior for unmarked abundance. The hierarchical multiyear M_{HB} model allows information about capture probability and abundance parameters during the same temporal period to be shared among years. Data scenarios may have excluded data for 4 or 8 temporal strata and may have reduced the number of marked and recaptured individuals by 60% across all strata. Because of predetermined P-spline knot characteristics, the M_{SPLINE} model was not able to produce estimates for data missing 8 strata.

Models	Data scenario	$\hat{U}_{Tot}$	Bias	95% CI	% CI width	% coverage of strata
M_{PS}	Full	25,944	2467	(25,214, 26,685)	6	34.3
	4 strata[1]	23,059	–418	(22,455, 23,682)	5	77.1
	4 strata 60% reduction†	24,205	728	(23,351, 25,163)	7	85.7
	8 strata 60% reduction†	26,640	3163	(25,528, 27,841)	9	31.4
M_{HW}	Full	24,020	543	(22,484, 25,717)	13	0.8
	4 strata	24,492	1015	(22,412, 35,035)	52	88.6
	4 strata 60% reduction	23,934	457	(21,771, 34,895)	55	88.6
	8 strata 60% reduction	30,541	7064	(25,780, 45,167)	63	82.9
M_{SPLINE}	Full	23,993	516	(21,939, 26,298)	18	82.9
	4 strata	22,659	–818	(20,955, 24,586)	16	77.1
	4 strata 60% reduction	22,697	–780	(20,401, 25,606)	23	77.1
	8 strata 60% reduction	–	–	–	–	–
M_{HB}	Full	23,245	–232	(22,538, 23,976)	6	100
	4 strata	23,216	–261	(22,517, 23,968)	6	100
	4 strata 60% reduction	22,509	–968	(21,536, 23,594)	9	100
	8 strata 60% reduction	22,552	–925	(21,534, 23,698)	10	100

[1] Posterior parameter distributions for strata that were missing data were removed from the analysis to simulate a naive Lincoln–Peterson estimator.

Table 2

Total abundance estimate ($\hat{U}_{Tot}$), 95% credible intervals (CIs), absolute CI width, and percent CI width for rotary screw trap mark-recapture data collected for juvenile Chinook salmon (*Oncorhynchus tshawytscha*) at Marsh Creek and Big Creek, Idaho, in 2014 from the pooled-simple (M_{PS}), hierarchical within-year (M_{HW}), hierarchical penalized-spline (M_{SPLINE}), and hierarchical multiyear (M_{HB}) models.

Model	$\hat{U}_{Tot}$	95% CI	CI width	% CI width
Marsh Creek				
M_{PS}[1]	104,594	(103,149, 106,064)	2915	3
M_{HW}	121,718	(110,295, 208,526)	98,231	81
M_{SPLINE}	112,299	(105,910, 120,212)	14,302	13
M_{HB}	114,035	(106,991, 123,920)	16,929	15
Big Creek				
M_{PS}†	106,141	(101,856, 104,729)	2873	3
M_{HW}	216,292	(154,931, 584,029)	425,498	197
M_{SPLINE}	NA	NA	NA	NA
M_{HB}	148,110	(119,758, 239,889)	120,131	81

[1] Posterior parameter distributions for temporal strata that were missing data were removed from the analysis.

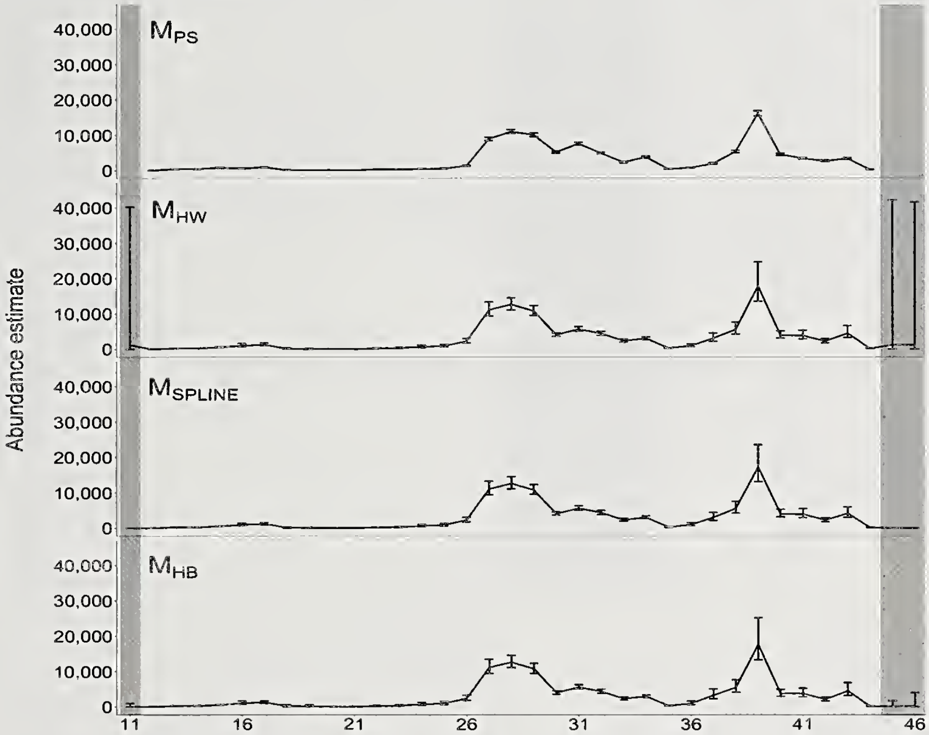

Figure 1

Abundance of juvenile Chinook salmon (*Oncorhynchus tshawytscha*) emigrating downstream during 2014 by ordinal week, estimated by using 4 competing models with data collected at a rotary screw trap deployed in Marsh Creek, Idaho, in 2014. The 4 models are the pooled-simple (M_{PS}), hierarchical within-year (M_{HW}), hierarchical penalized-spline (M_{SPLINE}), and hierarchical multiyear (M_{HB}) models. Gray regions denote estimates produced for temporal strata with missing data in 2014.

dence intervals did not overlap for all (Table 2). The M_{PS} model estimated total population abundance at levels 8000–17,000 fish less than the 3 other models but had the smallest 95% credible interval width. The total population abundance estimate for M_{PS} excluded potential fish migrating in ordinal weeks 11, 45, and 46 (Fig. 1). In addition, the precision of M_{PS} model estimates rely on the assumption that capture probabilities are constant across all weeks throughout the year and this condition is not likely satisfied because of fluctuating environmental and biological conditions. The M_{HW} model had the largest credible interval width that was nearly as large as the total population abundance estimate. Most of the uncertainty around the total population abundance estimate was acquired from strata with missing data at the beginning and end of the year. Posterior distributions for strata missing data using the M_{HW} model relied on capture probabilities and abundance characteristics from strata across the entire sample season. Models M_{HB} and M_{SPLINE} had similar total population estimates but the M_{HB} model produced 95% credible intervals wider by roughly 2500 individuals.

In contrast to estimates for Marsh Creek, total population estimates for Big Creek for 2014 varied greatly among models (Table 2). The M_{PS} model estimated total population abundances using 28 out of the 37 strata owing to the removal of strata missing data (Fig. 2). As with results for Marsh Creek, the precision associated with the total population estimate for the M_{PS} model is dependent on the assumption of homogeneous capture probabilities throughout the year and is likely overstated in this application. The population estimate produced by the MHW model was 216,291 fish with a credible interval width nearly double the median estimate. The variability of abundance estimates and capture probabilities throughout the year at Big Creek increased the uncertainty associated with estimates for missing data from the M_{HW} model. The M_{SPLINE} model was not able to run because of the large number of consecutive strata missing data. The M_{HB} model produced a $\hat{U}_{Tot}$ of 148,110 individuals with a 95% credible interval width of 120,131 fish.

To illustrate how the M_{HB} model used past data to inform the 2014 estimates at the Big Creek RST during the missing strata, we show *u*, *m*, and *n* from the

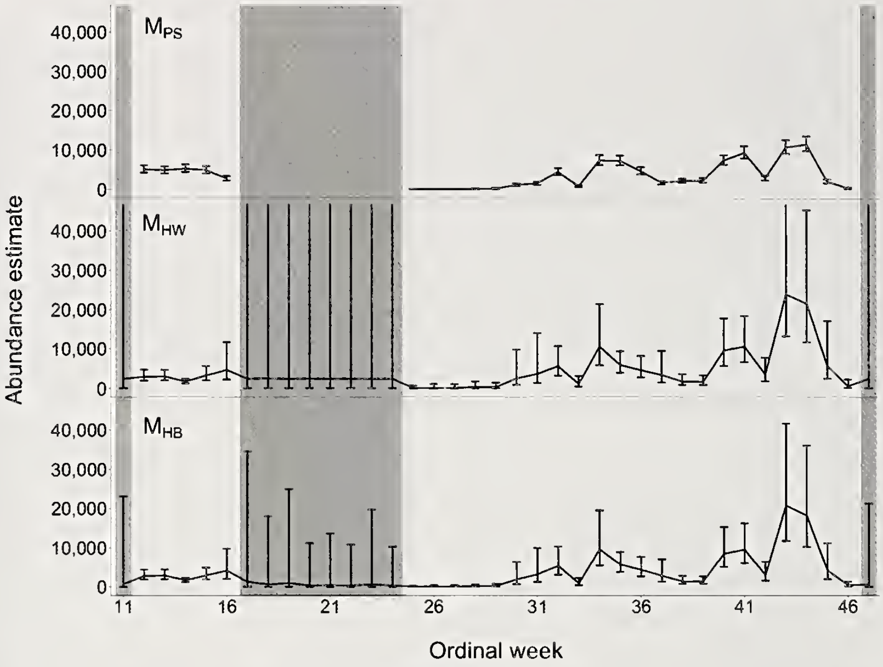

Figure 2

Abundance of juvenile Chinook salmon (*Oncorhynchus tshawytscha*) emigrating downstream during 2014 by ordinal week, estimated by using 3 competing models with data collected at a rotary screw trap for Big Creek, Idaho, in 2014. The 3 models are the pooled-simple (M_{PS}), hierarchical within-year (M_{HW}), and hierarchical multiyear (M_{HB}) models. A fourth model, the hierarchical penalized-spline M_{SPLINE} model, was unable to run and is not displayed. Gray regions denote estimates produced for temporal strata with missing data in 2014.

past record during the spring (Fig. 3). Spring peaks in catch varied in both timing and magnitude. Capture probabilities were variable but usually <0.10. Most gaps in operations start on the descending limb of the catch. These features influenced the 2014 estimates for weeks 17–19 such that the variable peak catches from the past record cause broad 95% credible intervals (Fig. 2). There were less past data after those strata but catches were not as variable; hence 95% credible intervals for strata 20–24 are not as wide. Note, however, that there were some data in every stratum in the past record and the M_{HB} model was able to use that information to estimate abundance with a precision measure during strata 17–24 in 2014. Because the past record is thin during these periods, the M_{HB} model estimate incorporates that uncertainty in the form of wide credible intervals.

Discussion

To our knowledge, this is the first time a hierarchical Bayesian model has been structured to incorporate data on annually recurring species behavior by using multiple years of data to improve abundance estimates from sparse and missing mark-recapture data. In the simulation, the hierarchical multiyear model produced comparable estimates to those of the best model when data were complete but also produced the most accurate and precise estimates when large periods of data were missing or reduced. Because the hierarchical multiyear model can incorporate information about recurring species behavior to improve the accuracy of abundance estimation, it can be applied beyond salmonids. Studies focused on species that express recurring behavior, particularly for species with low abundances, could benefit from similar hierarchical multiyear models to increase the accuracy and precision of abundance estimates obtained from sparse and missing mark-recapture data.

Current Lincoln–Petersen estimator approaches used for juvenile salmonids abundance estimation do not provide an effective method for addressing sparse or missing data. When strata have low numbers of recaptured individuals (less than 7), confidence intervals obtained from bootstrap approaches are largely uninformative (Steinhorst et al., 2004). Manual pooling, or the use of software that attempts to optimize the balance between satisfying model assumptions while maintaining fine-resolution run characteristics (e.g., Darroch analysis with rank reduction; Bjorkstedt[4]), of-

---

[4] Bjorkstedt, E. P. 2000. DARR (Darroch analysis with rank-reduction): a method for analysis of stratified mark-

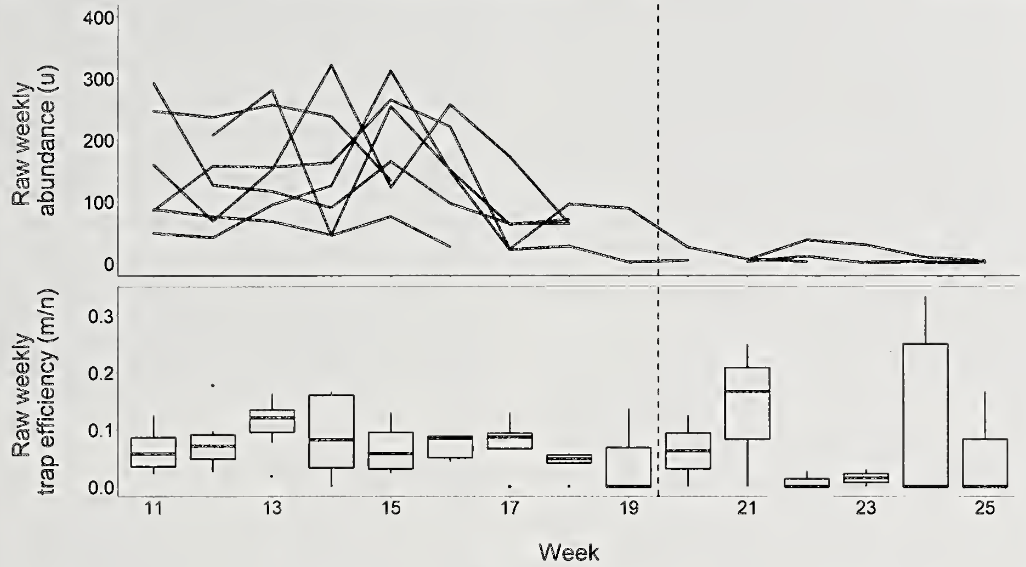

Figure 3

Raw weekly abundance (*u*) of Chinook salmon (*Oncorhynchus tshawytscha*) and raw weekly trap efficiencies, measured as the number of marked individuals in the population divided by the number of marked individuals counted or captured at a sampling event (*m*/*n*), at the rotary screw trap deployed in Big Creek, Idaho, during the spring from 2007 through 2013. In the top graph, catches within the same year are linked by a line. In the bottom panel, the middle line within the box represents the median, the upper and lower edges of the box represent the first and third quartiles (the 25th and 75th percentiles), the lines extending beyond the box correspond to the largest or smallest values or 1.5 times the interquartile range, and dots represent outliers (values outside of 1.5 times the interquartile range).

ten results in completely pooled strata, and therefore loses the power to distinguish real changes in sampling efficiency. Additionally, neither approach addresses missing periods when the trap is not able to operate but fish are known to be migrating, as was the case with the M_{PS} model in our study that was designed to represent these models. In the simulation, some of the M_{PS} model bias was offset by removal of missing strata. Because the M_{PS} model can use data only from sampled strata within a single year, it will contain inherent bias. Therefore the M_{PS} model precisions and biases reported in Tables 1 and 2 are misleading, because the model structure cannot incorporate the uncertainty associated with the missing strata. When data are not abundant and "well behaved," more complex models are necessary.

The hierarchical structures of the M_{SPLINE} and M_{HB} models incorporate information about the characteristics of salmonid migration to improve abundance estimates in situations with sparse or missing data. The M_{HW} and M_{SPLINE} models share information among temporal strata within years. The M_{HB} model shares information during the same temporal period between years, allowing data from previous years to inform periods of sparse or missing data. Because the M_{HB} model shares information among years, it effectively uses the entire data set.

Performance during the spring 2014 period in Big Creek shows best how the M_{HB} model is useful. The basic Lincoln–Petersen approach as implemented in the M_{PS} model provided no estimates in missing strata. Information from within 2014 was not very useful with the 2-month gap in operations, such that the M_{HW} model had extremely wide credible intervals and spline components of the M_{SPLINE} model could not bridge the missing period. The M_{HB} model provided an estimate based on data from previous years and included the appropriate uncertainty around that estimate (e.g., higher variability between years leads to increased uncertainty for estimates with missing data during that time period). The spring peak in migration becomes more pronounced closer to the coast and at lower elevations (Spence and Hall, 2010). hence the problems we address here may be greater elsewhere. Models that performed poorly with our data sets would fare even worse in more extreme environmental scenarios.

For the applications made in this study, we relied only on mark-recapture data but one could incorporate other types of information to make further improve-

---

recapture data from small populations, with application to estimating abundance of smolts from outmigrant trap data. NOAA, Natl. Mar. Fish. Serv., Southwest Fish. Sci. Cent. Admin. Rep. SC-00-02, 19 p. [Available from website.]

ments. For example, spawner abundance, flow characteristics, and data from co-migrating species could help explain variability in U and p in the respective examples. In particular, data on the number of previous-year spawners could explain annual differences in juvenile abundances, thus accounting for significant changes in abundances and timing of migration from year to year. Inclusion of data from co-migrating species could bolster estimates for species with extremely low abundances. With appropriate assumptions, a multi-species model could be a powerful approach to obtain information for threatened and endangered species.

The framework of the $\mathrm{M_{HB}}$ model is flexible and can easily be elaborated upon in other ways. For another example, one could combine the $\mathrm{M_{SPLINE}}$ model and $\mathrm{M_{HB}}$ model to create a multiyear spline model to apply within- and between-year information. Strata with consistent capture probabilities between years that would potentially benefit the most from the multiyear spline model may not improve much because capture and recapture rates are typically high and data are abundant in these strata. In addition, the use of the multiyear spline model would still be limited by large periods of missing data and running such a model would take substantial computing power and time. We surmise that it would be more beneficial to include environmental and biological covariates into the $\mathrm{M_{HB}}$ model than creating a multiyear spline model. We chose not to investigate the hybrid spline model or to include covariates because we wanted to illustrate the basic concept and functionality of the competing models and because additional data are not always available. However, if conditions are extreme, then these more complex options may be desirable.

Throughout this study we focused on 2 long-term monitoring projects with data sets ranging from 8 to 21 years; the $\mathrm{M_{HB}}$ model could produce estimates for missing data with fewer years of data. The accuracy and precision of abundance estimates produced for periods with sparse or missing data from short data sets will depend on the amount of data collected during years that the trap was able to operate and the consistency of recurring life-history characteristics between years. The effects of relevant factors on the quality of information in the data record can be tested but that is beyond the scope of this article. However, so long as the assumption that the species exhibits a recurring life-history characteristic that is expressed during the same temporal period between years, the estimates from sparse and missing data would be accurate but the uncertainty with these estimates will be expressed in wide, credible interval widths.

The hierarchical multiyear Bayesian model has broad application to fish and wildlife studies that employ mark-recapture approaches to obtain population abundance estimates, particularly when addressing issues of sparse or missing data. Other studies have used similar Bayesian approaches to calculate adult salmonid abundance estimates in Alaska (Sethi and Tanner, 2013), survival estimates of harbor seals (*Phoca vitulina*) in Scotland (Mackey et al., 2008), and wolverine (*Gulo gulo*) densities in Alaska (Royle et al., 2011) in order to address issues associated with sparse data. In this study, we were able to produce abundance estimates for populations of anadromous salmonids with sparse data by structuring a hierarchical model that incorporated prior biological information about the species behavior. The $\mathrm{M_{HB}}$ model has applicability to a wide range of fish and wildlife research that uses mark-recapture data to estimate species abundance. This model will be particularly useful in assessments of species for which long-term monitoring has occurred but for which low abundances and variable environmental conditions affect sampling efforts.

Acknowledgement

We thank the Idaho Department of Fish and Game (IDFG), University of Idaho, and Bonneville Power Administration (projects 1989-098-00, 1990-055-00 and 1991-073-00) for the opportunity and financial support to conduct this research. We greatly appreciate the discussion, reviews, and feedback provided by M. Quist, R. Kinzer, members of B. Kennedy's laboratory, and numerous other fisheries biologists from the IDFG and Nez Perce tribe. We are particularly grateful to K. Apperson, L. Jansen, D. Venditti, and B. Barnett for providing the RST data that made the analysis possible.

Literature cited

Bjornn, T. C.
1971. Trout and salmon movements in two Idaho streams as related to temperature, food, stream flow, cover, and population density. Trans. Am. Fish. Soc. 100:423–438.
1978. Survival, production, and yield of trout and Chinook salmon in the Lemhi River, Idaho. Univ. Idaho, Coll. For., Wildl. Range Sci. Bull. 27, 57 p.

Bonner, S. J., and C. J Schwarz.
2011. Smoothing population size estimates for time-stratified mark–recapture experiments using Bayesian P-splines. Biometrics 67:1498–1507.

Calambokidis, J., and J. Barlow.
2004. Abundance of blue and humpback whales in the eastern North Pacific estimated by capture recapture and line-transect methods. Mar. Mamm. Sci. 20:63–85.

Copeland, T. S., D. A. Venditti, and B. R. Barnett.
2014. The importance of juvenile migration tactics to adult recruitment in stream-type Chinook salmon populations. Trans. Am. Fish. Soc. 143:1460–1475.

Ellison, A. M.
2004. Bayesian inference in ecology. Ecol. Letters, 7:509–520.

Fryxell, J. M., A. R. E. Sinclair, and G. Caughley.
2014. Wildlife ecology, conservation, and management, 3rd ed., 509 p. John Wiley & Sons Ltd., Oxford, UK.

Johnson, D. H., B. M. Shrier, J. S. O'Neal, J. A. Knutzen, X. Augerot, T. A. O'Neil, T., and T. N. Pearsons.
2007. Salmonid field protocols handbook: techniques for

assessing status and trends in salmon and trout populations, 478 p. Am. Fish. Soc., Bethesda, MD.

Kareiva, P. M.
1983. Local movement in herbivorous insects: applying a passive diffusion model to mark-recapture field experiments. Oecologia. 57:322–327.

Lang, S., and A. Brezger.
2004. Bayesian P-splines. J. Comput. Graph. Stat. 13:183–212.

Mackey, B. L., J. W. Durban, S. J. Middlemas, and P. M. Thompson.
2008. A Bayesian estimate of harbour seal survival using sparse photo-identification data. J. Zool. 274:18–27.

Mäntyniemi, S., and A. Romakkaniemi.
2002. Bayesian mark-recapture estimation with an application to a salmonid smolt population. Can. J. Fish. Aquat. Sci. 59:1748–1758.

Mill, L. S.
2007. Conservation of wildlife populations: demography, genetics, and management, 407 p. Blackwell Publishing, Malden, MA.

Mowat, G., and C Strobeck.
2000. Estimating population size of grizzly bears using hair capture, DNA profiling, and mark-recapture analysis. J. Wildl. Manage. 64(1):183–193.

Nichols, J. D.
1992. Capture-recapture models. BioScience 42:94–102.

Otis, D. L., K. P. Burnham, G. C. White, and D. R. Anderson.
1978. Statistical inference from capture data on closed animal populations. Wildl. Soc., Wildl. Monogr. 62, 135 p.

Plummer, M.
2003. JAGS: a program for analysis of Bayesian graphical models using Gibbs sampling. *In* Proceedings of the 3rd international workshop on distributed statistical computing (DSC 2003); Vienna, Austria, 20–22 March (K. Hornik, F. Leisch, and A Zeileis, eds.), 10 p. [Available from website.]

R Core Team.
2015. R: a language and environment for statistical computing. R Foundation for Statistical Computing, Vienna, Austria. [Available from website, accessed September 2015].

Royle, J. A., and R. M. Dorazio.
2008. Hierarchical modeling and inference in ecology: the analysis of data from populations, metapopulations and communities. Academic Press, Inc., London.

Royle, J. A., A. J. Magoun, B. Gardner, P. Valkenburg, and R. E. Lowell.
2011. Density estimation in a wolverine population using spatial capture–recapture models. J. Wildl. Manage. 75:604–611.

Schwarz, C. J., and C. G. Taylor.
1998. Use of the stratified-Petersen estimator in fisheries management: estimating the number of pink salmon (*Oncorhynchus gorbuscha*) spawners in the Fraser River. Can. J. Fish. Aquat. Sci. 55:281–296.

Seber, G. A. F.
2002. The estimation of animal abundance and related parameters, 2nd ed., 654 p. Blackburn Press, Caldwell, NJ.

Sethi, S. A., and T. L. Tanner.
2013. Bayesian implementation of a time stratified Lincoln–Petersen estimator for salmon abundance in the upper Matanuska River, Alaska, USA. Fish. Res. 145:90–99.

Spence, B. C., and J. D. Hall.
2010. Spatiotemporal patterns in migration timing of coho salmon (*Oncorhynchus kisutch*) smolts in North America. Can. J. Fish. Aquat. Sci. 67:1316–1334.

Steinhorst, K., Y. Wu, B .Dennis, and P. Kline.
2004. Confidence intervals for fish out-migration estimates using stratified trap efficiency methods. J. Agric. Biol. Environ. Stat. 9:284–299.

Su, Y.-S., and M. Yajima.
2015. R2jags: using R to run 'JAGS'. R package, vers. 0.5-7. [Available from website.]

Zabel, R. W., T. Wagner, J. L. Congleton, S. G. Smith, and J. G. Williams.
2005. Survival and selection of migrating salmon from capture-recapture models with individual traits. Ecol. Appl. 15:1427–1439.

National Marine
Fisheries Service
NOAA

Fishery Bulletin
established in 1881

Spencer F. Baird
First U.S. Commissioner
of Fisheries and founder
of *Fishery Bulletin*

Abstract—Surveys of juvenile and larval stages can be useful for management of commercially important marine fishes but require definitive species identification. From May through October 2005–2008, midwater (30-m) trawls collected 78,407 late-larval and juvenile rockfish (*Sebastes* spp.) in shelf and slope waters off Oregon and Washington. Because of their small size and lack of pigmentation, we could identify only 4.1% (3266 individuals) of sampled rockfishes to species morphologically, representing a total of 17 species. An additional subsample (2534 individuals), representing 24 species and a 4-species complex, was identified by sequencing the mitochondrial cytochrome *b* gene and matching sequences to a reference data set. Incomplete overlap between identified species meant that a total of 29 species were identified overall. Community analyses showed that rockfish collected during the early upwelling season (May–June) were distinct from samples collected in the late upwelling season (July–October). Most rockfish were collected from outer-shelf or upper-slope stations, but distributions varied by month and year. Combining genetic and morphological identifications vastly improved our ability to assess seasonal distributions and abundances of planktonic rockfishes and is a step toward performing species-level surveys for this speciose and commercially important genus. Definitive identification based on visual and molecular methods as used here provides key information to enhance understanding of early-stage rockfish ecology.

Manuscript submitted 20 December 2017.
Manuscript accepted 19 June 2018.
Fish. Bull. 116:266–280 (2018)
Online publication date: 10 July 2018.
doi: 10.7755/FB.116.3-4.5

The views and opinions expressed or implied in this article are those of the author (or authors) and do not necessarily reflect the position of the National Marine Fisheries Service, NOAA.

Seasonal distribution of late larval and juvenile rockfish (*Sebastes* spp.) and associated environmental conditions off Oregon and Washington: new insights based on genetics

Mattias L. Johansson[1]
Marisa N.C. Litz[2]
Richard D. Brodeur[3]
Tristan A. Britt[2]
Camilo A. Vanegas[1]
John R. Hyde[4]
Michael A. Banks[1]

Email address for contact author: m.l.johansson@gmail.com

[1] Coastal Oregon Marine Experiment Station
Oregon State University
2030 SE Marine Science Drive
Newport, Oregon 97365
Present address for contact author: Biology Department
University of North Georgia
3820 Mundy Mill Road
Oakwood, Georgia 30566

[2] Cooperative Institute for Marine Resources Studies
Oregon State University
2030 SE Marine Science Drive
Newport, Oregon 97365

[3] Fish Ecology Division
Northwest Fisheries Science Center
National Marine Fisheries Service, NOAA
2030 S Marine Science Drive
Newport, Oregon 97365-5296

[4] Fisheries Resources Division
Southwest Fisheries Science Center
National Marine Fisheries Service, NOAA
8901 La Jolla Shores Drive
La Jolla, California 92037-1509

The larval and juvenile stages of many demersal fish species occur in pelagic waters, which may connect populations (Cowen and Sponaugle, 2009), and may promote survival of a subset of larval production by dispersing larvae among diverse habitats in an uncertain, variable environment while reducing the risk of inbreeding and density-dependent mortality (Gadgil, 1971; Levin et al., 2003). The dispersal of most larval fish seems to be highly diffusive and driven by ocean currents, although there is evidence that some rockfishes (particularly nearshore species) remain nearshore due to larval swimming behavior or limited water movement (Buonaccorsi et al., 2002, 2005; Johansson et al., 2008). Environmental conditions also vary with ocean currents, and habitat variability can affect species abundance and diversity.

In the California Current system of the eastern North Pacific, the genus *Sebastes* (the rockfishes) is known to be sensitive to shifts in environmental conditions associated with changes in prevailing currents. The rockfishes are among the most common of groups found in pelagic micronekton surveys in the eastern North Pacific. Larval and juvenile rockfishes may represent a great deal of unrecorded diversity because they are often difficult or impossible to identify to species based on body shape or pigmentation patterns. This highly diverse genus is represented by at least 65 species in the Pacific Ocean off the coast of North America, of which 36 to 40 occur in waters off southern Washington and northern Oregon (Love et al., 2002).

After parturition, the life history of all rockfish species includes a pelagic phase, consisting of both larval and juvenile stages (Boehlert, 1977; Moser and Boehlert, 1991). Settlement to the bottom occurs after a period of a few months to a year, and varies by species (Love et al., 2002). Larval and pelagic-juvenile-stage rockfish represent a significant proportion of the ichthyoplankton and micronekton community off Washington, Oregon, and California (Auth, 2009; Phillips et al., 2009; Thompson et al., 2016; Thompson et al., 2017).

The early-stage larvae of a number of species of rockfish occurring off the west coast of North America have been described morphologically (Sakuma and Laidig, 1995; Moser, 1996). However, misidentification of larval and juvenile fish often occurs even at the family level (Ko et al., 2013). Visual identification of field-caught late-larval and early-juvenile rockfishes is especially difficult because different but closely related species of *Sebastes* occur together and there are few distinguishing morphological characters (Seeb and Kendall, 1991; Sakuma and Laidig, 1995; Rocha-Olivares et al., 2000). This difficulty of identifying late larval and juvenile rockfishes is particularly problematic given their importance in the fisheries they support in the northeast Pacific Ocean (Love et al., 2002) and their history of being heavily fished.

Surveys of pelagic larval and juvenile fish are a widely used fishery-independent means of tracking abundances of marine fishes (Lasker, 1985; He et al., 2015). These surveys are both easier and cheaper than sampling adult fishes, and are likely to have a smaller impact on populations. In order to provide early indications of the potential recruitment of fishes to the northern California Current, the NOAA Northwest Fisheries Science Center (NWFSC) Fish Ecology Division has conducted surveys as part of the Stock Assessment Improvement Program (SAIP) during summer from 2004 through 2012 to collect late-larval and juvenile fish from southern Washington to central Oregon (Phillips et al., 2009).

The ability to efficiently identify large numbers of individual late-larval and pelagic juvenile rockfish would make it possible to characterize the distributions and abundances of the early life stages of species (Love et al., 2002; Ralston and Stewart, 2013), as well as conduct associated recruitment studies and estimate juvenile biomass (Sakuma and Laidig, 1995; Laidig et al., 2007). Molecular methods based on allozyme, microsatellite, or DNA sequence variation offer an alternative to morphological approaches to identify larvae to species quickly and efficiently (Seeb and Kendall, 1991; Rocha-Olivares et al., 2000; Gharrett et al., 2001; Taylor et al., 2004; Gray et al., 2006).

Our objectives were to identify to species late-stage larvae and juveniles of the genus *Sebastes* collected in SAIP tows of midwater trawls made during 2005–2008 by using visual meristic or pigmentation patterns. We used the cytochrome *b* sequence-based method of Taylor et al. (2004) to identify to species the remaining visually unidentifiable fraction. Using both of these techniques, we also sought to assess spatial and temporal variations in composition, concentration, and other characteristics of the late-larval and juvenile rockfish community off the coast of Oregon and Washington, and to relate their distributions to environmental conditions during the main upwelling season (May–October).

Materials and methods

Sampling procedure

Midwater trawls were used to sample micronekton, including juvenile fishes, from spring to fall during 2005–2008. With the exception of May 2005 and July 2006, monthly cruises were conducted from May through September of each year, and an additional cruise was included from October 2005. In each sampling cruise, the same 5 stations were sampled along each of 4 transects: Heceta Head (HH) (44.00°N), Newport (NH) (44.65°N), and the Columbia River (CR) (44.16°N) off Oregon and Willapa Bay (WB) (46.67°N) off Washington (Fig. 1). Stations ranged from approximately 20 to 100 km offshore along each transect. A single station, located 185 km (100 nautical miles) off the NH transect (the NH-100 station) was sampled just once in June 2008. Owing to weather or mechanical problems, some stations or transects (or both) were not sampled during some cruises.

To collect the samples used in this project, a Nordic 264 rope trawl was towed for 15 min with the head rope at a target depth of 30 m. The effective mouth area of the trawl was 12 m high and 28 m wide (336 m^2; Emmett et al., 2004). The main body of the net had variable mesh sizes (from 162.6 cm at the mouth to 8.9 cm at the codend), and a 6.1-m long, 3-mm stretched knotless web liner in the codend. All tows of the trawl were conducted at night. After all fish and invertebrates >10 cm in total length were removed, the remaining catch was subsampled as follows: samples with an unsorted volume of ≤ 0.25 m^3 were frozen in their entirety, whereas samples with an unsorted volume of >0.25 m^3 were subsampled in the amount of 0.25 m^3 or 20% of the entire sample, whichever was larger. The retained unsorted catches were frozen at sea and later thawed and sorted in the laboratory. For additional details on the collection method, see Phillips et al. (2007).

In the laboratory, individual rockfish were identified to the lowest possible taxonomic level by using a va-

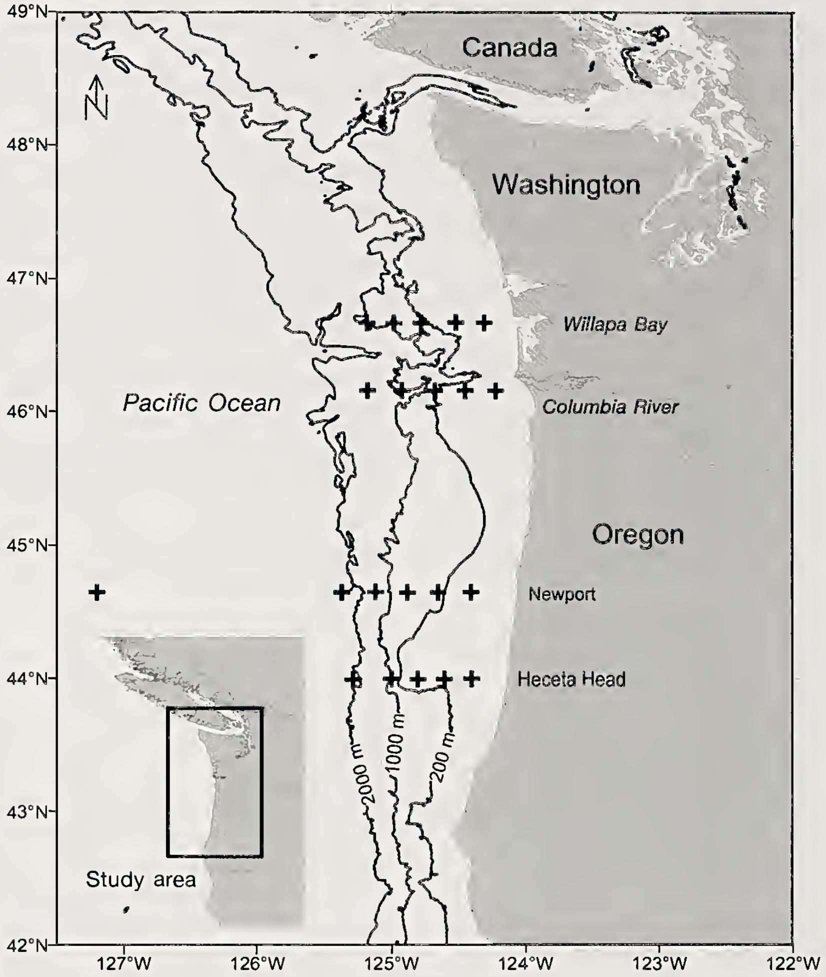

Figure 1

Map of stations (+) off Oregon and Washington sampled for species of *Sebastes* during 2005–2008. Along transects at Heceta Head, Newport, the Columbia River, and Willapa Bay, 5 stations were sampled during most sampling cruises. In addition, a single station located 185 km from shore on the Newport transect (the NH-100 station) was sampled once in June 2008.

riety of keys (Richardson and Laroche, 1979; Laroche and Richardson, 1980, 1981; Matarese et al., 1989; Laidig and Adams, 1991; Moser, 1996) and measured for standard length (SL, to the nearest mm). Densities for visually identified species were calculated by dividing catch by total distance towed (km) and assuming a relatively constant mouth opening for all the tows. Because of ambiguous and overlapping meristics, most (96%) late-larval and juvenile rockfishes could be identified only to the genus *Sebastes* and were stored in ethanol for genetic analysis.

DNA extraction and data collection

To perform genetic analysis, we took samples from caudal fin tissue of late-larval and juvenile rockfish (2534 individuals) collected in 144 different tows of the trawl. Samples were randomly selected from among the 96% of samples that could not be identified visually. On average, 26% of the individual rockfish from each haul were sampled for genetic material to obtain a representative sample of catch. Total genomic DNA was extracted by using a glass-fiber plate extraction protocol (Ivanova et al., 2006). Polymerase chain reaction (PCR) was used to amplify a 782-base-pair (bp) fragment of the mitochondrial DNA (mtDNA) cytochrome *b* gene by using previously published GluRF and CB3RF primers (Rocha-Olivares et al., 1999). Thermal cycling conditions included an initial denaturation at 94°C for 2.5 min, followed by 35 cycles of 94°C for 45 sec, 56°C for 1.5 min, and 72°C for 1.5 min. Final extension was carried out at 72°C for 3 min. PCR products were cleaned using a procedure with ExoSap-IT[1] reagent (Thermo Fisher Scientific, Waltham, MA), and were cycle sequenced by using BigDye Terminator cycle sequencing kits (Thermo Fisher Scientific) and internal primers CBInf2 and CBInr2 (Dauble et al., 2012). Sequencing products were cleaned with Sephadex (GE Healthcare Bio-Sciences, Pittsburgh, PA) and visualized on an Applied Biosystems 3730*xl* DNA Analyzer (Thermo Fisher Scientific). Sequence data were aligned and edited with Sequencher, vers. 4.7 (Gene Codes Corp., Ann Arbor, MI) software. All sequencing and analysis were performed by the authors. Reference and unknown sequence data are available from ScholarsArchive@OSU (available at website).

---

[1] Mention of trade names or commercial companies is for identification purposes only and does not imply endorsement by the National Marine Fisheries Service, NOAA.

Haplotype sequences from trawl-collected larvae were compared with a reference data set of 374 independent haplotypes from 67 species of morphologically identified adult rockfish (see Taylor et al., 2004 for species included in the reference data set). Identical sequences were identified in Sequencher, and all unique sequences were compared with the reference data set by using a custom script in R, vers., 3.3.1 (R Core Team, 2016) and the program PAUP*, vers. 4b10; Sinauer Associates, Sunderland, MA) with the optimality criterion set to distance (number of bp differences divided by total length of sequence in bp).

Nonparametric bootstrapping (1000 replicates) was used to cluster individual unknown sequences within the reference data set of 374 known adult sequences. Some species in the reference data set failed to form monophyletic clades: the widow rockfish (*S. entomelas*) and blue rockfish (*S. mystinus*) (EM complex) and pygmy rockfish (*S. wilsoni*), Puget Sound rockfish (*S. emphaeus*), harlequin rockfish (*S. variegatus*), and sharpchin rockfish (*S. zacentrus*) (WEVZ complex). Others, such as the splitnose rockfish (*S. diploproa*), have few differences from sister species, a feature that affects the robustness of bootstrap results. For samples that were identified as falling within the EM complex, we manually compared sequences in Sequencher with those of known widow rockfish and blue rockfish. Known widow and blue rockfish differ consistently at a single nucleotide in our database of known sequences (base position 627, where widow rockfish sequences contain a cytosine and blue rockfish sequences contain an adenine), allowing us to identify all our juveniles as widow rockfish. For all other samples, we performed identifications with 2 different levels of stringency and compared outcomes. If an individual clustered within a monophyletic single-species clade with a bootstrap value ≥70%, this result was considered a high-confidence identification of the individual. Bootstrap values between 50% and 69% were considered low-confidence identifications. Other outcomes (i.e., nonmonophyletic affinities, polytomies) were coded as failed identifications. We also calculated F84 distance (Felsenstein and Churchill, 1996) between unknown and reference haplotypes using the R package ape, vers. 3.5 (Paradis et al., 2004) to confirm that unknowns fell within the range of expected intraspecific diversity on the basis of reference data.

Physical data

Physical data were collated from local, regional, and basin-wide spatiotemporal scales for comparison with rockfish community composition to determine whether species of *Sebastes* were associated with a particular level of environmental variability. In situ measurements of temperature and salinity were collected at the surface (1 m) and at trawling depth (30 m) by using a cast of an SBE25*plus* Sealogger CTD conductivity, temperature, and pressure recorder (Sea-Bird Scientific, Bellevue, WA) at each sampling station. At the regional scale, monthly averaged upwelling indices, based on estimates of offshore Ekman transport driven by geostrophic wind stress at 45°N and 145°W, were obtained from the Pacific Fisheries Environmental Laboratory (website). At the basin scale, monthly indices of the Pacific Decadal Oscillation (PDO; Mantua et al., 1997) and the North Pacific Gyre Oscillation (NPGO; Di Lorenzo et al., 2008) were included in the analysis because they are oceanic expressions of the 2 dominant modes of North Pacific atmospheric variability—the Aleutian Low and the North Pacific Oscillation, which are linked to the different phases of the El Niño Southern Oscillation cycle (Di Lorenzo et al., 2010). The PDO captures variability in sea-surface temperature (SST) and the NPGO captures the variability in salinity, nutrients, and chlorophyll-*a*.

Community analyses

To evaluate seasonal and annual variability in the species numerical composition of late-larval and juvenile rockfish sampled for this study, nonmetric multidimensional scaling (NMS) was used to ordinate rockfish samples (densities of fish identified in the laboratory by visual means and proportions of rockfish identified on the basis of genetics) in n-dimensional space. NMS is an iterative process that searches for the best positions of n entities on k dimensions (axes) that minimize the stress of the k-dimensional configuration (McCune et al., 2002). The goal is to generate a plot of sample points (individual tows) such that the rank order of the dissimilarity values between all pairs of samples is preserved in the spatial arrangement of points in the final plot. A total of 17 rockfish species were visually identified in the laboratory from 3266 individuals collected at 93 sampling stations, but only 7 taxa that occurred in ≥10% of the sampling stations were included in the analysis (total number of individuals of the 7 visually identified taxa: 3072). Densities were ln $(x+1)$ transformed and relativized by species maxima to homogenize variance. For rockfishes identified by using genetics, 24 taxa (total number of individuals of the 24 genetically identified taxa: 915) were used, excluding individuals classified to species complexes as WEVZ (1489 individuals) or samples for which identification to species failed (25 individuals). This analysis was conducted with PC-ORD, vers. 6; MjM Software, Gleneden Beach, OR; McCune and Mefford, 2011) with

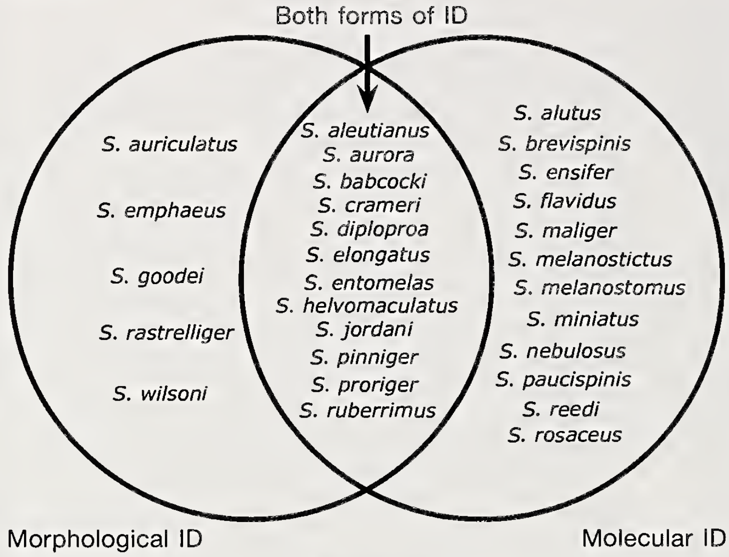

Figure 2

Venn diagram of species of *Sebastes* identified morphologically, by molecular technique, or both, from samples collected during 2005–2008 off Oregon and Washington.

the Sørensen distance measure, a maximum of 4 axes, and 200 iterations.

We examined monthly averages of temperature, salinity, and large-scale environmental indices by year to assess how the physical environment varied during the study. To determine the degree to which these variables were correlated with one another, we used Pearson correlation analysis. We also used correlation analysis to assess the relationship of the environment with the juvenile rockfish community by examining relationships between NMS scores and environmental covariates measured at the level of an individual haul. Physical variables included surface (1 m) and depth (30 m) temperature and salinity, as well as the large-scale indices of upwelling, PDO and NPGO. Distance from shore (km) was included as a spatial variable in the multivariate analysis because it has been shown in other studies that ichthyoplankton communities can vary along inshore and offshore gradients (Auth et al., 2011). Temporal variables included month, year, and season (spring=May and June, summer=July–October).

We also conducted indicator species analysis on each rockfish species matrix to detect within- and between-year variability and to identify statistically significant indicators for each month and year (Dufrêne and Legendre, 1997). An indicator species analysis combines information on relative abundance and frequency of occurrence to identify indicators that are most characteristic of a group. Indicator species analysis was performed separately for sampling months and years. Levels of significance were determined by using a Bonferroni adjustment and based on Monte Carlo tests with 5000 permutations for comparison with observed indicator values.

Results

Rockfish identification

Late-larval and juvenile rockfish were caught in 196 of the 271 tows made (72%) for a total of 78,407 specimens from 2005 through 2008. Using strictly visual means (meristics and pigmentation), we were able to identify 3266 (4.1% of total) late-larval/juvenile rockfish from 17 distinct taxa found in 93 hauls (Fig. 2). By far the most abundant species (81% of the identified rockfish) was the rosethorn rockfish (*S. helvomaculatus*), of which 2633 were identified. Other abundant rockfish species identified visually were the greenstriped rockfish (*S. elongatus*, 213 individuals), rougheye rockfish (*S. aleutianus*, 72 individuals), redbanded rockfish (*S. babcocki*, 66 individuals), brown rockfish (*S. auriculatus*, 66 individuals), and darkblotched rockfish (*S. crameri*, 52 individuals). Collectively, these 6 species accounted for 95% of the fish visually identified from 2005 through 2008.

Size distributions of late-larval and juvenile rockfish measured during this study ranged from 6 to 69 mm SL (Suppl. Figs. 1 and 2) (online only). There was a tendency toward greater visual identification of larger individuals, especially in May, when all specimens >35 mm SL were identifiable but none below this threshold (Suppl. Fig. 1) (online only). Similar patterns were observed in the annual size ranges that could be identified by visual means (Suppl. Fig. 2) (online only).

Subsampling among the visually unidentifiable larvae and juveniles, we successfully sequenced full-length (782 bp) cytochrome *b* fragments from a total of 2534 juvenile rockfish collected in 144 hauls, including 105 from the NH-100 station. We identified 20 species according to our high-confidence stringency criterion (Suppl. Fig. 3) (online only), and confidently assigned a large number (1489 individuals, 58.7%) of specimens to the multispecies WEVZ complex. Another 213 unknowns could not be assigned at high confidence and were coded as unassigned. Using the low-confidence (>50% bootstrap) criterion, we were able to identify 24 species (Fig. 2, Suppl. Fig 3 (online only) and assign many of the previous unknowns to the WEVZ group. The remaining 25 unknowns could not be assigned at low confidence and were coded as unassigned.

Of the species that occurred in the set of low-confidence identifications that were not found in the high-confidence set, 3 were represented by a single individual (aurora rockfish, *S. aurora*; rosy rockfish, *S. rosaceus*) or a few individuals (darkblotched rockfish, 3 individuals). Only the splitnose rockfish was present in greater numbers (43 individuals). Other differences between the sets of high- and low-confidence identifications were proportions of individuals that were as-

Table 1

Correlation matrix of average monthly values for temperature (T) and salinity (S) at the sea surface (1 m) and the depth of 30 m at sampling stations and for large-scale environmental indices off Oregon and Washington during 2005–2008. Pearson's correlation coefficients appear below and associated *P*-values are given above the diagonal. The environmental indices include the Upwelling Index (UI) measured off Oregon and Washington and the Pacific Decadal Oscillation (PDO) and North Pacific Gyre Oscillation (NPGO) indices. Bold values indicate significant correlations ($P<0.05$). SST=sea-surface temperature; SSS=sea-surface salinity.

	SST	SSS	30-m T	30-m S	UI	PDO	NPGO
SST	–	0.645	0.155	0.880	0.703	0.160	0.921
SSS	0.12	–	0.498	**0.011**	0.758	0.149	0.850
30-m T	0.35	0.17	–	0.621	0.827	0.137	**0.003**
30-m S	0.04	**0.58**	0.13	–	0.599	0.337	0.283
UI	–0.10	0.08	0.06	0.13	–	0.366	0.112
PDO	0.35	–0.35	–0.36	–0.24	0.23	–	0.101
NPGO	0.03	–0.05	**–0.66**	–0.27	–0.39	–0.40	–

signed to individual species versus the multispecies complex or unidentified. The WEVZ complex accounted for 58% of the high confidence, and 59% of the low-confidence data sets, respectively. Because the differences between sets were mainly differences of proportion rather than differences of identity, we chose to perform environmental analyses combining and using both high and low-confidence identification results.

There was some overlap between species identified by using morphological versus molecular techniques, with 12 species identified in both data sets (Fig. 2). However, both approaches also identified species that were not identified with the other method. Five species, the brown rockfish, Puget Sound rockfish, chilipepper (*S. goodei*), grass rockfish (*S. rastrelliger*), and pygmy rockfish, were identified only by visual means, whereas 12 species were identified only with the molecular technique (Fig. 2). Thus, the combined approach allowed us to identify a total of 29 species in our data set, plus those samples identified as belonging to the WEVZ complex.

Environmental data

During the 4 years of our study (2005–2008), ocean conditions during May–October off Oregon and Washington varied in terms of temperature, salinity, and upwelling intensity (Suppl. Fig. 4) (online only). Cooler average SST with low variation occurred in 2005 (13.9°C [standard deviation (SD) 1.7]) and 2006 (14.1°C [SD 1.3]) than in 2007 and 2008 (16.1°C [SD 2.0] and 14.2°C [SD 1.9], respectively). Warmest SST were measured during June–September 2007. At 30-m depth, warmest temperatures occurred in 2005, a year considered anomalous owing to delayed upwelling (Barth et al., 2007). Although the start of upwelling was delayed in 2005, once initiated in mid-July, it was strong and persistent, leading to cross-shelf transport of surface waters. Upwelling was strongest during June–August in 2006, which likely impacted offshore larval dispersal. Salinity varied little at 30 m during the study, but at the surface, freshwater input from the Columbia River was most detectable during May–June 2005, when upwelling was delayed.

Large-scale indices (PDO and NPGO) displayed values considered more favorable for productivity (more negative PDO and more positive NPGO; Chenillat et al., 2012; Sydeman et al., 2014) in the California Current system during 2007–2008 than during 2005–2006, reflected in the highest rockfish density occurring during 2007 and 2008 (Suppl. Fig. 5) (online only). In 2008, PDO values were the most negative and NPGO values the most positive throughout the entire sampling period (May–October), indicating that cool productive ocean conditions, coupled with less cross-shelf transport than in 2005 and 2006, were favorable for rockfish prerecruits in 2008. On average, total catches during 2007–2008 (59,779 rockfish) were >3 times larger than catches during 2005–2006 (18,628 rockfish). Effort was similar during the 2 time periods (129 hauls during 2005–2006 and 142 hauls during 2007–2008). Highest densities of late-larval and juvenile rockfish (identified and unidentified) were sampled in August and September of all years. Ten species/complexes accounted for >80% of the genetically identified rockfish over the entire study period (Suppl. Fig. 6) (online only).

Correlations between mean monthly temperature, salinity, and the large-scale environmental indices were low (coefficient of determination [r^2]=0.002–0.436); therefore all were retained for inclusion in the community analysis (Table 1). Correlation coefficients between salinity at the surface and at 30-m depth were positively and significantly correlated (coefficient of correlation [r]=0.58, P=0.011) and negatively correlated

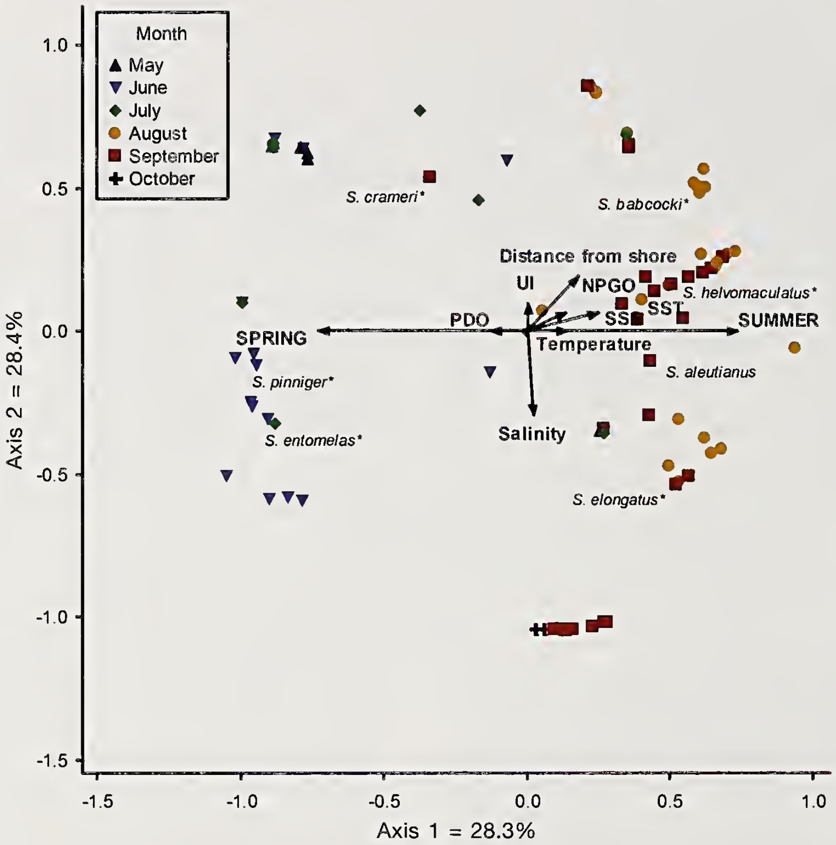

Figure 3

Nonmetric multidimensional scaling ordinations showing axes 1 and 2 for larval rockfishes (*Sebastes* spp.) identified visually and environmental covariates after collection off Washington and Oregon during 2005–2008. Environmental data include sea surface temperature (SST) and salinity at the sea surface (1 m; SSS) and at a depth of 30 m, Upwelling Index (UI), Pacific Decadal Oscillation (PDO) index, and North Pacific Gyre Oscillation (NPGO) index. Asterisks (*) denote species with coefficients of correlation >0.15. Each symbol represents the species composition of larvae collected in a single complete haul of a midwater trawl ordinated in species space (e.g. arranged so that similar hauls are near each other and dissimilar hauls are farther from each other). The arrows indicate the directionality and strength (by length of arrow) of physical correlations between hauls and physical variables measured during the collection period.

between temperature at 30 m and the NPGO (r=–0.66, P=0.003). However, because each variable represented a unique spatial scale or in situ habitat, they were all retained for subsequent analysis.

Community analyses

The NMS ordination of rockfishes identified by visual means (Figs. 3 and 4) contained 7 species caught in 89 of 93 tows where we had visual identifications, and described 73.8% of the variation in the data set (axis 1=28.3%, axis 2=24.8%, and axis 3=20.6%). The stress for the final solution was 17.0 (instability=0, 158 iterations), considered fair but interpretable (Kruskal, 1964). The largest variation in community structure was explained by seasonal differences along axis 1 (Suppl. Table 1) (online only). Summer months (July through October, r=0.767) and warmer SST at 1 m (r=0.446) were positively correlated with axis 1 scores; spring months (May and June) were negatively correlated (r=–0.767). The species most likely to be present during warm, summer months was the rosethorn rockfish. During spring, we were more likely to find canary rockfish (*S. pinniger*), darkblotched rockfish, and widow rockfish. Axis 2 was positively associated with offshore stations (r=0.394) and negatively associated with warmer temperatures at 50 m, indicating that axis 2 differentiated between on-shelf and off-shelf

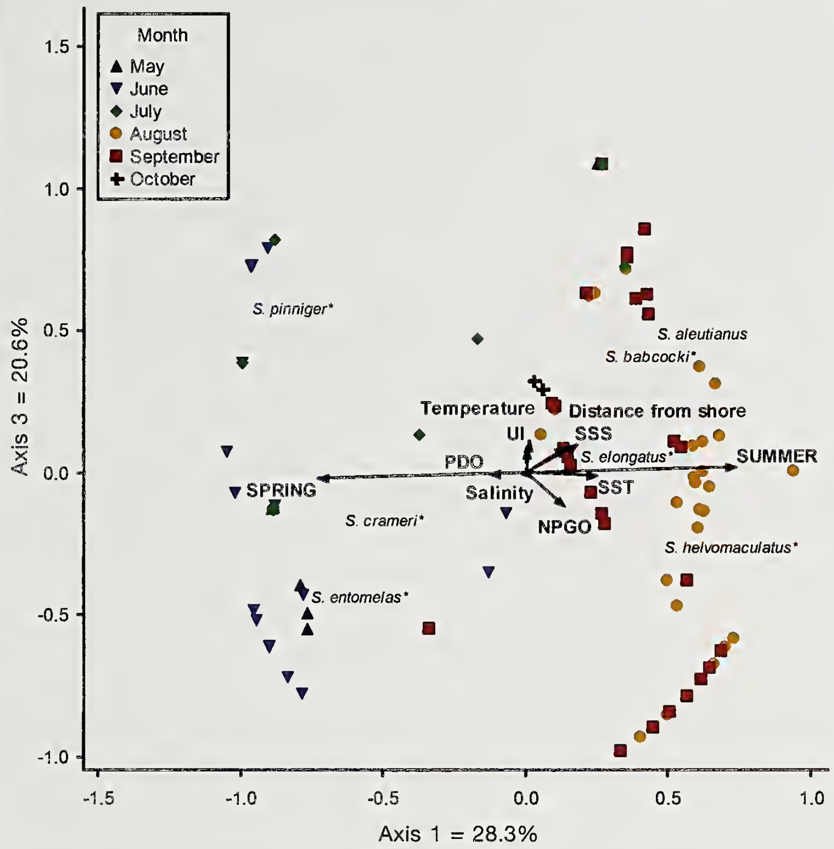

Figure 4

Nonmetric multidimensional scaling ordinations showing axes 1 and 3 for larval rockfishes (*Sebastes* spp.) identified visually after collection off Washington and Oregon during 2005–2008 and environmental covariates. Environmental data include sea surface temperature (SST) and salinity (SSS) at 1 m, and at a depth of 30 m, Upwelling Index (UI), Pacific Decadal Oscillation (PDO) index, and North Pacific Gyre Oscillation (NPGO) index. Asterisks (*) denote species with coefficients of correlation >0.15. Each symbol represents the species composition of larvae collected in a single complete haul of a midwater trawl ordinated in species space. The arrows indicate the directionality and strength (by length of arrow) of physical correlations between hauls and physical variables measured during the collection period.

catches. At offshore stations, we were more likely to encounter redbanded rockfish, whereas greenstriped rockfish were identified closer to the shelf break.

The NMS ordination of the proportion of rockfish identified by genetics (Figs. 5 and 6) contained 24 species caught in 126 of 143 tows where we had genetic data (excluding the station sampled 185 km offshore) and described 87.3% of the variation in the data set (axis 1=38.9%, axis 2=29.5%, and axis 3=18.9%). The stress for the final solution was 15.7% (instability=0, 131 iterations). The largest variation in community structure was also explained by seasonal differences along axis 1 (Suppl. Table 2) (online only). Summer months (r=0.729) and warmer SSTs (r=0.416, r^2<0.15) were positively associated with axis 1 along with redstripe rockfish (*S. proriger*), greenstriped rockfish, and yelloweye rockfish (*S. ruberrimus*) (r: 0.513, 0.482, and 0.445, respectively). Axis 1 was negatively associated with spring months (r= –0.761) and canary) and widow rockfish (r: –0.688 and –0.592). These were 2 of the species that were also identified in spring using visual identification, indicating that there was good agreement between visual and genetic identifications. Axis 2 showed a positive association with redstripe rockfish (r=0.776) and a negative association with rosethorn rockfish (r= –0.745, r^2<0.15), which was associated with warm, summer months based on the visual identification criteria. There were no physical variables associated with axis 2 or 3, but splitnose rockfish was negatively associated with axis 3 (r= –0.552).

Rockfish parturition timing varies seasonally by species. To better understand some of this variation, we

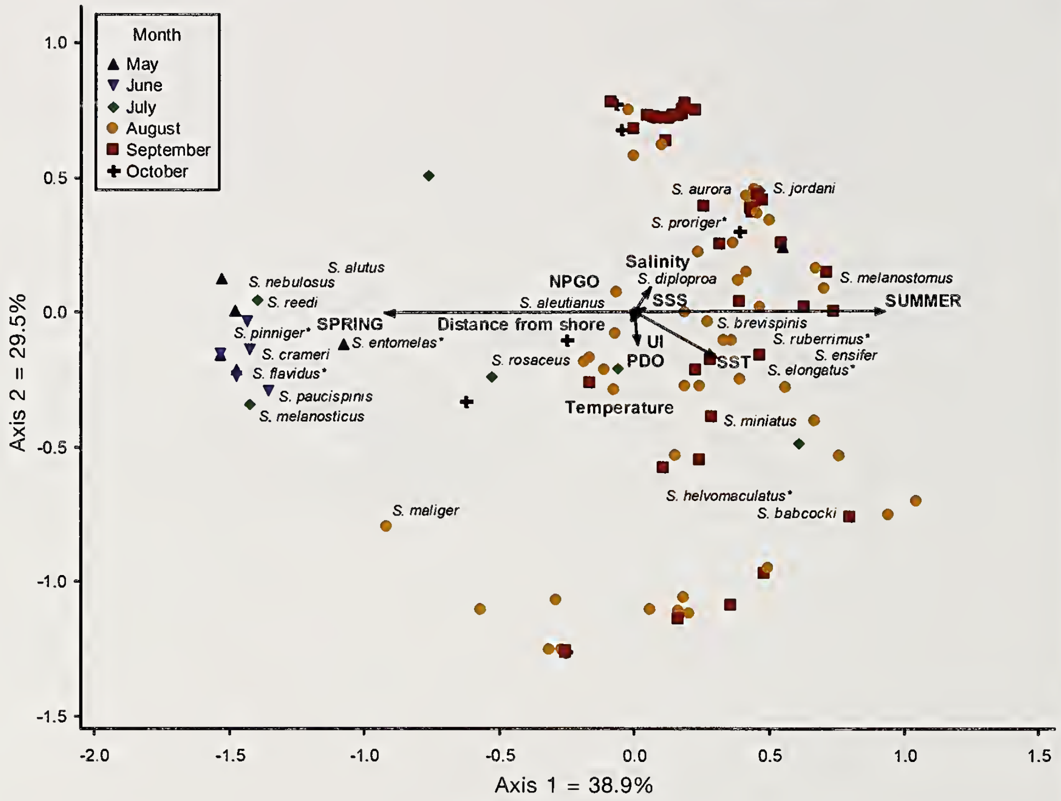

Figure 5

Nonmetric multidimensional scaling ordinations showing axes 1 and 2 for larval rockfishes (*Sebastes* spp.) identified by cytochrome *b* sequencing after collection off Washington and Oregon during 2005–2008 and environmental covariates. Environmental data include sea surface temperature (SST) and salinity at the sea surface (1 m; SSS), Upwelling Index (UI), Pacific Decadal Oscillation (PDO) index, and North Pacific Gyre Oscillation (NPGO) index. Asterisks (*) denote species with coefficients of correlation >0.15. Each symbol represents the species composition of larvae collected in a single complete haul of a midwater trawl ordinated in species space. The arrows indicate the directionality and strength (by length of arrow) of physical correlations between hauls and physical variables measured during the collection period.

conducted indicator species analysis to identify species' affinities to particular months and years (Table 2). Although month and year analyses were performed separately, results are combined in the table. In 2007 and 2008, years previously identified as having high mean concentrations (>60 individuals/1000 m^3) of rockfish larvae in the northern California Current ecosystem (Auth, 2011), we identified the rosethorn rockfish as an indicator species. This species was also more likely to be sampled in summer (August). Two of the species that were strongly associated with spring months (May and June) in NMS ordinations (canary and widow rockfish) were also significant indicators in spring months. Another spring indicator species that was not included in NMS ordinations was the yellowtail rockfish (*S. flavidus*). The NH-100 station was sampled only once during the study, in June 2008. Because widow and yellowtail rockfish were identified as significant indicator species in June and were identified in high abundance from the NH-100 station sampled in 2008, these results suggest that widow and yellowtail rockfish either spawn far off the shelf, were more abundant, or were more susceptible to offshore advection than other spring spawning species in 2008.

The spatial distribution patterns of the dominant rockfish taxa for selected cruises showed much overlap overall (Suppl. Figs. 7–9) (online only). The redstripe rockfish was found mainly later in the summer and predominantly at the outer stations at the shelf break and beyond, although the NH transect had high catches some years at the inshore station (Suppl. Fig. 7) (online only). In contrast, the greenstriped rockfish tended to show lower abundances and were caught almost exclusively beyond the shelf break (Suppl. Fig. 8) (online only). The rosethorn rockfish had a patchy distribution, but there were indications for some cruises that sampling did not extend far enough offshore to capture the full distribution of this species (Suppl. Fig. 9) (online only).

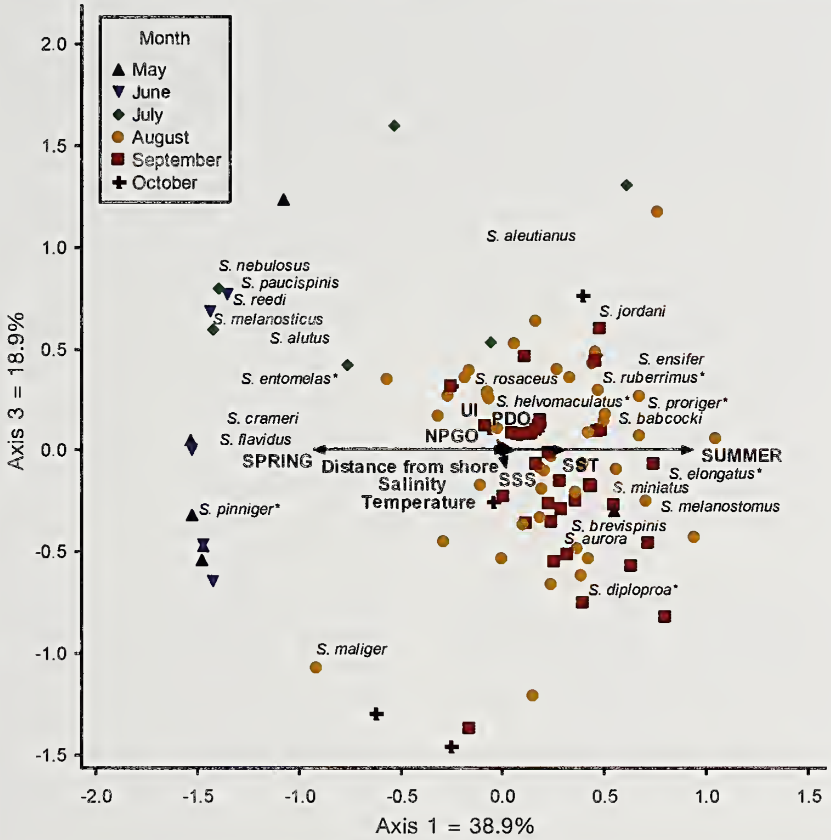

Figure 6

Nonmetric multidimensional scaling ordinations showing axes 1 and 3 for larval rockfishes (*Sebastes* spp.) identified by cytochrome *b* sequencing after collection off Washington and Oregon during 2005–2008 and environmental covariates. Environmental data include sea surface temperature (SST) and salinity at the sea surface (1 m; SSS), Upwelling Index (UI), Pacific Decadal Oscillation (PDO) index, and North Pacific Gyre Oscillation (NPGO) index. Asterisks (*) denote species with coefficients of correlation >0.15. Each symbol represents the species composition of larvae collected in a single complete haul of a midwater trawl ordinated in species space. The arrows indicate the directionality and strength (by length of arrow) of physical correlations between hauls and physical variables measured during the collection period.

Discussion

Before the widespread use of DNA-based identifications, much of what was known about larval and juvenile rockfishes off the west coast of North America came from bycatch in multiyear seasonal surveys made in the 1960s and 1970s by using strictly visual identifications (Richardson and Laroche, 1979; Laroche and Richardson, 1980, 1981). These authors used a variety of gear to sample both pelagic larvae and juveniles, as well as settled juveniles, providing useful information on the sizes and dates of occurrence and some information on spatial distribution for 7 common species, including several examined here. Using a similar approach, we were able to identify a total of 3266 rockfish from 17 species, using visual methods alone, acknowledging that visual identification is more commonly applicable for larger size classes. Previous studies found seasonal patterns similar to those we observed, in that darkblotched, canary, widow, and yellowtail rockfish were generally present early in the summer and settled by the end of June, whereas rosethorn rockfish reached peak catches later in the summer (July and August) (Richardson and Laroche, 1979; Laroche and Richardson, 1980, 1981). Building on the earlier studies, we were able to provide information on a larger number of taxa (24) by using both genetic and visual approaches than by visual identifications alone (17) and to capture a broader size range of juveniles given the larger nets used in our study compared with those used in earlier studies. Because the list of species identified with the 2 methods did not overlap completely, the combined ap-

Table 2

Results of the analysis of indicator species for species of *Sebastes* identified either visually or on the basis of genetics for samples collected off Oregon and Washington during 2005–2008, by month or year in which samples were collected. Separate analyses were conducted for months and years. Results are combined here for ease of presentation. Only the species that had significant ($P<0.05$) indicators for a particular month or year are shown.

	Indicator value	*P*-value	Month or year
Visual identification			
S. helvomaculatus	59.0/34.3	0.0002/0.002	August 2008
Genetic identification			
S. pinniger	38.2	0.002	May
S. entomelas	37.4	0.003	June
S. flavidus	33.3	0.002	June
S. helvomaculatus	22.7	0.009	2007
S. babcocki	16.7	0.001	2007

proach allowed us to identify a total of 29 species in our samples, and to assign individuals to the WEVZ complex. Of those 29 species, 5 were identified only in the morphological collection, whereas only 12 appeared in the molecular data set. We could also examine annual patterns and seasonal patterns in the presence or absence of larval and juvenile stages of specific rockfish species for spring and summer and relate these to environmental variables at local and regional scales (both cross- and along-shelf scales).

With the publication of mitochondrial and nuclear sequences from 105 of the 110 then-described *Sebastes* species (Taylor et al., 2004; Hyde et al., 2007), it became possible to identify larval juveniles at any size. Sequence-based identification methods have been previously used to identify morphologically unidentifiable rockfish larvae and to relate distributions of these larvae to oceanographic features and natal habitat (Taylor et al., 2004; Hitchman et al., 2012; Thompson et al., 2016; Thompson et al., 2017), to describe the early development of larval rockfishes (Watson et al., 2016), and to describe the early life history among lesser-known species (Yu et al., 2015). As with previously published research in Southern California utilizing cytochrome *b* sequencing, we identified 2509 rockfish from 24 different taxa and the 4-species WEVZ complex (plus 25 unknowns), and therefore adding this approach greatly increased the level of species identification and distribution details that could be made available.

Given the difficulty or impossibility of visually identifying the earliest life stages of larval rockfish, genetic approaches offer a way to explore the diversity of important previously unidentifiable rockfish species, thus providing new information on the timing of pelagic larval and juvenile stages and distribution of these previously unexamined species. For example, NMS and our observations from the indicator species analysis that the canary, darkblotched, and widow rockfish are more common among spring samples and the rosethorn rockfish is more prevalent in summer, revealed a clear relationship between abundances of certain species and the time of year sampled. Although some of these patterns have been previously identified, we were able to expand our identifications to include a much greater diversity of species, including many of those that are unidentifiable by visual means. This newly described diversity was then related to environmental factors, such as ocean temperature, upwelling intensity, and productivity regime (PDO and NPGO indices), and season to explore temporal and spatial drivers of species diversity or mating success (Taylor et al., 2004; Thompson et al., 2016; Thompson et al., 2017). Although a detailed seasonal and annual analysis of the abundance and distribution patterns of rockfish species is beyond the scope of this study, we did observe some months and years where individual species showed greater prominence through the indicator species analysis. The years examined in this study showed substantial differences in their oceanographic conditions which may have greatly affected the cross-shelf and along-shore distributions of rockfishes (Brodeur et al., 2006; Ralston and Stewart, 2013).

Previous research on ichthyoplankton diversity and concentration in the eastern North Pacific has shown spatial variation at the local (Richardson et al., 1980; Auth and Brodeur, 2006) and regional scale (Thompson et al., 2014) and temporal variation over the short- and long-term (Brodeur et al., 2008; Auth et al., 2011; Thompson et al., 2014), all of which are influenced by regional and basin-wide environmental fluctuations (Auth et al., 2011; Auth and Brodeur, 2013). One unifying feature of much of this previous research is that some groups of larval fishes cannot be identified to the species level based on pigmentation or meristics. These unidentifiable groups include larval smelts (7 species in the family Osmeridae), rockfishes (65 species), sanddabs (2 species of the genus *Citharichthys*), and snailfishes (17 species of the genus *Liparis*) (Richardson et al., 1980; Matarese et al., 1989; Love et al., 2002; Auth et al., 2011). Our work off the coast of Oregon, like previous research in and around Southern California (Taylor et al., 2004; Thompson et al., 2016; Thompson et al., 2017), has helped illuminate the diversity of the largest of these previously unidentifiable groups of fishes.

Because of the distributional patterns we observed, we may not have sampled the offshore extent of a number of our late-larval rockfishes sufficiently because the highest catches often were found at the most offshore station along our transects. Many species spawn well offshore and move progressively shoreward as they age before finally settling in most cases in demersal habitat over the continental shelf (Laroche and Richardson, 1980; 1981). Time constraints precluded us from sampling beyond our normal sampling grid during most cruises. However, on one occasion in June 2008, we were able to trawl at a station 185 km offshore along the Newport transect (Fig. 1). This single trawl tow sampled more than 60 km farther offshore than our target stations and captured 20,756 rockfish, which were mostly late-larval individuals and too small to be visually identified. We were able to run genetic analysis on a subsample from that haul of 105 individuals that were identified as mostly widow and yellowtail rockfish. In a study of larval fish distribution out to 364 km from shore along the Newport transect and from another transect off Northern California, Auth (2009) found that the majority of *Sebastes* larvae were seaward of 120 km during the spring of 2007, but were closer to the shore during the summer months. However, as acknowledged by the author, because the larvae could not be identified to species, these shifts in regional observations could be confounded by differences in cryptic species not observed in that study. Stable isotope analysis of juvenile rockfish caught on the continental shelf also revealed that they had derived much of their previous nutrition from taxa found off the shelf, indicating potential onshore advection before settlement (Bosley et al., 2014). However, as postulated by Kamin et al. (2014) for a Gulf of Alaska population of Pacific ocean perch (*S. alutus*), these offshore populations may be subjected to substantial mortality and only a small fraction of the larvae may subsequently return to shelf nursery areas.

Because some closely related groups of rockfishes are still undergoing lineage sorting (Hyde and Vetter, 2007) or may experience mtDNA introgression (Pearse et al., 2007), it was not possible to confidently identify some individuals to species. In our sampling, the WEVZ complex represented a substantial proportion of the larval catch, and is a still-unresolved diversity of species. Although microsatellites represent one approach to separate this (and potentially other multispecies complexes) (Pearse et al., 2007), microsatellite peak sizes can vary between sequencers and PCR chemistries, and therefore would require standardization between different laboratories to produce useful data (Weeks et al., 2002; Moran et al., 2006). This need for standardization makes it more difficult to compare and use microsatellites in databases of known samples than to use DNA sequences, as used here. Ultimately, the development of a suite of linked diagnostic single-nucleotide polymorphisms from genomes of all the members of the genus *Sebastes* (microhaplotypes) may prove most effective for confidently identifying any species by a molecular approach.

Our study combines the relative speed and ease of visually identifying more distinctive species of rockfish with the power of current sequence-based genetic identification methods. This combined approach provides new information on the distribution and seasonal timing of pelagic and larval juvenile stages of several rockfish species which have been challenging to identify on the basis of traditional morphological metrics and pigmentation. However, there remain some species (i.e., the WEVZ complex) that cannot be resolved to species level with the cytochrome *b* database of known samples. Analysis down to the species level for collections that contain a high proportion of rockfish (e.g., Thompson et al., 2016) can provide valuable information for ecosystem-based fishery management. Identifying *Sebastes* larvae to species may allow estimates of spawning biomass of the more abundant species (Ralston et al., 2003; Ralston and MacFarlane, 2010) and enable managers to track recruitment over time (Ralston et al., 2013). As the availability of high throughput sequencers bring the cost per sample down substantially, molecular identification of rockfish species should become more commonplace in the future.

Acknowledgments

The authors particularly thank the captain and crew of the FV *Piky* for their assistance with sampling. This research was funded by the NWFSC Stock Assessment Improvement Program; the Oregon State University Cooperative Institute for Marine Resources Studies; the National Science Foundation Research Experiences for Undergraduates program; and the NWFSC Conservation Biology Division. We especially thank A. Thompson, G. DiNardo, T. Auth, and 4 anonymous reviewers, whose helpful comments greatly improved the manuscript.

Literature cited

Auth, T. D.
2009. Importance of far-offshore sampling in evaluating the ichthyoplankton community in the northern California Current. CalCOFI Rep. 50:107–117.
2011. Analysis of the spring-fall epipelagic ichthyoplankton community in the northern California Current in 2004–2009 and its relation to environmental factors. CalCOFI Rep. 52:148–167.
Auth, T. D., and R. D. Brodeur.
2006. Distribution and community structure of ichthyoplankton off the coast of Oregon, USA, in 2000 and 2002. Mar. Ecol. Prog. Ser. 319:199–213.

2013. An overview of ichthyoplankton research in the northern California Current region: contributions to ecosystem assessments and management. CalCOFI Rep. 54:107–126.

Auth, T. D., R. D. Brodeur, H. L. Soulen, L. Ciannelli, and W. T. Peterson.

2011. The response of fish larvae to decadal changes in environmental forcing factors off the Oregon coast. Fish. Oceanogr. 20:314–328.

Barth, J. A., B. A. Menge, J. Lubchenco. F. Chan, J. M. Bane, A. R. Kirinich, M. A. McManus, K. J. Nielsen, S. D. Pierce, and L. Washburn.

2007. Delayed upwelling alters nearshore coastal ecosystems in the northern California Current. Proc. Nat. Acad. Sci. 104:3719–3724.

Boehlert, G. W.

1977. Timing of the surface-to-benthic migration in juvenile rockfish, *Sebastes diploproa*, off southern California. Fish. Bull. 75:887–890.

Bosley, K. L, T. W. Miller, R. D. Brodeur, K. M. Bosley, A. Van Gaest, and A. Elz.

2014. Feeding ecology of juvenile rockfishes off Oregon and Washington based on stomach content and stable isotope analyses. Mar. Biol. 161:2381–2393.

Brodeur, R. D., S. Ralston, R.L. Emmett, M. Trudel, T. D. Auth, and A. J. Phillips.

2006. Anomalous pelagic nekton abundance, distribution, and apparent recruitment in the northern California Current in 2004 and 2005. Geophys. Res. Lett. 33:L22S08.

Brodeur, R. D., W. T. Peterson, T. D. Auth, H. L. Soulen, M. M. Parnel and A. A. Emerson.

2008. Abundance and diversity of coastal fish larvae as indicators of recent changes in ocean and climate conditions in the Oregon upwelling zone. Mar. Ecol. Prog. Ser. 366:187–202.

Buonaccorsi V. P., C. A. Kimbrell, E. A. Lynn, R. D. Vetter.

2002. Population structure of copper rockfish (*Sebastes caurinus*) reflects postglacial colonization and contemporary patterns of larval dispersal. Can. J. Fish. Aquat. Sci. 59: 1374–1384.

2005. Limited realized dispersal and introgressive hybridization influence genetic structure and conservation strategies for brown rockfish, *Sebastes auriculatus*. Conserv. Genet. 6:697–713.

Chenillat, F., P. Rivière, X. Capet, E. Di Lorenzo, and B. Blanke.

2012. North Pacific Gyre Oscillarion modulates seasonal timing and ecosystem functioning in the California Current upwelling system. Geophys. Res. Lett. 39:L01606.

Cowen, R. K., and S. Sponaugle.

2009. Larval dispersal and marine population connectivity. Annu. Rev. Mar. Sci. 1:443–466.

Dauble, A. D., S. A. Heppell, and M. L. Johansson.

2012. Settlement patterns of young-of-the-year rockfish among six Oregon estuaries experiencing different levels of human development. Mar. Ecol. Progr. Ser. 448:143–154.

Di Lorenzo, E., N. Schneider, K. M. Cobb, P. J. S. Franks, K. Chhak, A. J. Miller, J. C. McWilliams, S. J. Bograd, H. Arango, E. Curchitser, et al.

2008. North Pacific Gyre Oscillation links ocean climate and ecosystem change. Geophys. Res. Lett. 35:L08607.

Di Lorenzo E., K. M. Cobb, J. C. Furtado, N. Schneider, B. T. Anderson, A. Bracco, M. A. Alexander, and D. J. Vimont.

2010. Central Pacific El Niño and decadal climate change in the North Pacific. Nat. Geosci. 3:762–765.

Dufrêne, M., and P. Legendre.

1997. Species assemblages and indicator species: the need for a flexible asymmetrical approach. Ecol. Monogr. 67:345–366.

Emmett, R. L., R. D. Brodeur, and P. M. Orton.

2004. The vertical distribution of juvenile salmon (*Oncorhynchus* spp.) and associated fishes in the Columbia River plume. Fish. Oceanogr. 13:392–402.

Felsenstein, J., and G. A. Churchill.

1996. A hidden Markov model approach to variation among sites in rate of evolution. Mol. Biol. Evol. 13:93–104.

Gadgil, M.

1971. Dispersal: population consequences and evolution. Ecology. 52:253–261.

Gharrett, A. J., A. K. Gray, and J. Heifetz.

2001. Identification of rockfish (*Sebastes* spp.) by restriction site analysis of the mitochondrial ND-3/ND-4 and 12S/16S rRNA gene regions. Fish. Bull. 99:49–62.

Gray, A. K., A. W. Kendall Jr., B. L. Wing, M. G. Carls, J. Heifetz, Z. Li, and A. J. Gharrett.

2006. Identification and first documentation of larval rockfishes in southeast Alaskan waters was possible using mitochondrial markers but not pigmentation patterns. Trans. Am. Fish. Soc. 135:1–11.

He, X., J. C. Field, D. E Pearson, L. Lefebvre, S. Lindley.

2015. Status of bocaccio, *Sebastes paucispinis*, in the Conception, Monterey and Eureka INPFC areas for 2015, 270 p. Pacific Fishery Management Council, Portland, OR. [Available from website.]

Hitchman, S. M., N. B. Reyns, and A. R. Thompson.

2012. Larvae define spawning habitat of bocaccio rockfish *Sebastes paucispinis* within and around a large southern California marine reserve. Mar. Ecol. Prog. Ser. 465:227–242.

Hyde, J. R., and R. D. Vetter.

2007. The origin, evolution, and diversification of rockfishes of the genus *Sebastes* (Cuvier). Mol. Phylogenet. Evol. 44:790–811.

Ivanova, N. V., J. R. Dewaard, and P. D.N . Hebert.

2006. An inexpensive, automation-friendly protocol for recovering high-quality DNA. Mol. Ecol. Notes, 6:998–1002.

Johansson, M. L., M. A. Banks, K. D. Glunt, H. M. Hassel-Finnegan, and V. P. Buonaccorsi.

2008. Influence of habitat discontinuity, geographical distance, and oceanography on fine-scale population genetic structure of copper rockfish (*Sebastes caurinus*). Mol. Ecol. 17:3051–3061.

Kamin, L. M., K. J. Palof, J. Heifetz, and A. J. Gharrett.

2014. Interannual and spatial variation in the population genetic composition of young-of-the-year Pacific ocean perch (*Sebastes alutus*) in the Gulf of Alaska. Fish. Oceanogr. 23:1–17.

Ko, H. L., Y. T. Wang, T. S. Chiu, M. A. Lee, M. Y. Leu, K. Z. Chang, W. Y. Chen, and K. T. Shao.

2013. Evaluating the accuracy of morphological identification of larval fishes by applying DNA barcoding. PLoS ONE 8:e53451.

Kruskal, J. B.
1964. Multidimensional scaling by optimizing goodness of fit to a nonmetric hypothesis. Psychometrika 29:1–27.

Laidig, T. E., and P. B. Adams.
1991. Methods used to identify pelagic juvenile rockfish (genus Sebastes) occurring along the coast of central California. NOAA Tech. Memo. NMFS-SWFSC-166, 180 p.

Laidig, T. E., J. R. Chess, and D. F. Howard.
2007. Relationship between abundance of juvenile rockfishes (*Sebastes* spp.) and environmental variables documented off northern California and potential mechanisms for the covariation. Fish. Bull. 105:39–48.

Laroche, W. A., and S. L. Richardson.
1980. Development and occurrence of larvae and juveniles of the rockfishes *Sebastes flavidus* and *Sebastes melanops* (Scorpaenidae) off Oregon. Fish. Bull. 77:901–924.
1981. Development of larvae and juveniles of the rockfishes *Sebastes entomelas* and *S. zacentrus* (family Scorpaenidae) and occurrence off Oregon, with notes on head spines of *S. mystinus*, *S. flavidus*, and *S. melanops*. Fish. Bull. 79:231–257.

Lasker, R. (ed.).
1985. An egg production method for estimating spawning biomass of pelagic fish: application to the northern anchovy, *Engraulis mordax*. NOAA Tech. Rep. NMFS 36, 99 p.

Levin, S. A., H. C. Muller-Landau, R. Nathan, and J. Chave.
2003. The ecology and evolution of seed dispersal: a theoretical perspective. Annu. Rev. Ecol. Evol. Syst. 34:575–604.

Love, M. S., M. Yoklavich, and L. Thorsteinson.
2002. The rockfishes of the northeast Pacific, 405 p. Univ. Calif. Press, Berkeley, CA.

Mantua, N. J., S. R. Hare, Y. Zhang, J. M. Wallace, and R. C. Francis.
1997. A Pacific interdecadal climate oscillation with impacts on salmon production. Bull. Am. Meteorol. Soc. 78:1069–1079.

Matarese, A. C., A. W. Kendall Jr., D. M. Blood, and B. M. Vinter.
1989. Laboratory guide to early life history stages of northeast Pacific fishes. NOAA Tech. Rep. NMFS 80, 652 p.

McCune, B., and M. J. Mefford.
2011. PC-ORD. Multivariate analysis of ecological data. Version 6 user's booklet, 25 p. MjM Software, Gleneden Beach, OR. [Available from website.]

McCune, B., J. B. Grace, and D. L. Urban.
2002. Analysis of ecological communities, 304 p. MjM Software Design, Gleneden Beach, OR.

Moran, P., D. J. Teel, E. S. LaHood, J. Drake, and S. Kalinowski.
2006. Standardizing multi-laboratory microsatellite data in Pacific salmon: an historical view of the future. Ecol. Freshw. Fish 15:597–605.

Moser, H. G.
1996. The early stages of fishes in the California Current region. CalCOFI Atlas 33, 1505 p.

Moser, H. G., and G. W. Boehlert.
1991. Ecology of pelagic larvae and juveniles of the genus *Sebastes*. Environ. Biol. Fish. 30:203–224.

Paradis E., J. Claude, and K. Strimmer.
2004. APE: analyses of phylogenetics and evolution in R language. Bioinformatics 20:289–290.

Pearse, D. E., L. Wooninck, C. A. Dean, and J. C. Garza.
2007. Identification of northeastern Pacific rockfish using multilocus nuclear DNA genotypes. Trans. Am. Fish. Soc. 136:272–280.

Phillips, A. J., S. Ralston, R. D. Brodeur, T. D. Auth, R. L. Emmett, C. Johnson, and V. G. Wespestad.
2007. Recent pre-recruit Pacific hake (*Merluccius productus*) occurrences in the northern California Current suggest a northward expansion of their spawning area. CalCOFI Rep. 48:215–229.

Phillips, A. J., R. D. Brodeur, and A. V. Suntsov.
2009. Micronekton community structure in the epipelagic zone of the northern California Current upwelling system. Prog. Oceanogr. 80:74–92.

R Core Team.
2016. R: a language and environment for statistical computing. R Foundation for Statistical Computing, Vienna, Austria. [Available from website, accessed June 2016.]

Ralston, S., and B. R. MacFarlane.
2010. Population estimation of bocaccio (*Sebastes paucispinis*) based on larval production. Can. J. Fish. Aquat. Sci. 67:1005–1020.

Ralston, S. and I.J. Stewart.
2013. Anomalous distributions of pelagic juvenile rockfish on the U.S. West Coast in 2005 and 2006. CalCOFI Rep. 54:155–166.

Ralston, S., J. R. Bence, M. B. Eldridge, and W. H. Lenarz.
2003. An approach to estimating rockfish biomass based on larval production, with application to *Sebastes jordani*. Fish. Bull. 101:129–146.

Ralston, S., K. M. Sakuma, and J. C. Field.
2013. Interannual variation in pelagic juvenile rockfish (*Sebastes* spp.) abundance—going with the flow. Fish. Oceanogr. 22:288–308.

Richardson, S. L., and W. A. Laroche.
1979. Development and occurrence of larvae and juveniles of the rockfishes *Sebastes crameri*, *Sebastes pinniger*, and *Sebastes helvomaculatus* (family Scorpaenidae) off Oregon. Fish. Bull. 77:1–46.

Richardson, S. L., J. L. Laroche, M. D. Richardson.
1980. Larval fish assemblages and associations in the north-east Pacific Ocean along the Oregon coast, winter–spring 1972–1975. Estuar. Coast. Mar. Sci. 11:671–699.

Rocha-Olivares, A., C. A. Kimbrell, B. J. Eitner, and R. D. Vetter.
1999. Evolution of a mitochondrial cytochrome *b* gene sequence in the species-rich genus *Sebastes* (Teleostei, Scorpaenidae) and its utility in testing the monophyly of the subgenus *Sebastomus*. Mol. Phylogenet. Evol. 11:426–440.

Rocha-Olivares, A., H. G. Moser, and J. Stannard.
2000. Molecular identification and description of pelagic young of the rockfishes *Sebastes constellatus* and *Sebastes ensifer*. Fish. Bull. 98:353–363.

Sakuma, K. M., and T. E. Laidig.
1995. Description of larval and pelagic juvenile chilipepper, *Sebastes goodie* (family Scorpaenidae), with an examination of larval growth. Fish. Bull. 93:721–731.

Seeb, L. W., and A. W. Kendall Jr.
1991. Allozyme polymorphisms permit the identification of larval and juvenile rockfishes of the genus *Sebastes*. Environ. Biol. Fish. 30:191–201.

Sydeman, W. J., S. A. Thompson, M. Garcia-Reyes, M. Kahru, W.T. Peterson, and J.L. Largier.
2014. Multivariate ocean-climate indicators (MOCI) for

the central California Current: environmental change, 1990–2010. Prog. Oceanogr. 120:352–369.

Taylor, C. A., W. Watson, T. Chereskin, J. Hyde, and R. Vetter.
2004. Retention of larval rockfishes, *Sebastes*, near natal habitat in the Southern California Bight as indicated by molecular identification methods. CalCOFI Rep. 45:152–166.

Thompson, A. R., T. D. Auth, R. D. Brodeur, N. M. Bowlin, and W. Watson.
2014. Dynamics of larval fish assemblages in the California Current System: a comparative study between Oregon and southern California. Mar. Ecol. Prog. Ser. 506:193–212.

Thompson, A.R., J.R. Hyde, W. Watson, D.C. Chen, and L.W. Guo.
2016. Rockfish assemblage structure and spawning locations in southern California identified through larval sampling. Mar. Ecol. Prog. Ser. 547:177–192.

Thompson, A. R., D. C. Chen, L. W Guo, J. R. Hyde, and W. Watson.
2017. Larval abundances of rockfishes that were historically targeted by fishing increased over 16 years in association with a large marine protected area. R. Soc. Open Sci. 4:170639.

Watson, W., S. R. Charter, and C. A. Taylor Lawley.
2016. Early larvae of the swordspine rockfish (*Sebastes ensifer*) identified by molecular methods. Fish. Bull. 114:135–143.

Weeks, D. E., Y. P. Conley, R. E. Ferrell, T. S. Mah, and M. B. Gorin.
2002. A tale of two genotypes: consistency between two high-throughput genotyping centers. Genome Res. 12:430–435.

Yu, H. J., Y. J. Im, H. S. Jo, S. J. Lee, and J.-K. Kim.
2015. Morphological development of eggs, larvae, and juvenile of *Sebastes koreanus* (Scorpaeniformes: Scorpaenidae) from the Yellow Sea. Ichthyol. Res. 62:439–449.

National Marine
Fisheries Service
NOAA

Fishery Bulletin
established in 1881

Spencer F. Baird
First U.S. Commissioner
of Fisheries and founder
of *Fishery Bulletin*

Movement and mortality of Atlantic salmon kelts (*Salmo salar*) released into the Penobscot River, Maine

George A. Maynard (contact author)[1]
Lisa K. Izzo[1]
Joseph D. Zydlewski[1,2]

Email address for contact author: galphonsemaynard@gmail.com

[1] Department of Wildlife, Fisheries, and Conservation Biology
University of Maine
5755 Nutting Hall, Room 210
Orono, Maine 04469-5755
Present address for contact author: Cape Cod Commercial Fishermen's Alliance
1566 Main Street
Chatham, Massachusetts 02633

[2] U.S. Geological Survey
Maine Cooperative Fish and Wildlife Research Unit
5755 Nutting Hall, Room 210
University of Maine
Orono, Maine 04469-5755

Abstract—The Penobscot River is home to the last remaining major run of Atlantic salmon (*Salmo salar*) in the United States and the subject of a century-long stocking effort. Since the 1970s, most kelts have been released to the estuary after they spawn in a hatchery, and the iteroparous share of the run has declined to <1%. We tagged with a radio transmitter 55 kelts that had spawned at a hatchery in 2015, and released them at two locations (head of tide and ~50 km upstream) to assess 1) when kelts leave the river, 2) whether release location influences the timing of river exit, and 3) whether kelts from the upper river could outmigrate through the hydroelectric complex of the river. The kelts were tracked from November 2015 to July 2016. Although fish from both release groups left the system within one month, the majority (84%) overwintered in freshwater. Many (71%) kelts that overwintered in freshwater made upstream movements in November and December. There was no difference in upstream movement rates, timing of outmigration, or survival between the release groups. Survival to outmigration was 23.6%. This low survival to outmigration may have contributed to the precipitous decline in iteroparous Atlantic salmon from the Penobscot River over the last four decades.

Manuscript submitted 8 March 2018.
Manuscript accepted 28 June 2018.
Fish. Bull. 116:281–290 (2018).
Online publication date: 20 July 2018.
doi: 10.7755/FB.116.3-4.6

The views and opinions expressed or implied in this article are those of the author (or authors) and do not necessarily reflect the position of the National Marine Fisheries Service, NOAA.

Atlantic salmon (*Salmo salar*) populations in the United States have declined precipitously over the last several decades, and the only remaining population segment is listed as endangered under the U.S. Endangered Species Act (Fay et al., 2006). The Penobscot River historically supported spawning runs of more than 100,000 individuals (Saunders et al., 2006), but recent returns have averaged only around 1000 fish annually (Cox[1]). The U.S. Government has identified restoration of the distinct population segment of the Gulf of Maine as a high priority (NMFS and USFWS, 2005). However, Atlantic salmon face a variety of threats because of their anadromous and iteroparous life history (Legault, 2005; Maynard et al., 2017), such as overfishing, pollution, and the presence of dams (Parrish et al., 1998; Nieland et al., 2015). Although many stages of Atlantic salmon life history have been well studied (Klemetsen et al., 2003), comparatively little is known about the survival and movements of kelts (postspawning adults) after successful spawning. Because repeat spawners have increased reproductive influence in salmonine populations (Kusterle et al., 2013; Trammell et al., 2016), ensuring survival of kelts could enhance restoration efforts.

Many anadromous salmonines can spawn multiple times during their life cycle, returning to sea after each spawning event to recondition (Klemetsen et al., 2003). Survival after spawning can be high in Atlantic salmon (~80%; Chadwick et al., 1978; Jonsson et al., 1990). However, a much smaller proportion of fish survive to spawn again (Ducharme, 1969). Broadly, the outmigration of kelts takes place in two stages. A small proportion of individuals migrate directly to the sea, whereas the majority overwinter in the river before outmigrating to the marine environment during the following spring (Ruggles, 1980). For those fish that overwinter in-river, survival to outmigration is >50% (Gray et al., 1987; Downton and Reddin[2]). Across systems (North American and European rivers) and species (Atlantic salmon and steelhead, *Oncorhynchus mykiss*), downstream kelt migrations in spring are generally finished by July (Halttunen et al., 2010; Marston et al., 2012; Lacroix, 2013). Once at sea, the time needed to rebuild energy stores varies according to several factors: the amount of time previously spent in freshwater (Niemelä et al., 2006), migratory distance to marine feeding areas (Lacroix, 2013), and fish condition after spawning (Jonsson et al., 1991).

---

[1] Cox, O. 2016. Personal commun. Maine Dep. Mar. Resour., 21 State House Station, Augusta, ME 04333-0021.

The ability of kelts to survive 1) a return migration to the sea, 2) a year or more of reconditioning, and 3) a return migration to spawning grounds affects the proportion of repeat spawners, which varies from 0 to 26% for Atlantic salmon populations (Fleming and Reynolds, 2004; Niemelä et al., 2006). However, spawning runs composed of >40% repeat spawners have been reported in undammed systems in Canada that are not subject to commercial exploitation (Jessop, 1976; Saunders and Schom, 1985). The number of broods a fish has is also variable in salmonines. In steelhead, nearly all iteroparous individuals spawn no more than twice in their lifetime (Seamons and Quinn, 2010). Atlantic salmon have been documented as returning for as many as eleven spawning runs during their lives (Ducharme, 1969; Hutchings and Morris, 1985; Saunders and Schom, 1985), but with at-sea kelt survival <10% (Jonsson and Jonsson, 2004), multiple returns is likely the exception, rather than the rule.

It is unknown how recent changes to the Penobscot River (Opperman et al., 2011) may have affected migration of naturally spawned kelts from the upper reaches of the river, particularly because the downstream bypasses at all dams are closed for much of the winter, and therefore may not be operational during the postspawning period. Kelts outmigrating down the upper mainstem of the Penobscot River must pass two dams to reach the middle portion of the river (upstream from Milford Dam, and downstream from the Piscataquis River confluence [Fig. 1]), whereas kelts moving through the Piscataquis River must pass three dams to reach the same location. Once reaching the confluence of the Piscataquis and Penobscot rivers, kelts may travel downstream through the main stem of the Penobscot River to the estuary (passing Milford Dam), or migrate through the Stillwater Branch of the river through Gilman Falls Dam, Stillwater Dam, and Orono Dam (Fig. 1).

The Penobscot River has been the focus of hatchery supplementation based on sea-run broodstock since

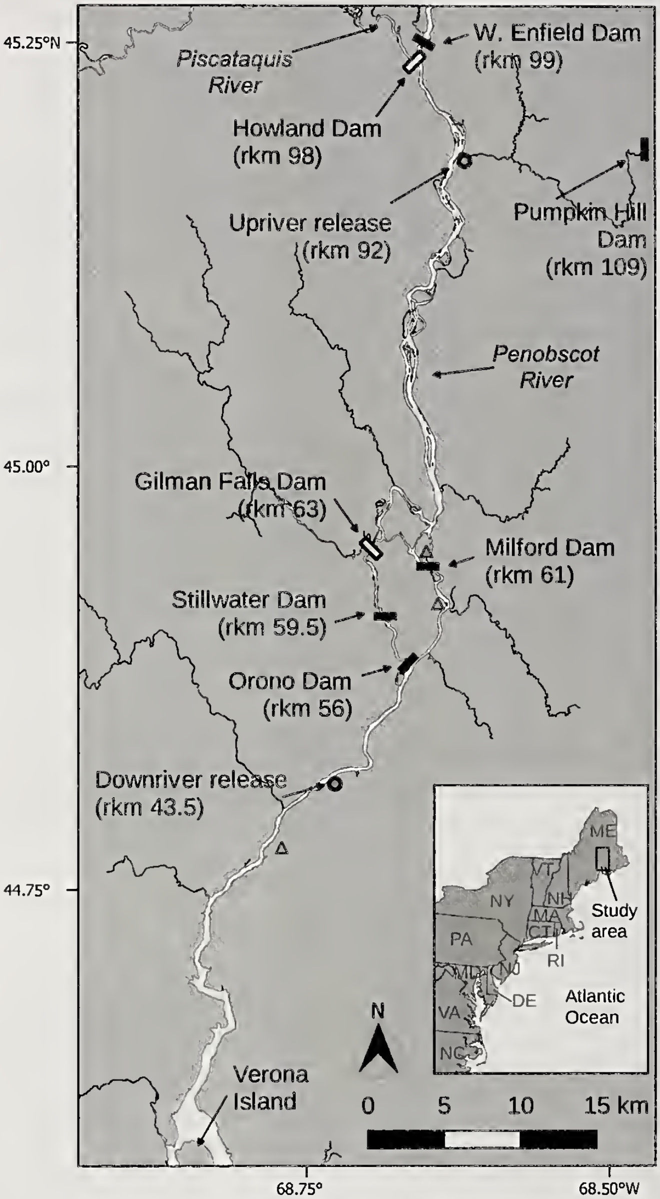

Figure 1

Map of the study area that included the Penobscot River from Orrington, Maine, at river kilometer (rkm) 33, to the West Enfield Dam. Black rectangles represent functioning hydroelectric dams that have no operable fish passage upstream from 15 November to 15 April. Open rectangles represent water control dams that are passable under certain conditions. Gray triangles represent the locations of stationary radio receivers, and circles indicate the sites where tagged kelt Atlantic salmon (*Salmo salar*) were released on 17 November 2015. River kilometer zero is located at the southwestern tip of Verona Island (516414E 4927755N, UTM Zone 19N). The area surrounded by the Milford, Orono, Stillwater, and Gilman Falls Dams is Marsh Island.

---

[2] Downton, P. R., and D. G. Reddin. 2004. Status of Atlantic salmon (*Salmo salar* L.) in Campbellton River, Notre Dame Bay (SFA 4), Newfoundland in 2003. Can. Sci. Adv. Secr., Res. Doc. 2004/043, 64 p. [Available from website.]

the late 1800s (Spidle et al., 2001). Current broodstock management practice requires the collection of mature adults from a trap at the terminus of the first fishway on the river (currently, Milford Dam) by the Maine Department of Marine Resources. These fish are transported to the U.S. Fish and Wildlife Service Craig Brook National Fish Hatchery in Orland, Maine, where they are held for up to five months before spawning is artificially induced in late October or early November. After spawning, kelts are released into the Penobscot River just downstream of the head of tide (at river kilometer [rkm] 43.5). This release point is thought to minimize spatial and temporal overlap with naturally spawning salmon and maximize survival by expediting their return to the sea (Bartron et al.[3]); however, neither of these assumptions have been tested. Because of record low returns in 2013 and 2014, 56% (18–98%) on average of all salmon returning to the Penobscot River have been taken to the hatchery as broodstock (USASAC[4]). Coinciding with decreased returns to the Penobscot River there has been a reduction in the percentage of the run of repeat spawners from an average of 1.7% in the 1980s to an average of 0.6% in recent years (Maynard et al., 2017).

Although the total number of repeat spawners in the Penobscot River has been low for several decades, their contribution to the total number of eggs produced in the system was likely important, historically. A review of salmon egg production in New England from the early 1980s to 2011 indicated that, on average, repeat spawners produced 2300 more eggs per female than virgin spawners in the Connecticut River, 3000 more eggs/female in the Sheepscot River, and 3100 more eggs/female in the Merrimack River (USASAC[3]). Similarly, research from the River Teno, Finland, found that although iteroparous Atlantic salmon numerically represented an average of 5% of the run, they accounted for an average of 7% of the total mass of salmon caught in the river (Niemelä et al., 2006). In the river systems of the Pacific Northwest, female iteroparous steelhead have a lifetime reproductive success that is 1.3 times higher than that of semelparous individuals, and iteroparous males have a lifetime reproductive success that is 2.8 times higher than that of semelparous individuals (Seamons and Quinn, 2010), indicating that this life history strategy allows some salmonines to produce more offspring than semelparity would. Previously spawned individuals may also provide an important buffer against years with low escapement (Saunders and Schom, 1985) because of their high fidelity to their natal rivers (Hansen and Jonsson, 1994) and high reproductive potential.

Research on kelt movements and survival is relatively sparse, compared with research on other life history stages of salmonines (Hubley et al., 2008). This sparsity of research is especially true in the context of individuals that are artificially induced to spawn at hatcheries. Because nearly all kelts in the Penobscot River system are the product of artificial spawning at hatcheries (i.e. the fish are anesthetized and stripped of gametes before release), a better understanding of postrelease movements may allow a targeted selection of release sites to match the need for suitable overwintering habitat, and therefore improve survival to outmigration.

Our goals were 1) to compare the postrelease movement and exit timing of kelts released at two sites in the Penobscot River, ~head of tide and upstream of the Marsh Island hydropower complex, which comprises the 4 dams that surround Marsh Island (Milford, Orono, Stillwater, and Gilman Falls), and 2) to evaluate differences in outmigration success between fish released upstream of the hydropower complex and those released downstream, in the free-flowing estuary.

Materials and methods

Study area

The Penobscot River, Maine, is the second largest watershed in New England (with an area of 22,000 km^2) and has been dammed in multiple locations since the late 1800s (Opperman et al., 2011). It also currently has the largest remaining run of Atlantic salmon in the United States and is dependent on hatchery stocking. Since the 1970s, an average of 82% of returning adult Atlantic salmon have originated from hatchery-reared smolts (USASAC[3]), and in recent years, the number is >95%.

Our study area (Fig. 1) included a 66-km section of the Penobscot River from Orrington, Maine (rkm 33), to the West Enfield Dam (rkm 99), as well as a 67-km stretch of the Piscataquis River from Howland Dam (rkm 98) to Brown's Mill Dam (rkm 165). There are 8 dams in the study area. Howland Dam has a newly constructed bypass channel that is operational in the winter months. Stillwater Dam and Gilman Falls Dam have no dedicated upstream passage facilities, and the remaining five dams (Orono, Milford, West Enfield, Pumpkin Hill, and Brown's Mill) have upstream passage facilities that are not operated between November 15 and April 15. Downstream passage facilities at Stillwater Dam, Orono Dam, and Milford Dam are closed between December 31 and April 1 because of ice, but passage may still be possible through the spillways or when water overflows the dams.

---

[3] Bartron, M. L., D. Buckley, T. King, M. T. Kinnison, G. Mackey, T. F. Sheehan, K. F. Beland and J. Marancik. 2006. Captive broodstock management plan for Atlantic salmon at Craig Brook National Fish Hatchery, 133 p. Report to the Maine Technical Advisory Committee. [Available from Protected Species Branch, Northeast Fish. Sci. Cent., Natl. Mar. Fish. Serv., NOAA, 166 Water St., Woods Hole, MA 02543-1026.]

[4] USASAC (U.S. Atlantic Salmon Assessment Committee). 2015. Annual report of the U.S. Atlantic Salmon Assessment Committee. Report No. 7—2014 activities. Kittery, Maine, February 9–12, 2015, 228 p. Prepared for U.S. Section to the North Atlantic Salmon Conservation Organization. [Available from website.]

Table 1

Minimum, median, and maximum values of total length (cm), mass (g), and body condition index for kelt Atlantic salmon (*Salmo salar*) released at an upriver and a downriver site on the Penobscot River, Maine, on 17 November 2015.

	Downriver			Upriver		
	Min	Med	Max	Min	Med	Max
Total length	72	76	85	73	77	81
Mass	3900	4481	5901	3338	4454	5561
Body condition index	−0.03	0	0.13	−0.13	0	0.16

Fish capture and tagging

Throughout the 2015 upstream migration, adult Atlantic salmon were collected at the Milford Dam lift and trap facility (rkm 61) by personnel of the Maine Department of Marine Resources. After collection, the fish were transported to Craig Brook National Fish Hatchery, approximately 56 km south of the dam, on a different river system. There, fish were held until they spawned in the fall. During the spawning process, fork length, mass, and sex of each fish were recorded. We used the residuals of log(*Mass*) regressed on log(*Total length*) to calculate body condition (Halttunen et al., 2013). On November 17, 2015, after several days of recovery from the artificial spawning procedure, 55 fish were anaesthetized with tricaine methanosufonate (MS-222) and surgically implanted with MCFT2-3L[5] radio transmitters (Lotek Wireless, Inc., Newmarket, Canada). A 16-mm incision was made offset from the ventral line and posterior to the pelvic fin girdle on the ventral side of the fish to enable closure with two or three sutures of Vicryl size 4-0 (Ethicon, Inc., Somerville, NJ). Tags had an air mass of 25.0 g and a water mass of 11.0 g, ensuring that they were <1% of the estimated body mass of the study fish, which ranged from 3.3 kg to 5.9 kg (median mass=4.4 kg). Transmitters had a 2.5- second burst rate and a tag life of < 170 days because of their use in a previous study. Of the 55 fish, 27 were released at the boat launch in Brewer, Maine (rkm 43.5, a 26-mile drive from the hatchery), downstream of the head of tide, and 28 were released at the boat launch in Passadumkeag, Maine (rkm 92, an 85 km drive from the hatchery). All releases took place within five hours of surgery on November 17, 2015.

Radio tracking

We monitored fish movements over a seven-month period from mid-November 2015 to mid-June 2016, primarily by mobile tracking with a portable receiver (SRX 800, Lotek Wireless, Inc.) during trips in the study area. These trips took place between Orrington (rkm 33) and Medway, Maine (rkm 149), on a weekly basis; more frequent trips (two or three/week) were made before ice-in (late December) and after ice-out (late April). Once a month, we used mobile tracking along the Piscataquis River to detect any fish that moved upstream through the Howland Dam bypass. All mobile tracking was conducted by using cars with omnidirectional antennas traveling along the side of the river on ME-116, U.S. Highway 2, and ME-178 at an average distance of 0.332 km (min 0.037 km, max 0.965 km), and an average speed of 64 km/h (40 mph). We also employed an array of three stationary radio receivers (SRX-DL, Lotek Wireless, Inc.) equipped with unidirectional Yagi antennas that were located between Orrington (rkm 33) and Indian Island, Maine (rkm 62; Fig. 1). One aerial survey, conducted aboard an airplane with a portable receiver, covered the mainstem Penobscot River, the Penobscot estuary, and the Piscataquis River on January 25, 2016.

Because a study with similar tagging methods found no tag loss in Atlantic salmon smolts (Stich et al., 2014), we assumed no tag loss. However, fish that remained in the same position throughout the winter, spring, and into the summer of 2016 were presumed dead. We used χ^2 tests to test for differences in survival, successful migration, and behavioral differences between the upper and lower release groups. Only fish that were detected at the most downstream receiver or fish that were detected in-river over the duration of the study were included in the survival analysis. Wilcoxon–Mann–Whitney tests were used to compare body condition index between groups of fish with different movements or survival outcomes. For the purposes of this study, we considered overwinter survival to take place between November and late April (ice-out); any movements after this were considered to take place during the spring, and we stopped tracking fish in early July 2016.

Results

We collected and tagged 55 fish from the hatchery: 53 females and two males (Table 1). All were multiseawin-

---

[5] Mention of trade names or commercial companies is for identification purposes only and does not imply endorsement by the National Marine Fisheries Service, NOAA.

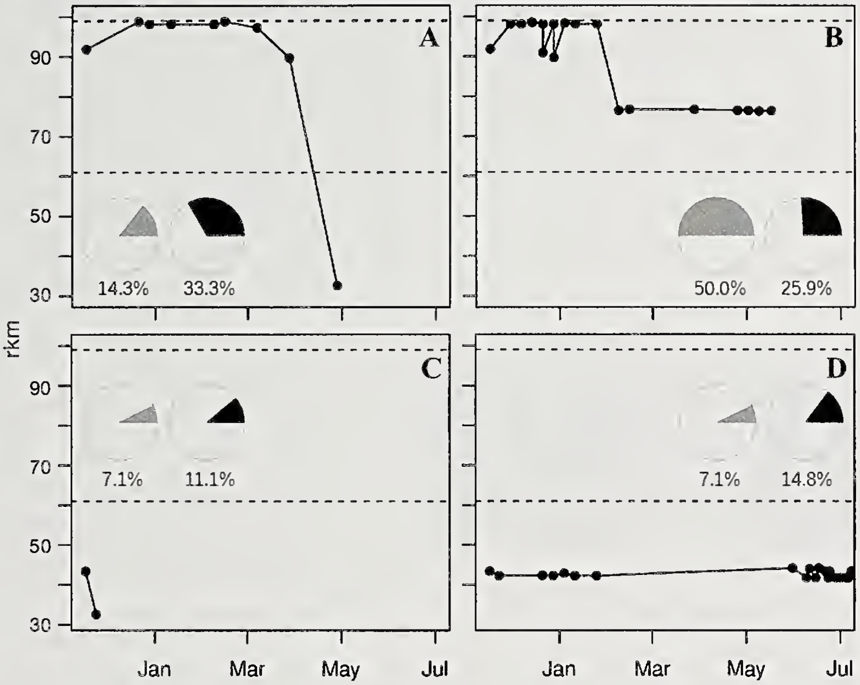

Figure 2

Representative paths of 4 tagged kelt Atlantic salmon (*Salmo salar*) tracked from mid-November 2015 to min-June 2016 on the Penobscot River, Maine. Pie charts indicate the proportion of fish that exhibited 1 of 2 movement patterns or 1 of 2 mortality types. The gray pie charts provide percentages for fish released at the upriver site at river kilometer (rkm) 92, and the black pie charts provide percentages for fish released at the downriver site at rkm 43.5. The tracks indicate fish that (**A**) overwintered in freshwater and then migrated to the estuary in the spring, (**B**) had an apparent overwinter mortality, (**C**) outmigrated rapidly (within 1 month) after release, and (**D**) had an apparent initial mortality. The dotted lines represent locations of hydroelectric dams on the main stem of the river. Because our lowest radio receiver in the Penobscot River system was located at rkm 30, detection at that point was considered successful outmigration.

ter fish (i.e. they spent ≥2 years maturing at sea), and because no grilse were tagged, only a limited number of males were available for the project. Total lengths ranged from 720 mm to 850 mm (median=770 mm). Fish masses ranged from 3.3 kg to 5.9 kg (median=4.4 kg), and body condition index ranged from −0.33 to 0.16 (median=0.01). Of the 55 fish released, 30 were detected at least once on the stationary radio array, and 49 were detected at least once during mobile tracking. Only three fish were never detected. Over half of all fish (56%) were tracked for more than 100 days (median=46 days). On the basis of detection histories (as described in the *Materials and methods* section) 19 fish from the upriver release and 20 fish from the downriver were included in the survival analysis.

Broadly considered, movement could be classified into 2 major groups overwintering in-system or rapid (within one month) downstream movement to the estuary (Fig. 2). Most of the tagged kelts (46 individuals) overwintered in the Penobscot River, and only 6 rapidly exited the system (Fig. 3). Of the 6 kelts that rapidly exited the system, 4 were initially released at the downriver site (rkm 43.5) and two were released at the upriver site (rkm 92). Many of the fish (36 individuals) that remained in the river over the winter made directed upstream movements (Fig. 4). Fish that overwintered in the system did so between rkm 33 and rkm 99, depending on where they were stocked (i.e. under most river conditions Milford Dam at rkm 61 impeded movement upstream). Of these, 15.4% of the fish were located downstream of the head of tide (~rkm 48), 34.6% were located between the head of tide and Milford Dam, and the remainder of our tagged fish (50%) overwintered between Milford Dam and the Piscataquis River confluence within the main stem of the river.

A total of 23 fish moved to the next dam upstream from their release location. Of these fish, 9 made repeated approaches to the dams over a period of days or weeks, indicating that the dams likely impeded their

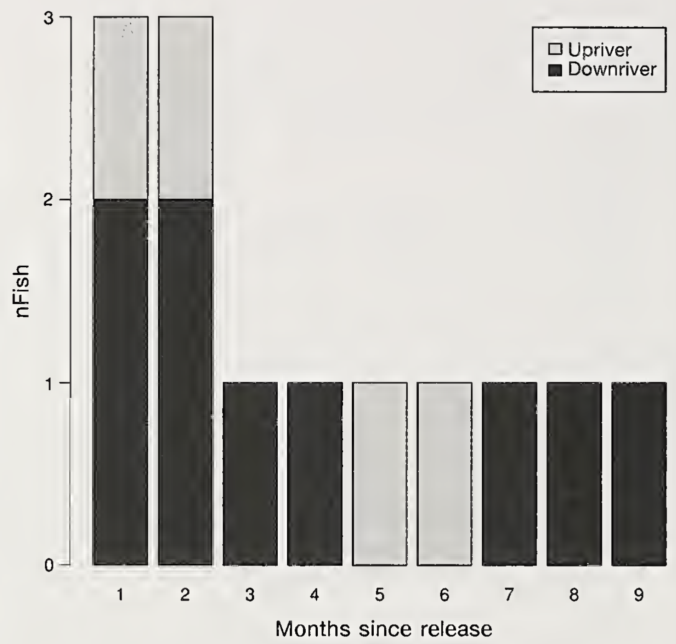

Figure 3

Timing of outmigration (in months after release) of kelt Atlantic salmon (*Salmo salar*) released in an upriver site (light gray, river kilometer [rkm] 92) and a downriver site (dark gray, rkm 43.5) on the Penobscot River, Maine, on 17 November 2015 and tracked with radio telemetry from release to mid-June 2016. The values on the y-axis represent the number of fish exiting each month.

upstream movement. Apparent overwinter survival was below 50%; 26 kelts were presumed dead in the river system and an additional 16 fish had an unknown outcome (8 from each release group).

The apparent survival for kelts released upriver was 43%. The maximum distance the 28 upper release fish could have moved upstream was 7 km before reaching the West Enfield Dam. Further movement was possible into the Passadumkeag River for up to 17 km before reaching the Pumpkin Hill Dam, although because of the absence of roads, this area was not tracked by a mobile receiver, except during our one flight. We found that 13 fish moved upstream from the release site (11 during the first month following release), and 10 of these approached the dam. Half of the fish (14/28) released upstream moved downstream past the Milford Dam. Most fish that successfully passed the dam did so before March, and only one fish descended from the upper river in May. Of the fish in this release group, 4 were documented leaving the system through the estuary, including 2 of those that initially moved upstream (Fig. 3). Of the 16 presumed fish that died in the upriver release group, 6 initially moved upstream, 8 initially moved downstream, and 2 remained within 1 rkm of the release site—a finding that indicated no relationship between initial movement choice and survival. Of the presumed mortalities, 6 occurred after the fish had moved downstream over the Milford Dam. For the purposes of these analyses, mortality and movement are not mutually exclusive (i.e. a fish that was counted as moving upstream could also be counted as a mortality).

The maximum distance that the 27 lower release fish could have moved upstream from the release point in Brewer was 17.5 km before reaching Milford Dam. Of the 23 fish that moved upstream from the release site; 13 of those approached the dam, and 1 passed the dam during a period of extreme high water in mid-December 2015, when river discharges were more than twice the 113-year median. All upstream movements originating from the downriver release site took place before the end of January. Of these fish 9 were eventually documented leaving the system, including 5 that initially moved upstream (Fig. 3). An additional 10 fish in this release group were presumed dead. Of these fish, 6 moved upstream initially, and 3 remained within 1 rkm of the release site.

A larger proportion of kelts released downriver were observed making directed upstream movements than the proportion of kelts released at the upriver location exhibiting the same behavior (85% vs. 46%, χ^2=7.498, df=1, *P*=0.006). There was no difference in apparent survival to the estuary between the upriver and downriver release groups (14% and 33%, respectively, χ^2=1.8084, df=1, *P*=0.179). Apparent mortality over the course of the study and apparent initial mortality (fish that remained within 1 rkm of the release site for the duration of the study) were not different for the upriver and downriver groups (Table 2). There was no difference in body condition index between the fish that were documented successfully leaving the system, and the fish that were presumed dead (Wilcoxon–Mann–Whitney [W]=367, *P*=0.899). There was also no difference in body condition index between the fish that made directed movements upstream and those that moved downstream (W=343, *P*=0.566).

Discussion

The results of this study suggest that the majority (88%) of kelts released into the Penobscot River overwinter in freshwater, regardless of where they are released. This finding is consistent with research from the River Teno, where about one third of individuals (35%) moved directly out to sea (Halttunen et al., 2010). Unlike Halttunen et al. (2013), we found no differences in body condition index between fish that emigrated quickly and fish that overwintered in the Penobscot River. However, our data set of outmigrating fish was considerably smaller than Halttunen et al.'s (13 vs. 166 individuals), the fish spawned artificially in a hatchery rather than naturally in the river, and our outmigrating fish were all females (as opposed to mixed sex in Haltunnen et al. (2013)).

Research from European rivers suggests that females are generally in better condition than males after spawning, likely because of low instances of aggression among female fish (Halttunen et al., 2013). Because their condition is generally better after spawning, it may be more advantageous for females to remain in the low-productivity, low-risk freshwater environment through the winter (Halttunen et al., 2013) to keep the risk of mortality low for those months, whereas males must enter the marine environment sooner to recondition. In our study, both males were presumed dead. Previous research has also documented low postspawning survival among males, which leads to a higher proportion of iteroparous fish being female (Niemelä et al., 2006; Halttunen et al., 2010). However, given that the sex-ratio of our study fish was so heavily skewed toward females, it is possible that our results are applicable only to female fish. With only 2 male fish (both released at the upriver release, and both mortalities), it is very likely that we were unable to capture the full range of male postspawning behavior.

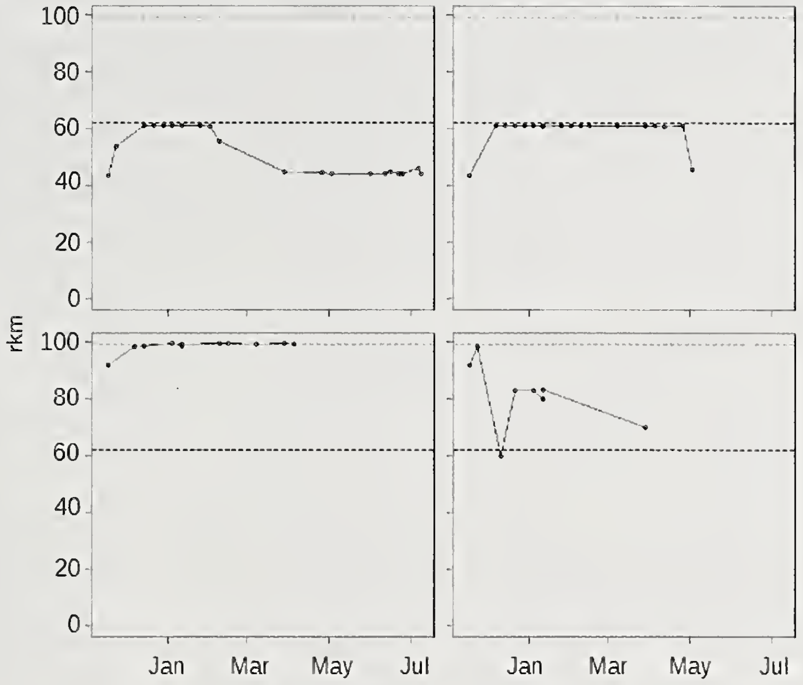

Figure 4

Representative paths of Atlantic salmon (*Salmo salar*) kelts tracked with radio telemetry from mid-November 2015 to min-June 2016 on the Penobscot River, Maine. The tracks in the top 2 graphs indicate movement of 2 kelts (from the release site at river kilometer [rkm] 43.5) after the first month of release and the tracks in the bottom 2 graphs indicate movement of 2 kelts from the release site at rkm 92. The horizontal dotted lines represent dams located at rkm 61 and rkm 99 on the main stem of the river.

Unlike the fish in several other studies of kelt movements (Baglinière and Porcher, 1994; Komandina-Douthwright et al., 1997; Cunjak et al., 1998), many fish in our study made directed, upstream movements after release. However, in our study, kelts were released downriver from where they would naturally spawn, if not taken to the hatchery. This provides at least 2 possible reasons why fish would move upstream: to seek more advantageous habitat conditions and because they may have been more physiologically similar to ripe adults than postspawning adults owing to the artificial spawning process at the hatchery.

Further study is needed to clarify the causes of upstream movements, such as those we observed in hatchery-spawned kelts. One possible explanation for upstream movement centers on habitat availability. Estuarine habitat may be most desirable for kelts during severe winters (Cunjak et al., 1998) because of the absence of frazil ice in that area. However, the winter of 2015–16 was unusually mild, which may have contributed to kelts overwintering farther upstream in the watershed during our study. Additionally, studies in other systems (Saunders, 1960; Komandina-Douthwright et al., 1997; Cunjak et al., 1998) have found that habitat complexity (e.g. lakes, large pools, islands, and other structure) was positively correlated with higher instream survival of postspawning fish and higher usage of freshwater habitat instead of marine or estuarine habitat. The first 38 rkm of the Penobscot River are commercially navigable, and relatively few islands (natural or artificial) exist downstream of rkm 48. In contrast, the reach between rkm 48 and rkm 61 is filled with artificial islands built for log drives, as well as several large natural islands. Therefore, for fish released at the downriver site, most of the complex habitat exists upriver of their release point. However, because the habitat between rkm 61 and rkm 99 is mostly complex, braided channel with many small islands, upstream migration would not be necessary for fish released at the upriver location to reach suitable overwintering habitat.

Another possible explanation for upstream migration after release is physiological. In our study, most of the fish in the lower release group and nearly half of the fish in the upper release group made directed movements upstream after release. However, other researchers have found that kelts move downstream after spawning (Baglinière and Porcher, 1994). Upstream movements late in the spawning season, as documented here, have only been documented in fish that were still ripe (Komandina-Douthwright et al.,

Table 2

Presumed mortality of kelt Atlantic salmon (*Salmo salar*) released at an upriver and a downriver site on the Penobscot River, Maine, on 17 November 2015 and tracked with radio telemetry from time of release to mid-June 2016. Fish presumed to be initial mortalities are those that remained within 1 km of their release site for the duration of the study. Fish presumed to be overwinter mortalities are those that remained at a fixed location in the river for several months, including the end of the study in mid-June 2016. Total presumed mortality includes both initial mortalities and overwinter mortalities. Mortality between the two release sites was compared using a chi-square (χ^2) test.

Mortality	Upriver (28 individuals)	Downriver (27 individuals)	χ^2	df	*P*
Initial	2 (0.071)	3 (0.111)	0.002	1	0.966
Overwinter	14 (0.500)	7 (0.259)	2.432	1	0.119
Total	16 (0.571)	10 (0.370)	1.496	1	0.221

1997). Because spawning of all the fish in our study was artificially induced in a hatchery, many still had gametes in the abdominal cavity when we surgically implanted tags. Physiological mechanisms to motivate upstream migration before spawning have been noted in previous studies (Bendall et al., 2012), therefore it is possible that our kelts were behaving more like ripe adults than postspawning adults, given that gametes were still present. The majority (95.3%) of upstream movements in individuals from both release sites ceased within a month of release. Therefore, without further knowledge of the physiology of each fish, it is difficult to determine a trigger for upstream movement.

Regardless of the mechanism behind upstream movement, the fact that kelts continue to move throughout the fall and early winter may be of concern to river managers. During this time of year, fish passage structures (in both upstream and downstream directions) are typically closed to avoid damage from ice and debris (Simpson[6]). Keeping these facilities operational in the winter may require substantial expenditures of effort and capital, but may also provide an opportunity for better survival, particularly for kelts moving in a downstream direction.

Because of the logistics of maintaining the radio receiver array, we were unable to place receivers on the Stillwater Branch of the river. Because of this gap in coverage, we were unable to determine the predominant path choice around Marsh Island (rkm 56–63) for fish outmigrating from the upriver release location. In the future, securing access to sites along this portion of the river could help determine whether path choice around the island influences mortality in the lower river. Previous research on Atlantic salmon smolts has shown that downstream passage at hydroelectric facilities results in decreased survival farther downriver (Stich et al., 2015). Because path choice influences the number of dams passed (e.g. there is one dam on the east side of the island and three on the west, Fig. 1), it may be also be linked to survival. Just as smolts are at risk of being descaled, of movement delays, and depredation at dams, these sites may also pose risks to downstream migrating kelts.

In both release groups, 8 tags were lost to the radio network, and we were unable to ascertain their area of disposition. The lack of transmissions from these tags could be due to a number of factors. First and foremost, the tags were all repurposed from an earlier study of upstream migrating Atlantic salmon, and therefore their batteries had already been somewhat depleted. Additionally, some tags may have been removed from the watershed either by poachers or wildlife (e.g. birds of prey). Finally, the most downriver receiver in the system covered a portion of the river that is inundated with salt water at high tide. Salt water can interfere with radio signals and likely reduced the probability of detection at that receiver during certain time periods.

Survival of kelts released into the Penobscot River was relatively low, compared with survival in European rivers, which may contribute to the observed declines in the number of multispawning individuals in the population (Maynard et al., 2017). Apparent initial mortality (fish that remained within 1 km of release for the duration of the study) was <15% in both release groups. There was no significant difference in apparent overwinter mortality between the groups. Apparent survival to outmigration was at least 23.6% (13/55 individuals) , which is considerably lower than documented survival to outmigration in the River Imsa (65–85%; Jonsson et al., 1990) in Norway and in the Burrishoole River in Ireland (40%; Piggins, 1990). Because 2015–2016 was an unusually warm winter, an absence of ice cover on the river may have contributed to low survival because kelts are known to use ice for refuge from aerial predators (Cunjak et al., 1998) such as bald eagles (Willson and Halupka, 1995). Since the initiation of the Penobscot River Restoration Project, the proportion of bald eagle diets made up of marine-derived nutrients has been increasing (Call, 2015). Although survival to repeat spawning varies among river systems (2–25%, Jonsson et al., 1991), multispawning returns to the Penobscot River have averaged 0.04% in the past decade. This percentage is below that of reports from degraded rivers in France where multispawning individuals made up 0.5–3% of spawning runs (Bardonnet and Baglinière, 2000).

---

[6] Simpson, M. 2017. Personal commun. Maine Dep. Mar. Resour., 21 State House Station, Augusta, ME 04333-0021.

The majority of kelts released into the Penobscot River overwintered in freshwater or the estuary rather than makimg a rapid exit to the marine environment. There was no measurable difference in migratory timing between fish released downstream of the head of tide and those released ~50 km upstream, and some fish stocked upstream were able to successfully migrate to the ocean through one or two hydroelectric facilities. Survival rates were comparable for the two release groups, but were lower than expected. Additionally, the majority of tagged fish exhibited directed, upstream movements more characteristic of ripe fish than spent fish. Survival and movement patterns may have been influenced by an unusually mild winter. Future research may benefit from a longer time-series of data, as well as better quantification of the reproductive status of the fish. The focus of this study was to document the possibility of adult Atlantic salmon requiring passage both upstream and downstream at dams in the Penobscot River during time periods when these facilities traditionally are nonoperational.

Acknowledgments

The Penobscot River Restoration Trust, the American Recovery and Reinvestment Act of 2009, the National Marine Fisheries Service, the U.S. Geological Survey, the U.S. Fish and Wildlife Service, and the University of Maine provided funding. C. Domina, D. Buckley, M. Simpson, S. Clark, A. Molina Moctezuma, K. Boyd, R. Spencer, H. Brinson, the Penobscot Indian Nation, the City of Old Town, the Pate family, and the Maine Warden Service provided additional support. This study was performed under the auspices of University of Maine IACUC protocol no. A2014-09-08.

Literature cited

Baglinière, J. L., and J. P. Porcher.
1994. Les stocks de reproducteurs et le comportement lors de la migration génésique. *In* Le saumon Atlantique: biologie et gestion de la ressource (J. C. Gueguen and P. Prouzet), p. 101–122. IFREMER, Brest, France.

Bardonnet, A., and J.-L. Baglinière.
2000. Freshwater habitat of Atlantic salmon (*Salmo salar*). Can. J. Fish. Aquat. Sci. 57:497–506.

Bendall, B., A. Moore, D. Maxwell, P. Davison, N. Edmonds, D. Archer, D. Solomon, V. Greest, R. Wyatt, and K. Broad.
2012. Modelling the migratory behaviour of salmonids in relation to environmental and physiological parameters using telemetry data. Fish. Manage. Ecol. 19:475–483.

Call, E.
2015. River birds as indicators of change in riverine ecosystems. Ph.D. diss., 129 p. Univ. Maine, Orono, ME.

Chadwick, E. M. P., T. R. Porter, and P. Downton.
1978. Analysis of growth of Atlantic salmon (*Salmo salar*) in a small Newfoundland river. J. Fish. Res. Board Can. 35:60–68.

Cunjak, R. A., T. D. Prowse, and D. L. Parrish.
1998. Atlantic salmon (*Salmo salar*) in winter: "the season of parr discontent"? Can. J. Fish. Aquat. Sci. 55(S1): 161–180.

Ducharme, L. J. A.
1969. Atlantic salmon returning for their fifth and sixth consecutive spawning trips. J. Fish. Res. Board Can. 26:1661–1664.

Fay, C., M. Bartron, S. Craig, A. Hecht, J. Pruden, R. Saunders, T. Sheehan, and J. Trial.
2006. Status review for anadromous Atlantic salmon (*Salmo salar*) in the United States, 294 p. Report by the Atlantic Salmon Biological Review Team to the National Marine Fisheries Service and US. Fish and Wildlife Service. [Available from website.]

Fleming, I. A., and J. D. Reynolds.
2004. Salmonid breeding systems. *In* Evolution illuminated: salmon and their relatives (A. P. Hendry and S. C. Stearns, eds.), p. 264–294. Oxford Univ. Press, Inc., New York.

Gray, R. W., J. D. Cameron, and A. D. McLennan.
1987. Artificial reconditioning, spawning and survival of Atlantic salmon, *Salmo salar* L., kelts in salt water and survival of their F1 progeny. Aquac. Fish. Manage. 18:309–326.

Halttunen, E., A. H. Rikardsen, E. B. Thorstad, T. F. Næsje, J. L. A. Jensen, and Ø. Aas.
2010. Impact of catch-and-release practices on behavior and mortality of Atlantic salmon (*Salmo salar* L.) kelts. Fish. Res. 105:141–147.

Halttunen, E., J. L. A. Jensen, T. F. Næsje, J. G. Davidsen, E. B. Thorstad, C. M. Chittenden, S. Hamel, R. Primicerio, and A. H. Rikardsen.
2013. State-dependent migratory timing of postspawned Atlantic salmon (*Salmo salar*). Can. J. Fish. Aquat. Sci. 70:1063–1071.

Hansen, L. P., and B. Jonsson.
1994. Homing of Atlantic salmon: effects of juvenile learning on transplanted post-spawners. Anim. Behav. 47:220–222.

Hubley, P. B., P. G. Amiro, A. J. F. Gibson, G. L. Lacroix, and A. M. Redden.
2008. Survival and behaviour of migrating Atlantic salmon (*Salmo salar* L.) kelts in river, estuarine, and coastal habitat. ICES J. Mar. Sci. 65:1626–1634.

Hutchings, J. A., and D. W. Morris.
1985. The influence of phylogeny, size and behaviour on patterns of covariation in salmonid life histories. Oikos 45:118–124.

Jessop, B. M.
1976. Distribution and timing of tag recoveries from native and nonnative Atlantic salmon (*Salmo salar*) released into Big Salmon River, New Brunswick. J. Fish. Res. Board Can. 33:829–833.

Jonsson, B., and N. Jonsson.
2004. Factors affecting marine production of Atlantic salmon (*Salmo salar*). Can. J. Fish. Aquat. Sci. 61:2369–2383.

Jonsson, N., B. Jonsson, and L. P. Hansen.
1990. Partial segregation in the timing of migration of Atlantic salmon of different ages. Anim. Behav. 40:313–321.

Jonsson, N., L. P. Hansen, and B. Jonsson.
1991. Variation in age, size and repeat spawning of adult Atlantic salmon in relation to river discharge. J. Anim. Ecol. 60:937–947.

Klemetsen, A., P.-A. Amundsen, J. B. Dempson, B. Jonsson, N. Jonsson, M. F. O'Connell, and E. Mortensen.
2003. Atlantic salmon *Salmo salar* L., Brown Trout *Salmo trutta* L. and Arctic Charr *Salvelinus alpinus* (L.): a review of aspects of their life histories. Ecol. Freshw. Fish 12:1–59.

Komandina-Douthwright, S. M., D. Caissie, and R. A. Cunjak.
1997. Winter movement of radio-tagged Atlantic salmon (*Salmo salar*) kelts in relation to frazil ice in pools of the Miramichi River. Can. Tech. Rep. Fish. Aquat. Sci. 2161, 66 p.

Kusterle, S., E. Halttunen, E. B. Thorstad, T. F. Naesje, J. L. A. Jensen, A. Gallo-Bueno, E. Olague, and A. H. Rikardsen.
2013. The gill maggot *Salmincola salmoneus* as an indicator of repeat spawning in Atlantic salmon *Salmo salar*. J. Fish Biol. 82:1068–1073.

Lacroix, G. L.
2013. Population-specific ranges of oceanic migration for adult Atlantic salmon (*Salmo salar*) documented using pop-up satellite archival tags. Can. J. Fish. Aquat. Sci. 70:1011–1030.

Legault, C. M.
2005. Population viability analysis of Atlantic salmon in Maine, USA. Trans. Am. Fish. Soc. 134:549–562.

Marston, B. H., R. E. Johnson, and S. Power.
2012. Steelhead studies from the Situk River in southeast Alaska, 2002–2008. Alaska Dep. Fish Game, Fish. Data Ser. 12–40, 26 p. [Available from website.]

Maynard, G. A., M. T. Kinnison, and J. D. Zydlewski.
2017. Size selection from fishways and potential evolutionary responses in a threatened Atlantic salmon population. River Research and Applications 33:1004–1015.

Nieland, J. L., T. F. Sheehan, and R. Saunders.
2015. Assessing demographic effects of dams on diadromous fish: a case study for Atlantic salmon in the Penobscot River, Maine. ICES J. Mar. Sci. 72:2423–2437.

Niemelä, E., J. Erkinaro, M. Julkunen, E. Hassinen, M. Länsman, and S. Brørs.
2006. Temporal variation in abundance, return rate and life histories of previously spawned Atlantic salmon in a large subarctic river. J. Fish Biol. 68:1222–1240.

NMFS and USFWS (National Marine Fisheries Service and U.S. Fish and Wildlife Service).
2005. Recovery plan for the Gulf of Maine distinct population segment of Atlantic salmon (*Salmo salar*), 268 p. National Marine Fisheries Service, Silver Spring, MD. [Available from website.]

Opperman, J. J., J. Royte, J. Banks, L. R. Day, and C. Apse.
2011. The Penobscot River, Maine, USA: a basin-scale approach to balancing power generation and ecosystem restoration. Ecol. Soc. 16(3):7.

Parrish, D. L., R. J. Behnke, S. R. Gephard, S. D. McCormick, and G. H. Reeves.
1998. Why aren't there more Atlantic salmon (*Salmo salar*)? Can. J. Fish. Aquat. Sci. 55(S1):281–287.

Piggins, D. J.
1990. Annual Report XXXIV. The Salmon Research Trust of Ireland, 34, Newport, Ireland.

Ruggles, C. P.
1980. A review of the downstream migration of Atlantic salmon. Can. Tech. Rep. Fish. Aquat. Sci. 952, 39 p.

Saunders, J. W.
1960. The effect of impoundment on the population and movement of Atlantic salmon in Ellerslie Brook, Prince Edward Island. J. Fish. Res. Board Can. 17:453–473.

Saunders, R. L., and C. B. Schom.
1985. Importance of the variation in life history parameters of Atlantic salmon (*Salmo salar*). Can. J. Fish. Aquat. Sci. 42:615–618.

Saunders, R., M. A. Hachey, and C. W. Fay.
2006. Maine's diadromous fish community: past, present, and implications for Atlantic salmon recovery. Fisheries 31:537–547.

Seamons, T. R., and T. P. Quinn.
2010. Sex-specific patterns of lifetime reproductive success in single and repeat breeding steelhead trout (*Oncorhynchus mykiss*). Behav. Ecol. Sociobiol. 64:505–513.

Spidle, A. P., W. B. Schill, B. A. Lubinski, and T. L. King.
2001. Fine-scale population structure in Atlantic salmon from Maine's Penobscot River drainage. Conserv. Genet. 2:11–24.

Stich, D. S., M. M. Bailey, and J. D. Zydlewski.
2014. Survival of Atlantic salmon (*Salmo salar*) smolts through a hydropower complex. J. Fish Biol. 85:1074–1096.

Stich, D. S., M. M. Bailey, C. M. Holbrook, M. T. Kinnison, and J. D. Zydlewski.
2015. Catchment-wide survival of wild- and hatchery-reared Atlantic salmon smolts in a changing system. Can. J. Fish. Aquat. Sci. 72:1352–1365.

Trammell, J. L. J., D. E. Fast, D. R. Hatch, W. J. Bosch, R. Branstetter, A. L. Pierce, J. W. Blodgett, and C. R. Frederiksen.
2016. Evaluating steelhead kelt treatments to increase iteroparous spawners in the Yakima River Basin. North Am. J. Fish. Manage. 36:876–887.

Willson, M. F., and K. C. Halupka.
1995. Anadromous fish as keystone species in vertebrate communities. Conserv. Biol. 9:489–497.

National Marine
Fisheries Service
NOAA

Fishery Bulletin
established in 1881

Spencer F. Baird
First U.S. Commissioner
of Fisheries and founder
of *Fishery Bulletin*

A comparison of length distributions of rockfishes (*Sebastes* spp.) from submersible and trawl surveys off central California

Diana L. Watters (contact author)
E. J. Dick

Email address for contact author: diana.watters@noaa.gov

Southwest Fisheries Science Center
National Marine Fisheries Service, NOAA
110 McAllister Way
Santa Cruz, California 95060

Abstract—Data from the West Coast Bottom Trawl Survey and from surveys conducted with a manned submersible in nearby untrawlable areas were used to compare length distributions for greenspotted rockfish (*Sebastes chlorostictus*), greenstriped rockfish (*S. elongatus*), canary rockfish (*S. pinniger*), and vermilion rockfish (*S. miniatus*) off central California. For all 4 species, broader size ranges and greater proportions of small fish were present in the data from the submersible surveys, and length distributions were significantly different ($P<0.01$) in comparisons of all lengths from the submersible surveys with all lengths from the trawl surveys, as well as in comparisons of lengths from the submersible surveys and trawl surveys over trawlable habitat. For 3 species, length distributions were significantly different in comparisons of lengths obtained from submersible surveys on trawlable and on untrawlable habitats. Trawl selectivity curves from recent stock assessments were evaluated in relation to the length data for greenspotted, greenstriped, and canary rockfish. Although derived from a larger spatiotemporal extent than our study, greenspotted and greenstriped rockfish selectivity curves appear to account for the reduced frequency of small fish in the trawl survey, whereas the canary rockfish selectivity curve does not. Similar comparisons between submersible and trawl-survey rockfish lengths from other regions of the west coast could help address spatial variability in trawl survey selectivity and further inform selectivity functions for stock assessments.

Rockfishes (genus *Sebastes*) have been historically significant for California commercial and recreational fisheries. Approximately 40 of the more than 60 species that occur off California have been harvested over the last 150 years (Love et al., 2002; Love, 2006). Most of these species occur at depths of 30–500 m on the continental shelf and upper continental slope off California, and associate with complex rocky seafloor habitats, such as pinnacles, rock ridges, boulders, canyon walls, and cobbles, mixed with varying amounts of low relief soft sediments (Love and Yoklavich, 2006). The diversity of deepwater rockfishes and the complex habitats that they occupy make them difficult to study and manage.

Most Pacific rockfishes are managed by the Pacific Fisheries Management Council in accordance with its Pacific Coast Groundfish Fishery Management Plan and stock assessment process (website), as first required by the Magnuson–Stevens Fishery Conservation and Management Act of 1976. Since 1999, several rockfish species have recovered from an overfished to a rebuilt status; currently, 2 species remain classified as overfished and in rebuilding status (cowcod [*S. levis*]; and yelloweye rockfish [*S. ruberrimus*]). However, regulatory measures implemented to reduce fishing mortality for rebuilding rockfish stocks have also reduced the amount of fishery-dependent data available for stock assessments (Field et al., 2006; Starr et al., 2016). A principal source of fishery-independent data for rockfish stock assessments is the Northwest Fisheries Science Center (NWFSC) West Coast Bottom Trawl Survey (hereafter referred to as the trawl survey; Keller et al., 2017), which cannot be conducted in complex rocky habitats where the highest densities of most deep-water rockfishes occur. Recognizing that trawl survey data may not represent many rockfish populations adequately, the Pacific Fisheries Management Council has encouraged the development of survey methods in untrawlable areas and research on the relative density, age, and length composition of rockfishes in trawlable and untrawlable areas (PFMC[1]). In particular, comparisons of length composition data between trawlable and untrawlable

Manuscript submitted 24 January 2018.
Manuscript accepted 9 July 2018.
Fish. Bull. 116: 291–301 (2018).
Online publication date: 31 July 2018.
doi: 10.7755/FB.116.3-4.7

The views and opinions expressed or implied in this article are those of the author (or authors) and do not necessarily reflect the position of the National Marine Fisheries Service, NOAA.

---

[1] PFMC (Pacific Fishery Management Council). 2013. Groundfish fishery management plan. *In* Research and data needs 2013, p. 21–31. Pacific Fishery Management Council, Portland, OR.. [Available at website.]

areas could increase understanding of trawl-survey selectivity, thereby improving model estimates of stock abundance.

Length composition data are among the fundamental sources of information used to assess fish populations (Ono et al., 2015), and sampled lengths ideally would represent the true distribution of lengths in a population. Length distributions are used to estimate critical population parameters (e.g., growth, mortality, recruitment), and the selectivity of fishing gear or scientific sampling methods. Length-dependent selectivity values are estimated from the fit of a stock assessment model to trawl survey data; selectivity can be thought of as a function of the availability of all lengths in the population to the trawl gear and the efficiency with which the gear samples those available lengths (Sampson, 2014; Weinberg et al., 2016). Selectivity also can be considered as the probability of a fish being sampled in relation to its length (Maunder et al., 2014). The selectivity function relates the index of abundance from the trawl survey to the estimate of total population abundance from the stock assessment model, and can interact with related model parameters, such as growth and natural mortality. Therefore, appropriate specification of selectivity is critical for reliable model outputs, evaluation of stock status, and resulting management recommendations (Maunder et al., 2014; Sampson, 2014; Weinberg et al., 2016).

Submersible surveys of demersal rockfishes that are most abundant in deepwater, untrawlable habitats can provide non-extractive, fishery-independent estimates of abundance, size composition, and biomass for stock assessments, e.g., cowcod (Yoklavich et al., 2007; Dick and MacCall, 2014); and yelloweye rockfish (O'Connell et al.[2]). Such surveys provide spatially explicit data that reveal patterns in abundance, size, and biomass, as well as habitat associations and community structure that are not possible with other survey methods (Yoklavich et al., 2000; Yoklavich and O'Connell, 2008; Wedding and Yoklavich, 2015). Length composition data from submersible surveys of rockfishes in areas of untrawlable habitat can be used to assess the extent to which length data from trawl surveys represent these populations on a regional basis, and to provide information to aid stock assessors with choosing a function that best represents trawl survey selectivity for a given species.

In this study, we examined length data collected off central California in trawl surveys and from surveys conducted with a manned submersible in nearby untrawlable areas. Our objectives were to compare length distributions of demersal rockfishes sampled in these two surveys, to evaluate the extent to which they might differ, and thereby to inform trawl survey selectivity functions used in stock assessments for selected species.

Materials and methods

Our study area was located off central California within the region bounded by latitudes 36°N (just south of Big Creek) and 37°N (Davenport), which was the geographic extent of the most recent submersible surveys conducted during a 7-yr period 2003–2009 (Fig. 1). We chose the period 2003–2009 for our study because our initial examination of length data for several species sampled during the trawl survey indicated that we would need to combine data from multiple years to ensure adequate data for comparison.

Submersible surveys of fishes and habitats were conducted with the 2-person *Delta* (Delta Oceanographics,[3] Torrance, CA) during daytime hours (typically 0700–1700) between late August and early November in years 2003, 2004, 2007, 2008, and 2009. Surveys of a total of 919 strip transects 2 m in width and averaging 248 m in length (standard deviation [SD] 54.4) were conducted at depths ranging from 24 to 326 m in submarine canyon and continental shelf locations. Strip-transect surveys of 10-min duration were directed by a scientific navigator aboard the support FV *Velero IV* and were located in areas of rocky substrata determined from maps of bathymetry and interpreted seafloor habitat (Monterey Bay Aquarium Research Institute, website; California State University Monterey Bay Seafloor Mapping Lab, website; Yoklavich et al., 1997; Eittreim et al., 2002). The position of the submersible was displayed in ArcGIS, vers. 9.0–9.3 (Esri, Redlands, CA) and tracked at 1- to 3-s intervals with an ORE Trackpoint II ultra-short baseline (USBL) acoustic system (EdgeTech, West Wareham, MA) and WinFrog software (Fugro, Leidschendam, Netherlands). The length of each transect was estimated either from the edited and smoothed USBL navigation data, or from a MiniRLG2 ring laser gyrocompass (Teledyne TSS, Watford, UK) and NavQuest 600 Micro Doppler Velocity Log (LinkQuest, Inc., San Diego, CA) mounted on the outside of the submersible. Details about the *Delta* survey vehicle, its associated equipment, and visual survey methods are described by Laidig and Yoklavich (2016) and Yoklavich and O'Connell (2008).

From inside *Delta*, a pilot and a scientist conducted the transect surveys. The pilot operated the submersible within 1 m of the seafloor at a speed of 0.3–0.5 m/s (0.5–1.0 kn), while the scientist identified and counted all fishes within the transect, and estimated their total lengths (TL) to the nearest 5 cm by direct observation in situ. A video camera and lights (Laidig and Yoklavich, 2016), mounted externally on the starboard side of

---

[2] O'Connell, V., C. Brylinsky, and D. Carlile. 2003. Demersal shelf rockfish stock assessment and fishery evaluation report for 2004. Alaska Dep. Fish Game., Reg. Inf. Rep. 1J03-39, 36 p. [Available from website]

[3] Mention of trade names or commercial companies is for identification purposes only and does not imply endorsement by the National Marine Fisheries Service, NOAA.

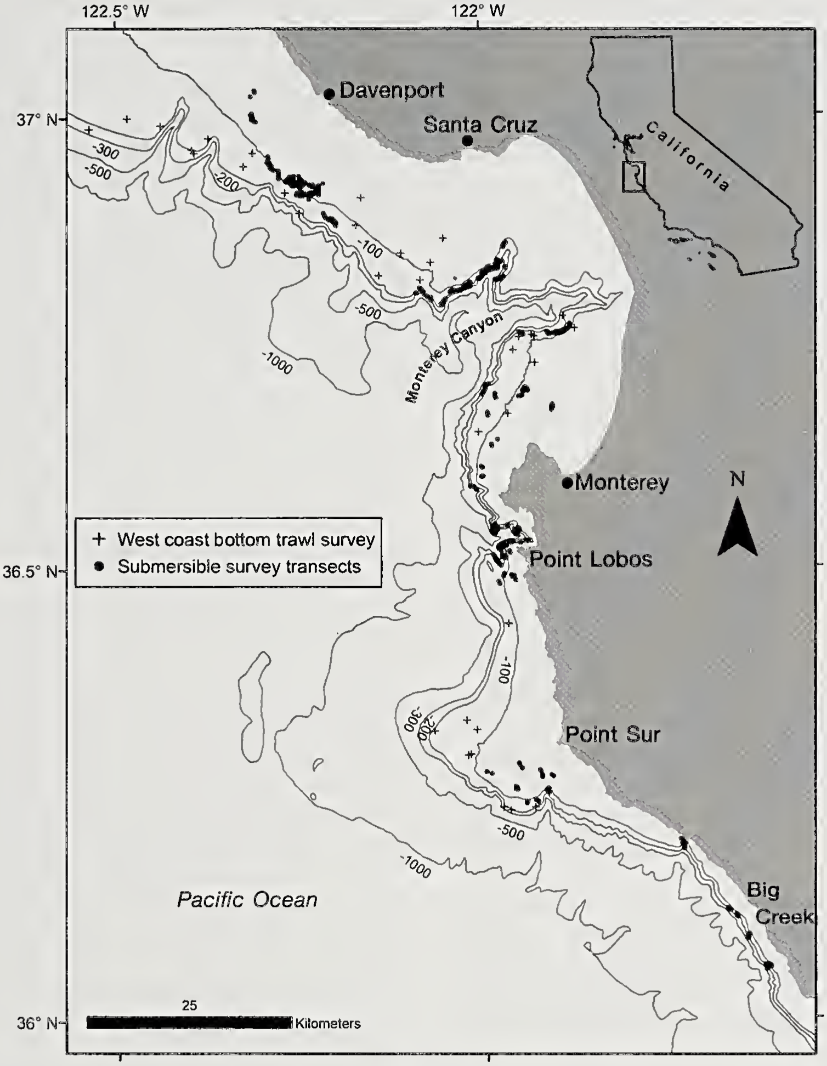
122.5° W
122° W
37° N
36.5° N
36° N
Davenport
Santa Cruz
California
Monterey Canyon
Monterey
Point Lobos
Point Sur
Big Creek
Pacific Ocean
N
+ West coast bottom trawl survey
● Submersible survey transects
-100
-200
-300
-500
-1000
25
Kilometers

Figure 1

The study area off central California with locations where transects of submersible surveys (black dots) and hauls of the Northwest Fisheries Science Center West Coast Bottom Trawl Survey (black crosses) were conducted from 2003 through 2009. Only transects and hauls with positive occurrence of one or more of the following 4 rockfish species at depths 55–326 m are shown: greenspotted rockfish (*Sebastes chlorostictus*), greenstriped rockfish (*S. elongatus*), vermilion rockfish (*S. miniatus*), and canary rockfish (*S. pinniger*). Depth contours are in meters.

the submersible above the scientist's viewport, recorded the view of the transect area and the scientist's narration. Two parallel lasers, spaced 20 cm apart on either side of the camera, aided estimates of fish lengths. A handheld sonar gun was used by the scientist to estimate and maintain the 2-m transect width. The time of each fish observation, along with counts and length estimates, was entered into a relational database during subsequent video analysis.

The amount and type of seafloor habitat within each subsmersible transect were defined from a video review. Contiguous patches comprised primary (>50% of the area) and secondary (>20% of the area) habitat types delineated by time (at least a 3-s duration) along each transect. Habitat types were 1) high-relief rock outcrop (>1 m and <3 m in-place rock), pinnacle (>3 m, isolated rock outcrop) and boulder (>25 cm); and 2) low-relief cobble (>6 cm and <25 cm), flat rock, brachiopod bed, pebble (>2 cm and <6 cm), gravel (>4 mm and <2 cm), sand, and mud. The area of each habitat patch was estimated by multiplying the 2-m transect width by the patch length. We categorized these habitat patches as untrawlable or trawlable after consulting with scientists familiar with the trawl survey and our habitat classification method (Whitmire,[4] Wakefield[5]). Untrawlable habitats were considered to be primary and secondary combinations of at least 1 high-relief type, e.g., boulder-boulder, rock-mud, or sand-pinnacle. Trawlable habitats were primary and secondary combinations of low-relief types, e.g., cobble-cobble, cobble-mud, mud-mud, flat rock-sand. Trawlable habitats within a transect were considered to be proxies for the type of area surveyed by a trawl, although these patches were too small to be trawled. We noted the occurrence of each fish on untrawlable or trawlable habitat patches.

The current trawl survey has been conducted annually off the U.S. west coast since 2003, from Cape Flattery, Washington (48.3°N latitude), to the border with Mexico (32.6°N latitude). Detailed descriptions of the survey design, sampling allocation, protocols, and equipment are provided by Keller et al. (2017). A stratified, random grid design and chartered commercial bottom trawlers were used to sample depths 55–1280 m during daylight (after sunrise and before sunset). Cells within the grid were 3.7 km (2.0 nautical mile [nmi]) latitude by 2.8 km (1.5 nmi) longitude in size and were selected randomly from depth and latitudinal strata. Within a selected cell, the captain of the vessel surveyed the seafloor with sonar to find suitable areas that were large enough to accommodate a 15-min trawl haul conducted at a speed of 1.1 m/s (2.2 kn). Trawlable habitat types were low to moderate in relief and included little substrata larger than cobble (Wakefield[5]).

The trawl net was an Aberdeen-type bottom trawl (NET Systems, Inc., Bainbridge Island, WA) with a 14.0-cm (5.5-in) stretch mesh and 3.8-cm (1.5-in) mesh liner that extended from the middle of the intermediate section to the codend. The spread of the net when deployed was approximately 5 m high and 14 m at the wing tips. The footrope had a continuous series of 25.4-cm (10-in) rubber disks that allowed the net to pass over cobbles (Wakefield[5]). Predetermined species of management concern or interest were subsampled randomly for individual length measurements. Depending on the species, up to 100 individuals were measured (fork length [FL]) to the nearest cm from each haul (Keller et al., 2017).

Trawl survey data were obtained from the NWFSC Data Warehouse: (website). We selected trawl hauls with the project name “Groundfish Slope and Shelf Combination Survey,” with a “satisfactory” performance (determined from sensors attached to the trawl net to monitor bottom contact and the net opening [Keller et al., 2017]), and from latitudes 36° to 37°N and years 2003–2009, resulting in a total of 139 hauls conducted at depths 60–1208 m from June through October.

We examined the length data from the trawl and submersible surveys for harvested deepwater rockfishes that commonly occur off central California within the overlapping depth range of the two surveys (55–326 m) (Love et al., 2002). Species with at least 50 length records from each survey were considered for comparison. We also considered species that have different orientations to the seafloor (i.e., on-the-bottom dwellers, near-the-bottom dwellers) and habitat associations, as described in Yoklavich et al. (2000), Love et al. (2002), and Laidig et al. (2009). On the basis of these considerations, we selected 4 rockfishes for analysis: greenspotted rockfish (*S. chlorostictus*), a bottom-dwelling species that occurs on a wide range of habitats; greenstriped rockfish (*S. elongatus*), a bottom-dwelling species that occurs primarily on low-relief cobble and mud; canary rockfish (*S. pinniger*), a near-bottom species that occurs over high-relief rock; and vermilion rockfish (*S. miniatus*), a near-bottom species that occurs over high-relief rock.

From submersible transects and trawl hauls (i.e., samples) with positive occurrences and length data for each of these 4 species, we examined the number of samples, total area sampled, and numbers and depths of fish measured from each survey. Fish length data from depths <55 m in the submersible survey were eliminated to match the shallow depth limit of the trawl survey. Fish length data from the trawl survey fell within the 326-m maximum depth of the submersible survey; therefore none was eliminated. Fish lengths measured from the trawl survey were converted from FL to TL by using conversions from Echeverria and Lenarz (1984). Within the 2 surveys, length data for each species were weighted by sampling effort.

For each species, we compared 1) all lengths from trawl and submersible surveys; 2) lengths from the submersible survey associated with untrawlable and trawlable habitats; and 3) lengths from trawl and submersible surveys associated with trawlable habitats. For these comparisons, we plotted lengths as the percentage of total frequency, using trawl data binned to 5-cm increments (bin as the midpoint) to match the format of the submersible data, and we added the trawl survey selectivity curve (not available for vermilion rockfish) from the most recent stock assessment to the plots with trawl data. To test whether 2 length-frequency distributions came from the same distribution, we used Pearson’s chi-square two-sample test in R statistical software, vers. 3.3.2 (R Core Team, 2016) and trawl data binned to 5-cm increments. The means of the length data and the 10%, 50%, and 90% quantiles were calculated (trawl data, however, not binned) with R statistical software (R Core Team, 2016).

Results

The spatial distribution of submersible transects and trawl hauls with 1 or more of the 4 species present in our study from depths ≥55 m was fundamentally

---

[4] Whitmire, C. 2017. Personal commun. Northwest Fish. Sci. Cent., Natl. Mar. Fish. Serv., NOAA, 99 Pacific St., Bldg. 255-A, Monterey, CA 93940.

[5] Wakefield, W. 2017. Personal commun. Northwest Fish. Sci. Cent., Natl. Mar. Fish. Serv., 2032 SE OSU Dr., Newport, OR 97365-5275.

Table 1

Characteristics of samples from submersible and bottom-trawl surveys used to compare length distributions of 4 species of rockfish (*Sebastes* spp.) off central California (36–37°N latitude) during 2003–2009. Habitats categorized as trawlable within the submersible surveys were considered rough proxies for the trawl survey because they were too small to be trawled. Common depth ranges for species are from Love et al. (2002).

Species	Survey	No. of transects or hauls	Total area sampled (m^2)	Area of trawlable habitat surveyed (%)	No. of fish measured	Avg. depth and depth range (m) of measured fish	Common depth range (m) of species
Greenspotted rockfish	Submersible	503	250,970	40	3282	132 (55–307)	30–363
	Trawl	20	318,699	100	292	109 (85–239)	
Greenstriped rockfish	Submersible	369	189,596	47	2157	125 (80–299)	100–250
	Trawl	28	461,814	100	601	126 (94–264)	
Vermilion rockfish	Submersible	139	65,846	22	695	111 (55–203)	50–150
	Trawl	6	90,812	100	80	111 (81–121)	
Canary rockfish	Submersible	120	53,313	27	667	108 (55–233)	80–200
	Trawl	9	144,062	100	90	98 (84–161)	

different (Fig. 1). A total of 609 submersible transects were clustered in canyons and areas of relief, whereas 35 trawl hauls were dispersed outside of these areas. Length data from the trawl and submersible surveys were collected from overlapping depths throughout the common depth range of all 4 species (Table 1). Range of depth was broader for the submersible data. Trawlable habitat represented less than 50% of the total habitat sampled along submersible transects and varied by species. Transects with vermilion and canary rockfishes present contained the least amount of trawlable habitat, while those with greenspotted and greenstriped rockfishes contained greater amounts of habitat categorized as trawlable. In general, the amount of seafloor area sampled in relation to the number of fish measured was considerably greater for trawl hauls than for submersible transects.

The first comparison, that of length distributions of all individuals of each of the 4 species, revealed significantly different distributions for the 2 surveys (Pearson's chi-square two-sample test, $P<0.001$), and there was a broader range of lengths and greater proportion of small fish in the submersible data (Fig. 2, Table 2). Greater proportions of greenspotted and greenstriped rockfishes <30 cm TL and <20 cm TL respectively, and canary and vermilion rockfishes <40 cm TL and <45 cm TL respectively, were present in the submersible data than in the trawl data. Binned maximum lengths from the 2 surveys were the same for greenstriped (40 cm TL) and vermilion (60 cm TL) rockfishes, 5 cm TL larger in the submersible survey for greenspotted rockfish (50 cm TL), and 15 cm TL larger in the submersible survey for canary rockfish (70 cm TL). Greenspotted rockfish length distributions were most similar between the surveys, although two peaks were present in the trawl survey data; all but the smallest (5 cm TL) and largest (50 cm TL) length bins were represented in trawl survey data for this species. Length distributions of vermilion and canary rockfishes were most dissimilar between the surveys; several length bins with data from the submersible survey were missing data from the trawl survey, and the 10% length quartiles differed by ca. 10-cm-TL.

Trawl survey selectivity curves for greenspotted and greenstriped rockfishes are consistent with a reduced proportion of small fish compared with the proportion from the submersible survey (Fig. 2). The disproportionate number of small canary rockfish in the submersible survey, compared with that in the trawl survey, is not consistent with the estimated trawl selectivity curve for that species. If canary rockfish larger than 15 cm TL are 100% vulnerable to the trawl survey, as implied by the selectivity curve, the expected proportions of small sizes would be at least as large as those in the submersible survey.

The second comparison, that of length distributions of fish from the submersible survey on untrawlable and trawlable habitats (Fig. 3), revealed significantly different distributions for greenspotted, greenstriped, and canary rockfishes (Pearson's chi-square two-sample test, $P<0.001$), whereas those of vermilion rockfish were not (Table 3). Mean lengths for all, except vermilion rockfish, were smaller on trawlable than on untrawlable habitat. All sizes of greenspotted rockfish were present on both habitat types; however, small (<20 cm TL) fish occurred in greater proportion on trawlable than on untrawlable habitat. Greenstriped rockfish, with almost equal numbers of lengths from the 2 habitats, had a greater proportion of small (<20 cm TL) fish on trawlable habitat. The small number of canary rockfish that were surveyed on trawlable habitat (35 individuals) also had a greater proportion of small (<20 cm TL) fish than the proportion of small fish present on untrawlable habitat. Although length distributions

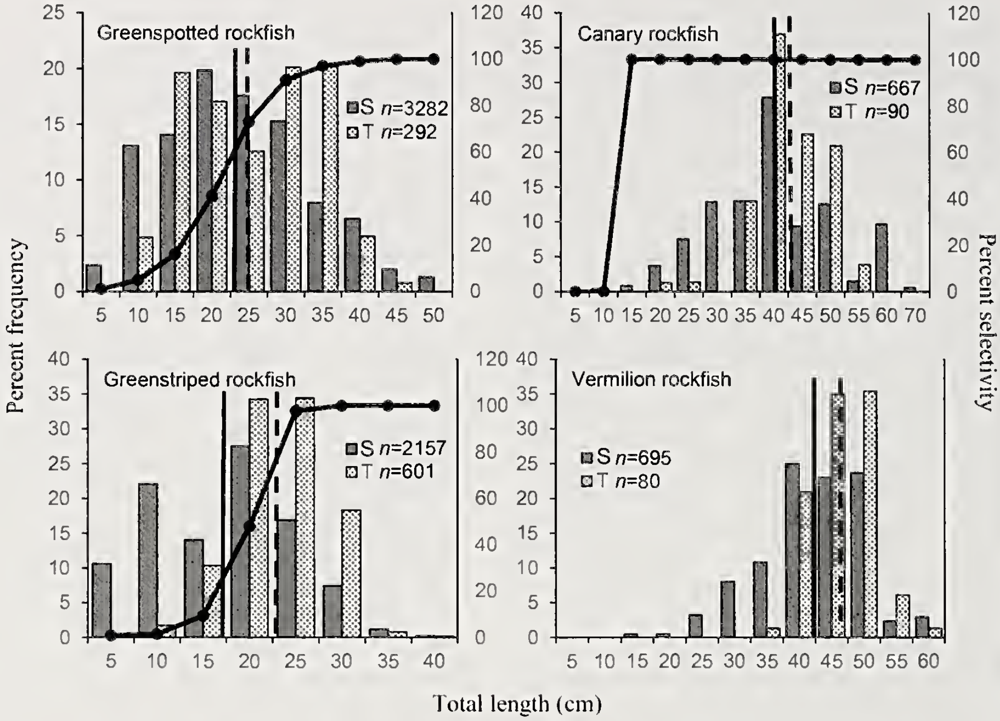

Figure 2

Length-frequency distributions of 4 species of rockfish (*Sebastes* spp.) sampled in submersible surveys (S, dark gray bars) and the Northwest Fisheries Science Center West Coast Bottom Trawl Survey (T, checkered bars) conducted off central California (36–37°N latitude) during 2003–2009. The curved line represents the bottom-trawl selectivity function from the most recent stock assessment for each species (not available for vermilion rockfish, *Sebastes miniatus*). The solid and dashed vertical lines indicate the mean lengths from submersible and bottom-trawl surveys, respectively.

Table 2

Values for 10%, 50%, and 90% total length quantiles (cm) and results of a chi-square two-sample test in comparing length distributions of all individuals of 4 species of rockfish (*Sebastes* spp.) from submersible surveys in untrawlable areas and trawl surveys conducted off central California (36–37°N latitude) during 2003–2009. Length data were estimated to the nearest 5 cm during submersible surveys and to the nearest 1 cm during trawl surveys. For the chi-square test, length data from trawl surveys were binned to 5-cm increments (bin as midpoint) to match the format of data from submersible surveys.

Species	Submersible 10%, 50%, 90% length quantiles	Trawl 10%, 50%, 90% length quantiles	Chi-square two-sample test
Greenspotted rockfish	10, 25, 35	14, 26, 36	88.311, df=9, *P*<0.001
Greenstriped rockfish	5, 20, 25	17, 23, 29	314.36, df=7, *P*<0.001
Vermilion rockfish	30, 45, 50	42, 47, 52	29.5, df=9, *P*<0.001
Canary rockfish	25, 40, 60	37, 42, 50	50.354, df=11, *P*<0.001

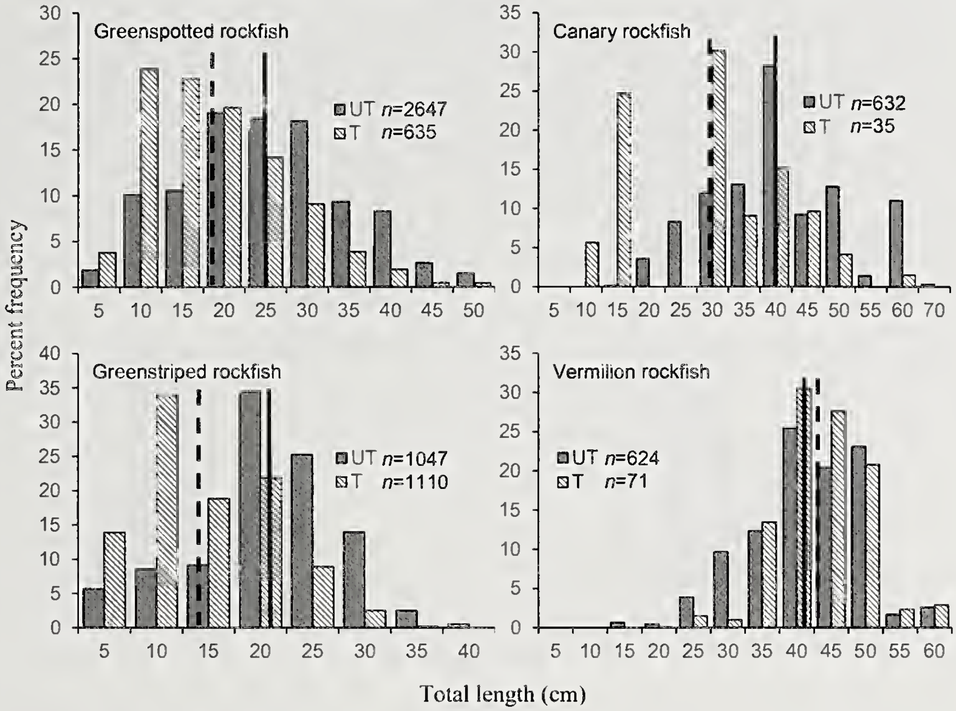

Figure 3

Length-frequency distributions of 4 species of rockfish (*Sebastes* spp.) on untrawlable high-relief habitat (UT, dark gray bars) and trawlable low relief habitat (T, hatched bars) from submersible surveys conducted off central California (36–37°N latitude) during 2003–2009. The solid and dashed vertical lines indicate the mean lengths of fish on untrawlable and trawlable habitats, respectively.

Table 3

Values of 10%, 50%, and 90% total length quantiles (cm) and results of a chi-square two-sample test in comparing length distributions of 4 species of rockfish (*Sebastes* spp.) from submersible surveys conducted in untrawlable and trawlable habitat off central California (36–37°N latitude) during 2003–2009. Length data were estimated to the nearest 5 cm.

Species	10%, 50%, 90% length quantiles, untrawlable habitat	10%, 50%, 90% length quantiles, trawlable habitat	Chi-square two-sample test
Greenspotted rockfish	10, 25, 40	10, 15, 30	235.33, df=9, $P<0.001$
Greenstriped rockfish	10, 20, 30	5, 15, 25	466.99, df=7, $P<0.001$
Vermilion rockfish	30, 40, 50	35, 45, 50	9.2217, df=9, $P=0.4171$
Canary rockfish	25, 40, 60	15, 30, 45	202.52, df=11, $P<0.001$

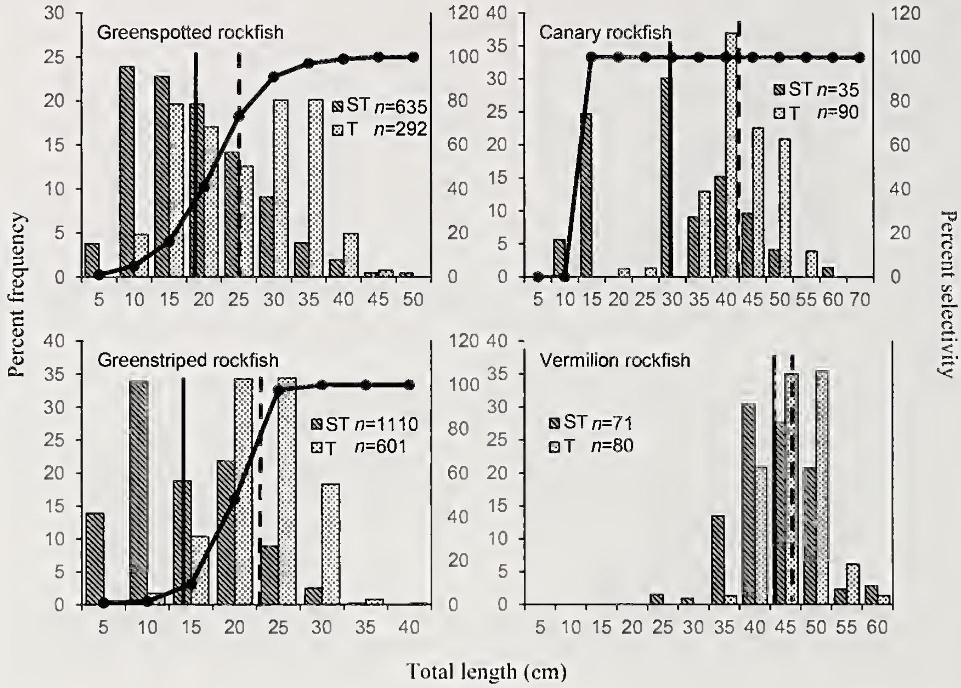

Figure 4

Length-frequency distributions of 4 species of rockfish (*Sebastes* spp.) on trawlable low-relief habitat from submersible surveys (ST, dark gray bars with diagonal hatches) and the Northwest Fisheries Science Center West Coast Bottom Trawl Survey (T, checkered bars) conducted off central California (36–37°N latitude) during 2003–2009. The curved line represents the bottom-trawl selectivity function from the most recent stock assessment for each species (not available for vermilion rockfish, *Sebastes miniatus*). The solid and dashed vertical lines indicate the mean lengths from submersible and bottom-trawl surveys, respectively.

of vermilion rockfish on the 2 habitats were not significantly different, fish <35 cm TL occurred in greater proportion on untrawlable habitat.

The third comparison, that of length distributions of fish from submersible surveys on low-relief trawlable habitat with those from the trawl survey (Fig. 4) was significantly different for all 4 species (Pearson's chi-square two-sample test, $P<0.001$; Table 4). In these comparisons, the dissimilarity in length distributions between the two surveys was even more apparent for greenspotted, greenstriped, and canary rockfishes than when all submersible survey data for these species, regardless of habitat, were compared with trawl survey data (Fig. 2, Table 2). The difference in the proportion of small fish present in the two surveys was particularly pronounced for greenstriped and canary rockfishes, with 10% length quartiles of 5 and 17 cm TL (greenstriped) and 15 and 37 cm TL (canary) in submersible and trawl survey data, respectively. In contrast, length distributions for vermilion rockfish were more similar between surveys than length distributions for the other species, owing to a greater proportion of large vermilion rockfish (>45 cm TL) on trawlable habitat in the submersible survey data.

Discussion

Our study provides a useful comparison of length data collected by the West Coast Bottom Trawl Survey and nearby submersible surveys in untrawlable areas, for some deepwater rockfishes off central California. Although the trawl survey samples areas of soft and low-relief habitats where relatively low densities of many rockfishes occur, there were enough length data for comparisons of some species that associate mostly with mixed and high-relief rocky habitats. The broader length and depth distributions present in the submersible survey data allowed informative comparisons with the trawl survey data. We could not directly address whether the low proportion of small sizes in the trawl data was due to habitat (i.e., small fish not available on trawlable habitat) or gear selectivity. However, the greater proportion of small sizes present on trawlable habitats in the submersible survey data (in particular for greenstriped rockfish), and the similar maximum lengths present in both surveys (Fig. 4) suggest that gear selectivity was the cause. Similarly, commercial trawl gear selects for larger sizes and would not be expected

Table 4

Values for 10%, 50%, and 90% total length quantiles (cm) and results of a chi-square two-sample test in comparing length distributions of 4 species of rockfish (*Sebastes* spp.) from submersible surveys in low-relief (<25 cm), trawlable habitat and from trawl surveys conducted off central California (36–37°N latitude) during 2003–2009. Length data were estimated to the nearest 5 cm during submersible surveys and to the nearest 1 cm during trawl surveys. For the chi-square test, length data from trawl surveys were binned to 5-cm increments (bin as midpoint) to match the format of data from submersible surveys.

Species	10%, 50%, 90% length quantiles, untrawlable habitat	10%, 50%, 90% length quantiles, trawlable habitat	Chi-square two-sample test
Greenspotted rockfish	10, 15, 30	14, 26, 36	138.9, df=9, $P<0.001$
Greenstriped rockfish	5, 15, 25	17, 23, 29	574.01, df=7, $P<0.001$
Vermilion rockfish	35, 45, 50	42, 47, 52	16.58, df=7, $P<0.02032$
Canary rockfish	15, 30, 45	37, 42, 50	73.905, df=10, $P<0.001$

to cause the reduced numbers of small sizes we observed in the trawl survey data.

An important consideration for our study was the accuracy of visually estimated fish lengths from the submersible survey. Trawl length data are in-hand measurements to the nearest cm, whereas submersible length data are visually estimated underwater to the nearest 5 cm with the aid of paired lasers. Yoklavich et al. (2007) conducted a study to address the error associated with visual estimates of fish length from the *Delta* submersible and found lengths were underestimated by 1.1 cm on average. Given that the trawl survey data were binned to 5-cm increments for plotting and the chi-square test, and maximum lengths from the submersible survey were similar or greater than those from the trawl survey, we did not consider the relatively small amount of error associated with visually estimated length data to have contributed greatly to the differences found in our study.

Before our comparisons of lengths, we surmised that lengths from the submersible survey would be more similar to lengths from the trawl survey for greenspotted and greenstriped rockfishes than for canary and vermilion rockfishes, on the basis of known habitat associations of these species that would make them more or less available to the trawl survey. To some extent, this assumption held true. Greenspotted rockfish, which associate with a wide variety of high- and low-relief habitats (Yoklavich et al., 2000; Love et al., 2002; Laidig et al., 2009), had similar length distributions and mean lengths between the surveys when all fish, regardless of habitat, were compared; the distributions were significantly different, however, because of the large amount of length data from the submersible survey. Canary and vermilion rockfishes associate strongly with high-relief rock habitats (Yoklavich et al., 2000; Love et al., 2002; Laidig et al., 2009), had the most dissimilar length distributions between the surveys for all fish regardless of habitat, and had the least amount of length data from the trawl survey. Our result for greenstriped rockfish was somewhat surprising because, given that this species associates most commonly with low-relief trawlable habitats (Yoklavich et al., 2000; Love et al., 2002; Jagielo et al., 2003; Laidig et al., 2009) and had the greatest amount of length data (601 measurements) from the trawl survey, we did not expect to find such strong dissimilarity in the length distributions between the surveys. However, the trawl survey selectivity curve from the stock assessment for greenstriped rockfish (Hicks et al., 2009) correctly assumes that smaller fish were not sampled by the trawl survey.

Given that adults of many rockfish species are known to associate with high-relief rocky habitats, for assessments based on trawl survey data, it is often assumed that selectivity for the survey is "dome-shaped," i.e., availability of larger fish to the survey may decline beyond a given size (Dick et al., 2011; Taylor and Wetzel, 2011; Hamel et al., 2013; He et al., 2015). One mechanism for this pattern could be ontogenetic movement into untrawlable habitat (Love and Yoklavich, 2008). Although limited in spatial and temporal extent compared with stock assessments based on trawl survey data from the entire U.S. west coast and multiple years, our results for these 4 species suggest that the major difference between size compositions from the submersible and trawl surveys may be a reduced frequency of smaller individuals in the trawl survey. The estimated selectivity curves in the assessments of greenspotted and greenstriped rockfishes appear to account for this difference, but for the selectivity curve for the canary rockfish assessment, all fishes larger than ~15 cm TL are assumed to be 100% available to the gear. It is important to note that the assessments are based on data from years and areas not represented in this analysis, which may be the reason for the differences in length composition observed in our study. These differences would imply that selectivity varies over time or space (or both). Time-varying selectivity is commonly assumed in rockfish assessments, although spatial variability in survey selectivity is considered less often, despite known latitudinal clines in size for many rockfishes (Fraidenburg, 1980; Gertseva et al., 2010; Keller et al., 2012). The differences we observed between surveys also could be due to a reduction in availability of large fish to the submersible survey, but that seems unlikely given that we found greater proportions of large sizes for 3 species on untrawlable habitat patches (Fig. 3, Table 3). With regard to survey efficiency, the probability of detection of fish in submersible surveys increases with fish size, and the reaction of large rockfishes to the *Delta* has been found to be minimal (Yoklavich et al., 2007; Laidig and Yoklavich, 2016).

A number of studies have compared other aspects of data collected during underwater visual surveys and trawl surveys of rockfishes, including fish density on trawlable habitat (Adams et al., 1995), trawl catch efficiency (Krieger, 1993), fish frequency of occurrence and weights on trawlable and untrawlable habitat (Starr et al., 2016), and species composition and densities on trawled and untrawlable habitat (Jagielo et al., 2003). Lauth et al. (2004) estimated size-specific selectivity for a trawl survey of thornyheads (*Sebastolobus* spp.) off Oregon, using independent estimates of density and lengths obtained with a video camera sled on trawlable habitat. Lauth et al. (2004) calculated much lower selectivity values for fish >30 cm TL than the most recent stock assessment (which was based on data from California, Oregon, and Washington), raising the question of spatial variability in trawl survey selectivity for thornyheads.

As far as we know, ours is the first study to compare length distributions of rockfishes from trawl surveys with those from submersible surveys conducted in nearby areas inaccessible to trawls. Additional comparisons can be made for other species from these central California data sets, and from existing submersible and trawl data sets from southern California. Similar comparisons of rockfish lengths estimated from submersible and trawl surveys from other regions of the west coast could help address spatial variability in trawl survey selectivity (Sampson, 2014) and assumptions about the trawl selectivity functions used in stock assessments for rockfishes.

Acknowledgments

We thank M. Yoklavich, principal investigator for submersible surveys; R. Starr, co-principal investigator in 2007-2008; T. Laidig, L. Snook, M. Love, M. Nishimoto, and D. Schroeder for field data collection and video processing; the *Delta* and R/V *Velero* crews; and the California Ocean Protection Council for partial funding. We appreciate T. Hay's assistance with the FRAM Data Warehouse, and the many NWFSC personnel and vessel crews that conduct the West Coast Bottom Trawl Survey. Comments from J. Field, A. Keller, M. Yoklavich, and three anonymous reviewers improved the manuscript.

Literature cited

Adams, P. B., J. L. Butler, C. H. Baxter, T. E. Laidig, K. A. Dahlin, and W. W. Wakefield.
1995. Population estimates of Pacific coast groundfishes from video transects and swept-area trawls. Fish. Bull. 93:446–455.

Dick, E. J., and A. D. MacCall.
2014. Status and productivity of cowcod, *Sebastes levis*, in the Southern California Bight, 2013, 166 p. Report to the Pacific Fishery Management Council, Portland, Oregon. Fish Ecol. Div., Southwest Fish. Sci. Cent., Natl. Mar. Fish. Serv., Santa Cruz, CA. [Available from website.]

Dick, E. J., D. Pearson, and S. Ralston.
2011. Status of greenspotted rockfish (*Sebastes chlorostictus*) in U.S. waters off California, 189 p. Report to the Pacific Fishery Management Council, Portland, OR. Fish Ecol. Div., Southwest Fish. Sci. Cent., Natl. Mar. Fish. Serv., Santa Cruz, CA. [Available from website.]

Echeverria, T., and W. H. Lenarz.
1984. Conversions between total, fork, and standard lengths in 35 species of *Sebastes* from California. Fish. Bull. 82:249–251.

Eittreim, S. L., R. J. Anima, and A. J. Stevenson.
2002. Seafloor geology of the Monterey Bay area continental shelf. Mar. Geol. 181:3–34.

Field, J. C., A. E. Punt, R. D. Methot, and C. J. Thomson.
2006. Does MPA mean “Major Problem for Assessments”? Considering the consequences of place-based management systems. Fish Fish. 7:284–302.

Fraidenburg, M. E.
1980. Yellowtail rockfish, *Sebastes flavidus*, length and age composition off California, Oregon, and Washington in 1977. Mar. Fish. Rev. 42(3–4):54–56.

Gertseva, V. V., J. M. Cope, and S. E. Matson.
2010. Growth variability in the splitnose rockfish *Sebastes diploproa* of the northeast Pacific Ocean: pattern revisited. Mar. Ecol. Prog. Ser. 413:125–136.

Hamel, O. S., J. M. Cope, and S. Matson.
2013. Stock assessment of aurora rockfish in 2013, 188 p. Pacific Fishery Management Council, Portland, OR. [Available from website.]

He, X., J. C. Field, D. E. Pearson, L. Lefebvre, and S. Lindley.
2015. Status of bocaccio, *Sebastes paucispinis*, in the Conception, Monterey and Eureka INPFC areas for 2015, 270 p. Pacific Fishery Management Council, Portland, OR. [Available from website.]

Hicks, A. C., M. A. Haltuch, and C. Wetzel.
2009. Status of greenstriped rockfish (*Sebastes elongatus*) along the outer coast of California, Oregon, and Washington, 125 p. Pacific Fishery Management Council, Portland, OR. [Available from website.]

Jagielo, T., A. Hoffman, J. Tagart, and M. Zimmerman.
2003. Demersal groundfish densities in trawlable and untrawlable habitats off Washington: implications for the estimation of habitat bias in trawl surveys. Fish. Bull. 101:545–565.

Keller, A. A., K. J. Molton, A. C. Hicks, M. Haltuch, and C. Wetzel.
2012. Variation in age and growth of greenstriped rockfish (*Sebastes elongatus*) along the U.S. west coast (Washington to California). Fish. Res. 119–120:80–88.

Keller, A. A., J. R. Wallace, and R. D. Methot.
2017. The Northwest Fisheries Science Center's west coast groundfish bottom trawl survey: history, design, and description. NOAA Tech. Memo. NMFS-NWFSC-136, 37 p.

Krieger, K. J.
1993. Distribution and abundance of rockfish determined from a submersible and by bottom trawling. Fish. Bull. 91:87–96.

Laidig, T. E., and M. M. Yoklavich.
2016. A comparison of density and length of Pacific groundfishes observed from 2 survey vehicles: a manned submersible and a remotely operated vehicle. Fish. Bull. 114:386–396.

Laidig, T. E., D. L. Watters, and M. M. Yoklavich.
2009. Demersal fish and habitat associations from visual surveys on the central California shelf. Est. Coast. Shelf Sci. 83:629–637.

Lauth, R. R., J. Ianelli, and W. W. Wakefield.
2004. Estimating the size selectivity and catching efficiency of a survey bottom trawl for thornyheads, *Sebastolobus* spp. using a towed video camera sled. Fish. Res. 70:27–37.

Love, M. S.
2006. Subsistence, commercial, and recreational fisheries. *In* The ecology of marine fishes: California and adjacent waters (L. G. Allen, D. J. Pondella, and M. H. Horn, eds.), p. 567–594. Univ. Calif. Press, Berkeley, CA.

Love, M. S., and M. Yoklavich.
2006.vDeep rock habitats. *In* The ecology of marine fishes: California and adjacent waters (L. G. Allen, D. J. Pondella, and M. H. Horn, eds.), p. 253–266. Univ. Calif. Press, Berkeley, CA.
2008. Habitat characteristics of juvenile cowcod, *Sebastes levis* (Scorpaenidae), in Southern California. Environ. Biol. Fish. 82:195–202.

Love, M. S., M. Yoklavich, and L. Thorsteinson.
2002. The rockfishes of the northeast Pacific, 405 p. Univ. Calif. Press, Berkeley, CA.

Maunder, M. N., P. R. Crone, J. L. Valero, and B. X. Semmens.
2014.vSelectivity: theory, estimation, and application in fishery stock assessment models. Fish. Res. 158:1–4.

Ono, K., R. Licandeo, M. L. Muradian, C. J. Cunningham, S. C. Anderson, F. Hurtado-Ferro, K. F. Johnson, C. R. McGilliard, C. C. Monnahan, C. S. Szuwalski, et al.
2015. The importance of length and age composition data in statistical age-structured models for marine species. ICES J. Mar. Sci. 72:31–43.

R Core Team.
2016. R: a language and environment for statistical computing. R Foundation for Statistical Computing, Vienna, Austria. [Available from website, accessed October 2016.]

Sampson, D. B.
2014. Fishery selection and its relevance to stock assessment and fishery management. Fish. Res. 158:5–14.

Starr, R. M., M. G. Gleason, C. I. Marks, D. Kline, S. Rienecke, C. Denney, A. Tagini, and J. C. Field.
2016. Targeting abundant fish stocks while avoiding overfished species: video and fishing surveys to inform management after long-term fishery closures. PLoS ONE 11(12):e0168645.

Taylor, I. G., and C. Wetzel.
2011. Status of the U.S. yelloweye rockfish resource in 2011 (update of 2009 assessment model), 68 p. Pacific Fishery Management Council, Portland, OR. [Available from website.]

Wedding, L., and M. M. Yoklavich.
2015. Habitat-based predictive mapping of rockfish density and biomass off the central California coast. Mar. Ecol. Prog. Ser. 540:235–250.

Weinberg, K. L., C. Y. Yeung, D. A. Somerton, G. G. Thompson, and P. H. Ressler.
2016. Is the survey selectivity curve for Pacific cod (*Gadus microcephalus*) dome-shaped? Direct evidence from trawl studies. Fish. Bull. 114:360–369.

Yoklavich, M. M., and V. O'Connell.
2008. Twenty years of research on demersal communities using the Delta submersible in the northeast Pacific. *In* Marine habitat mapping technology for Alaska (J. R. Reynolds and H. G. Greene, eds.), p. 143–155. Alaska Sea Grant Coll. Prog., Univ. Alaska, Fairbanks.

Yoklavich, M., R. Starr, J. Steger, H. G. Greene, F. Schwing, and C. Malzone.
1997. Mapping benthic habitats and ocean currents in the vicinity of central California's Big Creek Ecological Reserve. NOAA Tech. Memo. NMFS-SWFSC-245, 52 p.

Yoklavich, M. M., H. G. Greene, G. M. Cailliet, D. E. Sullivan, R. N. Lea, and M. S. Love.
2000. Habitat associations of deep-water rockfishes in a submarine canyon: an example of a natural refuge. Fish. Bull. 98:625–641.

Yoklavich, M. M., M. S. Love, and K. A. Forney.
2007. A fishery-independent assessment of an overfished rockfish stock, cowcod (s*Sebastes levis*), using direct observations from an occupied submersible. Can. J. Fish. Aquat. Sci. 64:1795–1804.

**National Marine
Fisheries Service**
NOAA

Fishery Bulletin
established in 1881

Spencer F. Baird
First U.S. Commissioner
of Fisheries and founder
of *Fishery Bulletin*

Daily deposition of growth increments in sagittae and lapilli of laboratory-reared larval northern pike (*Esox lucius*)

Dariusz P. Fey (contact author)[1]
Adam M. Lejk[2,3]
Martyna Greszkiewicz[1]

Email address for contact author: dfey@mir.gdynia.pl

[1] Department of Fisheries Oceanography and Marine Ecology
National Marine Fisheries Research Institute
ul. Kołłątaja 1
81-332 Gdynia, Poland

[2] Department of Logistics and Monitoring
National Marine Fisheries Research Institute
ul. Kołłątaja 1
81-332 Gdynia, Poland

[3] Department of Fish Biology and Pisciculture
University of Warmia and Mazury in Olsztyn
ul. Oczapowskiego 5
10-719 Olsztyn, Poland

Abstract—The daily deposition of growth increments within both sagittae and lapilli was validated for known-age laboratory-reared (18°C) larval northern pike (*Esox lucius*) (9–33 mm in standard length [SL]) sampled 1, 7, 14, 22, and 28 days after hatching. The mean otolith length at hatching was 58.1 µm (standard deviation [SD] 4.32) for sagittae (no. of larvae sampled [n]=30) and 39.04 µm (SD 4.04) for lapilli (n=30). For both sagittae and lapilli (the otoliths of which were examined without polishing), increments were formed daily and the first increment was deposited at time of hatching. The relationship of otolith size to fish size was linear for lapilli and exponential for sagittae. The size of the sagittae increased more than that of the lapilli at about 9 days after hatching—a size increase that corresponded with an increase in larval wet weight. The age of larval northern pike was moderately difficult to determine from otoliths; the difficulty varied according to the size of the larvae. Sagittae are preferable for fish larvae of up to approximately 25 mm SL, but for larger individuals, lapilli are more suitable. On some of the otoliths (79% of sagittae and 18% of lapilli), a "stress ring" was deposited that corresponded with the time of sampling from the aquaria.

Manuscript submitted 30 March 2018.
Manuscript accepted 14 August 2018.
Fish. Bull.: 116:302–309 (2018).
Online publication date: 5 September 2018.
doi: 10.7755/FB.116.3-4.8

The views and opinions expressed or implied in this article are those of the author (or authors) and do not necessarily reflect the position of the National Marine Fisheries Service, NOAA.

Identification of the survival mechanisms at early life stages of fish is exceedingly important, but it also requires the application of appropriate techniques to obtain essential information. One such technique is otolith microstructure analysis (Stevenson and Campana, 1992). This analysis provides a timeline of the life history of individuals, including the precise date of hatching, and analysis of growth rate and condition up to the observed size at capture (Campana and Jones, 1992). In fact, daily increments can be used not only for aging larvae and early juveniles, but also for fish that are several months old (Fey and Linkowski, 2006) and sometimes adults (Hüssy et al., 2010). Unfortunately, even the most precise analysis based on abundant, long-term material will be worthless if the underlying data are erroneous. The basic information that must be verified is daily increment formation and the time of first increment formation (Geffen, 1992; Campana, 2001). Obviously, such evaluations should be performed separately for each species and otolith type (i.e., sagittae and lapilli). However, even within the same species, otolith microstructure and frequency of increment deposition can vary depending on environmental variables and larval growth rates (Campana, 1983; Folkvord et al., 2000; Fukuda et al., 2009). Moreover, preparation technique (e.g., with a sagittal view with or without polishing, or with a transverse section with one or both sides polished, etc.) should be considered because the choice of preparation technique can affect the accuracy and precision of age estimates (Fey et al., 2005). Finally, as it was recently shown by Fey (2018) for larval Baltic herring (*Clupea harengus membras*), even the preservation of ichthyoplankton samples in alcohol may affect otolith quality and the results of age-determination and growth-rate analysis.

Several methods can be used for

the age validation of larval and juvenile fish (for a review, see Geffen, 1992; Campana, 2001). The most used method involves analysis of larvae of known age (e.g., Folkvord et al., 1997; Folkvord et al., 2000; Hill and Bestgen, 2014; Ding et al., 2015) and marking otoliths with alizarin or tetracycline (Secor et al., 1995; Fox et al., 2003). The marginal increment analysis method is more commonly used for adult fish, but it can be applied to larvae (Sepúlveda, 1994; Fey, 2002). Although most of such otolith microstructure analysis is performed with light microscopes, scanning electron microscopes can be used as well, especially if increment deposition occurs at low temperatures (Radtke and Fey, 1996) or during periods of starvation (Jones and Brothers, 1987; Fox et al., 2003).

The present study validates the aging method for larval northern pike (*Esox lucius*), a species of significant importance for both commercial and recreational fisheries and having a wide circumpolar distribution (i.e., in North America and Europe) (Craig, 2008). Although many populations of northern pike are not overexploited, in some geographical areas the species is close to extirpation, which is the case in many coastal areas of the Baltic Sea (Nilsson et al., 2014; Larsson et al., 2015; Skov and Nilsson, 2018). The reasons for population declines are over-exploitation, disappearance of suitable spawning grounds, and low recruitment (Larsson et al., 2015; Skov and Nilsson, 2018). Other factors related to human activities in coastal areas (e.g., presence of wind farms and underwater cables) should be considered, as well (Fey et al., 2019). Given their endangered status in some regions, there is a need to better understand the early life period, growth, and survival of northern pike. Therefore, it is also important to evaluate the methods applied for aging larvae and early juveniles (e.g., by enumeration of daily increments within otoliths). Unfortunately, only one publication validating age estimates of northern pike from lapilli is available (Wang and Eckmann, 1992), and no information of this kind exists on the basis of sagittae. Although Wang and Eckmann (1992) provided general information on sagittae and stated that lapilli were always much clearer to read than sagittae, no data have been presented to date on the rate of increment deposition for this otolith type.

Our goal was to estimate the periodicity of increment formation and the time of the first increment deposition on sagittae and lapilli of known-age laboratory-reared larval northern pike (9–33 mm in standard length [SL]). Changes in otolith size are described in relation to larval age, SL, and weight.

Material and methods

Rearing of fish larvae

Eyed-eggs of northern pike (12 days after fertilization) from wild spawners were transported in April 2015 from the Komorowo Hatchery (northern Poland) to the laboratory of the Center of Aquaculture and Ecological Engineering, University of Warmia and Mazury in Olsztyn. For the purpose of forcing the mass hatching of larvae, the eggs were subjected to a temperature that increased within one hour by 3–4°C. Pike larvae were kept in two separate aquaria with a water volume of 60 L each and initially at a density of approximately 22 indivduals/L per aquarium. Water in the aquaria was aerated and purified with a bio-filter at a constant water temperature of 18°C (standard deviation [SD] 0.5°C). The larvae were fed ad libitum every 1.5 h during day light hours with Perla Larva Proactive 4.0[1] commercial starter feed (Skretting, Stavanger, Norway). The aquaria were cleaned every morning, before feeding began, and dead larvae were removed. Throughout the rearing period, a natural photoperiod (14 h light/10 h dark) was applied that was characteristic of the spring photoperiod in East Central Europe.

Otolith analysis

A sample of 25 specimens was collected from each tank 7, 14, 22, and 28 days after hatching (dah)]. Additionally, 15 specimens were collected on the day of hatching. The fish samples were collected between 10:00 h. and 11:00 h. The fish were preserved in 96% alcohol. Otoliths (left and right sagittae and lapilli) were extracted from each larva and placed on microscope slides, distal surface down (sulcus up) and covered with DEPEX mounting medium (Electron Microscopy Sciences, Hatfield, PA). The otoliths without any preparation were used in the following analysis. At the time of otolith extraction, the SL of each larva was measured to the nearest 0.1 mm, and wet weight was estimated to the nearest 0.01 g. Length measurements were corrected for shrinkage before further analysis (Greszkiewicz and Fey, 2018). The length (i.e., maximum diameter) of all extracted otoliths (n=230 pairs) was measured by using an image analysis system (Image-Pro Premier, Media Cybernetics, Inc., Rockville, MD) under an Eclipse 80i transmitted light microscope (Nikon Corp., Tokyo, Japan). The mean value of the length measurements from the left and right otoliths was used for our analysis. The total number of increments was counted by the same person on two different occasions. If the difference in estimated numbers exceeded a given number of increments (2 increments for 7 dah, 3 for 14 dah and 22 dah, and 4 for 28 dah), the otolith was excluded (approximately 14–29% of the otoliths examined). Otherwise, the mean value from the two readings was used for the analysis. Some otoliths were excluded without increment counts if there was a lack of confidence in recognizing increments. The otoliths extracted on the day of hatching of the larvae were used to confirm the position of the hatching check on otoliths of older fish.

---

[1] Mention of trade names or commercial companies is for identification purposes only and does not imply endorsement by the National Marine Fisheries Service, NOAA.

Data analysis

The number of increments deposited in larval otoliths in each of the 2 aquaria (i.e., the replications) after 7, 14, 22, and 28 days were compared by using *t*-tests conducted separately for each of the 4 age groups. Age validation was completed by fitting linear regression to increment number-at-age data and by analyzing the slope for the difference from 1 (analysis of covariance [ANCOVA]). Otolith size-at-age and otolith size-at-SL data were described with best-fit functions to better visualize the patterns observed. Best-fit models for the relationship of fish growth to size (in SL) and weight at age are also presented. Statistica, vers. 12.0 (TIBCO Software, Inc., Palo Alto, CA) software was used for data analysis. Differences were considered statistically significant at $P<0.05$ ($\alpha=0.05$).

Results

The final number of otoliths on which increments were counted successfully was 78 for sagittae (21% and 24% of otoliths were excluded from aquarium 1 and 2, respectively) and 74 for lapilli (28% and 23% of otoliths were excluded from aquarium 1 and 2, respectively).

The mean otolith length at hatching was 58.1 µm (SD 4.32) for sagittae (n=30) and 39.04 µm (SD 4.04) for lapilli (n=30). The cores of both ototlith types were formed by a large number of primordia (Fig. 1).

The number of increments deposited in northern pike otoliths after 7, 14, 22, and 28 days was not statistically different for the 2 replications (*t*-test, $P>0.05$ for each of the 4 age groups). Therefore, the data from the replications were pooled for further analysis. The number of increments on otoliths, both sagittae (n=78) and lapilli (n=74), corresponded to the known age of the larvae, as was confirmed by fitting linear regression to the increment number-at-age data (Fig. 2). The

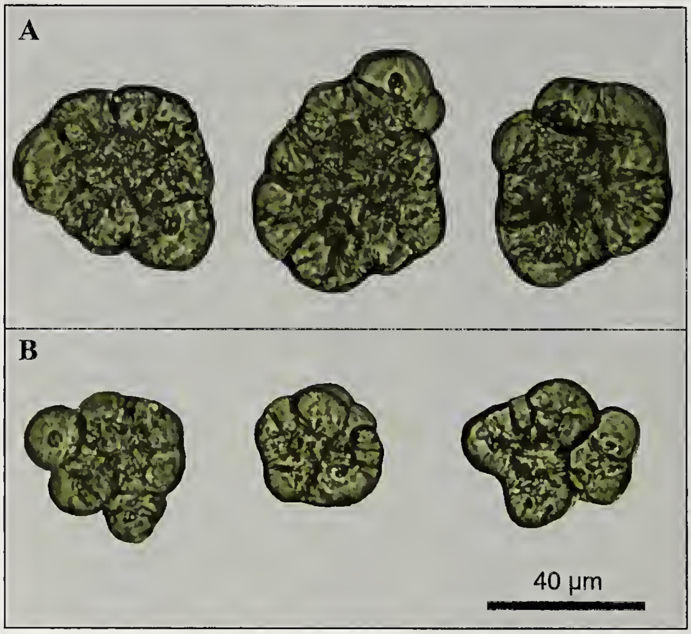

Figure 1

Images of otoliths at time of hatching of larval northern pike (*Esox lucius*) reared in a laboratory in 2015 at the Center of Aquaculture and Ecological Engineering, University of Warmia and Mazury in Olsztyn, Poland: (**A**) sagittae and (**B**) lapilli. Three examples are shown for each type of otolith.

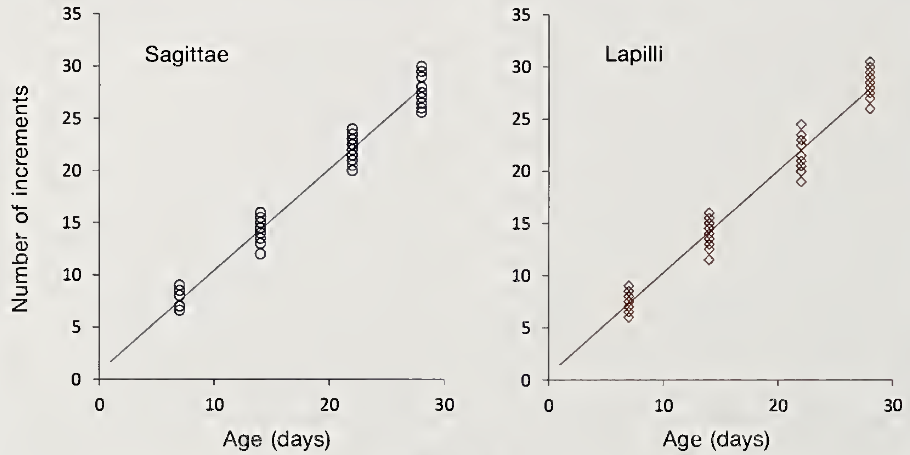

Figure 2

Number of increments counted from sagittae (n=78) and lapilli (n=74) of known-age laboratory-reared larval northern pike (*Esox lucius*). The data are described with linear regressions: sagittae, $y=0.972x+0.69$, coefficient of multiple determination (R^2)=0.98, $P<0.001$; lapilli, $y=0.977x + 0.53$, R^2=0.97, $P<0.001$). The slopes of the regressions are not statistically different from one, confirming the daily periodicity of increment formation.

Table 1

Number of increments deposited on sagittae and lapilli of known-age larval northern pike (*Esox lucius*) reared in a laboratory in 2015 at the Center of Aquaculture and Ecological Engineering, University of Warmia and Mazury in Olsztyn, Poland. *n*=the number otoliths analyzed (left or right otolith was used depending on which provided a clearer microstructure).

	Sagittae			Lapilli		
Number of days after hatching	*n*	Mean number of increments	SD	*n*	Mean number of increments	SD
7	17	7.6	0.88	16	7.4	0.97
14	21	14.4	0.65	18	13.9	1.47
22	22	22.0	0.97	20	21.6	1.51
28	18	27.8	1.41	20	28.1	1.26

slopes of these two regressions were not statistically different from 1 (ANCOVA, *P*>0.05). The intercept of these 2 regression lines was not statistically different from 0 (ANCOVA, *P*>0.05), indicating that the first increment was formed at hatching (when the temperature is 18°C). The mean number of increments counted in relation to real age is presented in Table 1. The SD for lapilli was higher than that of sagittae for all age classes (7, 14, and 22 days) except for the age of 28 days.

A stress check (i.e., a distinct dark band formed between regular increments) was formed on most (79%) of the sagittae on the days of handling, especially on day 7, and less frequently on days 14 and 22. Stress checks were less commonly observed on lapilli (18%). The mean number of increments between the sagittal edge and stress check formed on day 7 was 6.7 (SD 0.49, *n*=14; for 14-day-old fish), 14.8 (SD 0.67, *n*=17; for 22-day-old fish), and 21.4 (SD 0.51, *n*=19; for 28-day-old fish). Therefore, the number of increments between stress check and otolith edge corresponded to the number of days elapsed after the formation of the stress check. The lower SD for the counts from the stress check to the otolith edge described above compared with the SD for the counts from the otolith center to the edge (Table 1) indicate that the source of error in increment counts is related largely to the analysis of the area close to the otolith center.

The relationship of otolith size to fish size was linear for lapilli (*n*=115) and exponential for sagittae (*n*=115) (Fig. 3). The rapid change in otolith size between sagittae and lapilli, i.e., when daily increments on sagittae become significantly wider than those on lapilli, occurred around an SL of 17 mm and an age of 9–10 days (Fig. 3). This SL and age corresponded to the starting point of increase in fish weight (Fig. 4).

The clarity of the otolith microstructures in both sagittae (Fig. 5A) and lapilli (Fig. 5B) varied among all individuals from good, with easily distinguishable increments, to unclear and difficult to read. Generally, the lowest confidence in increment recognition was for the smallest fish (<17 mm SL), for both sagittae and lapilli. Differences between these two otolith types were evident when fish of different sizes were compared. Sagittae are preferable for northern pike larvae of up to approximately 25 mm, but lapilli are more suitable for larger specimens.

Discussion

The number of increments on otoliths, both sagittae and lapilli, corresponded in this study to the known age of the larvae. These results can be compared with those of Wang and Eckmann (1992) who also confirmed the daily deposition of increments on the lapilli of larval northern pike. No published data on increment formation exist for sagittae that could be used for comparison with data from the present results. The results obtained in the current study at a relatively high temperature of 18°C should be supplemented in the future with data obtained at lower temperatures that could potentially cause non-daily increment formation or the formation of increments that are too narrow to be identified with a transmitted light microscope. Wang and Eckmann (1992) analyzed increment development in lapilli at 16°C and 10°C, but it would still be valuable to analyze samples at temperatures below 10°C. Such temperatures that can result in age underestimation because the increments are too narrow to record have been previously reported for Atlantic herring (*Clupea harengus*) and turbot (*Scophthalmus maximus*) (Geffen, 1982) and Arctic charr (*Salvelinus alpinus*) (Radtke and Fey, 1996).

Depending on the species, the first increment occurs either at hatching, a day after hatching, or after the first feeding and yolk-sac absorption (Jones, 1986; Thorrold and Hare, 2002). In the present study on northern pike, conducted at a temperature of 18°C, increment deposition started at hatching in both the

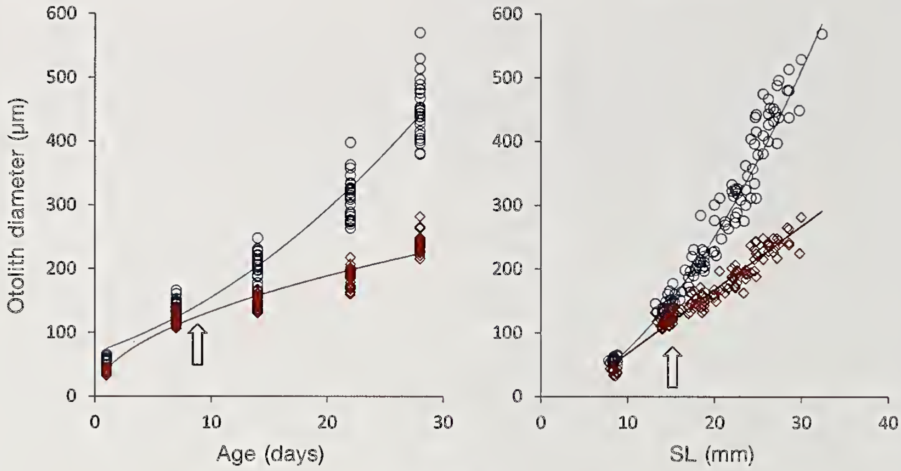

Figure 3

Changes in otolith size with age and standard length (SL) of laboratory-reared larval northern pike (*Esox lucius*), presented separately for sagittae (n=125, circles) and lapilli (n=125, diamonds). The data are described by best-fit regressions. Age from sagittae: $y=0.264x^2+6.234x+60.14$, coefficient of multiple determination (R^2)=0.97, $P<0.001$. Age from lapilli: $y=39.457x^{0.52}$, $R^2=0.97$, $P<0.001$. Standard length from sagittae: $y=1.307x^{1.76}$, $R^2=0.97$, $P<0.001$. Standard length from lapilli: $y=9.983x-31.96$, $R^2=0.95$, $P<0.001$. Arrows indicate approximate age and SL at which the growth of sagittae accelerated in contrast with that of lapilli.

sagittae and the lapilli, as has been reported before for many species (Isely and Noble, 1987; Bestgen and Bundy, 1998). Different results were obtained for northern pike by Wang and Eckmann (1992), who reported that increment formation in lapilli started 2–3 dah. Such a difference in first increment formation among different studies has been reported for other species. For example, increment formation starts at hatching in larval smallmouth bass (*Micropterus dolomieu*) in constantly fluctuating diel water temperatures (Hill and Bestgen, 2014). This finding contradicted the results of a previous study for the same species by Graham and Orth (1987), who reported that increment formation starts 7–11 dah. Similarly, Fey et al. (2005) reported that the first increment appeared at hatching in larval spot (*Leiostomus xanthurus*), whereas Peters et al.[2] identified it at five dah at first feeding. The reasons for such discrepancies could be related to the otolith preparation method or the lack of such preparation. The present study is based on unprepared otoliths, but the paper by Wang and Eckmann (1992) is based on increment counts from otoliths that were ground and polished. Although otolith preparation by grinding and polishing can reveal increments and facilitate correct

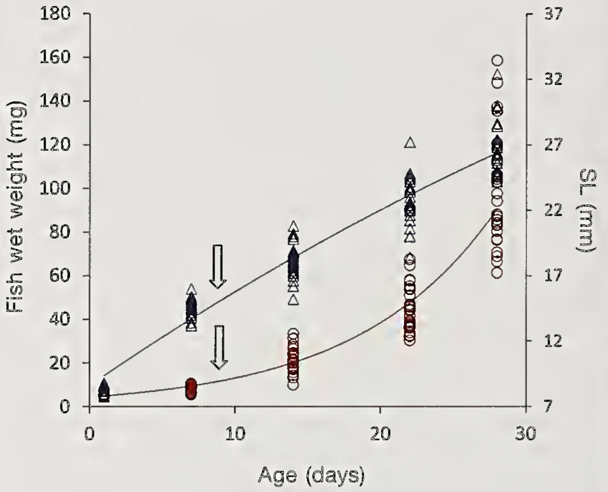

Figure 4

Growth of laboratory-reared larval northern pike (*Esox lucius*) in standard length (SL, n=125, triangles) and wet weight (n=125, circles) during the first 28 days of life. The data are described by best-fit regressions: SL, $y=-0.0045x^2+0.717x+8.61$, coefficient of multiple determination (R^2)=0.93, $P<0.001$; wet weight: $y=4.503e^{0.107x}$, $R^2=0.94$, $P<0.001$. Arrows indicate the age when growth in wet weight (bottom arrow) and SL (top arrow) of sagittae accelerated in contrast with that of lapilli.

---

[2] Peters, D. S., J. C. DeVane Jr., M. T. Boyd, L. C. Clements, and A. B. Powell. 1978. Preliminary observations on feeding, growth, and energy budget of larval spot (*Leiostomus xanthurus*). *In* Ann. Rep. Southeast Fish. Cent., Beaufort Lab. to U.S. Dep. Energy, p. 377–397. Beaufort Lab., Natl. Mar. Fish. Serv., NOAA, Beaufort, NC.

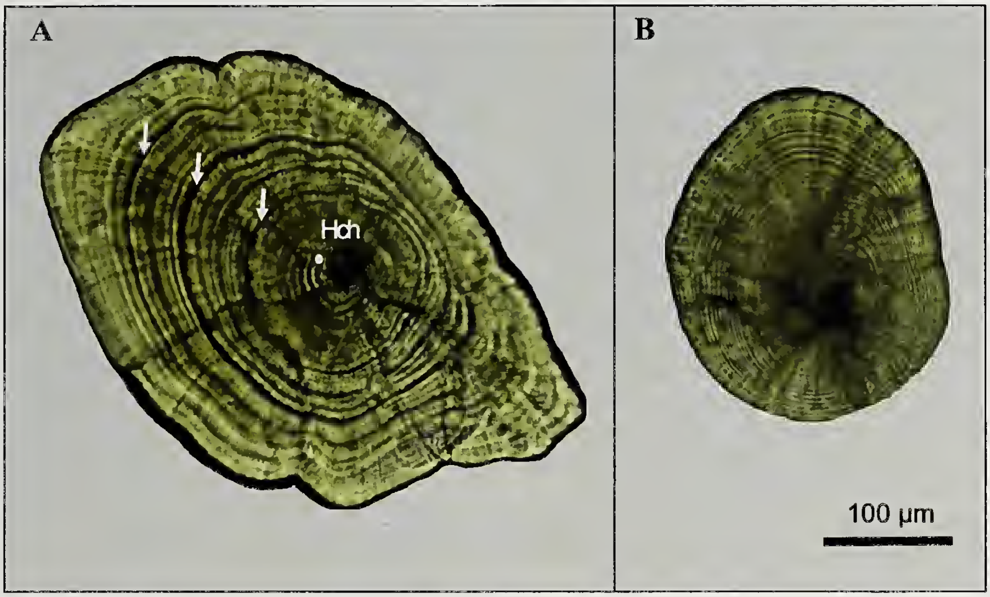

Figure 5

Images of otolith microstructure of a laboratory-reared larval northern pike (*Esox lucius*) 28 days after hatching: (**A**) sagitta and (**B**) lapillus. The white dot indicates the hatching check (Hch) and arrows indicate stress checks that correspond with days of handling (i.e., sampling of larvae from aquaria).

age estimates, it can also remove increments and lead to the underestimation of ages. The narrowest increments at the otolith center, in particular, can be affected during preparation (Secor et al.[3]; Fey et al., 2005). The most important source of inaccuracy is interpretation error among investigators (Campana, 1990). Interpretation depends on the experience of the reader and clarity of the otoliths, the latter of which may be affected by increment width. The increment width in turn is not only species specific, but it can also be affected by factors such as temperature, feeding conditions, and somatic growth (Campana, 1983; Folkvord et al., 2000; Fukuda et al., 2009). Although Wang and Eckmann (1992) reported that increment deposition started 2–3 dah, they referred to fish held in waters at a temperature of 10°C. For fish held at a temperature of 16°C, the delay in first increment formation described by Wang and Eckmann (1992) was only 1–2 days. It is possible that the clarity of the microstructure in the otoliths from the present study conducted with fish held at a temperature of 18°C was greater and therefore first increment formation was found to occur at hatching. Thus, it can be suggested that increment formation starts at hatching but, depending on the temperature at hatching, some age underestimation may occur because of problems with recognition of increments that are very narrow. Considering the above conditions, the importance of repeated evaluations of the timing of increment deposition and first increment formation is emphasized.

The relationship of otolith size to fish size was linear for lapilli and exponential for sagittae. Rapid differentiation in otolith size between sagittae and lapilli, i.e., when daily increments in sagittae become significantly wider than those in lapilli, occurred when fish growth in weight increased. Therefore, if larvae larger than 17 mm SL are used for age estimates, wider increments in sagittal otoliths would be more suitable for measurements of increment width otolith back-calculations of growth. Fey et al. (2005) made the opposite recommendation (i.e., lapilli are better for back-calculations of growth) for larval spot. Although sagittae had wider increments than lapilli, their irregular pattern made width measurements along one radius impossible.

When aging itself was concerned, in the present study sagittae provided slightly better visibility and clarity of increments than lapilli in fish of up to 25 mm SL. In larger specimens (25–33 mm SL), the usefulness of sagittae decreased, and that of lapilli increased slightly. In sagittae, difficulties resulted particularly from wide and relatively irregular increment formation with the result that many subdaily structures that can sometimes be difficult to distinguish from "real" increments. In lapilli, when optimal focus of the microscope is used, increment patterns are seen as more regular and are seen as daily increments, but when the focus is changed from that optimum, the daily increments have a tendency to merge and result in an underestimation of real age. Notice, however, that the quality of otolith microstructures in laboratory-reared fish is frequently worse than in fish occurring in the wild. For example Graham and Orth (1987) reported that the clarity of otolith increments in laboratory-reared smallmouth bass was less than that viewed in wild individuals. It could also have been the case that in the present study, the clarity of otoliths of northern pike larvae was not as good as it possibly could have been if the otoliths were collected from wild fish. As with the present results, lapilli are found to be useful for aging in many species (e.g., Hoff et al., 1997; Bestgen and Bundy, 1998). Ichimaru and Katsunori (1995) preferred lapilli for collecting age data for two species of flyingfish larvae (*Cheilopogon doederleini* and *Cypselurus hiraii*) because the increments in the lapilli were as clear as those in the sagittae and did not require any preparation. Bestgen and Bundy (1998) reported that increments deposited on the sagittae of Colorado pikeminnow (*Ptychocheilus lucius*) were difficult to distinguish after the fish were 30 days old. Therefore, those authors used lapilli to age older fish.

---

[3] Secor, D. H., J. M. Dean, and E. H. Laban. 1991. Manual for otolith removal and preparation for microstructural examination, 85 p. Electric Power Res. Inst., Palo Alto, CA, and Belle W. Baruch Inst. Mar. Biol. Coast. Res., Clemson, SC.

On some of the otoliths (mostly sagittae) a stress check was deposited on day 7 (and less frequently on days 14 and 22), which corresponded with the time of sample collection from the aquaria. Increment counts between the otolith edge and the check formed on day 7 provided additional confirmation of daily periodicity of increment deposition. Stress checks related to handling are frequently observed on larval fish otoliths, and some authors use them, as we did in this study, as markers for increment validation (Volk et al., 1984; Boehlert and Yoklavich, 1985). Moreover, lower SD for the counts from the stress check to the otolith edge, compared with SD for counts from the otolith center to the edge, suggests that the source of error in aging northern pike is related largely to distinguishing increments in the central otolith area (approximately first 7 days). A more irregular increment pattern in the otolith center was also reported in northern pike by Wang and Eckmann (1992).

Acknowledgments

This article is a contribution to statutory project Dot18/PIKE conducted at the National Fisheries Research Institute and financed by the Ministry of Science and Higher Education, Poland. Part of this work was co-financed by statutory project no. 18.610.001-300 conducted at the Department of Fish Biology and Pisciculture, University of Warmia and Mazury in Olsztyn. The authors would like to thank M. Teodorowicz from Komorowo Fish Farm for technical support during incubation of fish eggs and H. Wróblewska for help with otolith extraction.

Literature cited

Bestgen, K. R., and J. M. Bundy.
1998. Environmental factors affect daily increment deposition and otolith growth in young Colorado squawfish. Trans. Am. Fish. Soc. 127:105–117.

Boehlert, G. W., and M. M. Yoklavich.
1985. Larval and juvenile growth of sablefish, *Anoplopoma fimbria*, as determined from otolith increments. Fish. Bull. 83:475–481.

Campana, S. E.
1983. Feeding periodicity and the production of daily growth increments in otoliths of steelhead trout (*Salmo gairdneri*) and starry flounder (*Platichthys stellatus*). Can. J. Zool. 61:1591–1597.
1990. How reliable are growth back-calculations based on otoliths? Can. J. Fish. Aquat. Sci. 47:2219–2227.
2001. Accuracy, precision, and quality control in age determination, including a review of the use and abuse of age validation methods. J. Fish Biol. 59:197–242.

Campana, S. E., and C. M. Jones.
1992. Analysis of otolith microstructure data. *In* Otolith microstructure examination and analysis (D. K. Stevenson and S. E. Campana, eds.), p. 73–100. Can. Spec. Publ. Fish. Aquat. Sci. 117.

Craig, J. F.
2008. A short review of pike ecology. Hydrobiologia 601:5–16.

Ding, C., Y. Chen, D. He, and J. Tao.
2015. Validation of daily increment formation in otoliths for *Gymnocypris selincuoensis* in the Tibetan Plateau, China. Ecol. Evol. 5:3243–3249.

Fey, D. P.
2002. Formation of daily increments in otoliths of larval and juvenile herring (*Clupea harengus* L.) and early juvenile smelt (*Osmerus eperlanus* L.) in low-food conditions. Arch. Fish. Mar. Res. 49:189–197.
2018. The effect of preserving ichthyoplankton samples in alcohol on the accuracy of data obtained from otolith microstructure examinations. Fish. Res. 206:198–201.

Fey, D. P., and T. B. Linkowski.
2006. Predicting juvenile Baltic cod (*Gadus morhua*) age from body and otolith size measurements. ICES J. Mar. Sci. 63:1045–1052.

Fey, D. P., G. E. Bath Martin, J. A. Morris, and J. A. Hare.
2005. Effect of type of otolith and preparation technique on age estimation of larval and juvenile spot (*Leiostomus xanthurus*). Fish. Bull. 103:544–552.

Fey, D. P., M. Greszkiewicz, Z. Otremba, and E. Andrulewicz.
2019. Effect of static magnetic field on the hatching success, growth, mortality, and yolk-sac absorption of larval northern pike *Esox lucius*. Sci. Total Environ. 647:1239–1244.

Folkvord, A., K. Rukan, A. Johannessen, and E. Moksness.
1997. Early life history of herring larvae in contrasting feeding environments determined by otolith microstructure analysis. J. Fish Biol. 51(suppl. A):250–263.

Folkvord, A., G. Blom, A. Johannessen, and E. Moksness.
2000.v Growth-dependent age estimation in herring (*Clupea harengus* L.) larvae. Fish. Res. 46:91–103.

Fox, C. J., A. Folkvord, A. J. Geffen.
2003. Otolith micro-increment formation in herring *Clupea harengus* larvae in relation to growth rate. Mar. Ecol. Prog. Ser. 264:83–94.

Fukuda, N., M. Kuroki, A. Shinoda, Y. Yamada, A. Okamura, J. Aoyama, and K. Tsukamoto.
2009. Influence of water temperature and feeding regime on otolith growth in *Anguilla japonica* glass eels and elvers: does otolith growth cease at low temperatures? J. Fish Biol. 74:1915–1933.

Geffen, A. J.
1982. Otolith ring deposition in relation to growth rate in herring (*Clupea harengus*) and turbot (*Scophthalmus maximus*) larvae. Mar. Biol. 71:317–326.
1992. Validation of otolith increment deposition rate. *In* Otolith microstructure examination and analysis (D. K. Stevenson and S. E. Campana, eds.), p. 101–113. Can. Spec. Publ. Fish. Aquat. Sci. 117.

Graham, R. J., and D. J. Orth.
1987. Otolith aging of young-of-the-year smallmouth bass. *In* Age and growth of fish (R. C. Summerfelt and G. E. Hall, eds.), p. 486-491. Iowa State Univ. Press, Ames, IA.

Greszkiewicz, M., and D. P. Fey.
2018. Effect of preservation in formalin and alcohol on the growth rate estimates of larval northern pike. North Am. J. Fish. Manage. 38:601–605.

Hill, A. A., and K. R. Bestgen.
2014. Otolith daily increment deposition in age-0 smallmouth bass reared in constant and fluctuating water temperatures. North Am. J. Fish. Manage. 34:774–779.

Hoff, G. R., D. J. Logan, and D. F. Markle.
1997. Notes: otolith morphology and increment validation in young Lost River and shortnose suckers. Trans. Am. Fish. Soc. 126:488–494.

Hüssy, K., H.-H. Hinrichsen, D. P. Fey, Y. Walther, and A. Velasco.
2010. The use of otolith microstructure to estimate age in adult Atlantic cod (*Gadus morhua*). J. Fish Biol. 76:1640–1654.

Ichimaru, T., and T. Katsunori.
1995. Otolith increment formation of flyingfishes larvae, *Cypselurus heterurus doederleini* and *Cypselurus hiraii* under rearing conditions. Bull. Nagasaki Prefect. Inst. Fish. 21:1–6.

Isely, J. J., and R. L. Noble.
1987. Validation of daily ring deposition in otoliths of wild young-of-the-year largemouth bass. Tex. J. Sci. 39:273–277.

Jones, C.
1986. Determining age of larval fish with the otolith increment technique. Fish. Bull. 84:91–103.

Jones, C., and E. B. Brothers.
1987. Validation of otolith increment aging technique for striped bass, *Morone saxatilis*, larvae reared under suboptimal feeding conditions. Fish. Bull. 85:171–178.

Larsson, P., P. Tibblin, P. Koch-Schmidt, O. Engstedt, J. Nilsson, O. Nordahl, and A. Forsman.
2015. Ecology, evolution, and management strategies of northern pike populations in the Baltic Sea. Ambio 44(suppl. 3):451–61.

Nilsson, J., O. Engstedt, and P. Larsson.
2014. Wetlands for northern pike (*Esox lucius* L.) recruitment in the Baltic Sea. Hydrobiologia 721:145–154.

Radtke, R., and D. P. Fey.
1996. Environmental effects on primary increment formation in the otoliths of newlyhatched Arctic charr. J. Fish Biol. 48:1238–1255.

Secor, D. H., E. D. Houde, and D. M. Monteleone.
1995. A mark-release experiment on larval striped bass *Morone saxatilis* in a Chesapeake Bay tributary. ICES J. Mar. Sci. 52:87–101.

Sepúlveda, A.
1994. Daily growth increments in the otoliths of European smelt *Osmerus eperlanus* larvae. Mar. Ecol. Prog. Ser. 108:33–42.

Skov, C., and P. A. Nilsson, (eds.).
2018. Biology and ecology of pike, 402 p. CRC Press, Boca Raton, FL.

Stevenson, D. K., and S. E. Campana (eds.).
1992. Otolith microstructure examination and analysis. Can. Spec. Publ. Fish. Aquat. Sci. 117, 126 p.

Thorrold, S. R., and J. A. Hare.
2002. Otolith applications in reef fish ecology. *In* Coral reef fishes: dynamics and diversity in a complex ecosystem (P. F. Sale, ed.), p. 243–264. Academic Press, San Diego, CA.

Volk, E. C., R. C. Wissmar, C. A. Simenstad, and D. M. Eggers.
1984. Relationship between otolith microstructure and the growth of juvenile chum salmon (*Oncorhynchus keta*) under different prey rations. Can. J. Fish. Aquat. Sci. 41:126–133.

Wang, N., and R. Eckmann.
1992. Effects of photoperiod, feeding regime and water temperature on the formation of daily growth increments in otoliths of larval pike (*Esox lucius* L.). J. Appl. Ichthyol. 8:246–250.

National Marine
Fisheries Service
NOAA

Fishery Bulletin
established in 1881

Spencer F. Baird
First U.S. Commissioner
of Fisheries and founder
of *Fishery Bulletin*

Food habits of the blue shark, *Prionace glauca* (Linnaeus, 1758), in waters off northern Peru

Francisco Córdova-Zavaleta (contact author)[1,2]
Jaime Mendo[2]
Sergio A. Briones-Hernández[3]
Nicolas Acuña-Perales[1]
Adriana Gonzalez-Pestana[1,4]
Joanna Alfaro-Shigueto[1,4,5]
Jeffrey C. Mangel[1,5]

Email address for contact author: fcordova@prodelphinus.org

[1] ProDelphinus
Calle Jose Galvez 780-e
15074 Lima, Peru

[2] Facultad de Pesquería
Universidad Nacional Agraria la Molina
Avenida La Molina s/n
15024 Lima, Peru

[3] Centro Interdisciplinario de Ciencias Marinas
Instituto Politécnico Nacional
Avenida Instituto Politécnico Nacional s/n
Colonia Playa Palo de Santa Rita Apdo.
23096 La Paz, Baja California Sur, Mexico

[4] Facultad de Biología Marina
Universidad Científica del Sur
Panamericana Sur Km 19
15067 Lima, Peru

[5] Center for Ecology and Conservation
College of Life and Environmental Sciences
University of Exeter, Penryn Campus
Penryn, Cornwall TR10 9FE, United Kingdom

Abstract—The blue shark (*Prionace glauca*) is the most landed shark species in Peruvian shark fisheries, representing 42% of total landings. Despite its importance for fisheries, the ecological role of the blue shark in Peruvian waters remains poorly understood. Therefore, in this study, we aimed to assess the food habits of blue sharks off northern Peru through stomach content analysis. Between February and December of 2015, 143 stomachs were collected and 28 found to be were empty. Individuals measured from 110.0 to 299.4 cm in total length. The results indicate that blue sharks have epipelagic and mesobathypelagic feeding habits, preying upon a wide number of prey taxa (42 species) but with a diet dominated by cephalopods, especially *Argonauta* spp. and *Ancistrocheirus lesueurii*. Diets differed by size class and location, suggesting that longitudinal movements are related to increments in body size. In addition, we propose that blue sharks scavenge for food on the basis of finding the cyprid larval stage and juvenile cosmopolitan duck barnacle (*Lepas anatifera*) associated with the prey item 'unidentified cephalopods.' The present study contributes new information on the diet of blue sharks.

Manuscript submitted 14 December 2017.
Manuscript accepted 16 August 2018.
Fish. Bull. 116:310–322 (2018).
Online publication date: 11 September 2018.
doi: 10.7755/FB.116.3-4.9

The views and opinions expressed or implied in this article are those of the author (or authors) and do not necessarily reflect the position of the National Marine Fisheries Service, NOAA.

In the southeastern Pacific Ocean, the area off northern Peru is an important area of convergence between temperate (Humboldt Current) and tropical (South Equatorial Current) waters (Spalding et al., 2007). This particular area hosts a diversity of marine species (Chirichigno and Cornejo, 2001), including a large number of sharks (Cornejo et al., 2015). One of these is the blue shark (*Prionace glauca*), which is considered a key cosmopolitan pelagic species that exerts top-down control on community structure (Stevens et al., 2000).

On a global scale, the blue shark is the most landed shark species (as target and nontarget catch) and the major component of the international shark fin trade (Clarke et al., 2006; Nakano and Stevens, 2008). It is also the most landed species by Peruvian shark fisheries, representing 42% of total landings (Gonzalez-Pestana et al.,[1] 2016). Seventy percent of blue shark landings come from the small-scale longline fishery operating along the coast (Doherty et al., 2014), especially off southern Peru where cold to temperate waters support higher abundances of pelagic sharks (Adams et al., 2016). Likewise, it is one of the most frequently species caught in Peruvian small-scale driftnet shark fisheries (Alfaro-Shigueto et al., 2010). However, despite its importance for fisheries, biological studies describing the ecological role of blue sharks in Peruvian waters are few.

There have been several studies regarding the diet of blue sharks in

---

[1] Gonzalez-Pestana, A., C. Kouri, and X. Velez-Zuazo. In review. Shark fisheries in the southeast Pacific: a 61-year analysis from Peru. F1000Research 3:164. [Available at website.]

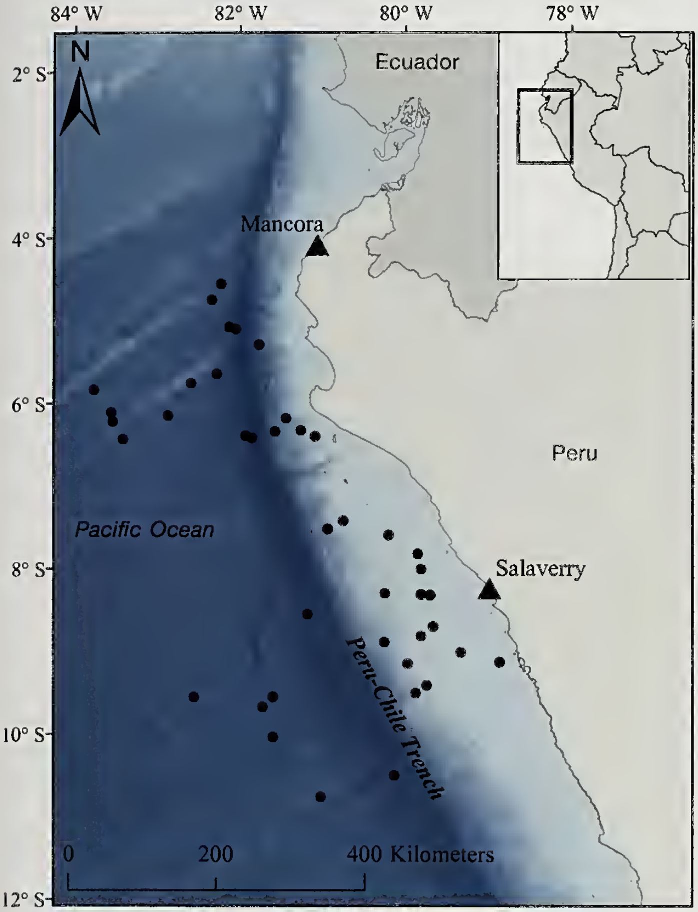

Figure 1

Map of locations where blue sharks (*Prionace glauca*) were collected in northern Peru between February and December 2015. The blue vertical gradient defines the position of the Peru–Chile Trench (with an average distance from shore of 130 km or 70 nautical miles).

the eastern Pacific Ocean. For example, Tricas (1979) and Harvey (1989) reported that blue sharks consume euphausiids (mostly *Thysanoessa spinifera*), small fish (e.g., the northern anchovy, *Engraulis mordax*), and a variety of cephalopods (e.g., Loliginidae and Histioteuthidae). Studies from the Mexican Pacific Ocean have revealed a high consumption of the pelagic red crab (*Pleuroncodes planipes*), as well as a variety of squid, including *Histioteuthis heteropsis*, *Gonatus californiensis*, and *Ancistrocheirus lesueurii* (Markaida and Sosa-Nishizaki, 2010; Hernández-Aguilar et al., 2016). Loor-Andrade et al. (2017) showed that *A. lesueurii*, *Stigmatoteuthis hoylei*, and the jumbo squid (*Dosidicus gigas*) were the most consumed species off Ecuador. In Chilean waters, prey species included a variety of fishes: mackerels (*Trachurus murphyi* and the Pacific chub mackerel, *Scomber japonicus*) and tunas (*Thunnus* spp.), as well as jumbo squid (Lopez et al., 2010; Klarian et al., 2018).

In Peru, three studies of blue shark diet have revealed that they feed on jumbo squid, Peruvian anchoveta (*Engraulis ringens*), Pacific sardine (*Sardinops sagax*), Peruvian hake (*Merluccius gayi peruanus*), and eggs from flying fish (Exocoetidae) and Chilean silverside (*Odontesthes regia*) (Hoyos et al., 1991; Elliot et al., 1995, 1996). Although these previous studies provide valuable insights into prey species of blue sharks off the coast of Peru, their results have been limited by sample size, time series, and size classes. Therefore, to determine the ecological role of blue sharks in the Peruvian marine ecosystem, we focused on providing broader information on blue shark food habits off northern Peru by analyzing stomach contents and assessing diet variability by sex, size class, season, and fishing ground.

Materials and methods

Sampling and stomach content analysis

Stomach contents of blue sharks were collected between February and December 2015 by onboard observers during small-scale driftnet and longline fishing trips that landed in Mancora and Salaverry ports in northern Peru (Fig. 1). Sex of each shark was determined and total length (TL) was measured to the nearest centimeter (Bigelow and Schroeder, 1948). Stomachs were extracted and preserved in 10% formalin for analysis (Galván-Magaña et al., 1989). Stomach samples were examined at the Laboratorio de Recursos Hidrobiológicos of the Universidad Nacional Agraria la Molina, where prey items were identified to the lowest possible taxon and weighed (wet weight) to the nearest 0.01 g. Fish items (entire specimens and skeletons) were identified according to Chirichigno and Velez (1998) and Clothier (1950), and fish otoliths were identified according to Rivaton and Bourret (1999) and García-Godos (2001). Cephalopods were identified by examination of beaks (Wolff, 1982, 1984; Clarke, 1986; Xavier and Cherel, 2009). Crustaceans and marine mammals were identified according to Moscoso (2013) and Jefferson et al. (2015), respectively. Reconstruction of cephalopod weights by regression equations was based on measurements of the lower rostral length of cephalopod beaks (Wolff, 1982, 1984; Clarke, 1986; Smale et al., 1993; Xavier and Cherel, 2009), whereas reconstruction of fish weights was based on the relationship of length to weight (Fernández, 1987; IMARPE[2]) and the relationship of otolith radius to total length (Goicochea and Arrieta, 2008) when possible.

To assess whether the sample size collected was appropriate to describe the diet of blue sharks, we constructed a cumulative prey curve at the family level from the total number of prey species identified, excluding 'unidentified remains' (i.e., cephalopod, fish, and crustacean) prey items by using the software EstimateS, vers. 9.1.0 (Colwell, 2013). The order of samples was permuted 1000 times to reduce bias. Following the method of Jiménez-Valverde and Hortal (2003), we plotted the results to analyze the suitability of the sample size. When the curve approaches the asymptote (slope<0.1), the number of samples is deemed to be sufficient to describe the diet (Soberón and Llorente, 1993). Furthermore, we used the calculation method proposed by Bizzarro et al. (2007) to reinforce the sampling assessment. This method states that the slope of the line generated from the curve endpoints (mean cumulative number of prey taxa generated for the final 4 stomach samples) should be compared to a line of 0 slope to establish whether a cumulative prey curve has reached an asymptote. Slopes are compared by using Student's *t*-test, where slopes that are not significant ($P>0.05$) indicate that the curve has reached an asymptote (Bizzarro et al., 2007).

---

[2] IMARPE (Instituto del Mar del Peru). 2012. Crucero 1202-04 de "Evaluación hidroacústica de los recursos pelágicos." Inst. Mar Peru, Inf. Ejec., 49 p. [Available from website.]

The relative importance of each prey species to the diet of the blue shark was established by the prey-specific index of relative importance (%PSIRI) (Brown et al., 2012), by using the equation:

$$\%PSIRI = 0.5\%FO_i \times (\%PN_i + \%PW_i), \tag{1}$$

where $\%FO_i$ = the number of stomachs containing prey category i, divided by the total number of stomachs n;
$\%PN_i$ = prey-specific numeric abundance; and
$\%PW_i$ = prey-specific wet-weight abundance.

Prey-specific abundance ($\%PA_i$) was calculated by

$$\%PA_i = \Sigma_{j=1}^{n} \%A_{ij} n_i^{-1},$$

where $\%A_{ij}$ = the abundance (by counts [$\%PN_i$] or weight [$\%PW_i$]) of prey category i in stomach sample j; and
n_i = the number of stomachs containing prey i.

The %PSIRI, is a modification of the index of relative importance (%IRI [Cortés, 1997]) that avoids %FO redundancies taken in the %IRI and is additive with respect to taxonomic levels. As a result, the %PSIRI of a family will be equal to the sum of the %PSIRI of the species within the taxon (Brown et al., 2012).

Niche breadth was calculated according to Levin's standardized index by using %PSIRI converted to proportions at the family level (Krebs, 1999). The index values ranged between 0 and 1, where values closer to 0 indicate a diet dominated by few prey species (i.e., by a greater degree of specialization) and values closer to 1 indicate a lesser degree of specialization (Munroe et al., 2014). In addition, the graphical analysis proposed by Amundsen et al. (1996) was performed to explore prey importance at the family level and predator feeding strategy. The analysis is based on a 2-dimensional graph representation of prey-specific abundance ($\%PA_i$) in relation to the frequency of occurrence of the different prey types in the diet ($\%FO_i$).

Trophic position was calculated based on percent weight values of the prey species identified with the equation proposed by Christensen and Pauly (1992):

$$TP = 1 + \left(\Sigma_{j=1}^{n} DC_{ij}\right) \times \left(TP_j\right), \tag{2}$$

where DC_{ij} = the composition of the prey j in the diet of the predator I;
TP_j = to the trophic level of prey j; and
n = the number of prey species in the diet of predator j.

Values of trophic position for fish prey were obtained from Froese and Pauly[3] and Espinoza (2014); and for cephalopod prey from Cortés (1999) and Espinoza (2014).

To identify possible differences in diet, individual sharks were analyzed according to 5 factors: sex, season, size class, latitude of fishing ground, and longitude of fishing ground. The analysis by sex was performed to clarify whether the composition of diets of females and males is related to the reported spatial segregation by sex (Nakano and Stevens, 2008). Specimens analyzed per season were grouped into warm (February–May and December) and cold (June–November) seasons according to established patterns of sea-surface temperatures (SST) (Flores et al., 2013). Cluster analysis was employed with 20-, 30-, and 40-cm-TL intervals to define size classes (Markaida and Sosa-Nishizaki, 2010) by using the numeric abundance (at family levels) of identified preys. Calculations were performed by the unweighted pair-group method with arithmetic mean and by using the Bray–Curtis index as a measure of dissimilarity. A 50% of dissimilarity distance indicated major divisions between size classes (Ebert and Bizzarro, 2007). Fishing grounds based on latitude were grouped into 2 biogeographical marine provinces, where 'northern' corresponds to the Tropical Eastern Pacific marine province and 'Northern–Central' to the Warm Temperate Southeastern Pacific marine province (Spalding et al., 2007). Fishing grounds based on longitude were grouped into 'coastal' and 'oceanic' groups, with the Peru–Chile Trench (which occurs at an average distance from the coast of 130 km or 70 nautical miles) as the boundary between these 2 groups (Macharé et al., 1986) (Fig. 1).

Statistical analysis

To assess differences in the diet of blue sharks by factors, we performed two multivariate techniques: nonmetric multidimensional scaling (MDS) ordinations and analysis of similarity (ANOSIM). These techniques were conducted with the Bray–Curtis index of dissimilarity generated from the numeric abundance of each prey grouped by family (Mendoza-Ávila et al., 2016), pretreated by fourth-root transformation and standardized to percentages. The stress value generated by the nonmetric MDS model indicates the reliability of the representation, where values closer to 0 indicate excellent representation and values larger than 0.2 indicate that interpretation of the data is unreliable (Clarke,

---

[3] Froese, R., and D. Pauly (eds.). 2018. FishBase, vers. 02/2018. World Wide Web electronic publication. [Available from website.]

Table 1

Diet composition of blue sharks (*Prionace glauca*), based on analysis of stomach contents collected between February and December 2015 off northern Peru, by percent frequency of occurrence (%FO), percent prey-specific number (%PN), percent number (%N), percent prey-specific weight (%PW), percent weight (%W) and the prey-specific index of relative importance (%PSIRI).

Prey species	%FO	%N	%PN	%W	%PW	%PSIRI
CEPHALOPODA						
Decapodiformes						
Oegopsida	4.35	0.27	6.18	<0.01	<0.01	0.13
Ancistrocheiridae						
Ancistrocheirus lesueurii	14.78	5.07	34.31	7.37	49.86	6.22
Chiroteuthidae						
Chiroteuthis veranyi	3.48	1.45	41.83	0.93	26.85	1.19
Grimalditeuthis bonplandi	11.30	1.88	16.66	<0.01	<0.01	0.94
Cranchiidae						
Galiteuthis pacifica	2.61	1.14	43.63	0.88	33.55	1.01
Leachia danae	4.35	1.06	24.34	0.24	5.42	0.65
Enoploteuthidae						
Abraliopsis affinis	1.74	0.51	29.35	0.28	16.34	0.40
Gonatidae						
Gonatus antarcticus	11.30	4.06	35.90	5.88	51.98	4.97
Gonatus sp.	0.87	0.87	100.00	0.87	100.00	0.87
Histioteuthidae						
Histioteuthis cerasina	0.87	0.14	16.67	0.05	6.00	0.10
Stigmatoteuthis hoylei	6.96	2.12	30.44	2.91	41.83	2.51
Mastigoteuthidae						
Mastigoteuthis dentata	2.61	1.53	58.59	0.88	33.64	1.20
Octopoteuthidae						
Octopoteuthis sicula	6.09	1.65	27.15	1.30	21.35	1.48
Ommastrephidae						
Dosidicus gigas	6.09	1.58	26.03	4.03	66.17	2.81
Ommastrephes bartramii	1.74	0.61	35.00	1.22	70.40	0.92
Onychoteuthidae						
Onychoteuthis banksii	4.35	0.89	20.46	0.07	1.72	0.48
Pholidoteuthidae						
Pholidoteuthis massyae	3.48	0.27	7.74	0.11	3.05	0.19
Thysanoteuthidae						
Thysanoteuthis rhombus	12.17	5.53	45.41	6.43	52.79	5.98
Myopsida						
Loliginidae						
Doryteuthis (Amerigo) gahi	2.61	0.49	18.88	1.39	53.43	0.94
Octopodiformes						
Argonautidae						
Argonauta spp.	26.09	17.60	67.46	14.52	55.65	16.06
Bolitaenidae						
Japetella diaphana	7.83	3.61	46.18	3.15	40.21	3.38
Japetella heathi	1.74	0.34	19.64	<0.01	<0.01	0.17
Enteroctopodidae						
Muusoctopus sp.	0.87	0.14	16.67	0.01	0.73	0.08
Octopodidae						
Eledone spp.	0.87	0.05	5.71	<0.01	<0.01	0.02
Tremoctopodidae						
Tremoctopus violaceus	1.74	0.10	5.72	0.01	0.77	0.06
Vitreledonellidae						
Vitreledonella richardi	1.74	0.07	4.26	<0.01	0.00756	0.04
Vampyromorphida						
Vampyroteuthidae						
Vampyroteuthis infernalis	6.96	2.42	34.82	2.96	42.55	2.69
Unidentified cephalopods	33.04	29.57	89.47	33.04	99.98	31.30

Table continued

Table 1 (*continued*)

Prey species	%FO	%N	%PN	%W	%PW	%PSIRI
TELEOSTEI						
Clupeiformes						
Engraulidae						
Engraulis ringens	2.61	1.12	42.91	1.52	58.43	1.32
Gadiformes						
Macrouridae						
Coryphaenoides sp.	0.87	0.02	2.86	<0.01	<0.01	0.01
Merlucciidae						
Merluccius gayi peruanus	0.87	0.05	6.25	0.56	63.94	0.31
Myctophiformes						
Myctophidae						
Myctophum aurolaternatum	0.87	0.09	10.00	<0.01	0.03	0.04
Perciformes						
Coryphaenidae						
Coryphaena hippurus	1.74	0.43	25.00	1.65	94.84	1.04
Scombridae						
Auxis thazard	0.87	0.08	9.09	0.02	2.87	0.05
Sphyraenidae						
Sphyraena idiastes	0.87	0.11	12.50	<0.01	<0.01	0.05
Unidentified fishes	22.61	8.71	38.53	3.51	15.51	6.11
MAMMALIA						
Cetacea						
Delphinidae	1.74	0.23	12.96	0.91	52.29	0.57
Delphinus capensis	0.87	0.29	33.33	0.25	28.61	0.27
CRUSTACEA						
Decapoda						
Galatheidae						
Pleuroncodes monodon	0.87	0.84	97.14	0.81	92.64	0.83
Unidentified crustaceans	5.22	0.70	13.42	<0.01	0.06	0.35
AVES						
Unidentified bird	0.87	0.11	12.50	<0.01	0.31	0.06
EGGS						
Exocoetidae eggs	7.83	2.17	27.76	2.25	28.75	2.21

1993). The *R*-statistic values from ANOSIM describe the extent of similarity, where $R=0$ refers to an identical diet and $R= \pm 1$ is indicative of the most divergent diet (Clarke, 1993). Similarity percentages (SIMPER) were used, as well, to determine the prey categories, by family, that typified particular groups, or contributed most to the similarities between groups, or both (Clarke, 1993). Finally, the semiparametric permutation multivariate analyses of variance (PERMANOVA) test on the Bray–Curtis index of dissimilarity (based on numeric abundance) was used to test whether an interaction was present between factors that were significant according to the pairwise tests (ANOSIM).

Statistical analyses were conducted with the software RStudio, vers. 1.1.453 (RStudio, 2018) with R, vers. 3.5.0 (R Core Team, 2018). Descriptive statistics are presented with mean standard deviations (SDs).

Results

A total of 143 stomachs of blue sharks were obtained from the ports of Mancora (n=43) and Salaverry (n=100). Of these, 115 (80.4%) had food remains and 28 (19.6%) were empty. Of those individuals with food remains, 47 were female (range: 165–293 cm TL; mean: 214 cm TL [SD 35] and 68 were male (range: 110–288 cm TL; mean: 220 cm TL [SD 41]). A cumulative prey curve was constructed on the basis of 74 stomach contents because 41 stomachs containing only ‘unidentified remains’ were excluded. The curve slope was 0.9, indicating that the sampling size was sufficient to describe the diet of blue sharks. However, according to the Bizzarro’s et al. (2007) method, the curve did not reach an asymptote (P<0.05), and therefore suggests that the results presented here do not fully describe the blue shark diet.

Prey comprised 42 taxonomic levels (Table 1). Cephalopods represented the main prey group (87.4% PSIRI), followed by fishes (8.5% PSIRI), flying fish eggs (2.1% PSIRI), crustaceans (1.1% PSIRI), and marine mammal and bird remains (0.8% and 0.1% PSIRI, respectively). The prey item ‘unidentified cephalopods’ (represented by flesh, gladii, and eye lenses) was the most important (31.3% PSIRI) in the overall analysis, followed by *Argonauta* spp. (16.1% PSIRI) and *A. lesueurii* (6.2% PSIRI) (Table 1; Fig. 2).

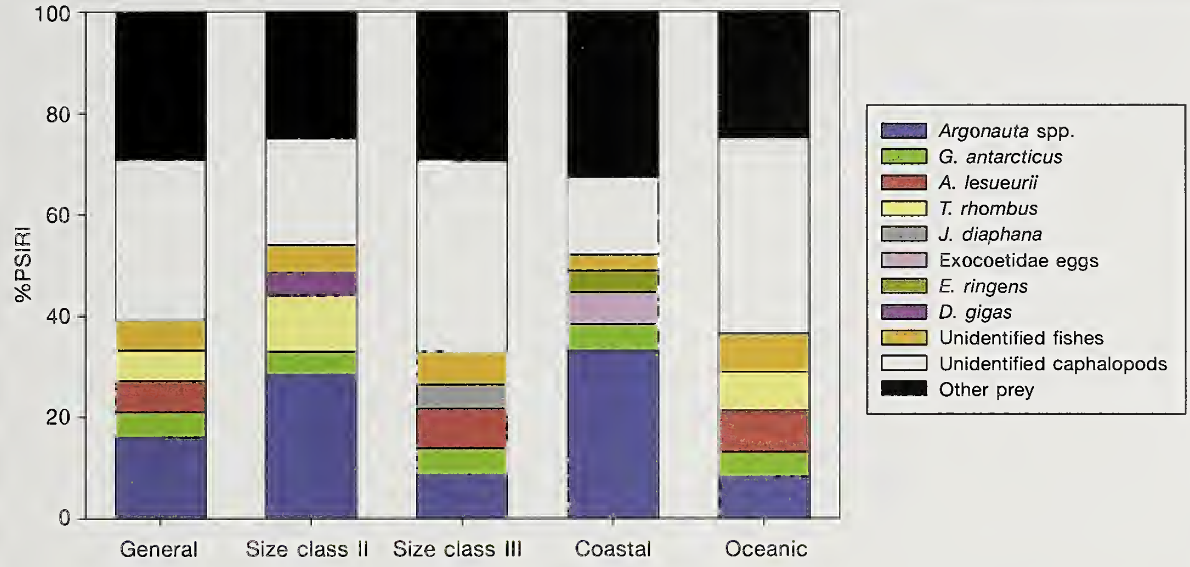

Figure 2

Prey-specific index of relative importance (%PSIRI) of the overall diet of blue sharks (*Prionace glauca*) sampled in northern Peru between February and December 2015, by size class and longitude of fishing ground. Size class II represents fish 150.0–229.9 cm in total length (TL) and size class III represents fish 230.0–309.9 cm TL; size class I had only 2 samples and was excluded from most analyses. Two regions were used for analyses with longitudes: coastal and oceanic, delineated by the Peru–Chile Trench (which has an average distance from shore of 130 km or 70 nautical miles). Taxa include *Argonauta* spp., *Gonatus antarcticus*, *Ancistrocheirus lesueurii*, the diamond squid (*Thysanoteuthis rhombus*), *Japetella diaphana*, flying fish (Exocoetidae) eggs, the Peruvian anchoveta (*Engraulis ringens*), and the jumbo squid (*Dosidicus gigas*).

Table 2

Levin's standardized index (B_i), analysis of similarity (ANOSIM), and trophic position (TP) of blue sharks (*Prionace glauca*) from which stomach contents were collected between February and December 2015 off northern Peru, by size class and longitude of fishing ground. Size class II represents fish 150.0–229.9 cm in total length (TL) and size class III represents fish 230.0–309.9 cm TL; size class I had only 2 samples and was excluded from most analyses. Two regions, coastal and oceanic, were used for the analyses with longitudes of fishing grounds: these regions are separated by the Peru–Chile Trench (which has an average distance from shore of 130 km or 70 nautical miles). General=overall analysis.

Factor	Subfactor	ANOSIM	B_i	TP
General	–	–	0.26	4.4
Size class	II	II vs III (R=0.05; P<0.05*)	0.19	4.4
	III		0.42	4.4
Fishing ground longitude	Coastal	Coastal vs. oceanic (R=0.10; P<0.01*)	0.18	4.4
	Oceanic		0.40	4.4

The niche breadth of the blue shark was considered narrow according to Levin's standardized index (Table 2), indicating a higher degree of specialization. The graphical analysis suggests a similar feeding pattern, with a clear dominance of the Argonautidae family (Fig. 3). Additionally, the trophic position of the blue shark was calculated as 4.4, indicating that the blue shark is a high trophic-level consumer within the food web off northern Peru.

Size class groups were evaluated at 20- and 30-cm-TL intervals and showed no clear organization of size classes. Nevertheless, cluster analysis with a 40-cm-TL interval showed positive results, with 3 size classes identified at 50% of Bray–Curtis dissimilarity (Fig. 4).

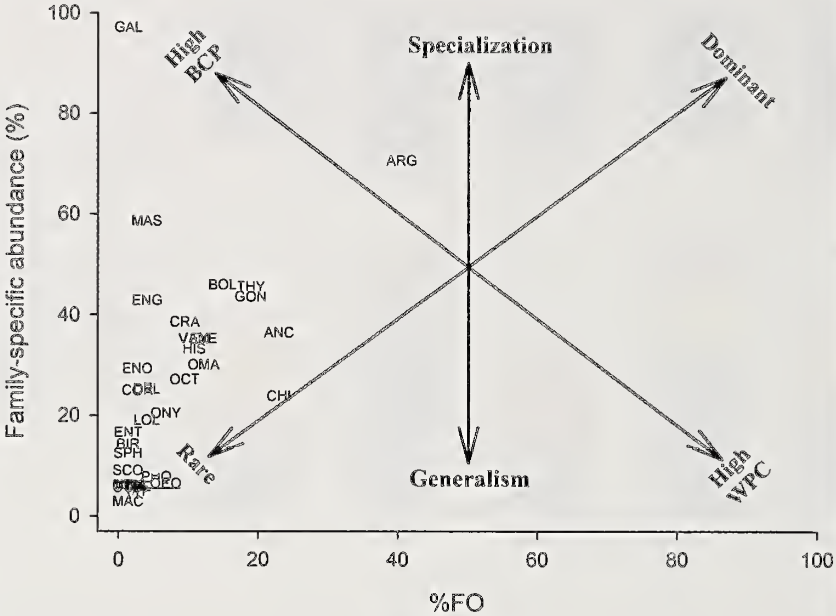

Figure 3

Prey-specific abundance at a family level plotted against the frequency of occurrence (%FO) for families of prey species found in analysis of stomach contents of blue sharks (*Prionace glauca*) sampled in northern Peru between February and December 2015. The explanatory axes for foraging patterns are those modified by Amundsen et al. (1996). The 2 diagonal axes represent the importance of prey (dominant versus rare) and the contribution to niche width (high between-phenotype contribution [BPC] versus high within-phenotype contribution [WPC]). The vertical axis defines the predator feeding strategy. The families include Ancistrocheiridae (ANC), Argonautidae (ARG), Bolitaenidae (BOL), Chiroteuthidae (CHI), Coryphaenidae (COR), Cranchiidae (CRA), Delphinidae (DEL), Engraulidae (ENG), Enoploteuthidae (ENO), Enteroctopodidae (ENT), Galatheidae (GAL), Gonatidae (GON), Histioteuthidae (HIS), Loliginidae (LOL), Macrouridae (MAC), Mastigoteuthidae (MAS), Merlucciidae (MER), Myctophidae (MYC), Octopodidae (OCD), Octopoteuthidae (OCT), Oeogopsidae (OEO), Ommastrephidae (OMA), Onychoteuthidae (ONY), Pholidoteuthidae (PHO), Scombridae (SCO), Sphyraenidae (SPH), Thysanoteuthidae (THY), Tremoctopodidae (TRE), Vampyroteuthidae (VAM), and Vitreledonellidae (VIT). Other stomach contents include one bird (BIR) and flying fish (Exocoetidae) eggs (EXO).

However, because size class I (110.0–149.9 cm TL) was represented by only 2 samples, only size class II (150.0–229.9 cm TL, n=32) and size class III (230.0–309.9 cm TL, n=40) were considered for subsequent analyses.

From all the factors assessed (sex, season, size class, and fishing ground [by latitude and longitude]), ANOSIM showed a significant difference in the diet by size class and fishing ground longitude. These differences were small (Table 2), but indicated that an overlap exists between the composition of dietary factors (Clarke, 1993). A small difference in diet composition existed between size class II and III (Table 2). The nonmetric MDS plot showed that this small difference is explained by an overlap of diets (Fig. 5A). According to SIMPER analysis, in order of importance, the prey families that most contributed to the diet of size class II were Argonautidae and Thysanoteuthidae, whereas in size class III they were Argonautidae and Ancistrocheiridae. The %PSIRI for size classes showed a similar trend (Fig. 2). *Argonauta* spp. represented the main prey taxon for both size classes, although a considerable decrease in this taxon was observed from size class II (28.5%) to size class III (8.6%). Furthermore, larger size individuals (size class III) exhibited a tendency to forage on other prey species such as *A. lesueurii* (7.8%) and *Japetella diaphana* (4.7%), in addition to an increase in the importance of 'unidentified cephalopods' in the diet. Niche breadth analysis revealed that both groups had high degrees of specialization, even though higher values were estimated for size class III (Table 2). Blue sharks of both groups were considered top predators (Table 2).

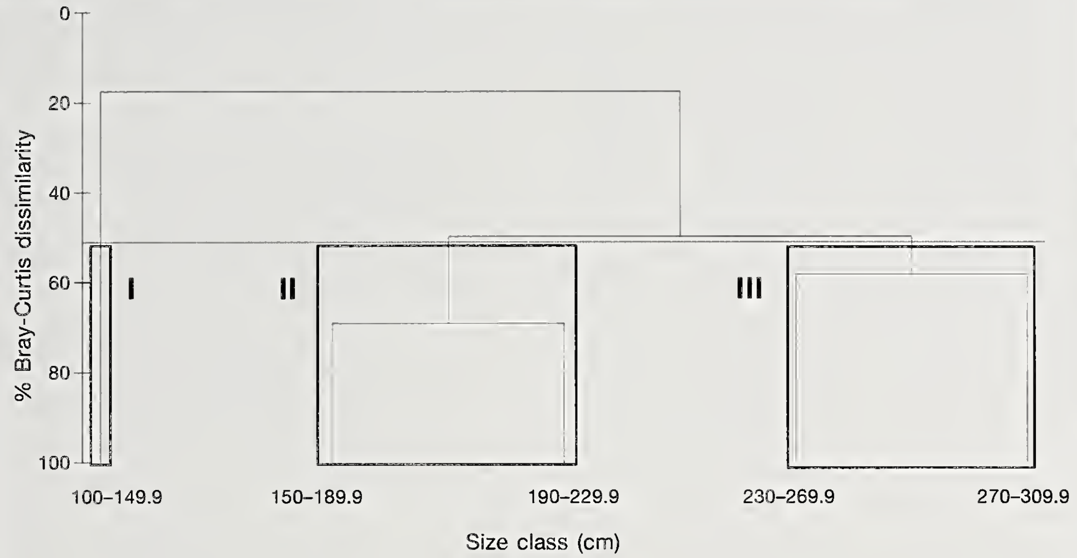

Figure 4

Cluster analysis of 3 size classes with total length intervals of 40 cm for blue sharks (*Prionace glauca*) sampled off northern Peru between February and December 2015. Hierarchical clustering was performed by using the Bray–Curtis index of dissimilarity.

The nonmetric MDS ordination for fishing ground longitude showed that the diets of both groups overlapped (Fig. 5B). This overlap explains the small difference calculated with ANOSIM (Table 2). SIMPER analysis revealed that, in order of importance, Argonautidae and Chiroteuthidae contributed more to the diet of blue sharks in the coastal zone, whereas Ancistrocheiridae and Argonautidae contributed more to the diet of individuals in the oceanic zone. Trophic positions in both longitudinal zones were similar and Levin's standardized index revealed that blue sharks had a higher degree of diet specialization in both zones, although higher values were estimated for the oceanic zone (Table 2). Values of %PSIRI for longitudinal zones (Fig. 2) showed that the coastal zone diet (n=36) was predominated by *Argonauta* spp. (33.2%), flying fish eggs (6.3%), *Gonatus antarcticus* (5.2%), and Peruvian anchoveta (4.2%). In contrast, the oceanic zone (n=79 stomachs) had a much lower percentage of *Argonauta* spp. (8.3%), in addition to *A. lesueurii* (8.2%) and diamond squid (*Thysanoteuthis rhombus*, 7.6%). Furthermore, 'unidentified cephalopods' varied greatly between coastal (15.3%) and oceanic (38.6%) zones.

Finally, the PERMANOVA test (pseudo-F=0.7961, P>0.05) indicated no interaction between the 2 size classes and coastal and oceanic fishing grounds.

Discussion

The present study provides important new information on the diet of blue sharks in Peruvian waters. In this study, cephalopods represented 87.4% PSIRI of overall diet, and 66.7% of total prey species identified. These results validate, for Peruvian waters, the preference of blue sharks to prey on squid in the eastern Pacific Ocean (Markaida and Sosa-Nishizaki, 2010; Loor-Andrade et al., 2017). Furthermore, our results showed that small quantities of fish were consumed (8.5% PSIRI). It is important, however, to note that fish consumption is likely underestimated because both fish flesh and otoliths degrade faster than cephalopod flesh and beaks (Tricas, 1979; Hernández-García, 1995).

Blue sharks have been described as meso- and bathypelagic predators (Clarke et al., 1996). They are known to swim at depths near the thermocline at night, whereas during daylight hours, they prefer to dive and complete long incursions to great depths (Carey and Scharold, 1990). Campana et al. (2011) stated that this behavior was highly related to the diel vertical migrations of their preferred prey (i.e., cephalopods), which feed in the epipelagic zone at night and move to greater depths during daylight hours. Our identification of mesopelagic (e.g., Ancistrocheiridae, Histioteuthidae, Gonatidae cephalopods) and bathypelagic (i.e., *Vampyroteuthis infernalis*) prey in significant quantities, suggests that, at least for the area studied, they also completed vertical migrations to feed on preferred or available prey, or both (Roper and Young, 1975).

Argonauta spp. off the coast of northern Peru have been studied little and have been described only as fauna associated with prospections associated with the Peruvian anchoveta fishery in the northern Humboldt ecosystem (between 4–16°S and 0–148 km from shore)

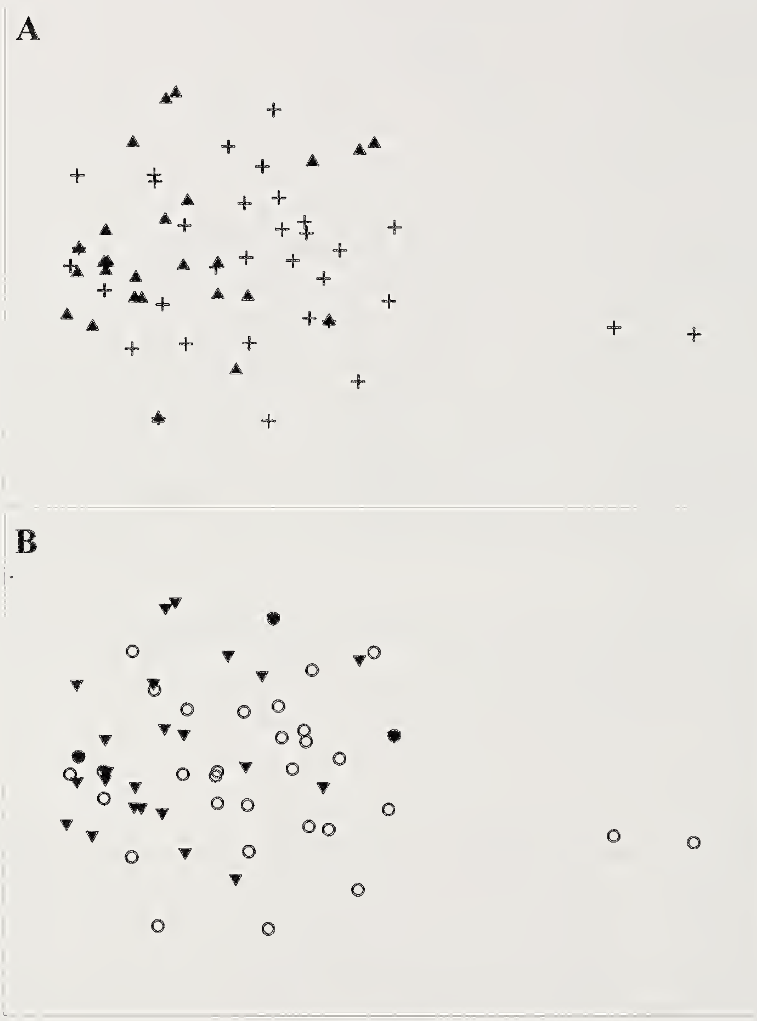

Figure 5

Nonmetric multidimensional scaling plots comparing distributions of (A) size classes II (▲) and III (+) and (B) oceanic (▼) and coastal (O) fishing grounds for blue sharks (*Prionace glauca*) collected off northern Peru between February and December 2015. Size class II represents fish 150.0–229.9 cm in total length (TL), and size class III represents fish 230.0–309.9 cm TL. The coastal and oceanic fishing grounds were categorized by using the Peru–Chile Trench (with an average distance from shore of 130 km or 70 nautical miles) as the boundary. The stress level of this plot is 0.06.

(IMARPE[4]) and as a component of the diet of dolphinfish (*Coryphaena hippurus*) (Solano et al., 2015). However, recent investigations have begun to assess basic aspects of its ecology. Orosco-Montenegro (2016) reported that the abundance of larvae of *Argonauta* spp. is higher during the summer (318 individuals/m^2) than during the fall (9 individuals/m^2) along the Peruvian coast, while Sajinez et al. (2016) mentioned that *Argonauta* spp. abundance is highly related to SST, with increased abundance during positive anomalies. During the sampling year, an SST positive anomaly of 1.7°C (SD 1.2) (DHN[5]) was reported for the Niño 1+2 region (in the eastern equatorial Pacific Ocean between 0–10°S and 90–80°W). Therefore, the elevated consumption of *Argonauta* spp. that we observed (16.1% PSIRI) may have been a response to higher abundances of this species during the SST positive anomaly if we consider the opportunistic foraging behavior of the blue shark upon abundant available prey (Stevens, 1973). The elevated consumption of *Argonauta* spp. is what most makes the blue shark a consumer with a high degree of specialization. However, further investigations are needed to further confirm this feeding pattern and to evaluate how this degree of specialization varies during La Niña periods.

The consumption of flying fish eggs (in patches) recorded in this study may suggest, as Nakano and Seki (2003) proposed, the ingestion of prey (or objects) whose silhouettes are detected against light from the sea surface. However, the maximum number of individuals of certain small-size species (e.g., *Argonauta* spp.=102, *P. monodon*=34, *Doryteuthis (Amerigo) gahi*=25, Peruvian anchoveta=24, *Grimalditeuthis bonplandi*=14) reported in different samples may also reflect a habit of foraging upon shoals of small-size species (Tricas, 1979). Furthermore, Tricas (1979) indicated that blue sharks benefit from schools of spawning squid, such as those of the opalescent inshore squid (*Loligo opalescens*). Therefore, *Argonauta* spp. could be prey of blue sharks within spawning areas of *Argonauta* spp. off northern Peru, as well, especially considering that abundant fertilized and nonfertilized Argonautidae eggs were found in 21 stomachs.

Scavenger behavior

Blue sharks are considered active scavengers in the open ocean (Garibaldi and Orsi Relini, 2000). However, this behavior has only been discussed because of the discovery of cephalopod and marine mammal parts in stomachs of blue sharks (Markaida and Sosa-Nishizaki, 2010; Klarian et al., 2018). In this study we sought to reinforce these studies with a new approach, i.e., with the consideration of the cosmopolitan duck barnacle (*Lepas anatifera*) as a bioindicator of scavenging behavior.

---

[4] IMARPE (Instituto del Mar del Peru). 2015. Crucero 1502-04 de "Evaluación hidroacústica de los recursos pelágicos." Inst. Mar Peru, Inf. Ejec., 42 p. [Available from website]

[5] DHN (Dirección de Hidrografía y Navegación). 2015. Anomalías de la temperatura superficial del mar en el Pacífico ecuatorial. Bol. Oceanogr., December 2015, 9 p. [Available from website]

The duck barnacle is a cosmopolitan species that as an adult is commonly found attached to floating objects (Hinojosa et al., 2006). Its cyprid larval stage denotes the shift from a free-swimming organism to a sessile organism. During this stage, cyprid larvae are forced to find a favorable place to settle and metamorphose into juvenile duck barnacles (Høeg et al., 2012). The most common substrate used by cyprid larvae are animals and floating objects, such as boats, buoys (Sneli, 1983), wood (Minchin, 1996), macroalgae (Hinojosa et al., 2006), turtles (Casale et al., 2012), and even fish (Zevina and Memmi, 1981). However, we believe that other substrates could be used by duck barnacle in the open ocean, for example, moribund spent females of many deep-water cephalopods that float passively to the ocean surface and die (Nesis, 1996). Indeed, Markaida and Sosa-Nishizaki (2010) stated that blue sharks may easily scavenge on these dead buoyant cephalopods. In our study, two stages of duck barnacle—cyprid larvae (60.1%, range: 1–200 individuals) and juveniles (9.1%, range: 1–3) (Suppl.Fig.)—were found in stomachs containing only the prey 'unidentified cephalopods' (n=40). We believe that at least some of the ingestion of cephalopods was the result of scavenging behavior. The possible scavenging behavior of blue sharks is also reinforced by findings of duck barnacle cyprid larvae in samples containing skin, blubber, muscle tissue, and dorsal fin of marine mammals, and in the keeled sternum of an 'unidentified bird' (Klarian et al., 2018).

Dietary variability by ontogenetic factors

Ontogenetic shifts have been described in the diets of several shark species—shifts that are mainly due to energetics, metabolism, or changes in foraging ability (Grubbs, 2010). In the case of blue sharks, some studies have tried to prove these ontogenetic shifts, however, with no success (Markaida and Sosa-Nishizaki, 2010; Hernández-Aguilar et al., 2016).

Length at first maturity of blue sharks in the southeastern Pacific Ocean has been reported to be around 200 cm TL (Bustamante and Bennett, 2013). Therefore, size class II in our study was considered to comprise both juvenile and small adults, with a large predominance (82%) of juveniles. Juvenile blue sharks (TL<200 cm) have a narrow coastal distribution before they take part in larger-scale migrations (Vandeperre et al., 2014). Litvinov (2006) supported the idea that this spatial isolation of juvenile blue sharks is caused by limitations on prey consumption at the earliest age, specifically during the period of development of teeth cusps. In addition, Vandeperre et al. (2014) stated that coastal areas may provide juvenile blue sharks (fork length<185 cm) with optimal growth conditions because of the availability of food resources that are associated with the diversity of topographic features (seamounts and islands), and localized oceanographic processes. In our study, the large abundance of small-size octopods, such as *Argonauta* spp., in the diet of individuals from size class II and in the diet of those captured in the coastal zone (Fig. 2), reaffirms the hypothesis that small-size blue sharks occur in coastal areas and feed upon available prey items.

Vertical and horizontal movements of blue sharks expand progressively as body size increases, and according to migratory patterns throughout their life history (Nakano and Stevens, 2008). The smaller quantities of *Argonauta* spp. and the appearance of the oceanic squid *A. lesueurii* in the diet of individuals from size class III (100% adults) and from oceanic areas (Fig. 2) may indicate longitudinal movements of larger blue sharks from coastal to oceanic areas (Vögler et al., 2012). Moreover, the presence of cephalopods from deeper depths, such as *J. diaphana* or *V. infernalis,* in the diet of size class III may indicate progressive dives to greater depths by larger individuals (Roper and Young, 1975).

In this article we have provided important new information about the food habits of blue sharks off northern Peru. Blue sharks feed on small-size (*Argonauta* spp.) and larger size (*A. lesueurii*) prey species, which indicate a surface and mesobathypelagic foraging behavior. In addition, we identified prey items with commercial importance, such as jumbo squid, *D. gahi*, Peruvian anchoveta, and flying fish eggs in the diet of blue sharks, which highlight the importance of the results from this study for Peruvian ecosystem management.

Acknowledgments

We thank F. Galván-Magaña and J. Xavier for assisting with cephalopod beak identification, as well as J. Ramón-Ortega for his advice with statistics. The authors also thank all onboard observers who participated in this study, as well as E. Alfaro, J. Coasaca, S. Pingo, A. Jimenez, and ProDelphinus staff. This study was funded by the Fondo para la Innovación, la Ciencia y la Tecnología (contract no. 369-PNICP-PIBA-2014), the Darwin Initiative, and the U.S. State Department through the U.S. Embassy in Lima.

Literature cited

Adams, G. D., D. Flores, O. Galindo Flores, K. Aarestrup, and J. C. Svendsen.
2016. Spatial ecology of blue shark and shortfin mako in southern Peru: local abundance, habitat preferences and implications for conservation. Endang. Species Res. 31:19–32.

Alfaro-Shigueto, J., J. C. Mangel, M. Pajuelo, P. H. Dutton, J. A. Seminoff, and B. J. Godley.
2010. Where small can have a large impact: structure and

characterization of small-scale fisheries in Peru. Fish. Res. 106:8–17.

Amundsen, P.-A., H.-M. Gabler, and F. J. Staldvik.
1996. A new approach to graphical analysis of feeding strategy from stomach contents data—modification of the Costello (1990) method. J. Fish Biol. 48:607–614.

Bigelow, H. B., and W. C. Schroeder.
1948. Sharks. *In* Fishes of the western North Atlantic, part 1: lancelets, cyclostomes, sharks (A. E. Parr and Y. H. Olsen, eds.), p. 59–546. Sears Found. Mar. Res. Mem. 1, Yale Univ., New Haven, CT.

Bizzarro, J. J., H. J. Robinson, C. S. Rinewalt, and D. A. Ebert.
2007. Comparative feeding ecology of four sympatric skate species off central California, USA. Environ. Biol. Fish. 80:197–220.

Brown, S. C., J. J. Bizzarro, G. M. Cailliet, and D. A. Ebert.
2012. Breaking with tradition: redefining measures for diet description with a case study of the Aleutian skate *Bathyraja aleutica* (Gilbert 1896). Environ. Biol. Fish. 95:3–20.

Bustamante, C., and M. B. Bennett.
2013. Insights into the reproductive biology and fisheries of two commercially exploited species, shortfin mako (*Isurus oxyrinchus*) and blue shark (*Prionace glauca*), in the south-east Pacific Ocean. Fish. Res. 143:174–183.

Campana, S. E., A. Dorey, M. Fowler, W. Joyce, Z. Wang, D. Wright, and I. Yashayaev.
2011. Migration pathways, behavioural thermoregulation and overwintering grounds of blue sharks in the northwest Atlantic. PLoS ONE 6(2):e16854.

Casale, P., M. D'Addario, D. Freggi, and R. Argano.
2012. Barnacles (Cirripedia, Thoracica) and associated epibionts from sea turtles in the central Mediterranean. Crustaceana 85(4–5):533–549.

Chirichigno, N., and J. Velez.
1998. Clave para identificar los peces marinos del Perú, 2nd ed., 496 p. Publ. Espec., Inst. Mar Peru, Callao, Peru.

Chirichigno, N., and R. M. Cornejo.
2001. Catálogo comentado de los peces marinos del Perú, 314 p. Publ. Espec., Inst. Mar Peru, Callao, Peru.

Christensen, V., and D. Pauly.
1992. ECOPATH II—a software for balancing steady-state ecosystem models and calculating network characteristics. Ecol. Model. 61:169–185.

Carey, F. G., and J. V. Scharold.
1990. Movements of blue sharks (*Prionace glauca*) in depth and course. Mar. Biol. 106:329–342.

Clarke, K. R.
1993. Non-parametric multivariate analysis of changes in community structure. Aust. J. Ecol. 18:117–143.

Clarke, M. R. (ed.).
1986. A handbook for the identification of cephalopod beaks, 273 p. Clarendon Press. Oxford, UK.

Clarke, M. R., D. C. Clarke, H. R. Martins, and H. M. Da Silva.
1996. The diet of the blue shark (*Prionace glauca* L.) in Azorean waters. Arquipélago Life Mar. Sci. 14A:41–56.

Clarke, S. C., M. K. McAllister, E. J. Milner-Gulland, G. P. Kirkwood, C. G. J. Michielsens, D. J. Agnew, E. K. Pikitch, H. Nakano, and M. S. Shivji.
2006. Global estimates of shark catches using trade records from commercial markets. Ecol. Lett. 9:1115–1126.

Clothier, C. R.
1950. A key to some southern California fishes based on vertebral characters. Calif. Dep. Fish Game Fish Bull. 79, 83 p.

Colwell, R. K.
2013. EstimateS: statistical estimation of species richness and shared species from samples. Version 9.1.0 user's guide. [Available from website.]

Cornejo, R., X. Vélez-Zuazo, A. González-Pestana, C. Kouri, and G. Mucientes.
2015. An updated checklist of Chondrichthyes from the southeast Pacific off Peru. Check List 11(6):1809.

Cortés, E.
1997. A critical review of methods of studying fish feeding based on analysis of stomach contents: application to elasmobranch fishes. Can. J. Fish. Aquat. Sci. 54:726–738.
1999. Standardized diet compositions and trophic levels of sharks. ICES J. Mar. Sci. 56:707–717.

Doherty, P. D., J. Alfaro-Shigueto, D. J. Hodgson, J. C. Mangel, M. J. Witt, and B. J. Godley.
2014. Big catch, little sharks: insight into Peruvian small-scale longline fisheries. Ecol. Evol. 4:2375–2383.

Ebert, D. A., and J. J. Bizzarro.
2007. Standardized diet compositions and trophic levels of skates (Chondrichthyes: Rajiformes: Rajoidei). Environ. Biol. Fish. 80:221–237.

Elliot, W., F. Paredes, and M. Bustamante.
1995. Biología y pesquería de tiburones de las Islas Lobos, Perú. Inf. Prog. Inst. Mar Peru 16:5–22.
1996. II prospección biológico-pesquera de "tiburones" al oeste de las Islas Lobos, ynero 1996. Inf. Prog. Inst. Mar Peru 41:3–17.

Espinoza, P.
2014. Trophic dynamics in the northern Humboldt Current system: insights from stable isotopes and stomach content analyses. Ph.D. diss., 131 p. Univ. Bretagne Occidentale, Brest, France.

Fernández, F.
1987. Edad y crecimiento de la merluza Peruana (*Merluccius gayi peruanus*). Bol. Inst. Mar Peru 11:191–220.

Flores, R., M. Espino, G. Luque, and J. Quispe.
2013. Patrones de variabilidad ambiental en el mar peruano. Rev. Peru Biol. 20:21–28.

Galván-Magaña, F., H. J. Nienhuis, and A. P. Klimley.
1989. Seasonal abundance and feeding habits of sharks of the lower Gulf of California, Mexico. Calif. Fish Game 75(2):74–84.

García-Godos, I.
2001. Patrones morfológicos del otolito *Sagitta* de algunos peces óseos del mar Peruano. Bol. Inst. Mar Perú 20:1–83.

Garibaldi, F., and L. Orsi Relini.
2000. Summer abundance size and feeding habits of the blue shark, *Prionace glauca*, in the pelagic sanctuary of the Ligurian Sea. Biol. Mar. Mediterr. 7:324–333. [In Italian with English abstract.]

Goicochea, C., and S. Arrieta.
2008. Variaciones en crecimiento de la anchoveta peruana expresadas en los radios de otolitos. Inf. Inst. Mar. Peru 35:241–244.

Grubbs, R. D.
2010. Ontogenetic shifts in movements and habitat use. *In* Sharks and their relatives II: biodiversity, adaptive physiology, and conservation (J. C. Carrier, J. A. Musick,

and M. R. Heithaus, eds.), p. 319–350. CRC Press, Boca Raton, FL.

Harvey, J. T.
1989. Food habits, seasonal abundance, size, and sex of the blue shark, *Prionace glauca*, in Monterey Bay, California. Calif. Fish Game 75(1):33–44.

Hernández-Aguilar, S. B., O. Escobar-Sánchez, F. Galván-Magaña, and L. A. Abitia-Cárdenas.
2016. Trophic ecology of the blue shark (*Prionace glauca*) based on stable isotopes ($\delta^{13}C$ and $\delta^{15}N$) and stomach content. J. Mar. Biol. Assoc. U.K. 96:1403–1410.

Hernández-García, V.
1995. The diet of the swordfish *Xiphias gladius* Linnaeus, 1758, in the central east Atlantic, with emphasis on the role of cephalopods. Fish. Bull. 93:403–411.

Hinojosa, I., S. Boltaña, D. Lancellotti, E. Macaya, P. Ugalde, N. Valdivia, N. Vásquez, W. A. Newman, and M. Thiel.
2006. Geographic distribution and description of four pelagic barnacles along the south east Pacific coast of Chile—a zoogeographical approximation. Rev. Chil. Hist. Nat. 79:13–27.

Høeg, J. T., D. Maruzzo, K. Okano, H. Glenner, and B. K. K. Chan.
2012. Metamorphosis in balanomorphan, pedunculated, and parasitic Barnacles: a video-based analysis. Integr. Comp. Biol. 52:337–347.

Hoyos, L., J. Tarazona, G. Marquina, D. Velarde, and S. Valle.
1991. Ecologia trofica de *Prionace glauca* "tintorera" de la costa central del Peru. *In* I Reunión Anual del ICBAR libro de resúmenes; Lima, Peru, 4–6 November, p. 75. Instituto de Investigación de Ciencias Biológicas "Antonio Raimondi" (ICBAR), Universidad Nacional Mayor de San Marcos, Lima, Peru.

Jefferson, T., M. Webber, and R. Pitman
2015. Marine mammals of the world: a comprehensive guide to their identification, 2nd ed., 616 p. Academic Press, Cambridge, MA.

Jiménez-Valverde, A., and J. Hortal.
2003. Las curvas de acumulación de especies y la necesidad de evaluar la calidad de los inventarios biológicos. Rev. Ibér. Aracnología 8:151–161.

Klarian, S. A., C. Canales-Cerro, P. Barría, P. Zárate, F. Concha, S. Hernández, M. Heidemeyer, P. Sallaberry-Pincheira, and R. Meléndez.
2018. New insights on the trophic ecology of blue (*Prionace glauca*) and shortfin mako sharks (*Isurus oxyrinchus*) from the oceanic eastern South Pacific. Mar. Biol. Res. 14:173–182.

Krebs, C. J.
1999. Ecological methodology, 2nd ed., 620 p. Addison-Wesley Educational Publishers, Inc. Menlo Park, CA.

Litvinov, F. F.
2006. On the role of dense aggregations of males and juveniles in the functional structure of the range of the blue shark *Prionace glauca*. J. Ichthyol. 8:613–624.

Loor-Andrade, P., J. Pincay-Espinoza, and R. Rosas-Luis.
2017. Diet of the blue shark *Prionace glauca* in the Ecuadorian Pacific Ocean during the years 2013 to 2015. J. Appl. Ichthyol. 33:558–562.

Lopez, S., R. Meléndez, and P. Barría.
2010. Preliminary diet analysis of the blue shark *Prionace glauca* in the eastern South Pacific. Rev. Biol. Mar. Oceanogr. 45:745–749.

Macharé, J., M. Sebrier, D. Huaman, and J.-L. Mercier.
1986. Tectónica cenozoica de la margen continental Peruana. Bol. Soc. Geol. Peru 76:45–77.

Markaida, U., and O. Sosa-Nishizaki.
2010. Food and feeding habits of the blue shark *Prionace glauca* caught off Ensenada, Baja California, Mexico, with a review on its feeding. J. Mar. Biol. Assoc. U.K. 90:977–994.

Mendoza-Ávila, M., G. Zavala-Zambrano, F. Galván-Magaña, and P. Loor-Andrade.
2016. Feeding habits of wahoo (*Acanthocybium solandri*) in the eastern Pacific Ocean. J. Mar. Biol. Assoc. U.K. 97:1505–1510.

Minchin, D.
1996. Tar pellets and plastics as attachment surfaces for lepadid cirripedes in the North Atlantic Ocean. Mar. Pollut. Bull. 32:855–859.

Moscoso, V.
2013. Clave para identificación de crustáceos decápodos y estomatópodos del Peru. Bol. Inst. Mar Peru 28:8–25.

Munroe, S. E. M., C. A. Simpfendorfer, and M. R. Heupel.
2014. Defining shark ecological specialisation: concepts, context, and examples. Rev. Fish Biol. Fish. 24:317–331.

Nakano, H., and M. P. Seki.
2003. Synopsis of biological data on the blue shark, *Prionace glauca* Linnaeus. Bull. Fish. Res. Agency 6:18–55.

Nakano, H., and J. D. Stevens.
2008. The biology and ecology of the blue shark, *Prionace glauca*. *In* Sharks of the open ocean: biology, fisheries and conservation (M. D. Camhi, E. K. Pikitch, and E. A. Babcock, eds.), p. 140–151. Blackwell Publishing, Oxford, UK.

Nesis, K. N.
1996. Mating, spawning, and death of oceanic cephalopods: a review. Ruthenica 6:23–64.

Orosco-Montenegro, L. X.
2016. Variabilidad espacio-temporal de paralarvas de cefalópodos en el mar peruano entre los años 2013 y 2014. B.S. diss., 89 p. Universidad Ricardo Palma, Lima, Perú.

R Core Team.
2018. R: a language and environment for statistical computing. R Foundation for Statistical Computing, Vienna, Austria. [Available from website, accessed May 2018.]

Rivaton, J., and P. Bourret.
1999. Les otolithes des poissons de l'Indo Pacifique. Doc. Sci. et Tech. II 2, 378 p. Inst. Rech. Dev., Nouméa, New Caledonia.

Roper, C. F. E., and R. E. Young.
1975. Vertical distribution of pelagic cephalopods. Smithson. Contrib. Zool. 209, 51 p.

RStudio.
2018. RStudio: integrated development environment for R. RStudio, Inc., Boston, MA. [Available from website, accessed May 2018.]

Sajinez, M., J. Ledesma, and J. Salcedo.
2016. Presencia del género *Argonauta* en el norte del ecosistema de Humboldt, asociadas a las variables oceanográficas 2009–2015. *In* Libro de resúmenes. V Congreso de Ciencias del Mar del Perú; Lambayeque, Peru, 21–25 November (W. Carbajal, J. Chanamé, E. Angulo, and J. Fupuy, eds.), p. 337. Univ. Pedro Ruiz Gallo, Lambayeque, Peru.

Smale, M. J., M. R. Clarke, N. T. W. Klages, and M. A. C. Roeleveld.
1993. Octopod beak identification—resolution at a regional level (Cephalopoda, Octopoda: southern Africa). S. Afr. J. Mar. Sci. 13:269–293.

Sneli, J.-A.
1983. Larvae of *Lepas anatifera* L., 1758, in the North Sea (Cirripedia). Crustaceana 45:306--308.
Soberón, J., and J. Llorente.
1993. The use of species accumulation functions for the prediction of species richness. Conserv. Biol. 7:480–488.
Solano, A., Á. Tresierra, V. García, C. Goicochea, V. Blaskovic, B. Buitrón, and G. Chacón.
2015. Biología y pesquería del perico o dorado Coryphaena hippurus, febrero 2010. Inf. Inst. Mar Peru 42:35–73.
Spalding, M. D., H. E. Fox, G. R. Allen, N. Davidson, Z. A. Ferdaña, M. Finlayson, B. S. Halpern, M. A. Jorge, A. Lombana, S. A. Lourie, et al.
2007. Marine ecoregions of the world: a bioregionalization of coastal and shelf areas. BioScience 57:573–583.
Stevens, J. D.
1973. Stomach contents of the blue shark (*Prionace glauca* L.) off south-west England. J. Mar. Biol. Assoc. U. K. 53:357--361.
Stevens, J. D., R. Bonfil, N. K. Dulvy, and P. A. Walker.
2000. The effects of fishing on sharks, rays, and chimaeras (chondrichthyans), and the implications for marine ecosystems. ICES J. Mar. Sci. 57:476–494.
Tricas, T. C.
1979. Relationships of the blue shark, *Prionace glauca*, and its prey species near Santa Catalina Island, California. Fish. Bull. 77:175–182.
Vandeperre, F., A. Aires-da-Silva, J. Fontes, M. Santos, R. Serrão Santos, and P. Alfonso.
2014. Movements of blue sharks (*Prionace glauca*) across their life history. PLoS ONE 9(8):e103538.
Vögler, R., E. Beier, S. Ortega-García, H. Santana-Hernández, J. J. Valdez-Flores.
2012. Ecological patterns, distribution and population structure of *Prionace glauca* (Chondrichthyes: Carcharhinidae) in the tropical-subtropical transition zone of the north-eastern Pacific. Mar. Environ. Res. 73:37–52.
Wolff, G. A.
1982. A beak key for eight eastern tropical pacific cephalopod species with relationships between their beak dimensions and size. Fish. Bull. 80:357–370.
1984. Identification and estimation of size from the beaks of 18 Species of cephalopods from the Pacific Ocean. NOAA Tech. Rep. NMFS 17, 50 p.
Xavier, J. C., and Y. Cherel.
2009. Cephalopod beak guide for the southern ocean, 129 p. British Antarctic Survey, Cambridge, UK.
Zevina, G. N., and M. Memmi.
1981. Distribution of the pelagic barnacle crustaceans in the Atlantic ocean with respect to anthropogenic factors. *In* Epiboly and biological corrosion in aquatic medium (N. A. Rudyakova, ed.), p 99–109. Nauka, Moscow, Russia.

National Marine
Fisheries Service
NOAA

Fishery Bulletin
established in 1881

Spencer F. Baird
First U.S. Commissioner
of Fisheries and founder
of *Fishery Bulletin*

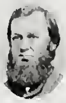

Reproduction, first-year growth, and expansion of spawning and nursery grounds of black sea bass (*Centropristis striata*) into a warming Gulf of Maine

Richard S. McBride (contact author)[1]
Matthew K. Tweedie[2]
Kenneth Oliveira[2]

Email address for contact author: richard.mcbride@noaa.gov

[1] Northeast Fisheries Science Center
National Marine Fisheries Service, NOAA
166 Water Street
Woods Hole, Massachusetts 02543

[2] Department of Biology
University of Massachusetts Dartmouth
285 Old Westport Road
North Dartmouth, Massachusetts 02747-2300.

Abstract—The black sea bass (*Centropristis striata*) is extending its range northward, into a warming Gulf of Maine. Here, we plot the geographic distribution of specific life stages to examine whether spawning and settlement, and therefore productivity, are extending northward. In order to align these life stages with the correct sampling season, we first resolve confusion about the spawning seasonality of this species, by collecting age-0 individuals from coastal waters of southeastern Massachusetts (Buzzards Bay and Nantucket Sound) and aging them by using daily otolith microincrements. Wild-caught age-0 fish (n=381), ranged in size from 32 to 88 mm total length (mean: 53 mm [standard deviation (SD) 11]), and in age from 50 to 129 d old (84 d [SD 16]). They hatched from May 2 to July 21 (June 6 [SD 14 d]), and grew at linear rates from 0.32 to 1.22 mm/d (0.65 mm/d [SD 0.15]). The literature and two 40-year trawl surveys confirm that black sea bass have spawned in Buzzards Bay and Nantucket Sound since the 1880s. Farther north, in the southern Gulf of Maine, spawning has likely occurred in the last 15 years. Settlement has increased about 1°N latitude over the recent 4 decades in association with warming sea temperatures in the southern Gulf of Maine.

The black sea bass (*Centropristis striata*) is an important fishery species in temperate and subtropical latitudes of the western North Atlantic Ocean (Musick and Mercer, 1977; Hood et al., 1994; NEFSC[1]) and is the only serranid that spawns north of Cape Hatteras, North Carolina (Kendall, 1972). The northernmost stock, subject of this study, has been historically distributed in temperate waters from Cape Hatteras to Cape Cod, Massachusetts (Roy et al., 2012; McCartney et al., 2013; McBride, 2014), but in recent years its range has been extending northward into the colder Gulf of Maine (Klein-MacPhee, 2002; Miller et al., 2016). Coastal warming along the U.S. northeast coast is accompanied by the shifting distributions for many marine species (Nye et al., 2009; Pershing et al., 2015; Henderson et al., 2017), and has led to predictions of "winning and losing" species as climate changes (Graham and Harrod, 2009; Hare et al., 2016). Unlike some New England species that appear to be losing ground in the region, the warm-temperate black sea bass may be a winner; however, our ability to predict the effects of climate on fish remains difficult (Brander, 2015; Kleisner et al., 2017; Frank et al., 2018). For example, it is unclear whether random individuals or a specific subset of adults are simply moving farther north on a seasonal basis, or whether spawning or settlement is increasing in previously unoccupied or sparsely populated habitats of the Gulf of Maine.

Fish movements may be a cause for distributional shifts. This northern stock is composed of subregional 'contingents' that provide evidence of phenotypic, particularly meristic, variation along a latitudinal cline (Shepherd, 1991). A potential mechanism underlying this phenotypic cline is contingent-specific seasonal

---

[1] NEFSC (Northeast Fisheries Science Center). 2017. 62nd Northeast Regional Stock Assessment Workshop (62nd SAW) assessment summary report. Northeast Fish. Sci. Cent. Ref. Doc. 17-01, 37 p. [Available from website.]

Manuscript submitted 30 March 2018.
Manuscript accepted 29 August 2018.
Fish. Bull. 116:323–336 (2018).
Online publication date: 27 September 2018.
doi: 10.7755/FB.116.3-4.10

The views and opinions expressed or implied in this article are those of the author (or authors) and do not necessarily reflect the position of the National Marine Fisheries Service, NOAA.

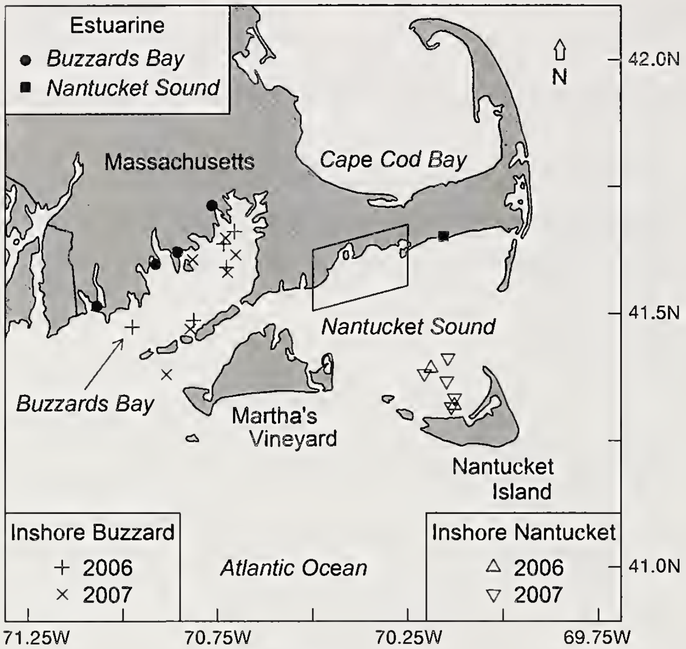

Figure 1

Map of estuarine and inshore sites where black sea bass (*Centropristis striata*) were collected off southeastern Massachusetts during 2006–2007. Collections were used for otolith microincrement analyses. The rhombus indicates the spawning area identified by Kolek (1990), from Succonnesset Shoal to Point Gammon in Nantucket Sound.

migrations, because individuals move offshore and south in autumn and back inshore and north in spring and show a substantial degree of site-fidelity evident from tag-recapture data (Moser and Shepherd, 2009; Fabrizio et al,. 2013). One or more contingents may be leading the way in expanding northward.

Climate change may also be affecting reproduction by shifting spawning seasons or grounds in a manner that could affect productivity rates (Pankhurst and Munday, 2011), which is our focus here. Testing this hypothesis is challenging given that the first year of life of black sea bass at the northern extent of its historical range is poorly understood. Kendall (1972; p. 1254) advanced the idea: “Seasonally, there seems to be some northerly progression of spawning” but added “Details of the suggested northward progression of spawning need clarification” (p. 1257). Differences in modal peaks in spawning seasonality north versus south of Cape Hatteras are not in dispute here (Table 1). To the south, black sea bass spawn in a protracted manner, beginning as early as January, peaking in March, and ending with a smaller peak in September (Mercer, 1978; Wenner et al., 1986). Juveniles, 3–17 cm standard length, are reported year-round off South Carolina, within a coastal, subtropical range of practical salinities (11–35) and temperatures (10–32°C) (Lehnert and Allen, 2002). Farther north, in Maryland and Virginia, Musick and Mercer (1977) concluded that spawning peaked in June. Klein-MacPhee (2002) stated that spawning between Chesapeake Bay and Long Island peaked in August. Age-0 black sea bass, 3–11 cm total length (TL), have occurred in New Jersey coastal habitats during summer–autumn, but they cannot survive winter temperatures, and instead migrate offshore (Able and Hales, 1997; Hales and Able, 2001; Fabrizio et al., 2013).

Although sparse, such data fit Kendall's (1972) initial proposal that spawning progresses seasonally from south to north. However, Caruso's (1995) and Wuenschel et al.'s[2] sampling of black sea bass off Massachusetts, at the northernmost range limit of this species, provide evidence of peak spawning activity early, in late May or mid-June, not later in the season. They examined gonads macroscopically for evidence of spawning, whereas much of the other research was based on ichthyoplankon collections (Table 1). Ichthyoplankton surveys in waters off Massachusetts are not representative of black sea bass spawning, because such surveys did not sample in Nantucket or neighboring sounds (Table 1), where black sea bass have been observed in spawning condition during May–June and juveniles are present in autumn (Fig. 1; Wilson, 1889; Lux and Nichy, 1971; Kolek, 1990; Able et al., 1995; Caruso, 1995; Drohan et al., 2007). We conclude that spawning seasonality and the first year of life have not been adequately described for this species at the northern extent of its range.

To resolve the issue of spawning seasonality, age-0 black sea bass were collected with multiple gears in Buzzards Bay and Nantucket Sound during summer and autumn of 2006 and 2007 to determine age, by day, within that annual age class. Herein and elsewhere (Hales and Able, 1995), this otolith microincrement method has been validated as both accurate and precise with respect to daily increment formation. In addition to defining spawning seasonality based on backcalculated hatch dates, we examined growth rates and resulting size of age-0 fish entering their first overwintering period.

To check for shifting spawning and nursery grounds, we examined geographic distributions of spawning adults and age-0 black sea bass from 2 time series of fishery-independent groundfish (otter trawl) surveys since at least the 1980s. We plot the distributions of these fish roughly by decade and correlate the annual distributions of settled, age-0 fish by both latitude and temperature.

---

[2] Wuenschel, M. J., G. R. Shepherd, R. S. McBride, R. Jorgensen, K. Oliveira, E. Robillard, and J. Dayton. 2011. Sex and maturity of black sea bass collected in Massachusetts and Rhode Island waters; preliminary results based on macroscopic staging of gonads with a comparison to survey data. A working paper for SARC 53- Black Sea Bass Data Meeting. *In* 53rd Northeast Regional Stock Assessment Workshop (53rd SAW) assessment report. Northeast Fish. Sci. Cent. Ref. Doc. 12-05, p. 529–559. [Available from website.]

Materials and methods

Daily age validation and precision

Age-0 black sea bass were collected from the Swan River (Dennis, Massachusetts) on August 10, 2008, with minnow traps (42 cm×20 cm in size, with 7-mm mesh, and a 2.5-cm opening) baited with surf clams. Fifty-nine individuals were transferred to a 90-L aquarium and immersed in a 500 µg/L solution of oxytetracycline (OTC) for 5 h at a salinity of 15 and temperatures of 21–22°C on August 13 (McBride, 2002). These fish were then held in a 970-L tank with a supply of flow-through sea water at 30–32 salinity and 21–22°C and fed to satiation a daily diet of squid and clams. After 24 h (day 2), 5 fish were sacrificed to verify that an OTC mark was present (these fish were not aged later). On day 7, 1 fish was sacrificed to check again the formation of an OTC mark. On day 16, 10 fish were sacrificed for daily ring counts along the distal edge of the OTC mark. Also on day 16, 15 fish were re-marked by immersing them in OTC, in a similar manner as before. On day 30, all remaining fish, some with double OTC marks, were sacrificed for additional counts. There was no other evidence of mortality during the experiment. After fish were sacrificed, sagittal otoliths were removed, cleaned, and stored dry.

Of the 54 marked fish, 17 were selected from each date in a simple random fashion: 1 fish at day 7, 8 fish at day 16, 8 fish at day 30 (including 1 fish with a double mark). One otolith per fish was embedded in epoxy resin, and a 300-µm transverse section was cut with a double-bladed IsoMet Low Speed Saw[3] (Buehler, Lake Bluff, IL). These sections were mounted on microscope slides with a clear, thermoplastic adhesive (Crystalbond 509, Electron Microscopy Sciences, Hatfield, PA) and polished with 3-µm and 5-µm metallurgical lapping film. OTC marks were identified with an ultraviolet light, and microincrements were counted with a light microscope (200×) and imaging software (Image-Pro Plus, vers. 7.0, Media Cybernetics, Inc., Rockville, MD). Standard tests for accuracy, bias, and precision of these daily ages included plotting the data, using Chang's coefficient of variation (CV; Chang, 1982), and using Evans and Hoenig's test of symmetry (Evans and Hoenig, 1998). Age-bias plots follow the bubble format advocated by McBride (2015), and the statistic tests were produced by the FSA package, vers. 0.8.20 (Ogle, 2018) in R software, vers. 3.5.0 (R Core Team, 2018) (Ogle, 2016).

Precision (i.e., repeatability) of daily age estimates from wild-caught fish was checked for 37 otoliths (10% of the 372 fish examined). These otoliths—from 5 randomly selected fish over 10-d intervals (range: 51–129 d)—were aged a second time, independently but by the same reader. Bias and precision tests were performed as described above.

Hatching dates and growth rates

In the estuary, age-0 black sea bass were collected during August–September, 2006 and 2007, off southeastern Massachusetts, by using minnow traps as described in the previous section (Fig. 1). Four sites were sampled in Buzzards Bay (Westport River; Clarks Cove; Nasketucket Bay; Sippican River) and 1 site was sampled in Nantucket Sound (Swan River). Estuarine surface salinity ranged from 17 to 23 and surface temperature ranged from 14° to 23°C during the sampling period.

Inshore, off southeastern Massachusetts, age-0 black sea bass were also collected during the Massachusetts Division of Marine Fisheries (MA-DMF) autumn survey in September 2006 and 2007 by trawl (with 7-mm codend liner). Trawl sites were selected following a stratified-random design (King et. al.[4]), and these sites were then stratified into two areas (Buzzards Bay and Nantucket Sound [Fig. 1]) in analyses. Inshore bottom salinity ranged from 31 to 33 and bottom temperature ranged from 6° to 20°C in September.

The TL of each fish was measured to the nearest mm from the snout to the posterior of the medial caudal fin ray. Sagittal otoliths were removed, cleaned, and stored dry. Otoliths were embedded, sectioned, and mounted as described above; however, 400-µm sections were initially produced, and these became thinner (150–200 µm) after subsequent wet sanding with 1200-grit wet or dry sandpaper. These otoliths were also soaked for 24–96 h in a 2% trypsin solution to enhance the visibility of the rings (Roemer and Oliveira, 2007), and were then polished with metallurgical lapping film, to finish.

Prepared otoliths were dabbed with immersion oil and viewed under a light microscope (100×), aided by imaging software (Image-Pro Plus). Counts began with the first visible ring near the nucleus and continued to the edge of the otolith. Variation in clarity of different areas of the otolith section meant that no single axis was used to count microincrements ('images' in Tweedie, 2014).

A total of 1131 black sea bass were collected in 2006 and 2007 from 5 estuarine sites and 18 different inner shelf sites. Fish were selected for age determination by simple, random subsampling when more than 20 fish were collected within a month-year-area (estuarine, inshore, Buzzards Bay, or Nantucket Sound) aggregate, which resulted in 34% (n=381) of these fish being aged (Fig. 2). Selected fish were statistically smaller than all fish collected in 2006 (Student's t=2.7, df=636, P=0.006), but by <3 mm; therefore this difference was

---

[3] Mention of trade names or commercial companies is for identification purposes only and does not imply endorsement by the National Marine Fisheries Service, NOAA.

[4] King, J. R., M. J. Camisa, and V. M. Manfredi. 2010. Massachusetts Division of Marine Fisheries trawl survey effort, lists of species recorded, and bottom temperature trends, 1978–2007. Mass. Div. Mar. Fish. Tech. Rep TR-38, 151 p. [Available from website.]

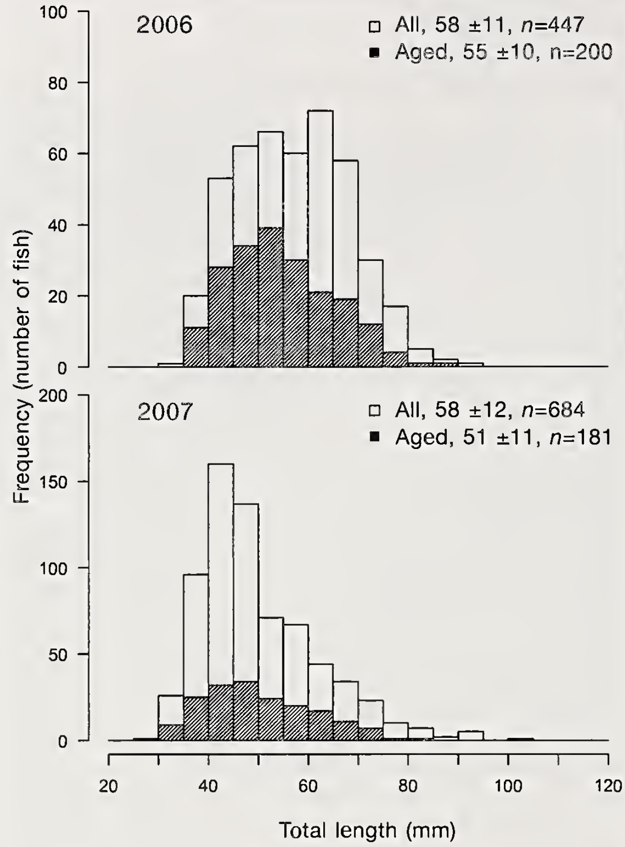

Figure 2

Length–frequency distributions for all (white bars) and aged (overlayed black hatched bars) black sea bass (*Centropristis striata*) collected in 2006 (upper panel) and 2007 (lower panel) in southeastern Massachusetts. Mean values, with standard deviations, (SDs) for sizes and number of fish (*n*) are indicated.

of limited biological significance; there was no difference in aged and all fish collected in 2007 (Student's t=−0.27, df=863, P=0.78) (Fig. 2).

Hatching dates were calculated by subtracting the total count of microincrements for each fish from the date of capture, assuming that the first ring observed corresponded to the hatching date and that there was negligible time difference between spawning and hatching (unknown but considered in the discussion). Capture dates were similar between years (mean: August 28 or 29 [standard deviation (SD) 18–19 d], in 2006 and 2007) and areas (August 28–31 [SD 18–20 d], Buzzards Bay and Nantucket Sound); however, capture dates were 1 month earlier for estuarine than for inshore collections (August 18 [SD 13 d] vs. September 19 [SD 3 d]). Therefore, capture date was a confounding variable, which precluded a comparison of a full 3-way analysis of variance (ANOVA) of hatching dates between years, and between estuarine and inner shelf sites in both Buzzards Bay and Nantucket Sound. Also, because different sampling gears (traps, trawls), were used in estuarine and inshore habitats, there may also have been a gear effect, although this effect would not arise from mesh selectivity, which was the same for both gears (7-mm mesh). Because of these potential confounding variables, hatching dates are described and plotted separately by year and location.

Daily increments and TL at capture were also used to calculate mean growth (in millimeters per day). As reported above for hatching dates, capture date had a significant effect when included in a full multifactorial ANOVA comparison of growth rates between years, and between estuarine and inner shelf sites in both Buzzards Bay and Nantucket Sound. Consequently, size at age and growth rates are also described separately by year and sampling location.

A time series of fish distributions

Annual time series, from 2 otter trawl surveys conducted since the late 1970s and early 1980s, were examined to map the distribution of adult female and age-0 black sea bass collected in coastal waters and on the continental shelf. Plots of different maturity classes depict distributions of adult females and spawning grounds. Maturity classification, completed at sea, followed Burnett et al. (1989). For graphical clarity, 3 classes were plotted: 1) developing fish (prespawning females but also likely to include spawning fish between batch spawning events [Klibansky and Scharf, 2015]); 2) spawning fish (females with hydrated oocytes), and 3) postspawning fish (spent females). Immature and resting fish were not plotted because these were reproductively inactive at time of capture. Distributions of age-0 fish depict nursery grounds. Identification of age-0 fish followed the methods of Penttila and Dery (1988) for examinations of prepared otoliths. Subsequently, it was determined that age-0 fish were readily identified by size (Suppl. Material), and a proxy size (<12 cm TL) was used to select age-0 fish in order to include individuals that were age-0 but that had not been specifically examined for age.

Site selection for these 2 otter trawl surveys followed a stratified-random sampling design. The first survey (MA-DMF), in coastal waters off Massachusetts, was the inshore bottom trawl survey described in the previous section; sampling occurred during spring (May) and autumn (September). The second survey was performed by the National Marine Fisheries Service's Northeast Fisheries Science Center (NMFS-NEFSC) in the spring (March–May) and autumn (September–November). It was conducted in federal waters primarily, covering offshore waters across the continental shelf to the shelf break, from North Carolina to the northern Gulf of Maine, including adjacent territorial seas of Canada. For both surveys, the time series of age-0 fish started in 1978, the time series of mature adults started in 1983, and the terminal year of all data was 2016. Further details are summarized in Reid et al. (1999).

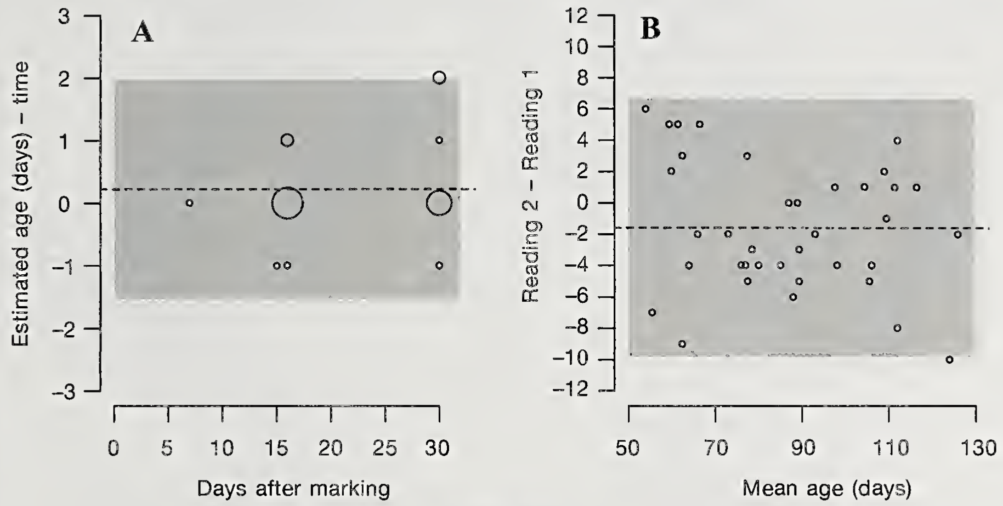

Figure 3

Accuracy and precision of daily otolith microincrement readings in black sea bass (*Centropristis striata*) collected in southeastern Massachusetts during 2006–2007. (**A**) Accuracy: estimated age minus days after marking with oxytetracycline in relation to the days after marking of captive fish held in an aquarium. Bubble size corresponds to number of marks on otoliths from 17 fish (1 fish of which had 2 marks). (**B**) Precision: estimated age difference between 2 independent readings by the same reader in relation to the mean age of both readings for wild-caught fish. Each bubble represents one fish. In both panels, the dashed line indicates the mean of all differences, and the gray box depicts +2 standard deviations.

For later examination in relation to age-0 fish distributions, local sea-surface temperature data were measured from NOAA Buoy Station 44013, 30 km (or 16 nautical miles) east of Boston, Massachusetts (42°21′N, 70°39′W, National Data Buoy Center, website), 1984–2016.

Results

Microincrement analyses

Otolith microincrements were validated as daily in marked fish held captive for up to 30 d (Fig. 3A). The mean bias, 0.22 d, was not significant (test of symmetry: χ^2=2.0, df=2, P=0.37) and there was agreement between known-age and estimated ring count along the distal edge of the OTC mark (Chang's CV=1.8). Microincrement counts made from wild-caught individuals were also repeatable (Fig. 3B). The mean bias, −1.6, was not significant (test of symmetry: χ^2=11.0, df=10, P=0.36) and there was high precision between the first and second paired readings (Chang's CV=3.3). Wild-caught age-0 fish ranged in size from 32 to 88 mm TL (mean: 53 mm TL [SD 11]), and in age from 50 to 129 days old (84 d [SD 16]) (n [no. of fish sampled]=381).

Results based on daily age counts showed that black sea bass spawn from early May to mid-July off southern New England. Individual hatching dates for all aged black sea bass ranged from May 2 to July 21 (mean: June 6 [SD 14 d], n=381) (Fig. 4). Mean hatching dates, pooled by year, were at least a week later in 2006 (June 11 [SD 13 d], n=200) than in 2007 (June 1 [SD 13 d], n=181). They were only 1 d apart between Buzzards Bay and Nantucket Sound (June 6 [SD 14 d], n=273 and June 7 [SD 14 d], n=108, respectively), and they were 2 weeks earlier in fish collected in estuaries (June 1 [SD 11 d], n=257) than at inshore sites (June 16 [SD 12 d], n=124).

Age-0 black sea bass had variable growth rates ranging from 0.32 to 1.22 (mean: 0.65 mm/d [SD 0.15]) (Fig. 5). Mean growth rates, pooled by year, were faster in 2006 (0.70 [SD 0.14]) than in 2007 (0.58 [SD 0.12]); pooled by locations, they were less variable between Buzzards Bay and Nantucket Sound regions (0.66 [SD 0.15] and 0.61 [SD 0.12], respectively), than between estuaries (0.68 [SD 0.14]) and inshore sites (0.57 [SD 0.13]).

Trawl survey analyses

Black sea bass have been spawning farther north for the last 40 years (Fig. 6). Before 2000, spawning was focused in Buzzards Bay and Nantucket Sound, and there were no indications of spawning in the Gulf of Maine. In the 2000s, developing females appeared in Cape Cod Bay. Since 2010, developing females have been caught as far north as Cape Ann off northeastern Massachusetts (42°39′N, 70°36′W). Few spawning females were observed in the Gulf of Maine—a finding

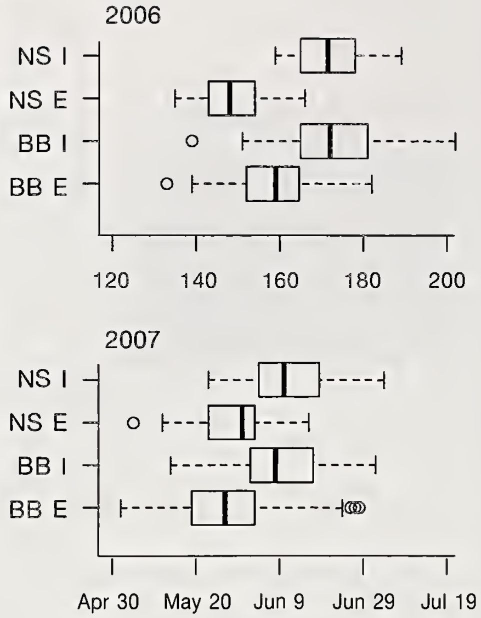

Figure 4

Hatching dates of black sea bass (*Centropristis striata*) in 2006 (upper panel, with numerical days of the year along the bottom axis) and 2007 (lower panel, with corresponding calendar dates). Box-whisker plots represent aged individuals collected from estuarine (E) and inshore (I) sites within Nantucket Sound (NS) and Buzzards Bay (BB) in southeastern Massachusetts, each with the median (thick line), the 25–75 percentile (boxes), the approximate 95% confidence limits (whiskers), and outliers (dots).

that would provide the most direct evidence of spawning. Few spent females were found.

Black sea bass nursery grounds have also been moving northward over the last 40 years (Fig. 7). Overall, age-0 black sea bass were found distributed from the southern Gulf of Maine, specifically Cape Cod and Massachusetts Bay, to North Carolina (Suppl. Material). In the Gulf of Maine, they have been most frequently collected during the last decade, but they have been present in the southern Gulf of Maine since both surveys operated together in the late 1970s. Although the NMFS-NEFSC trawled well into Canadian waters (> 45°N), the maximum latitude of age-0 black sea bass occurrence during 1978–2016 ranged from 41°35′N in 1993 to 42°56′N in 2014.

The maximum latitude of age-0 black sea bass has steadily increased 0.021 degrees annually, on average, since 1978, for a total of about 1°N during the last 40 years (Fig. 8). Most relevant for future monitoring is the association between autumn sea temperature and the maximum latitude of age-0 fish. This association is modeled in Figure 8 as a linear relationship, but also suggests a break point pattern, with a break value around 16–17°C, below which this species is found much farther south and above which it is found much farther north.

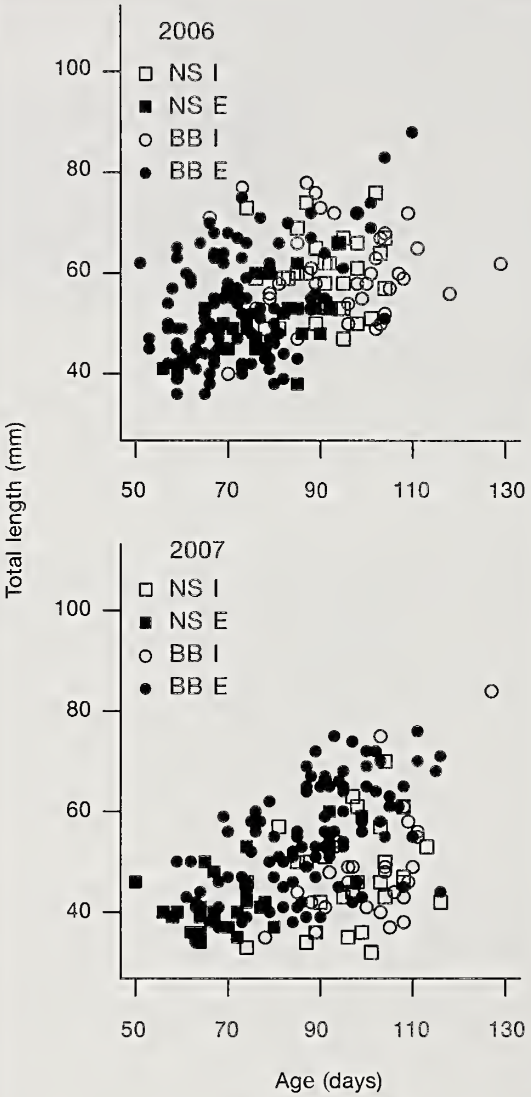

Figure 5

Size at age of black sea bass (*Centropristis striata*) in 2006 (upper panel) and 2007 (lower panel). Individuals are represented according to the location of collections from estuarine (E) and inshore (I) sites within Nantucket Sound (NS) and Buzzards Bay (BB) off southeastern Massachusetts.

Discussion

Black sea bass is already a winner under conditions of warming temperatures. Earlier spring warming has led to earlier and more extensive spring migrations,

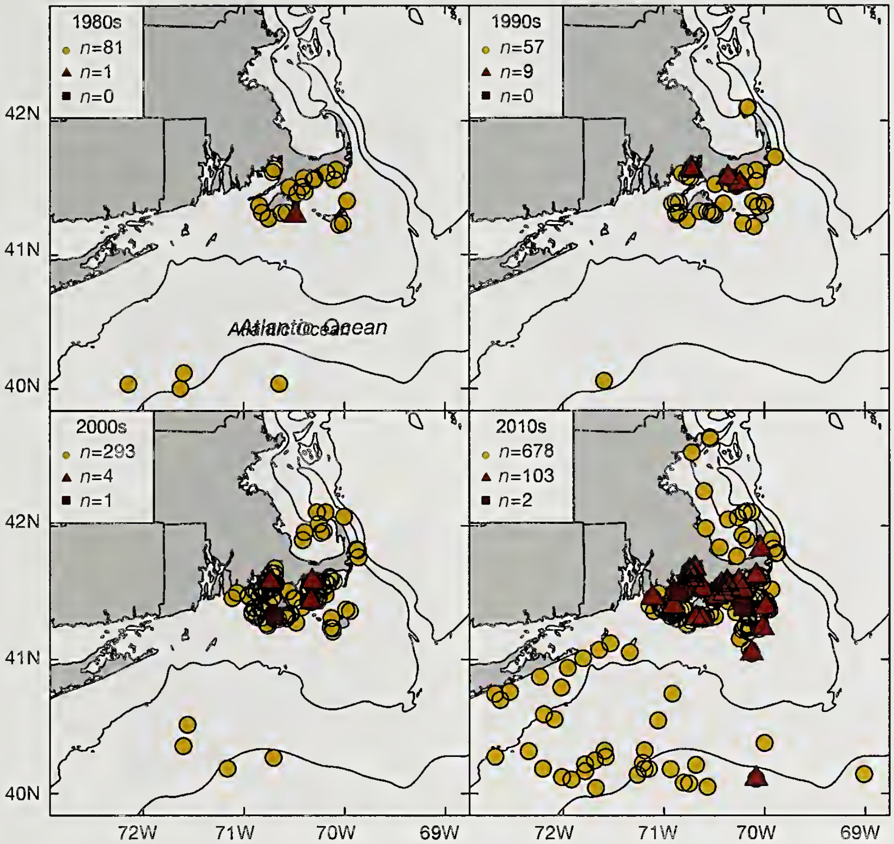

Figure 6

Occurrence of mature female black sea bass (*Centropristis striata*) in trawl surveys conducted during spring by the Massachusetts Division of Marine Fisheries (MA-DMF) and the Northeast Fisheries Science Center (NEFSC) at the northern distributional limit of this species off southeastern Massachusetts, from 1983 to 2016. Most fish are from the MA-DMF survey (Suppl. Material), but we examined fish from both surveys because the NEFSC survey shows broader spawning across the continental shelf. Mature fish are depicted in 3 spawning conditions: developing (orange circles), spawning (red triangles), and postspawning (brown squares). Numbers of fish in each spawning condition (*n*) are provided. Black lines indicate the 50- and 100-m isobaths.

and longer summer durations appear to favor growth, which increases their biomass (Henderson et al., 2017). Our new analyses support a hypothesis that increasing reproductive productivity by the northernmost spawning contingents is driving the broader increasing abundance of this northern stock. As evidence, we define black sea bass spawning seasonality at the northern extent of its range, comment on juvenile growth rates, and examine geographic shifts in spawning females and settled juveniles. Trends in the northward expansion of settled age-0 fish are also correlated with a warming trend in the southern Gulf of Maine.

Spawning seasonality

Using an otolith microincrement method, we found that black sea bass spawning seasonality does not conform to Kendall's (1972) preliminary proposal that spawning for this species occurs progressively later with latitude. True, peak spawning is much earlier in the year south versus north of Cape Hatteras, North Carolina, but black sea bass also have the potential for a very prolonged spawning period in some regions but not others. In the south, in offshore waters of South Carolina and Georgia, Wenner et al. (1986) documented an early and prolonged spawning peak, from January to April, and a smaller peak in September. Farther north, in offshore waters of the middle Atlantic seaboard, from North Carolina to New York, spawning appears protracted from as early as April to as late as November (Table 1). At the northernmost extent of black sea bass distribution, as shown herein, spawning begins later but appears less prolonged: from May to July, peaking in June. Earlier spawning is not likely, because adults return to Massachusetts waters in spring, from an overwintering migration. We postulate that later

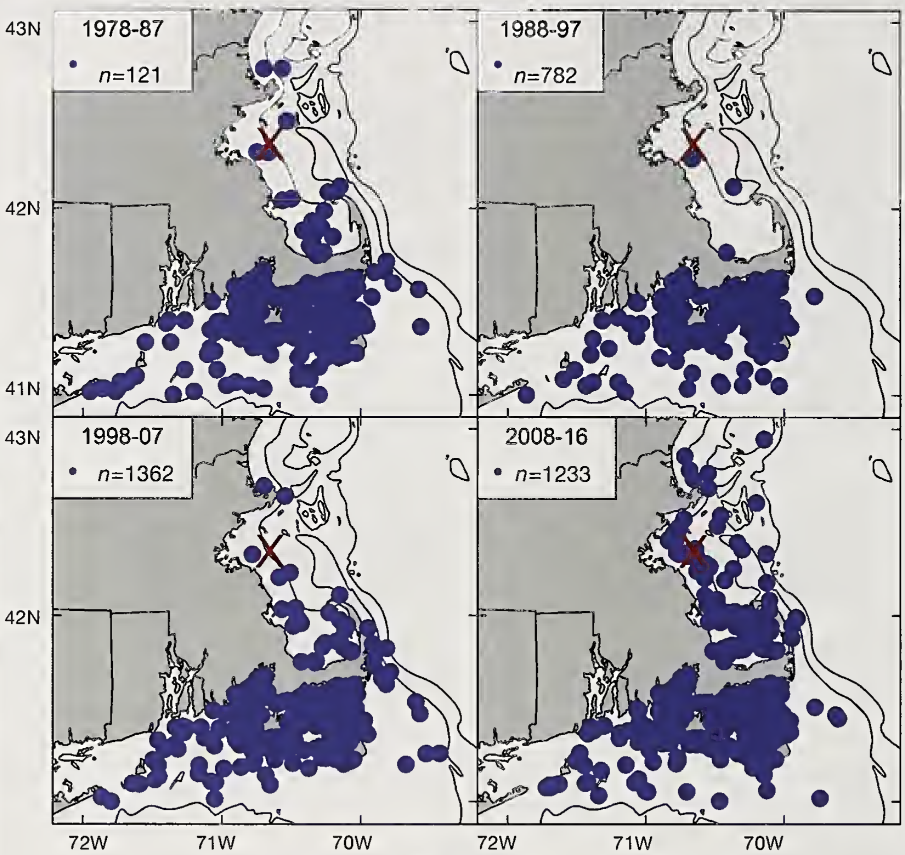

Figure 7

Occurrence (blue dots) of age-0 black sea bass (*Centropristis striata*) in trawl surveys conducted during autumn by the Massachusetts Division of Marine Fisheries and the Northeast Fisheries Science Center (NEFSC) at the northern distributional limit of this species off southeastern Massachusetts, from 1978 to 2016. See Supplementary Material for areal extent of the NEFSC sampling coverage (~36–44°N). Numbers of age-0 fish (*n*) are provided. Black lines indicate the 50- and 100-m isobaths. A red X indicates the position of the sea-surface temperature buoy referred to in Figure 8.

spawning is not favored in southern New England waters because the resulting age-0 fish would not grow to a sufficient size or store sufficient energy to avoid overwintering mortality (Munch et al., 2003; Bell, 2012). The timing and length of the spawning season may itself be subject to change, if warming continues, as suggested by supplemental data in Walsh et al. (2015); therefore further monitoring is warranted.

Our estimates of hatching dates are both accurate and precise. Daily microincrement formation in black sea bass otoliths has been validated by Hales and Able (1995) using OTC marked fish released and recaptured in the wild. Our effort confirms the age validation step of Hales and Able (1995) and shows the level of precision in our specific estimates. Nonetheless, we have assumed that the first microincrement corresponds with hatching specifically, but it could be laid down earlier during embryogenesis. In general, we assume a negligible difference between the times of deposition of the first growth ring, hatching, and spawning. A review of the literature suggests that our estimates of hatching dates may differ from spawning dates by as much as a week. Egg incubation is reported to range from 38 h at 23°C to 75–120 h at 15–16°C (Wilson, 1889; Hoff[5]; Kendall, 1972). The difference between spawning, hatching, and the first microincrement may be more than 5 d in Buzzards Bay and Nantucket Sound with May bottom temperatures of 10–12°C (King et al.[2]), but would be shorter later, June or July, as temperature increases and survival of eggs would improve (optimized at 22–25°C; Watanabe et al., 2003). These potential adjustments would push the calculation of spawning seasonality earlier, especially when sea temperatures are

---

[5] Hoff, F. H. 1970. Artificial spawning of the black sea bass *Centropristis striata melanus* (Ginsberg), aided by chorionic gonadotrophic hormones. Fla. Dept. Nat. Resour. Mar. Res. Lab. Spec. Sci. Rep. 25, 17 p.

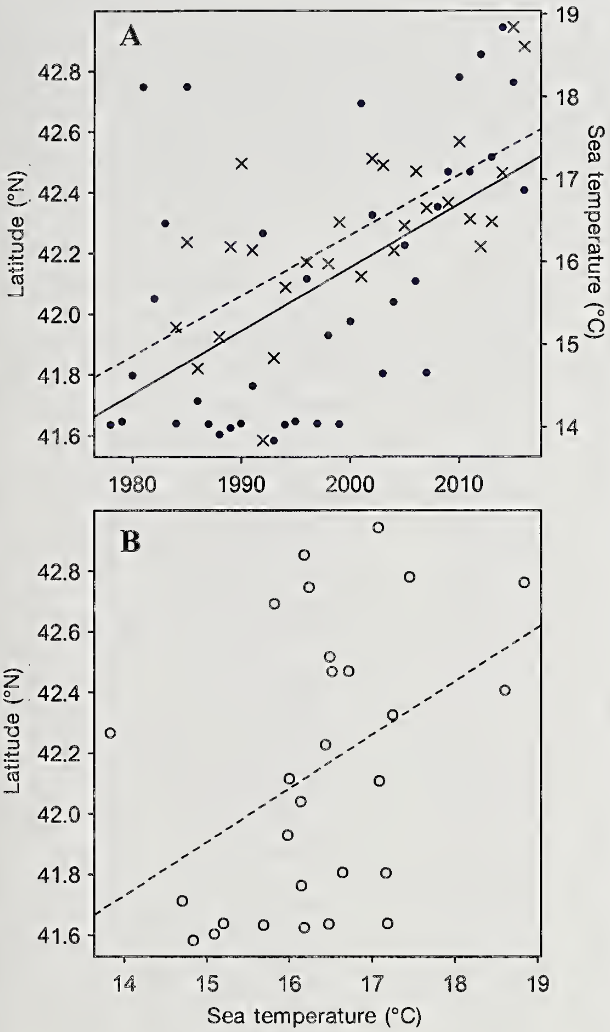

Figure 8

(**A**) Increasing distribution (solid circles= maximum latitude) of age-0 black sea bass (*Centropristis striata*) in trawl surveys conducted during autumn by the Massachusetts Division of Marine Fisheries and the Northeast Fisheries Science Center from 1978 to 2016, plotted with increasing sea-surface temperatures (x=mean for September of each year) in the southern Gulf of Maine. Both regression slopes were significantly different than zero (autumn distribution, solid line: $y=0.38+0.021x$, $P<0.001$, coefficient of determination [r^2]=0.29; September temperatures, dashed line: $y=-130+0.073x$, $P<0.001$, $r^2=0.46$). (**B**) Year-to-year comparison of maximum latitude and mean September sea-surface temperature (dashed line, $y=39.3+0.177x$, $P=0.03$, $r^2=0.18$). Temperature data for 1984–2016 come from NOAA Buoy Station 44013, 30 km east of Boston, Massachusetts (see Fig. 7).

cooler, but such adjustments would not push spawning or hatching outside a May–July period.

We note few differences in hatching dates among our sampling years or locations. There was no difference between years, and although temperature may drive spawning seasonality, June temperatures at the buoy in offshore waters of Boston varied by less than 0.5°C between 2006 and 2007 (14.2°C vs 14.5°C), leaving little contrast between our years of sampling. It may be that—with the longer-term pattern of warming temperatures—black sea bass spawning seasonality is undergoing a directional selection so that spawning begins earlier in the year (Pankhurst and Munday, 2011), which would justify replicating our study design to test such a hypothesis in Massachusetts waters. We were curious whether there was a spatial difference in hatching dates between neighboring Buzzards Bay and Nantucket Sound but found no difference. Finally, earlier hatching dates for fish that settle in estuarine sites, as opposed to inshore sites, may arise from early warming in estuarine waters, if warmer water initiates earlier seasonal spawning. However, our sampling design was confounded in two specific ways. First, different gears were used in estuarine and inshore sites, which may lead to gear selectivity, although this seems unlikely because the smallest mesh was a similar size in both gears. Second, sampling at estuarine sites began earlier than at inshore sites: if all fish originated across the same hypothetical hatching date distribution, then fish sampled earlier (versus later) would experience less cumulative mortality, resulting in different back-calculated hatching dates between early and late samples. Or they may have experienced different dispersal patterns with respect to age and habitat. These may be interesting considerations to pursue in the future, but their resolutions are not likely to reveal a radically different perception of spring–summer spawning by black sea bass in coastal waters off southeastern Massachusetts.

It is unlikely that spawning occurs later, such as in August, but our study design may not have captured late spawning. For example, larvae from a hypothetical August spawning may have been too small to be retained by traps or they may have had a high mortality rate. However, spawning after July by local fish is not consistent with the predominance of immature or spent individuals observed by Kolek (1990), Caruso (1995) and Wuenschel et al.[2] in late summer. Late summer spawning is occurring farther south. For example, a check of the NMFS-NEFSC data base from 35°N to 41°N shows an average of 8.9% (range: 3–19% by 1° latitude) of mature females are in spawning condition (ripe or ripe and running) during autumn, whereas the percentage of spawning females drops to 0.3% north of 41°N. Thus, if black sea bass spawn into autumn in Massachusetts waters, it is rare.

The dynamics and overlap between spawning and targeted fishing seasons is relevant for managing the reproductive potential of a fish population (Peer and Miller, 2014). For example, the (Massachusetts and

Table 1

Evidence from literature of black sea bass (*Centropristis striata*) spawning seasons by locations, ordered from north to south: Gulf of Maine (GOM, >42°N), southern New England (SNE, ~42–41°N), Long Island Sound (LIS, 41.5–41°N), New York Bight (NYB, 41–39°N), Chesapeake Bight (CB, 39–35°N), and South Carolina and Georgia (SC/GA, 33.5–31.5°N). Sampling habitats are identified as estuarine (E) or offshore (O). Months indicate the period during which eggs or larvae were present or when ripe or ripe and running gonads were observed by ichthyoplankton sampling (I) or by macroscopic or histological examination of gonads (G). Years of sampling are indicated, as are the citations for the sources of evidence.

Location	Habitat	Months present	Method	Year	Citation
GOM	O	–	I (larvae)	1977–87	Able et al., 1995
GOM	O	–	I (eggs)	1977–87	Berrien and Sibunka, 1999
GOM	O	–	I (larvae)	1969–70	Chenoweth, 1973
SNE	–	Jun[a]	–	1898	Bumpus, 1898
SNE	–	May–Jun	–	–	Bigelow and Schroeder, 1953
SNE	E	Jul	I (larvae)[b]	1957–8	Herman, 1963
SNE	E	–	I (eggs and larvae)	1972–3	Bourne and Govoni, 1988
SNE	O[c]	–	I (larvae)	1966	Kendall, 1972
SNE	O[c]	–	I (eggs)	1977–87	Berrien and Sibunka, 1999
SNE	O[c]	–	I (larvae)	1977–87	Able et al., 1995
SNE	O	May–July	G (macro)	1993	Caruso, 1995
SNE	O	May–Jun[d]	G (macro)	2010	Wuenschel et al. (fn. 2 in main text)
LIS	E	–	I (eggs and larvae)	1950s	Richards, 1959
NYB	–	May–Jun	–	–	Bigelow and Schroeder, 1953
NYB	O	Aug–Oct	I (larvae)	1966	Kendall, 1972
NYB	O	Jun–Oct	I (eggs)	1977–87	Berrien and Sibunka, 1999
NYB	O	Jul–Nov	I (larvae)	1977–87	Able et al., 1995
NYB	O	May–Jul	G (macro)	1974–5	Wilk et al., 1990
CB	E[e]	Jun–Jul	I (larvae)	1929–30	Pearson, 1941
CB	–	May	–	–	Bigelow and Schroeder, 1953
CB	O	Jun, Aug, Oct–Nov	I (larvae)	1966	Kendall, 1972
CB	O	Apr–Oct, Jan	I (eggs)	1977–87	Berrien and Sibunka 1999
CB	O	Apr–Nov	I (larvae)	1977–87	Able et al., 1995
CB	O	Jul–Aug	G (macro)	1987	Eklund and Targett,1990
SC/GA	O	Jan–Apr (Sep)	G (histology)	1978–81	Wenner et al., 1986

[a] Spawns in June (sampling locations and method not explicit).

[b] n=2 at mouth of Narragansett Bay, probably a product of offshore spawning.

[c] No sampling in Nantucket Sound.

[d] Sampling May–Oct but not July.

[e] Most taken in July at the mouth of the Chesapeake Bay.

federal) fishing season begins in mid-May and extends until at least August, completely overlapping the spawning season. Migrants that may arrive or start spawning after fishing starts are more vulnerable than earlier migrants to mortality and the potential disruption of spawning behavior, and their vulnerabilities may vary on a yearly basis or could be reduced over time if the spawning season is pushed earlier.

First year growth

Farther south, off New Jersey (39.5°N; Able and Hales, 1997) and Maryland (38.0-38.4°N; Peters and Chigbu, 2017), autumn age-0 fish size distributions overlap (range: 50–110 mm TL, mode: 70 mm TL) with what we observed off southern New England. If anything, age-0 growth was slower to the south (mean: 0.43 mm/d, Able and Hales, 1997; 0.58 mm/d, Peters and Chigbu, 2017), but a counter gradient pattern of juvenile growth has not been described for this species (Conover, 1992) and more data across its range appear necessary before speculating further on growth patterns. Growth is likely affected by temperature and by salinity as well: Berlinsky et al. (2000) reported higher growth at a salinity of 20 in relation to salinities of 10 and 32. Able and Hales (1997) observed high site fidelity of age-0 black sea bass, at least until they migrate offshore as winter approaches; therefore local conditions are relevant to juvenile growth and survival (Miller et al., 2016). Although more experimental work would be useful to define a full response to temperature and salinity combinations, first-year growth conditions off southern New England do not appear to be suboptimal in relation to the central portions of the middle Atlantic seaboard.

Spawning and nursery habitats

Black sea bass spawning during June was historically documented in Nantucket Sound by Wilson (1889), and later, Kolek (1990) identified spawning black sea bass in shallow waters, <6 m, along the south shore of Cape Cod during May–July. In our analysis of spawning fish from trawl samples, ripe females were deeper and more variable in deeper water (mean: 18.7 m [SD 21.1], range: 6–146 m, n=341) than that reported for running ripe females (mean: 12.2 m [SD 5.3], range: 5–35 m, n=83; MADMF and NEFSC spring surveys, 1984-2017). These characterizations of spawning depth are similar to, or even shallower than, Drohan et al.'s (2007) characterization of black sea bass spawning: at 20–50 m depth. Recaptures of spawning fish in subsequent years, on the spawning grounds where they were tagged, indicate homing behavior to Nantucket Sound (Kolek, 1990).

We assume limited movements by spawning fish between locations of capture and spawning, which appears reasonable on the basis of field observations of tagged fish (Fabrizio et al., 2013). Our conclusion that spawning is expanding into the Gulf of Maine is dependent on whether the developing females observed there since 2000 do spawn there. Our prediction is that actively spawning females (i.e., ovulating) will eventually be documented in the Gulf of Maine, or that with gonad histological methods, partially spent females (i.e., with fresh postovulatory follicles) between batch spawning events will be identified there.

The NMFS-NEFSC trawling data may reflect a bias caused by a switch to a larger trawl and research vessel in 2008, which increased catches (NEFSC[1]). However, expansion of mature adults into the southern Gulf of Maine was also evident in the MA-DMF survey, which has not switched gear or ships during this period (Suppl. Material). Another concern is to explain why some age-0 fish were present in the southern Gulf of Maine in the 1980s, before spawning adults were documented. Some researchers have suggested early life stages of bass are transported through the Cape Cod Canal, but no ichthyoplankton data exist to confirm such transport.

These first approximations of areal extent and dynamics of spawning suggest additional avenues for research. Tagging returns from previous years by Kolek (1990) and Moser and Shepherd (2009) indicate that a combined use of acoustic tags may not only be successful for documenting philopatry, but may also be successful for contrasting spawning activity in different habitats and elucidating details of black sea bass mating systems, as has occurred recently for Atlantic cod (*Gadus morhua*) (e.g., Dean et al., 2014; Zemeckis et al., 2014).

Further focus on age-0 fish appears warranted. For example, the success of newly settled fish in habitats in the Gulf of Maine depends on the prey base there. Are there aspects of habitat at time of settlement that are being preconditioned by warming or is there already suitable habitat there now, but the area lacked competent larvae (i.e., larvae capable of undergoing metamorphosis) previously. Black sea bass do not use estuarine habitats extensively as nurseries, but age-0 juveniles do use polyhaline, subtidal habitats in estuaries (this study; Able and Hales, 1997; Peters and Chigbu, 2017), and larvae and juveniles are tolerant of a wide range of salinities (10–32; Berlinsky et al., 2000). The expansion of early life stages, those of both larvae and settled juveniles, on Georges Bank off the coast of New England (Suppl. Material) is quite recent and warrants continued scrutiny, as well. Given this breath of possible settlement habitats, examining the microchemistry and isotopic signatures of otolith cores may be fruitful to test the hypothesis that fish settling at more northern latitudes have been responsible for the recent trend in increasing biomass of the northern stock.

This study details black sea bass spawning and nursery habitats in a poorly studied region, noting that habitat use has been dynamic over the last 4 decades. Spawning adults and juveniles have extended northward as coastal waters warm, and possibly to the east, on Georges Bank (Suppl. Material). Nye et al. (2009) did not include black sea bass in their review of changing fish distributions in continental shelf waters of the U.S. Northeast, but more recent examinations of the same data set show that the distribution range of this species is moving northward (Bell et al., 2015; Kleisner et al., 2016; Miller et al., 2016). Such analyses have been conducted at a coarse level, i.e., by examining changes in geographic centroids, without consideration of life stage. The most recent stock assessment (NEFSC[1]) showed that the northern (north of Hudson Canyon off the New Jersey coast) but not the southern contingents of black sea bass have been increasing in abundance, which could give the impression that the fish are moving north, when what is changing is the productivity rates of each set of contingents. Also, the geographic distribution of this species may appear to be moving 'north' in spring because warmer temperatures initiate an earlier migration to inshore waters off Long Island, New York, as well as north of Cape Cod (Suppl. Material). Warm-temperate species, like black sea bass, are preconditioned to wide seasonal fluctuations in temperature, and thus may be better able to expand into new habitats caused by warming seas at high latitudes. Still, just because this stock migrates seasonally, we should not assume that aggregate changes in the distribution of this population are solely the result of individuals per se moving farther north.

Details, such as described here, will help form predictions about the ways in which population abundance and geographic distribution may change (Cheung et al., 2016). In this regard, black sea bass is an informative stock to watch in the future.

Looking farther north, there is scant but growing evidence of black sea bass reaching the northern Gulf of Maine. Bigelow and Schroeder (1953) regarded black sea bass as 'a rare stray from the south,' mostly captured in offshore waters off Massachusetts, and not known north of Maine's Matinicus Island (43°51′N). Even today, evidence that black sea bass are moving seasonally into the northern Gulf of Maine is the result more of anecdotal accounts than survey records. Recent state records have been reported in New Hampshire (Xu[6]), there have been accounts of increased bycatch of black sea bass in lobster pots (Rudalevige, 2015), and rare catches (3 fish from 2012 to 2016) have been reported in an inshore trawl survey along coastal New Hampshire and Maine (Sherman et al.[7]). During the NMFS-NEFSC trawl survey, few black sea bass were captured in offshore waters of Maine, either in the spring (Suppl. Material) or in the autumn (data not depicted but only 2 adults north of 43°N). Still, the northward expansion of this species led to the implementation of fishing regulations in 2014.[8]

Will this expansion of spawning and nursery grounds contribute to greater population productivity or resiliency? Maybe, but another phase of the first year needs to be recognized. Miller et al. (2016) report that cohort strength is limited by overwintering survival, a juvenile phase later than that examined here. Therefore warming near the shelf break may be more important to recruitment variability than warming in the Gulf of Maine. However, these relationships often break down when new data are added. If expansion of spawning and nursery grounds continues northward, then the corresponding effect on increasing local productivity could interact, perhaps nonlinearly, with Miller et al.'s (2016) predictive model of year-class strength. The information reported in this study provides additional context regarding the dynamics of the early life history of black sea bass, because year class strength may be set at multiple stages of ontogeny.

Acknowledgments

This research was in partial fulfillment of a M.S. thesis (M. Tweedie) from the University of Massachusetts Dartmouth. Many, many hands supported the groundfish surveys, in particular, from the MA-DMF, J. King, V. Manfredi. J. Dayton (NEFSC), and S. Elzey (MA-DMF) aged, in years, black sea bass. R. Jakuba, J. Kocik, C. Lipsky, K. Mills, H. Walsh provided data or information used herein or in the supplemental materials, and D. Bernal, A. Miller, and G. Shepherd, provided constructive comments on earlier drafts.

Literature cited

Able, K. W., and L. S. Hales Jr.
1997. Movements of juvenile black sea bass *Centropristis striata* (Linnaeus) in a southern New Jersey estuary. J. Exp. Mar. Biol. Ecol. 213:153–167.

Able, K. W., M. P. Fahay, and G. R. Shepherd.
1995. Early life history of black sea bass, *Centropristis striata*, in the mid-Atlantic Bight and a New Jersey estuary. Fish. Bull. 93:429–445.

Bell, R. J.
2012. Winter feeding as an overwintering survival strategy in young-of-the-year winter flounder. Trans. Am. Fish. Soc. 141:855–871.

Bell, R. J., D. E. Richardson, J. A. Hare, P. D. Lynch, and P. S. Fratantoni.
2015. Disentangling the effects of climate, abundance, and size on the distribution of marine fish: an example based on four stocks from the Northeast US shelf. ICES J. Mar. Sci. 72:1311–1322.

Berlinsky, D., M. Watson, G. Nardi, and T. M. Bradley.
2000. Investigations of selected parameters for growth of larval and juvenile black sea bass *Centropristis striata* L. J. World Aqua. Soc. 31:426–435.

Berrien, P., and J. Sibunka.
1999. Distribution patterns of fish eggs in the U. S. northeast continental shelf ecosystem, 1977–1987. NOAA Tech. Rep. NMFS 145, 310 p.

Bigelow, H. B., and W. C. Schroeder.
1953. Fishes of the Gulf of Maine. Fish. Bull. 53:1–577.

Bourne, D. W., and J. J. Govoni.
1988. Distribution of fish eggs and larvae and patterns of water circulation in Narragansett Bay, 1972–1973. Am. Fish. Soc. Symp. 3:132–148.

Brander, K.
2015. Improving the reliability of fishery predictions under climate change. Current Climate Change Rep. 1:40–48.

Bumpus, H. C.
1898. The breeding of animals at Woods Holl during the month of May, 1898. Science 8:58–61.

Burnett, J., L. O'Brien, R. K. Mayo, J. A. Darde, and M. Bohan.
1989. Finfish maturity sampling and classification schemes used during Northeast Fisheries Center bottom trawl surveys, 1963–89. NOAA Tech. Memo. NMFS-F/NEC-76, 9 p.

Caruso, P. G.
1995. The biology and fisheries of black sea bass (*Centropristis striata*) in Massachusetts waters. M.S. thesis, 118 p. Univ. Rhode Island, Kingston, RI.

Chang, W. Y. B.
1982. A statistical method for evaluating the reproducibility of age determination. Can. J. Fish. Aquat. Sci. 39:1208–1210.

---

[6] Xu, D. 2015. New Hampshire angler catches potential record black sea bass. Outdoorhub [Available from website, accessed May 2018.]

[7] Sherman, S. A., K. L. Stepanek, F. Pierce, R. Tetrault, and R. Eckert. 2014. Annual report on the Maine-New Hampshire Inshore Trawl Survey, January 1, 2013–December 31, 2013, Contract #NA07NMF4720357, 9 p. Submitted to the NOAA Fisheries Northeast Region Cooperative Research Partners Program. [Available from website.]

[8] Department of Marine Resources, 13-188, C.M.R. chap. 51 [Available from website.]

Chenoweth, S. B.
1973. Fish larvae of the estuaries and coast of central Maine. Fish. Bull. 71:105–113.

Cheung, W. W. L., G. Reygondeau, and T. L. Froicher.
2016. Large benefits to marine fisheries of meeting the 1.5°C global warming target. Science 354:1591–1594.

Conover, D. O.
1992. Seasonality and the scheduling of life history at different latitudes. J. Fish Biol. 41:161–178.

Dean, M. J., W. S. Hoffman, D. R. Zemeckis, and M. P. Armstrong.
2014. Fine-scale diel and gender-based patterns in behaviour of Atlantic cod (*Gadus morhua*) on a spawning ground in the Western Gulf of Maine. ICES J. Mar. Sci. 71:1474–1489.

Drohan, A. F., J. P. Manderson, and D. B. Packer.
2007. Essential Fish Habitat Source Document: black sea bass, *Centropristis striata*, life history and habitat characteristics, 2nd ed. NOAA Tech. Memo. NMFS-NE-200, 68 p.

Eklund, A.-M., and T. E. Targett.
1990. Reproductive seasonality of fishes inhabiting hard bottom areas in the Middle Atlantic Bight. Copeia 1990:1180–1184.

Evans, G. T., and J. M. Hoenig.
1998. Testing and viewing symmetry in contingency tables, with application to readers of fish ages. Biometrics 54:620–629.

Fabrizio, M. C., Manderson J. P., and Pessutti J. P.
2013. Habitat associations and dispersal of black sea bass from a mid-Atlantic Bight reef. Mar. Ecol. Prog. Ser. 482:241–253.

Frank, K. T., B. Petrie, W. C. Leggett, and D. G. Boyce.
2018. Exploitation drives an ontogenetic-like deepening in marine fish. Proc. Natl. Acad. Sci. U.S.A. 115:6422–6427.

Graham, C. T., and C. Harrod.
2009. Implications of climate change for the fishes of the British Isles. J. Fish Biol. 74:1143–1205.

Hales, L. S., Jr., and K. W. Able.
1995. Effects of oxygen concentration on somatic and otolith growth rates of juvenile black sea bass, *Centropristis striata*. *In* Recent developments in fish otolith research. Belle W. Baruch Lib. Mar. Sci. 19 (D. H. Secor, J. M. Dean, and S. E. Campana, eds.), p. 135–154. Univ. South Carolina Press, Columbia, SC.
2001. Winter mortality, growth, and behavior of young-of-the-year of four coastal fishes in New Jersey (USA) waters. Mar. Biol. 139:45–54.

Hare, J. A., W. E. Morrison, M. W. Nelson, M. M. Stachura, E. J. Teeters, R. B. Griffis, M. A. Alexander, J. D. Scott, L. Alade, R. J. Bell, et al.
2016. A vulnerability assessment of fish and invertebrates to climate change on the Northeast U.S. continental shelf. PLoS ONE 11(2):e0146756.

Henderson, M. E., K. E. Mills, A. C. Thomas, A. J. Pershing, and J. A. Nye.
2017. Effects of spring onset and summer duration on fish species distribution and biomass along the Northeast United States continental shelf. Rev. Fish Biol. Fish. 27:411–424.

Herman, S. S.
1963. Planktonic fish eggs and larvae of Narragansett Bay. Limnol. Oceanogr. 8:103–109.

Hood, P. B., M. F. Godcharles, and R. S. Barco.
1994. Age, growth, reproduction, and the feeding ecology of black sea bass, *Centropristis striata* (Pisces: Serranidae), in the eastern Gulf of Mexico. Bull. Mar. Sci. 54:24–37.

Kendall, A. W., Jr.
1972. Description of black sea bass, *Centropristis striata* (Linnaeus), larvae and their occurrences north of Cape Lookout, North Carolina, in 1966. Fish. Bull. 70:1243–1260.

Klein-MacPhee, G.
2002. Sea basses. Family Serranidae. *In* Bigelow and Schroeder's fishes of the Gulf of Maine, 3rd ed. (B. B. Collette, and G. Klein-MacPhee, eds.), p. 391–395. Smithsonian Institution Press, Washington, D.C.

Kleisner, K. M., M. J. Fogarty, S. McGee, A. Barnett, P. Fratantoni, J. Greene, J. A. Hare, S. M. Lucey, C. McGuire, J. Odell, et al.
2016. The effects of sub-regional climate velocity on the distribution and spatial extent of marine species assemblages. PLoS ONE 11(2):e0149220.

Kleisner, K. M., M. J. Fogarty, S. McGee, J. A .Hare, S. Moret, C. T. Perretti, and V. S. Saba.
2017. Marine species distribution shifts on the U.S. Northeast Continental Shelf under continued ocean warming. Prog. Oceanogr. 153:24–36.

Klibansky, N., and Scharf F. S.
2015. Success and failure assessing gonad maturity in sequentially hermaphroditic fishes: comparisons between macroscopic and microscopic methods. J. Fish Biol. 87:930–957.

Kolek, D.
1990. Homing of black sea bass, *Centropristis striata*, in Nantucket Sound with comments on seasonal distribution, growth rates, and fisheries of the species, 12 p. Mass. Div. Mar. Fish. Pocassett, MA.

Lehnert, R. L., and D. M. Allen.
2002. Nekton use of subtidal oyster shell habitat in a southeastern U.S. estuary. Estuaries 25:1015–1024.

Lux, F. E., and F. E. Nichy.
1971. Number and lengths, by season, of fishes caught with an otter trawl near Woods Hole, Massachusetts, September 1961 to December 1962. NOAA Natl. Mar. Fish. Serv., Spec. Sci. Rep. Fish. 662, 15 p.

McBride, R. S.
2002. Spawning, growth, and overwintering size of searobins (Triglidae: *Prionotus carolinus* and *P. evolans*). Fish. Bull. 100:641–647.
2014. Managing a marine stock portfolio: stock identification, structure, and management of 25 fishery species along the Atlantic coast of the United States. North Am. J. Fish. Manage. 34:710–734.
2015. Diagnosis of paired age agreement: a simulation of accuracy and precision effects. ICES J. Mar. Sci. 72:2149–2167.

McCartney, M. A., M. L. Burton, and T. G. Lima.
2013. Mitochondrial DNA differentiation between populations of black sea bass (*Centropristis striata*) across Cape Hatteras, North Carolina (USA). J. Biogeogr. 40:1386–1398.

Mercer, L. P.
1978. The reproductive biology and population dynamics of black sea bass, *Centropristis striata*. Ph.D. diss., 195 p. Coll. William Mary, Williamsburg, VA.

Miller, A. S., G. R. Shepherd, and P. S. Fratantoni.
2016. Offshore habitat preference of overwintering juvenile and adult black sea bass, *Centropristis striata*, and the relationship to year-class success. PLoS ONE 11(1):e0147627.

Moser, J., and G. R. Shepherd.
2009. Seasonal distribution and movement of black sea bass (*Centropristis striata*) in the northwest Atlantic as determined from a mark-recapture experiment. J. Northwest Atl. Fish. Sci. 40:17–28.

Munch, S. B., M. Mangel, and D. O. Conover.
2003. Quantifying natural selection on body size from field data: winter mortality in *Menidia menidia*. Ecology 84:2168–2177.

Musick, J. A., and L. P. Mercer.
1977. Seasonal distribution of black sea bass, *Centropristis striata*, in the Mid-Atlantic Bight with comments on the ecology and fisheries of the species. Trans. Am. Fish. Soc. 106:12–25.

Nye, J. A., J. S. Link, J. A. Hare, and W. J Overholtz.
2009. Changing spatial distribution of fish stocks in relation to climate and population size on the Northeast United States continental shelf. Mar. Ecol. Prog. Ser. 393:111–129.

Ogle, D. H.
2016. Introductory fisheries analysis with R, 317 p. CRC Press, Boca Raton, FL.
2018. FSA: fisheries stock analysis. R package vers. 0.8.20. [Available from website.]

Pankhurst, N. W., and P. L. Munday.
2011. Effects of climate change on fish reproduction and early life history stages. Mar. Freshw. Res. 62:1015–1026.

Pearson, J. C.
1941. The young of some marine fishes taken in lower Chesapeake Bay, Virginia, with special reference to the gray sea trout *Cynoscion regalis* (Bloch). Fish. Bull. 50:78–102.

Peer, A. C., and T. J. Miller.
2014. Climate change, migration phenology, and fisheries management interact with unanticipated consequences. North Am. J. Fish. Manage. 34:94–110.

Penttila, J., and L. M Dery (eds.).
1988. Age determination methods for northwest Atlantic species. NOAA Tech. Rep. NMFS 72, 132 p.

Pershing, A. J., M. A. Alexander, C. M. Hernandez, L. A. Kerr, A. Le Bris, K. E. Mills, J. A. Nye, N. R. Record, H. A. Scannell, J. D. Scott, et al.
2015. Slow adaptation in the face of rapid warming leads to collapse of the Gulf of Maine cod fishery. Science 350:809–812.

Peters, R., and P. Chigbu.
2017. Spatial and temporal patterns of abundance of juvenile black sea bass (*Centropristis striata*) in Maryland coastal bays. Fish. Bull. 115:504–516.

R Core Team.
2018. R: a language and environment for statistical computing. R Foundation for Statistical Computing, Vienna, Austria. [Available from website, accessed May 2018]

Reid, R. N., F. P. Almeida, and C. A. Zetlin.
1999. Essential fish habitat source document: fishery-independent surveys, data sources, and methods. NOAA Tech. Memo. NMFS-NE-122, 39 p.

Richards, S. W.
1959. Pelagic fish eggs and larvae of Long Island Sound. Bull. Bingham Oceanogr. Collect. 17:95–124.

Roemer, M. E., and K. Oliveira.
2007. Validation of back-calculation equations for juvenile bluefish (*Pomatomus saltatrix*) with the use of tetracycline-marked otoliths. Fish. Bull. 105:305–309.

Roy, E. M., J. M. Quattro, and T. W. Greig.
2012. Genetic management of black sea bass: influence of biogeographic barriers on population structure. Mar. Coast. Fish. 4:391–402.

Rudalevige, C. B.
2015. A new fish for Maine waters—and dinner plates. Portland Press Herald, April 26, 2015. [Available from website.]

Shepherd, G.
1991. Meristic and morphometric variation in black sea bass north of Cape Hatteras, North Carolina. North Am. J. Fish. Manage. 11:139–148.

Tweedie, M. K.
2014. Hatch dates and growth of young-of-the-year black sea bass, *Centropristis striata*, in southeastern Massachusetts coastal waters. M.S. thesis, 114 p. Univ. Massachusetts Dartmouth., Dartmouth, MA.

Walsh, H. J., D. E. Richardson, K. E. Marancik, and J. A. Hare.
2015. Long-term changes in the distributions of larval and adult fish in the northeast U.S. shelf ecosystem. PLoS ONE 10(9):e0137382.

Watanabe, W. O., T. I. J. Smith, D. L. Berlinsky, C. A. Woolridge, K. R. Stuart, K. A. Copeland, and M. R. Denson.
2003. Volitional spawning of black sea bass *Centropristis striata* induced with pelleted luteinizing hormone releasing hormone-analogue. J. World Aqua. Soc. 34:319–331.

Wenner, C. A., W. A. Roumillat, and C. W. Waltz.
1986. Contributions to the life history of black sea bass, *Centropristis striata*, off the southeastern United States. Fish. Bull. 84:723–741.

Wilk, S. J., W. W. Morse, and L. L. Stehlik.
1990. Annual cycles of gonad-somatic indices as indicators of spawning activity for selected species of finfish collected from the New York Bight. Fish. Bull. 88:775–786.

Wilson, H. V.
1889. The embryology of the sea bass (*Serranus atrarius*). Bull. U.S. Fish Comm. 9:209–277.

Zemeckis, D. R., W. S. Hoffman, M. J. Dean, M. P. Armstrong, and S. X. Cadrin.
2014. Spawning site fidelity by Atlantic cod (*Gadus morhua*) in the Gulf of Maine: implications for population structure and rebuilding. ICES J. Mar. Sci. 71:1356–1365.

National Marine
Fisheries Service
NOAA

Fishery Bulletin
established in 1881

Spencer F. Baird
First U.S. Commissioner
of Fisheries and founder
of *Fishery Bulletin*

Distribution of angel sharks (Squatinidae) in United States waters of the western North Atlantic Ocean

William B. Driggers III (contact author)[1]
Matthew D. Campbell[1]
David S. Hanisko[1]
Kristin M. Hannan[1]
Eric R. Hoffmayer[1]
Christian M. Jones[1]
Adam G. Pollack[1]
David S. Portnoy[2]

Email address for contact author: william.driggers@noaa.gov

[1] Mississippi Laboratories
Southeast Fisheries Science Center
National Marine Fisheries Service, NOAA
P.O. Drawer 1207
Pascagoula, Mississippi 39567

[2] Marine Genomics Laboratory
Department of Life Sciences
Texas A&M University—Corpus Christi
6300 Ocean Drive
Corpus Christi, Texas 78412

Abstract—The distributions of sharks inhabiting deepwater ecosystems (>200 m) remain largely speculative because of limited collection efforts for species of relatively low commercial value and because of difficulties associated with sampling in deepwater habitats. As a result, ranges of deepwater shark species are often considered continuous across broad expanses despite records of occurrence, in many cases, being spatially fragmented. Within United States (US) waters of the western North Atlantic Ocean (WNA), the range of angel sharks (Squatinidae) in continental shelf and slope waters has been variously reported as both continuous and disjunct. The objective of this study was to use fishery-independent data to describe the range of angel sharks in US waters of the WNA and identify potential spatial discontinuities that could be consistent with the idea of multiple species or populations in the region. Results indicate that angel sharks in US waters of the WNA have a disjunct distribution and discontinuities occur from approximately Georgia through southern Florida and within a well-defined area off the coast of Louisiana. Evidence suggests spatial discontinuities could be related to thermal, salinity or current velocity barriers, or to a combination of these factors.

Historically, distributions of shark species were based on the amalgamation of observational and fishery-dependent data (e.g., Jordan and Evermann, 1896; Bigelow and Schroeder, 1948). Since the advent of fishery-independent surveys, the true spatial extent of shark distributions has come into greater focus, particularly for species occupying neritic habitats. However, distributions of sharks inhabiting deepwater ecosystems (>200 m) remain largely speculative owing to limited collections because of their relatively low commercial value and difficulties associated with sampling in deepwater habitats. Additionally, the use of satellite tagging technology is of limited applicability for monitoring movements of species found beyond the photic zone because of the dependence on light-based geolocation. As a result, the ranges of deepwater shark species are often considered continuous across broad expanses despite occurrence records being spatially fragmented.

Within United States (US) waters of the western North Atlantic Ocean (WNA), sharks from the orders Hexanchiformes, Squaliformes, Lamniformes, Squatiniformes, and Carcharhiniformes occur in benthic habitats of the outer continental shelf and slope (Castro, 2011). Of these fishes, angel sharks are of particular concern because the family Squatinidae is reported to be the most threatened family of sharks globally (Dulvy et al., 2014). Conservation concern for angel sharks results from high bycatch rates, regional extinctions, relatively *k*-selected life history characteristics, data deficiencies (e.g., Colonello et al., 2007; Baremore, 2010; Tagliafico et al., 2017), and, importantly, the

Manuscript submitted 2 July 2018.
Manuscript accepted 13 September 2018.
Fish. Bull. 116:337–347 (2018).
Online publication date: 2 October 2018.
doi: 10.7755/FB.116.3-4.11

The views and opinions expressed or implied in this article are those of the author (or authors) and do not necessarily reflect the position of the National Marine Fisheries Service, NOAA.

Table 1

Data sources for trawl surveys used to examine the spatial distribution of squatinid sharks in the western North Atlantic Ocean. Data were collected by the Marine Resources Monitoring, Assessment, and Prediction Program (MARMAP), the Northeast Area Monitoring and Assessment Program (NEAMAP), the Northeast Fisheries Science Center (NEFSC), Southeast Area Monitoring and Assessment Program South Atlantic (SEAMAP-SA) and Gulf of Mexico (SEAMAP-GOM) surveys, the Southeast Fisheries Science Center (SEFSC) Small Pelagics/Acoustic Trawl Survey, and SEFSC Mississippi Laboratories historical and exploratory trawl surveys (MSLABS). n=the total number of trawls conducted over each time series.

Data source	Years	Months sampled	n	Spatial coverage	Depth (m)
MARMAP	1973–1980	Jan–Nov	1196	Cape Hatteras, NC, to Cape Canaveral, FL	3–108
NEAMAP	2007–2016	Apr–May, Sep–Nov	2870	Cape Cod, MA, to Cape Hatteras, NC	4–57
NEFSC	1963–2016	Jan–Dec	43,121	Halifax, Nova Scotia, to Cape Canaveral, FL	2–1164
SEAMAP-SA	1989–2015	Apr–Nov	16,046	Cape Hatteras, NC, to Cape Canaveral, FL	2–20
MSLABS	1950–1997	Jan–Dec	29,392	Rhode Island to Brownsville, TX	4–3085
SEAMAP-GOM	1987–2016	Jun–Jul, Oct–Nov	16,794	Key West, FL, to Brownsville, TX	2–113
SEFSC	2002–2016	Oct–Nov	1538	Key West, FL, to Brownsville, TX	12–555

limited spatial distribution of some species (Compagno et al., 2005). For example, Walsh and Ebert (2007) confirmed the validity of 4 species of squatinids around Taiwan in the western North Pacific Ocean: Taiwan angel shark (*Squatina formosa*); Japanese angel shark (*S. japonica*), clouded angel shark (*S. nebulosa*); and ocellated angel shark (*S. tergocellatoides*). Similarly, Vaz and de Carvalho (2013) described the overlapping range of three sympatric squatinids within the western South Atlantic Ocean off the coast of Brazil: Argentine angel shark (*S. argentina*); angular angel shark (*S. guggenheim*); and hidden angel shark (*S. occulta*).

Angel sharks inhabiting the WNA off the US east coast of the US (EC) and throughout the Gulf of Mexico (GOM) are largely thought to consist of a single species, the Atlantic angel shark (*S. dumeril*) (e.g., Bigelow and Schroeder, 1948; Castro, 1983; Compagno, 1984). However, Applegate et al. (1979) reported the possible presence of an undescribed squatinid in the GOM on the basis of a specimen collected in a fish market in Mexico. Later, Castro-Aguirre et al. (2006) described 2 new species of angel sharks, Gulf angel shark (*S. heteroptera*) and Mexican angel shark (*S. mexicana*), from the GOM. Shortly thereafter, Ebert et al. (2013) placed the 2 newly described species in synonymy with *S. dumeril* leaving the validity of these species in question, a conclusion supported by Eschmeyer and Fricke[1] but in disagreement with Castro (2011). Despite the taxonomic uncertainty associated with angel sharks in the GOM, the range of Atlantic angel sharks in continental shelf and slope waters of the WNA has been reported as continuous by some and disjunct by others. For example, Compagno (2002) indicated angel sharks within the WNA have a continuous range from Massachusetts to Veracruz, Mexico, whereas Bigelow and Schroeder (1948) reported that the range extends from southern New England to North Carolina off the east coast and from the Florida Keys into the northern GOM.

On the basis of conflicting information regarding the range of the genus in US waters of the WNA, our goal was to examine fishery-independent data collected throughout the region to determine the distribution of angel sharks. Our goal was 1) to determine whether the range is continuous (or discontinuous) throughout US waters of the WNA and 2) to identify spatial discontinuities in distribution that could be consistent with the idea of multiple species or populations in the region.

Materials and methods

To examine the broad- scale distribution of squatinids in US waters of the WNA, catch data from 7 fishery-independent trawl surveys were obtained and analyzed. Data were collected from Nova Scotia to the Florida Keys off the EC and in the northern GOM from the Florida Keys to Brownsville, Texas. The boundary between the EC and the GOM was designated to be at 81.0°W. All data sources were trawl based; however, because of a lack of consistency in survey design and gear configurations among and, in some cases, within data sources, we did not compare relative abundance (i.e., catch-per-unit-of-effort) throughout the sampling area. Additionally, because of numerous changes in the experimental design and gear of most surveys, research design and gear specifications are not provided in the present study. Data sources from the east coast of the US included the 1) National Marine Fisheries Service (NMFS), Northeast Fisheries Science Center (NEFSC), Spring, Autumn and Winter Bottom Trawl surveys (1963–2016); 2) the Northeast Area Monitoring and Assessment Program (NEAMAP) (2007–2016) Survey; 3) the joint South Carolina Department of Nat-

---

[1] Eschmeyer, W. N., and R. Fricke (eds.). 2017. Catalog of fishes. Electronic version, updated 1 November 2017. [Available from website,]

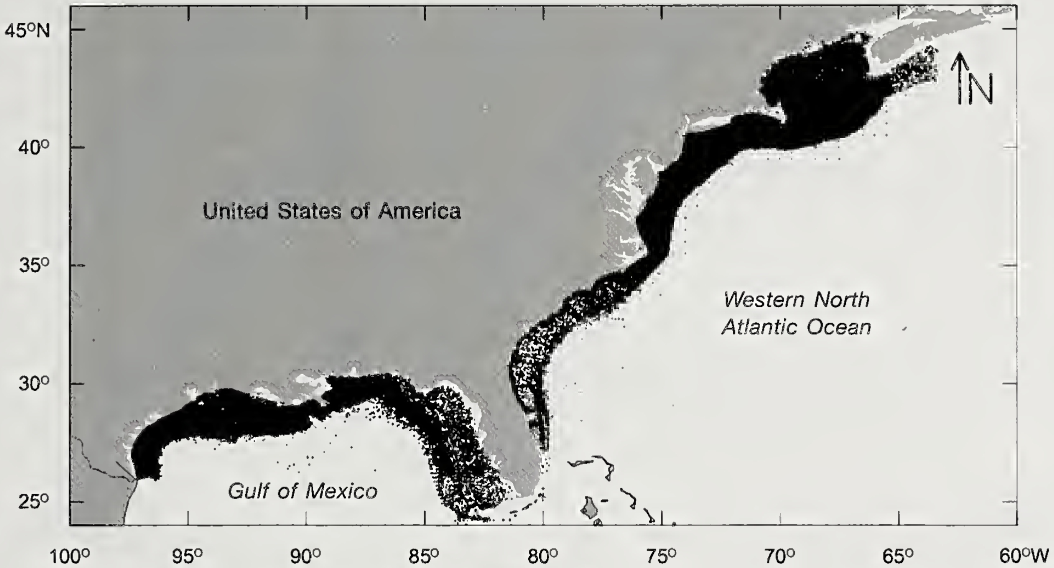

Figure 1

Locations of 104,957 trawls conducted during 7 fishery-independent surveys in the western North Atlantic Ocean between 1950 and 2016. Black dots represent a single sampling station, and many dots overlap because of high sampling density, most notably in the northern and western parts of the sampling area.

ural Resources and NMFS, Marine Resources Monitoring, Assessment, and Prediction (MARMAP) Survey (1973–1980); and 4) the Southeast Area Monitoring and Assessment Program-South Atlantic (SEAMAP-SA) Survey (1989–2015); and 5) NMFS, Mississippi Laboratories historical and exploratory trawl surveys (MSLABS) (1950–1997). Data collected from the GOM included the 1) MSLABS surveys, 2) the SEAMAP-GOM Survey (1982–2014), and the 3) NMFS, Southeast Fisheries Science Center, Small Pelagics/Acoustics Trawl Survey (2002–2014) (Table 1).

The position of each trawl and the locations where angels sharks were captured were plotted to determine the distribution of squatinids within the surveyed area. Median depth and depth distributions of all trawls conducted and locations where angel sharks were captured were compared for both regions by using Mann–Whitney–Wilcoxon (W) and Kolmogorov–Smirnov (K–S) tests, respectively. Results of the K–S test were used in conjunction with histograms to determine whether angel sharks were uniformly distributed throughout sampled depths. Additionally, bottom temperature and salinity (measured according to the practical salinity scale) information were available for a subset of the data and were compared, by using W and K–S tests, to determine whether these abiotic factors significantly affect the distribution of angel sharks in the two areas. To describe region-specific depth, temperature, and salinity preferences, the upper and lower quartiles are presented for each variable, as suggested by Magnuson et al. (1979) for skewed data. Logistic regression was used to examine the relationship between binomial catch (i.e., no catch versus positive catch), depth, temperature, and salinity. Because of a significant collinearity between depth and temperature within some seasons, logistic models were run that included and excluded depth.

Data were obtained from the NOAA National Centers for Environmental Information (Boyer et al.[2]; Seidov et al.[3]) to generate maps of bottom temperature and salinity off the southeastern EC and throughout the GOM in order to visualize potential barriers to movements between the two regions. Mean values for both variables were obtained for grids of 1/10° latitude by 1/10° longitude and plotted with ArcGIS[4] software, vers. 10.3.1 (Esri, Redlands, CA). Temperature data were limited to winter months (i.e., January, February and March), whereas salinity data was pooled over all months.

Results

Data were obtained from 104,957 trawls conducted from Nova Scotia to the Florida Keys (n=66,161) and throughout the northern GOM (n=38,796) (Fig. 1). Off

---

[2] Boyer, T. P., M. Biddle, M. Hamilton, A. V. Mishonov, C. Paver, D. Seidov, and M. Zweng. 2015. Gulf of Mexico regional climatology (NCEI accession 0123320). Vers. 1.1. NOAA Natl. Cent. Environ. Inf. Data set. [Available from website, accessed March 2018.]

[3] Seidov, D., O. K. Baranova, D. R. Johnson, T. P. Boyer, A. V. Mishonov, and A. R. Parsons. 2016. Northwest Atlantic regional climatology, Regional Climatology Team (NCEI accession 0155889). Vers. 1.1. NOAA Natl. Cent. Environ. Inf. Data set. website, accessed March 2018.]

[4] Mention of trade names or commercial companies is for identification purposes only and does not imply endorsement by the National Marine Fisheries Service, NOAA

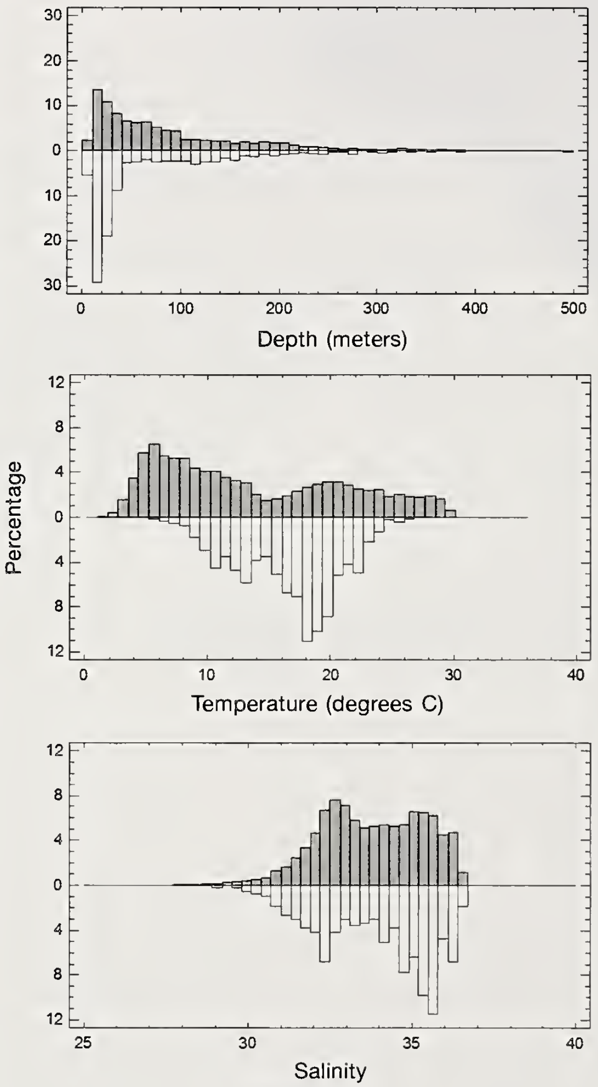

Figure 2

Comparison of depth (<500 m), temperature, and salinity (>24) at all sampled locations (gray bars) and at locations where angel sharks (Squatinidae) were collected (white bars) off the East Coast of the United States between 1950 and 2016, expressed as percentages of total number of trawls conducted (N=49,887) and trawls in which angel sharks were captured (n=1001).

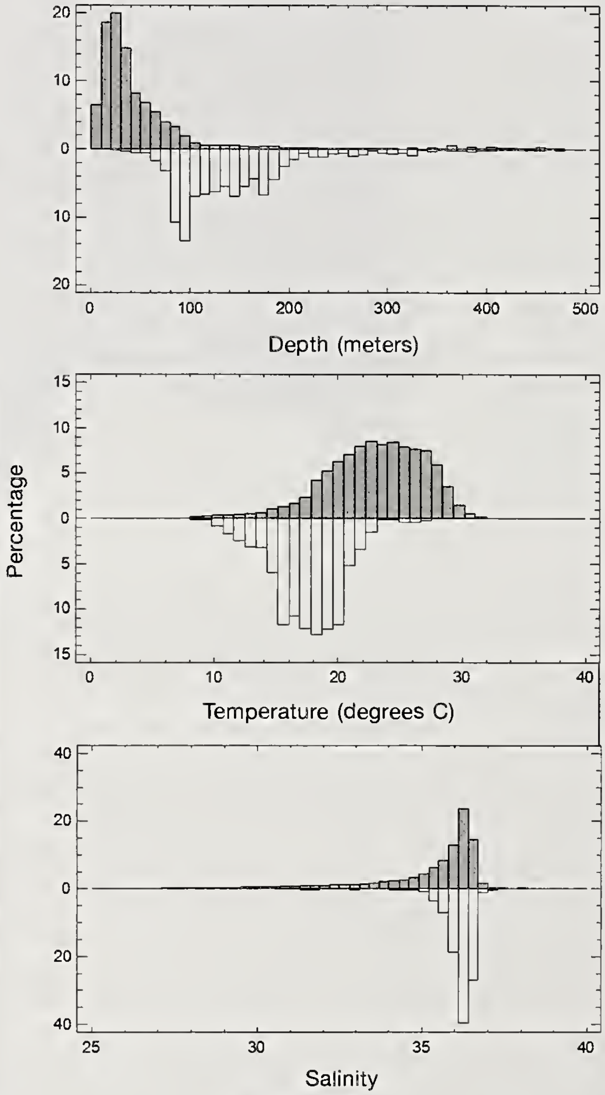

Figure 3

Comparison of depth (<500 m), temperature, and salinity (>24) at all sampled locations (gray bars) and locations where angel sharks (Squatinidae) were collected (white bars) in the northern Gulf of Mexico between 1950 and 2016, expressed as percentages of total number of trawls conducted (N=38,520) and trawls in which angel sharks were captured (n=1223).

the EC, trawls were conducted from 24.67° to 44.87°N at depths from 3.7 to 3840.0 m (mean: 92.07 m [standard error (SE) 0.46]) and 89 trawls were conducted at depths greater than 500 m (Fig. 2). In the GOM, trawls were conducted at depths from 1.8 to 3085.2 m (mean: 62.07 m [SE 0.54]) and 49 trawls were conducted at depths greater than 1000 m (Fig. 3). In both regions, sampling occurred in all months; however, effort was lowest during January, February, and December (Fig. 4). A total of 4999 angel sharks were collected during the trawl surveys; 2465 were caught off the EC and 2534 were captured in the GOM. Angel sharks were collected off the EC from 32.93° to 39.29°N at depths between 5.4 and 494.0 m (Figs. 2 and 5). Off the EC there was a significant difference in the distribution of depths sampled and depths where angel sharks were collected (K–S statistic: 8.92, P<0.01). Angel sharks were captured at higher rates at depths less than ~60 m and between 100 and 160 m than would be expected if their spatial distribution were uniform (Fig. 2).

In the GOM, angel sharks were collected at depths between 25.6 and 473.6 m; however, only 2.2% of indi-

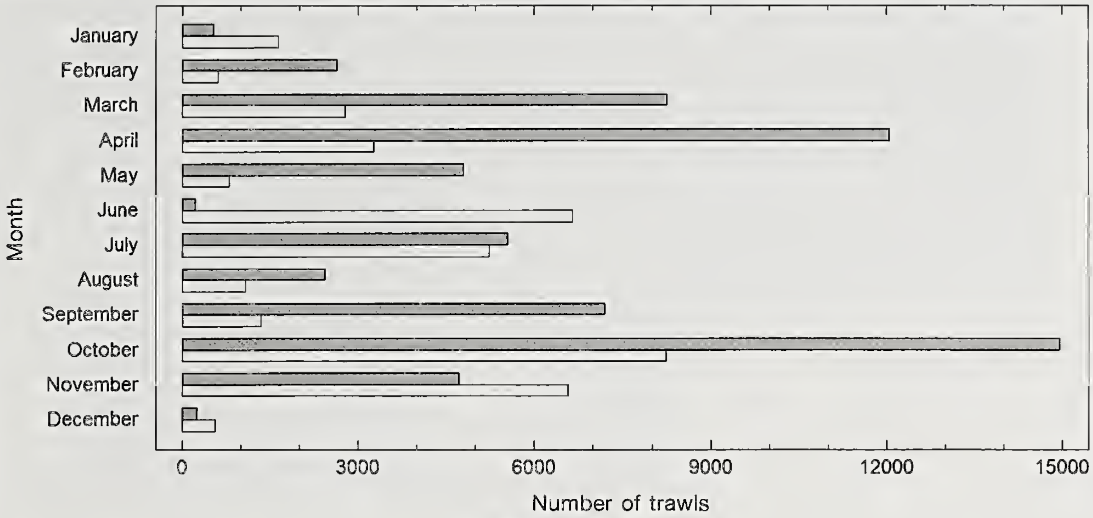

Figure 4

Monthly sampling effort, measured as number of trawls, during the varied time series (1950–2016) of 7 different fishery-independent surveys (*N*=104,957) from which data were examined for this study. Gray bars represent effort off the East Coast of the United States, and white bars represent effort within the northern Gulf of Mexico.

viduals were collected at a depth less than 70 m, despite that 80.0% of the total trawling effort occurred in shallower water. There was a significant difference in the distributions of depths sampled and depths where angel sharks were collected in the GOM (K–S statistic: 26.93, $P<0.01$), and no individuals were captured at depths less than 25 m. However, 97.8% of individuals were caught between 70 and 474 m where 19.2% of the total sampling effort occurred (Fig. 3). The distribution of squatinids was relatively continuous throughout outer continental shelf waters of the GOM; however, only 2 individuals were observed between the Mississippi River Delta and the western boundary of the Mississippi Canyon (~150 linear km, Fig. 5), despite 3600 trawls that were conducted within this area. The 2 sharks were caught in 1950 and 1951 at depths of 73.1 m and 82.3 m, respectively, east of Mississippi Canyon.

Angel sharks off the EC (13.5–19.5°C) and in the GOM (15.7–19.4°C) were collected in relatively cool waters and showed similar temperature preferences (median preferred temperature for EC=17.5°C, median for the GOM=17.6°C) (Table 2; Figs. 2 and 3). Depth preference for angel sharks was deeper in the GOM (92.3–171.9 m; minimum depth observed=25.6 m) than off the EC (17.0–94.0 m; minimum depth observed=5.4 m) (Table 2). Of the sharks captured that had corresponding salinity data available, only 7 out of 2266 individuals were collected in brackish water (salinity <30.0). In both regions, angel sharks indicated a preference for high salinity (Table 2; Figs. 2 and 3); however, sharks were caught over a broader range of salinity off the EC.

There were 20,566 stations off the EC and 18,116 stations in the GOM that had a full complement of depth, temperature, and salinity data. Within the GOM, there was a significant relationship between temperature (χ^2=437.76, $P<0.01$), salinity (χ^2=387.05, $P<0.01$), and positive catch (deviance=2220.71, $P<0.01$); however, depth was not significant when included in the logistic model (χ^2=0.03, P=0.87). When excluding depth from the model, the relationship between temperature (χ^2=1725.18, $P<0.01$), salinity (χ^2=391.06, $P<0.01$), and positive catch remained significant (deviance=2223.75, $P<0.01$). Similarly, off the EC, there was a significant relationship between temperature (χ^2=420.35, $P<0.01$), salinity (χ^2=89.82, $P<0.01$), and positive catch (deviance=658.72, $P<0.01$); however, depth (χ^2=1.12, P=0.29) was not a significant factor. The relationship between temperature (χ^2=420.35, $P<0.01$), salinity (χ^2=89.82, $P<0.01$), and positive catch remained significant when depth was not included as a factor (deviance=658.72, $P<0.01$). Visual inspection of mapped abiotic conditions in the sampled region indicated that relatively high temperatures associated with waters off the southern Florida peninsula during the winter could represent a barrier to movements of squatinids between the EC and GOM (Fig. 6). There was no indication of a barrier to movements between the EC and the northern GOM in relation to salinity (Fig. 7).

Discussion

All current sources describing the distribution of Atlantic angel sharks off the EC list the species as oc-

Table 2

Abiotic characteristics of bottom water associated with all stations sampled and stations where squatinid sharks were captured in waters along the East Coast (EC) of the United States and throughout the northern Gulf of Mexico (GOM) over varied time series during 1950–2016. All *P*-values for the Mann–Whitney–Wilcoxon (W) and Kolmogorov–Smirnov (K–S) tests were less than 0.01. Mean values are given with standard errors (SEs).

Variable	*n*	Range	Mean (SE)	Lower quartile	Upper quartile	Median	W	K–S
Depth (m)								
EC all stations	49,976	3.7–3840.0	92.07 (0.46)	28.0	128.0	64.0	1.81E+07	8.92
EC sharks present	1001	5.4–494.0	61.86 (2.13)	17.0	94.0	28.0		
GOM all stations	38,789	1.8–3085.2	62.07 (0.54)	20.1	60.4	32.9	4.27E+07	26.93
GOM sharks present	1223	25.6–473.6	144.3 (1.96)	92.3	171.9	128.6		
Temperature (°C)								
EC all stations	56,273	−1.4–30.71	13.75 (0.03)	7.1	20.2	11.8	3.26E+07	10.94
EC sharks present	907	5.5–26.7	16.72 (0.13)	13.5	19.5	17.5		
GOM all stations	19,665	6.1–39.1	22.94 (0.03)	20.4	26.0	23.3	2.25E+06	18.89
GOM sharks present	899	8.5–26.7	17.47 (0.09)	15.7	19.4	17.6		
Salinity								
EC all stations	36,550	22.1–37.8	33.75 (0.01)	32.6	35.1	33.8	1.06E+07	3.19
EC sharks present	530	22.1–36.5	34.02 (0.08)	32.5	35.5	34.5		
GOM all stations	18,026	2.3–38.0	36.13 (0.02)	34.7	36.3	35.9	1.09E+07	9.64
GOM sharks present	879	28.8–37.4	36.13 (0.02)	36.0	36.4	36.3		

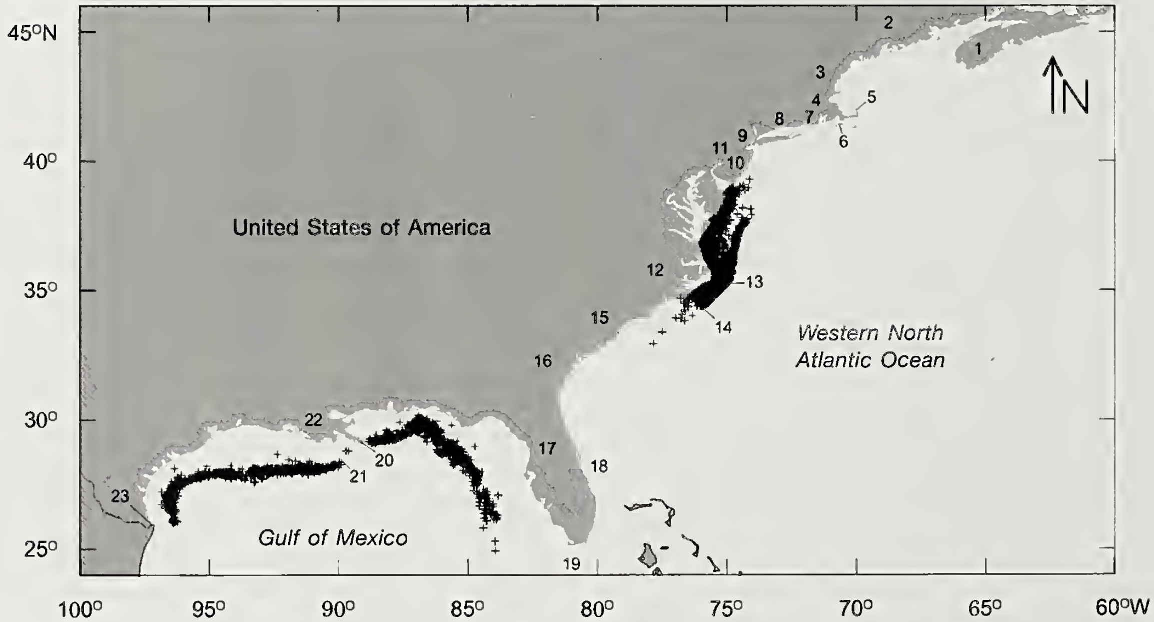

Figure 5

Locations where angel sharks (Squatinidae, n=2315) were captured during 7 fishery-independent surveys conducted in the western North Atlantic Ocean between 1950 and 2016. Numbers indicate key geographic locations mentioned in the text: 1=Nova Scotia, Canada; 2=Maine; 3=New Hampshire; 4=Massachusetts (MA); 5=Cape Cod, MA; 6=Martha's Vineyard, MA; 7=Rhode Island; 8=Connecticut; 9=New York; 10=New Jersey; 11=Philadelphia, Pennsylvania; 12=North Carolina (NC); 13=Cape Hatteras, NC; 14=Cape Lookout, NC; 15=South Carolina; 16=Georgia; 17=Florida (FL); 18=Jupiter and Port St. Lucie, FL; 19=Florida Keys; 20=Mississippi River Delta; 21=Mississippi Canyon; 22=Louisiana; and 23=Brownsville, Texas.

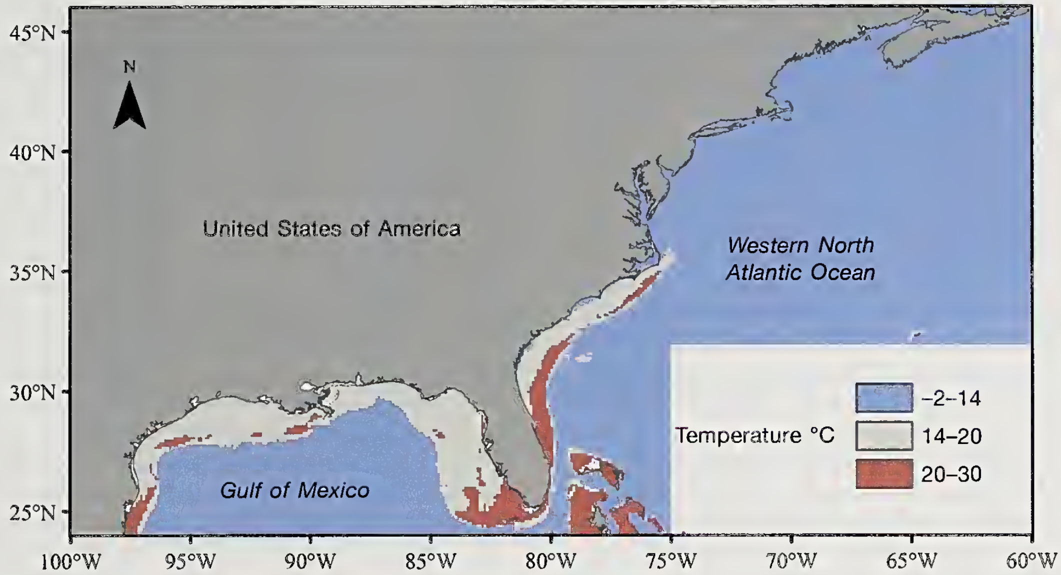
45°N
40°N
35°N
30°N
25°N
N
United States of America
Western North Atlantic Ocean
Gulf of Mexico
Temperature °C
-2–14
14–20
20–30
100°W
95°W
90°W
85°W
80°W
75°W
70°W
65°W
60°W

Figure 6

Bottom temperatures (°C) associated with winter months (January, February, and March) off the coast of the southeastern United States and throughout the northern Gulf of Mexico, based on data from the NOAA National Centers for Environmental Information (northwest Atlantic Ocean, website; Gulf of Mexico, website).

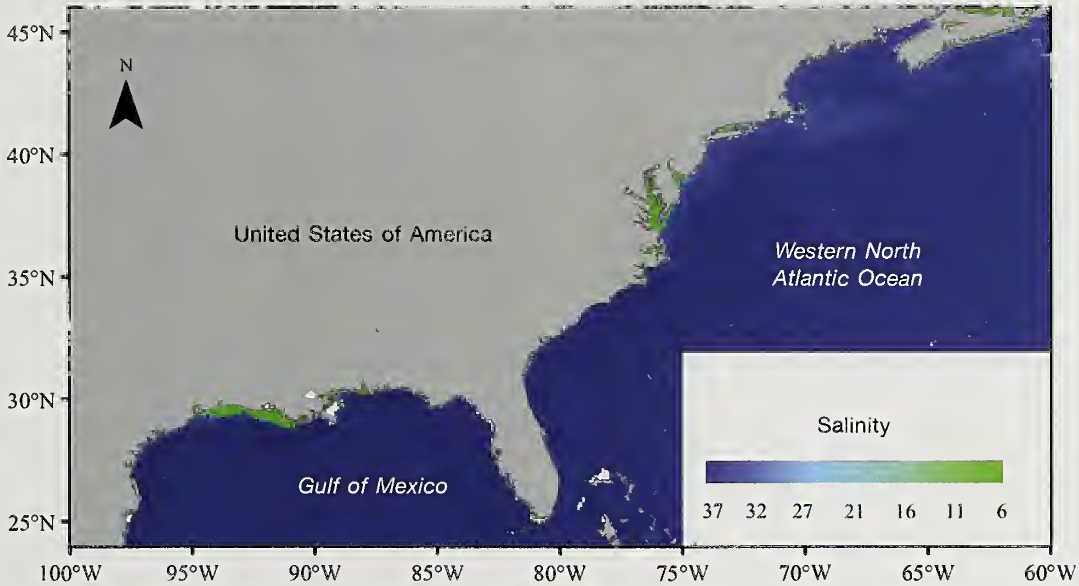
45°N
40°N
35°N
30°N
25°N
N
United States of America
Western North Atlantic Ocean
Gulf of Mexico
Salinity
37 32 27 21 16 11 6
100°W
95°W
90°W
85°W
80°W
75°W
70°W
65°W
60°W

Figure 7

Annual composite of bottom salinity off the east coast of the southeastern United States and throughout the northern Gulf of Mexico based on data from the NOAA National Centers for Environmental Information (northwest Atlantic Ocean, website; Gulf of Mexico, website).

curring from New England to southern Florida (e.g., Compagno, 1984; McEachran and Fechhelm, 1998; Castro, 2011; Ebert et al., 2013). The results of our study indicate that angel sharks in US waters of the WNA have a discontinuous distribution with gaps approximately from Georgia through Florida, off the EC, and across the Mississippi Canyon in the GOM. The first assessment of the distribution of *Squatina* in the WNA is attributable to Jordan (1885) who considered the angel shark (*S. squatina*, with *S. dumeril* considered a junior synonym at the time) to occur only off the northeastern United States. Several years later, Jordan and Evermann (1896) reported this species occurring "from Cape Cod southward." However, within the junior synonym list, the authors state the location of the source material for the original description of

S. dumeril by Le Sueur (1818) was "probably Florida." Similarly, Bigelow and Schroeder (1948) stated that one of the original specimens examined by Le Sueur (1818) in his original description of the species was possibly collected off of eastern Florida.

The speculations of Jordan and Evermann (1896) and Bigelow and Schroeder (1948) were almost certainly based on one of Le Sueur's syntypes that were collected by Titian Peale, an artist and naturalist, who participated in the 1817 Florida Expedition of the Academy of Natural Sciences of Philadelphia (ANSP). The description of *S. dumeril* by Le Sueur (1818) was based on three specimens. Although Le Sueur (1818) did not specifically state where these specimens were collected, the syntype accessioned in the Museum National D'Histoire Naturelle (MNHN-IC-A-9692), by Le Sueur himself, lists New York as the locality of collection. Le Sueur (1818) wrote "My observations on this species are derived from three individuals, perfectly alike; and the drawing was made from one which Mr. Titian Peale kindly put into my hands for examination, before preparing it for the museum." Peale, who was from Philadelphia, Pennsylvania, took his first collecting trip abroad during the 1817 ANSP Florida Expedition, which lasted from 25 December 1817 until late April 1818 (Porter, 1983, 1985; Bennett, 2002); however, Le Sueur's description of *S. dumeril*, which included the specimen provided by Peale, was read to the ANSP on 3 March 1818 (Le Sueur, 1818). Because Peale did not return from his collecting trip in Florida until over a month after *S. dumeril* had been described by Le Sueur, and because Peale's detailed logs do not mention the collection of any sharks; the specimen in question was therefore not collected as part of the ANSP Florida Expedition. Further, no angel sharks were collected during 12,451 trawls conducted south of 32.93°N off the EC, an area extending from the central coast of South Carolina to the Florida Keys. Additionally, no angel sharks were reported within observer data collected during 942 commercial trawls for penaeid and rock shrimp that were conducted from Cape Hatteras, North Carolina (35.20°N) to Port St. Lucie, Florida (~27.0°N) from 2007 to 2010 (Scott-Denton et al., 2012). However, 2 records of angel sharks having been captured and tagged by recreational fishermen in shallow water off the east coast of Florida are present within the NMFS Cooperative Shark Tagging Program database (Kohler[5]). One shark was tagged off Ponte Vedra Beach, Florida, on 17 June 1973 and the other near Fort Lauderdale, Florida, on 3 October 1979. Both sharks were caught off the EC at latitudes lower than those at which any angel sharks have been reported before or since. Further, because there is no way to verify identifications of these specimens (i.e., photographs) and because angel sharks are morphologically similar (e.g., dorsoventrally depressed, two relatively large dorsal fins) to the lesser electric ray (*Narcine bancroftii*), which commonly occurs off the east coast of Florida (McEachran and de Carvalho, 2002), we suspect these records are anomalies or the result of misidentification.

The northern extent of the distribution of Atlantic angel sharks was recently reported by Ebert et al. (2013) to extend into New England waters (i.e., Connecticut, Rhode Island, Massachusetts, New Hampshire, and Maine). However, the northernmost documented occurrence of the Atlantic angel shark off the EC that we are aware of is off Massachusetts (e.g., Smith, 1922), which is the northern distribution extent of Atlantic angel sharks acknowledged by Castro (1983) and Compagno (2002). Additionally, no angel sharks were collected during 15,074 NEFSC trawls conducted north of Martha's Vineyard, Massachusetts (~41.5°N). Furthermore, among all survey data examined for our study, no Atlantic angel sharks were collected north of southern New Jersey (39.30°N) and only 2.6% of all angel sharks collected during fishery-independent surveys off the EC were found south of Cape Lookout, North Carolina (34.58°N). Therefore, we conclude that the primary range of Atlantic angel sharks off the EC of the US extends from southern New Jersey to Cape Lookout, North Carolina.

The distribution of angel sharks off the EC appears to be temperature driven because this variable had the highest level of significance in the logistic models. Off the EC, the Labrador Current brings relatively cool water southward from northern latitudes, terminating near Cape Hatteras, North Carolina at ~35.2°N (Fratantoni and Pickart, 2007). North of Cape Hatteras, angel sharks are present year-round; however, south of this area in the waters of southern North Carolina and northern South Carolina, the species occurs offshore in relatively deep waters during winter. From December through March, the mean bottom temperature of inshore waters from Cape Hatteras to Charleston, South Carolina, is less than 13°C (Grieve et al., 2016), below the minimum preferred temperature for angel sharks (13.5°C). By February, mean bottom temperatures of these coastal waters are less than 12°C south of Cape Lookout, North Carolina (Atkinson et al., 1983). Although water temperatures in offshore waters along much of the continental shelf in the region are within the preferred temperature range of angel sharks during the winter, the influx of warm waters from the Florida Current during this time results in bottom temperatures above the preferred temperature (19.5°C) of angel sharks south of central Florida (Fig. 6; Atkinson et al., 1983; Grieve et al., 2016). Therefore, we hypothesize that a thermal barrier prevents angel sharks inhabiting waters off the EC from moving into the GOM.

Temperature also limits the movement of angel sharks from the GOM into waters within the Straits of Florida and northward along the EC. The preferred water temperature of angel sharks in the GOM was found to be 15.7–19.4°C. However, mean annual temperatures in relatively shallow waters of the Dry Tortugas and Florida Keys are in excess of 24°C (Lee and Williams, 1999),—temperatures above the preferred temperature range for angel sharks. Therefore, if angel sharks do occur in shallow waters of the eastern GOM, the relatively high water temperatures of the Dry Tortugas and Florida Keys year-round could act as a barrier for angel shark movement into the Straits of Florida. To our knowledge, the only record of angel sharks occurring in shallow waters of the eastern GOM is attributable to Fowler (1906) who stated that local fishermen reported *Rhina squatina* (a junior synonym for *S. dumeril*) was "occasionally taken in summer" in the Florida Keys. Because of the morphological similarity between angel sharks and guitarfishes (Rhinobatidae) and because the Atlantic guitarfish (*Pseudobatos lentiginosus*) is "often encountered in shallow waters around the Florida Keys" (Bigelow and Schroeder, 1953), we believe Fowler's (1906) report of angel sharks occurring in the area to be in error.

---

[5] Kohler, N. 2018. Personal commun. Northeast Fish. Sci. Cent., Natl. Mar. Fish. Serv., NOAA, 28 Tarzwell Dr., Narragansett, RI 02882.

South of the Dry Tortugas, the South Florida Escarpment is within the preferred depth range for angel sharks and could represent a relatively narrow corridor through which angel sharks could move from the GOM into the Florida Straits. Additionally, based on our data (Fig. 6) and on visual inspection of temperature data presented by Soto (1985), bottom temperature on the South Florida Escarpment at depths between approximately 150 and 250 m is within the preferred temperature range of angel sharks during a portion of the year. However, Longley and Hildebrand (1941) did not list angel sharks among the fishes collected in dredges conducted across the South Florida Escarpment, south of the Dry Tortugas, and on the Tortugas Terrace, despite having documented other shark species, such as the chain dogfish (*Scyliorhinus retifer*) and Caribbean lanternshark (*Etmopterus hillianus*). Additional sampling will be required to determine whether angel sharks are present within the Straits of Florida, particularly along the South Florida Escarpment and on the Pourtales Terrace where bottom temperatures are within the preferred range of this species.

Velocity and direction of the Florida Current as it moves through the Straits of Florida and changes trajectory to the north off the southeastern tip of Florida are other possible mechanisms acting, possibly in concert with temperature, to limit movements of angel sharks between the EC and GOM. Although information on the swimming performance of Atlantic angel sharks is scant, Standora and Nelson (1977) examined the diel activity patterns of Pacific angel sharks (*S. californica*) associated with Santa Catalina Island, California. The authors concluded the species is relatively sedentary during daylight hours and becomes more active at night. Mean sustained swimming speeds during nocturnal periods were approximately 11 cm/s and maximum reported sustained swimming speed was approximately 25 cm/s. Lee et al. (1992) deployed an acoustic Doppler current profiler to a depth of 200 m in the Straits of Florida south of Looe Reef and recorded bottom currents up to 40 cm/s. Hamilton et al. (2005) analyzed data from buoy arrays moored off Jupiter in southeastern Florida and reported current speeds of over 70 cm/s at a depth of 300 m. Relatively high bottom current speeds and seasonal bottom current reversals (e.g., Düing and Johnson, 1972), coupled with the comparatively low maximum sustained swimming speed of angel sharks, could make the Straits of Florida energetically demanding to traverse and thus a potential barrier for exchange between basins.

Unlike angel sharks off the EC, angel sharks were not collected inshore in the GOM during fishery-independent surveys despite extensive sampling efforts in shallow waters. However, of the 60,827 commercial shrimp trawl catches sampled by fishery observers from 1981 through 2015 in the GOM from January to April, angel sharks were observed in 9 trawls conducted at depths less than 70 m (Hart[6]). Furthermore, an experienced commercial shark fisherman provided photographs of an angel shark captured in nearshore waters of the northern GOM during the winter of 2018 and reported frequent captures of angel sharks in gill nets off Mississippi and Alabama at depths as shallow as 18 m during winter months of January and February (Stiller[7]). Therefore, more sampling will be needed in the northern GOM during winter months to fully describe seasonal variability in the depth range of angel sharks within the region.

Angel sharks were collected throughout the northern GOM. However, in an area off Louisiana, between the Mississippi River Delta and the western edge of Mississippi Canyon, only 2 individuals were collected over the 67-year sampling period, despite 3600 trawls conducted in that area during that period. This hypothesized discontinuity in distribution could be related to a number of factors, including the steepness of the narrow shelf at the terminus of the Mississippi Delta, upwelling of cold water through the Mississippi Canyon, or abiotic conditions related to discharge from the Mississippi River. A similar discontinuity in the distribution and genetic population structure of blacknose sharks (*Carcharhinus acronotus*) associated with the same area was identified by Portnoy et al. (2014) using molecular techniques. The authors speculated that the freshwater plume associated with the Mississippi River potentially acts as a physiological barrier between the eastern and western GOM for stenohaline species. Like blacknose sharks, angel sharks in the GOM appear to be stenohaline because they were collected in a narrow range of preferred salinity (i.e., 34.7–36.3). Future research will be needed to address the discontinuity in distribution in this region and whether it is related to salinity.

---

[6] Hart. R. 2016. Unpubl. data. Southeast Fish. Sci. Cent., Natl. Mar. Fish. Serv., NOAA, 4700 Ave. U, Bldg. 306, Galveston, TX 77551.

[7] Stiller, D. 2018. Personal commun. Commercial fisherman.

The spatial disjunction of squatinid sharks between the EC and the GOM suggests the possibility of genetic isolation between angel sharks in the 2 regions. Therefore, we hypothesize that squatinid sharks in the GOM and the EC are separate evolutionary units. Although current research cannot address the species status of squatinid sharks in US waters of the WNA, our findings do suggest an evaluation is warranted. Further, on the basis of the presence of what appears to be a distributional break at the Mississippi River Delta/Mississippi Canyon, we hypothesize that squatinids in the eastern and western GOM represent, at a minimum, 2 separate populations. As human activities intensify in offshore waters of the GOM (e.g., commercial fishing, petroleum industry), it will become increasingly imperative to understand the species composition and population structures of marine organisms in poorly studied areas so that conservation efforts can effectively mitigate potentially deleterious effects.

Acknowledgments

We thank J. Gartland (Virginia Institute of Marine Science), R. Hart (NMFS), P. Kostovick (NMFS), and T. Smart (South Carolina Department of Natural Resources) for providing data from various surveys. We also thank the numerous persons who spent an extraordinary amount of time at sea collecting the data used in our study.

Literature cited

Applegate, S. P., L. Espinosa, L. Menchaca, and F. Sotelo.
1979. Tiburones Mexicanos, 146 p Subsecretaria de Educacion e Investigacidn Tecnolbgica, Dirección General de Ciencias y Tecnologia del Mar, Mexico City, Mexico.

Atkinson, L. P., T. N. Lee, J. O. Blanton, and W. S. Chandler.
1983. Climatology of the southeastern United States continental shelf waters. J. Geophys. Res., C 88:4705–4718.

Baremore, I. E.
2010. Reproductive aspects of the Atlantic angel shark *Squatina dumeril*. J. Fish Biol. 76:1682–1695.

Bennett, T. P.
2002. The 1817 Florida Expedition of the Academy of Natural Sciences. Proc. Acad. Nat. Sci. Phila. 152:1–21.

Bigelow, H. B. and W. C. Schroeder.
1948. Sharks. *In* Fishes of the western North Atlantic. Part one: lancelets, cyclostomes, sharks (A. E. Parr and Y. H. Olsen, eds.), p. 59–546. Mem. Sears Found. Mar. Res., Yale Univ., New Haven, CT.
1953. Sawfishes, guitarfishes, skates and rays. *In* Fishes of the western North Atlantic. Part two: sawfishes, guitarfishes, skates, rays, and chimaeroids (A. E. Parr and Y. H. Olsen, eds.) p. 1–514. Mem. Sears Found. Mar. Res., Yale Univ., New Haven, CT.

Castro, J. I.
1983. The sharks of North American waters, 180 p. Texas A&M Univ. Press, College Station, TX.
2011. The sharks of North America, 640 p. Oxford Univ. Press, Oxford, UK.

Castro-Aguirre, J. L., H. E. Pérez, and L. H. Campos.
2006. Dos nuevas especies del género *Squatina* (Chondrichthyes: Squatinidae) del Golfo de México. Rev. Biol. Trop. 54:1031–1040.

Colonello, J. H., L. O. Lucifora, and A. M. Massa.
2007. Reproduction of the angular angel shark (*Squatina guggenheim*): geographic differences, reproductive cycle, and sexual dimorphism. ICES J. Mar. Sci. 64:131–140.

Compagno, L. J. V.
1984. FAO species catalogue. Vol. 4. Sharks of the world. An annotated and illustrated catalogue of shark species known to date. Part 1. Hexanchiformes to Lamniformes. FAO Fish. Synop. 125, 249 p. FAO, Rome.
2002. Sharks. *In* The living marine resources of the Western Central Atlantic. Vol. 1: introduction, molluscs, crustaceans, hagfishes, sharks, batoid fishes, and chimaeras. FAO species identification guide for fishery purposes and American Society of Ichthyologists and Herpetologists Spec. Publ. 5 (K. E. Carpenter, ed.), p. 357–505. FAO, Rome.

Compagno, L., M. Dando, and S. Fowler.
2005. Sharks of the world, 368 p. HarperCollins Publishers, London.

Düing, W., and D. Johnson.
1972. High resolution current profiling in the Straits of Florida. Deep-Sea Res. 19:259–274.

Dulvy, N. K., S. L. Fowler, J. A. Musick, R. D. Cavanagh, P. M. Kyne, L. R. Harrison, J. K. Carlson, L. N. K. Davidson, S. V. Fordham, M. P. Francis, et al.
2014. Extinction risk and conservation of the world's sharks and rays. eLife 3:e00590.

Ebert, D. A., S. Fowler, and L. Compagno.
2013. Sharks of the world: a fully illustrated guide. Wild Nature Press, Plymouth, UK.

Fowler, H. W.
1906. Some cold-blooded vertebrates of the Florida Keys. Proc. Acad. Nat. Sci. Phila. 58:77–113.

Fratantoni, P. S., and R. S. Pickart.
2007. The western North Atlantic shelfbreak current system in summer. J. Phys. Oceanogr. 37:2509–2533.

Grieve, B. D., E. N. Curchitser, and R. R. Rykaczewski.
2016. Range expansion of the invasive lionfish in the northwest Atlantic with climate change. Mar. Ecol. Prog. Ser. 546:225–237.

Hamilton, P., J. C. Larsen, K. D. Leaman, T. N. Lee, and E. Waddell.
2005. Transports through the Straits of Florida. J. Phys. Oceanogr. 35:308–322.

Jordan, D. S.
1885. A catalogue of the fishes known to inhabit the waters of North America, north of the Tropic of Cancer, with notes on the species discovered in 1883 and 1884, 185 p. U.S. Gov. Print. Off., Washington, D. C.

Jordan, D. S., B. D. Evermann.
1896. The fishes of North and Middle America: a descriptive catalogue of the species of fish-like vertebrates found in the waters of North America, north of the Isthmus of Panama. Part I. Bull. U. S. Natl. Mus. 47, 1240 p.

Lee, T. N., and E. Williams.
1999. Mean distribution and seasonal variability of coastal currents and temperature in the Florida Keys with

implications for larval recruitment. Bull. Mar. Sci. 64:35–56.

Lee, T. N., C. Rooth, E. Williams, M. McGowan, A. F. Szmant, and M. E. Clarke.
1992. Influence of Florida Current, gyres and wind-driven circulation on transport of larvae and recruitment in the Florida Keys coral reefs. Cont. Shelf Res. 12:971–1002.

Le Sueur, C. A.
1818. Descriptions of several new species of North American fishes. J. Acad. Nat. Sci. Phila. 1:222–235.

Longley, W. H., and S. F. Hildebrand.
1941. Systematic catalogue of the fishes of Tortugas, Florida. Carnegie Inst. Wash. Publ. 535, 331 p. Carnegie Inst. Wash., Washington, D.C.

Magnuson, J. J., L. B. Crowder, and P. A. Medvick.
1979. Temperature as an ecological resource. Am. Zool. 19:331–343.

McEachran, J. D., and J. D. Fechhelm.
1998. Fishes of the Gulf of Mexico. Vol. 1: Myxiniformes to Gasterosteiformes, 1120 p. Univ. Texas Press, Austin, TX.

McEachran, J. D., and M. R. de Carvalho.
2002. Batoid fishes. *In* The living marine resources of the Western Central Atlantic. Vol. 1: introduction, molluscs, crustaceans, hagfishes, sharks, batoid fishes, and chimaeras. FAO species identification guide for fishery purposes and American Society of Ichthyologists and Herpetologists Spec. Publ. 5. (K. E. Carpenter, ed.), p. 507–590. FAO, Rome.

Portnoy, D. S., C. M Hollenbeck, C. N. Belcher, W. B. Driggers III, B. S. Frazier, J. Gelsleichter, R. D. Grubbs, and J. R. Gold.
2014. Contemporary population structure and post-glacial genetic demography in a migratory marine species, the blacknose shark, *Carcharhinus acronotus*. Mol. Ecol. 23:5480–5495.

Porter, C. M.
1983. Following Bartram's "track": Titian Ramsay Peale's Florida journey. Fla. Hist. Q. 61:431–444.
1985. The lifework of Titian Ramsay Peale. Proc. Am. Philos. Soc. 129:300–312.

Scott-Denton, E., P. F. Cryer, M.R. Duffy, J. P. Gocke, M. R. Harrelson, D. L. Kinsella, J. M. Nance, J. R. Pulver, R. C. Smith, and J. A. Williams.
2012. Characterization of the U.S. Gulf of Mexico and South Atlantic penaeid and rock shrimp fisheries based on observer data. Mar. Fish. Rev. 74(4):1–27.

Smith, H. M.
1922. Second occurrence of Squatina in New England. Copeia 106:33.

Soto, L. A.
1985. Distributional patterns of deep-water brachyuran crabs in the Straits of Florida. J. Crustac. Biol. 5:480–499.

Standora, E. A., and D. R. Nelson.
1977. A telemetric study of the behavior of free-swimming Pacific angel sharks, *Squatina californica*. Bull. South. Calif. Acad. Sci. 76:193–201.

Tagliafico, A., S. Rangel, and M. K. Broadhurst.
2017. Reproductive aspects of the Atlantic angel shark *Squatina dumeril* in the southern Caribbean Sea. J. Fish Biol. 91:1062–1071.

Vaz, D. B. F. and de Carvalho, M .R.
2013. Morphological and taxonomic revision of species of *Squatina* from the southwestern Atlantic Ocean (Chondrichthyes: Squatiniformes: Squatinidae). Zootaxa 3695:1–81.

Walsh, J. H., and D. A. Ebert.
2007. A review of the systematics of western North Pacific angel sharks, genus *Squatina*, with redescriptions of *Squatina formosa*, *S. japonica*, and *S. nebulosa* (Chondrichthyes: Squatiniformes, Squatinidae). Zootaxa 1551:31–47.

National Marine
Fisheries Service
NOAA

Fishery Bulletin
established in 1881

Spencer F. Baird
First U.S. Commissioner
of Fisheries and founder
of *Fishery Bulletin*

Sex change and oscillating growth pattern of the picarel (*Spicara smaris*) in the Saronikos Gulf (Greece)

Constantina Karlou-Riga (retired)[1]
Dimitra Petza (contact author)[1,2,3]
Konstantinos Ganias[4]

Email address for contact author: d.petza@marine.aegean.gr

[1] Fisheries Laboratory
Hellenic Ministry of Rural Development and Food
15 Karaoli and Demetriou Street
Piraeus 18531, Greece

[2] Department of Marine Sciences
University of the Aegean
University Hill
Mytilene 81100, Greece

[3] Directorate General for Fisheries
Hellenic Ministry of Rural Development and Food
150 Syggrou Avenue
Athens 17671, Greece

[4] School of Biology
Aristotle University of Thessaloniki
University Campus
Thessaloniki 54124, Greece

Abstract—The picarel (*Spicara smaris*) is an interesting species of the Mediterranean Sea fishery, yet little information is available on life history of this protogynous species. A total of 6458 picarel (4.3 to 20.7 cm total length [TL]) were sampled from the Saronikos Gulf, an important fishing area in the eastern Mediterranean, during 1998 and 1999 to assess their age structure, sex-based growth, and sex-change pattern. Marginal-increment analysis combined with otolith edge analysis (n=1694) showed that the time of annulus formation was around July (i.e., at the end of the spawning season). The length and age at sex change were estimated to be 15.3 cm TL and 3.0 years, respectively. The proportion of early maturing males, or males maturing before the length at sex change (L_{50}), was 2.4%, whereas the ratio of L_{50} to maximum length was 0.74, approximating the dimensionless theory. Males were shown to become longer than females, and the decreasing growth rate noticed between summer and autumn in fish older than 2 years, resulted in a strong oscillating growth pattern, clearly attributed to the synergistic effect of sex change and to large differences in summer and winter temperatures. Additionally, an alternative method for assigning fish to age groups, based on clusters derived from length distributions, is proposed.

Manuscript submitted 18 January 2018.
Manuscript accepted 14 September 2018.
Fish. Bull. 116:348–359 (2018).
Online publication date: 22 October (2018).
doi: 10.7755/FB.116.3-4.12

The views and opinions expressed or implied in this article are those of the author (or authors) and do not necessarily reflect the position of the National Marine Fisheries Service, NOAA.

The picarel (*Spicara smaris*) is a very common species in the Mediterranean Sea and the Black Sea, but also occurs in the Sea of Marmara in Turkey and the southern part of the Sea of Azov, which connects Ukraine and Russia (Russell et al., 2015). Species of the genus *Spicara* occur in shallow rocky and muddy bottoms throughout the Mediterranean Sea and the Black Sea, in the Atlantic Ocean from Portugal to Morocco, and around the Canary Islands (Froese and Pauly[1]). These species contribute to inshore fisheries in Greece (Mytilineou and Papaconstantinou, 1991; Stergiou et al., 2011), and represent a major proportion of the total catch for coastal fisheries in Croatia (Dulčiç et al., 2000). These species are also part of bycatch in the Mediterranean Sea but have low commercial value (Ragonese et al., 2004).

The picarel has been observed at depths from 15 to 170 m (Froese and Pauly[1]) and down to 328 m in the eastern Ionian Sea (Mytilineou et al., 2005). This species has been used as a bio-indicator of the coastal and neritic environment (Wacquant and Lamare[2]).

In Greece, the picarel is rather popular as a food item and commer-

---

[1] Froese, R., and D. Pauly. 2018. *Spicara smaris* (Linnaeus, 1758): Picarel. FishBase. World Wide Web electronic publication. [Available from website.]

[2] Wacquant, C., and V. Lamare. 2014. *Spicara smaris* (Linnaeus, 1758). *In* Données d'Observations pour la Reconnaissance et l'Identification de la faune et la flore Subaquatiques (DORIS), 30/03/2014. [Available from website.]

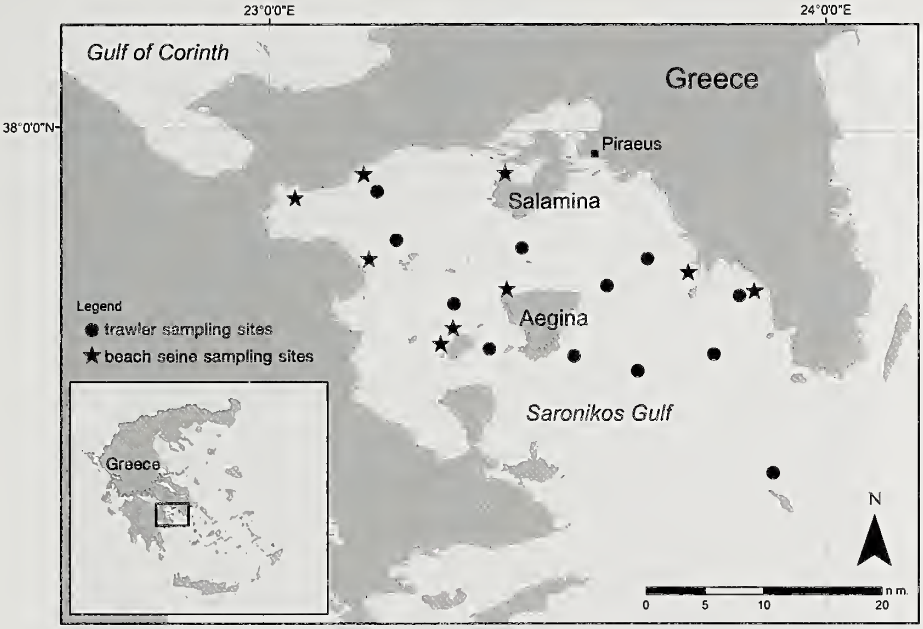

Figure 1

Map of the Saronikos Gulf in Greece showing sites where picarel (*Spicara smaris*) were sampled by trawler (black circles) or by beach seine (stars) from September 1998 through August 1999.

cially important. The ratio of picarel production to the total production for the period between 1990 and 2009 varied from 3.91 to 8.32 (sea fisheries statistics, National Statistical Service of Greece, available from website). It is caught by beach seines, trawlers, nets, and purse seines, but the catch by beach seines accounts for almost half of the catch by the other gears. Picarel represents the major target species of beach seine vessels; other congeneric species do not significantly contribute to the beach seine catch (Karlou-Riga et al., 1997; Papaconstantinou et al., 2007).

The picarel is a protogynous species and presents sexual dimorphism (Zei, 1950; Salekhova, 1979; Whitehead et al., 1986). Protogyny in picarel has also been confirmed histologically. During sexual transition, ovarian tissue degenerates and testicular tissue proliferates (Mitcheson and Liu, 2008). The fish occur in schools, except during time of breeding (Tsangridis and Filippousis, 1992). According to Harmelin and Harmelin-Vivien (1976), each nest is guarded by a brightly colored male. After incubation, the males lose their coloration and swim in schools to feeding areas. Regarding the age and growth of picarel in the Mediterranean Sea, the literature is quite extensive (Salekhova, 1979; Tsangridis and Filippousis, 1989, 1991, 1992; Ismen, 1995; Vidalis and Tsimenidis, 1996; Rizkalla, 1997; Dulčiç et al., 2003). Despite the number of publications, discrepancies do exist in both age determination and growth rates. It is noted, however, that Denaxa et al. (2014), who studied ages of picarel in Greek waters by means of otolith microstructure, gave important information on the first annulus formation.

Oscillating growth rates have been observed to influence sex change, but have never been studied in detail (Tsangridis and Filippousis, 1992). However, they have been recognized as the cause of discrepant length-at-age estimates (Vidalis and Tsimenidis, 1996). Spawning seasonality and body sizes at sex change have, also, been identified as important in developing management plans for sustainable extraction of sequentially hermaphroditic species (DeMartini et al., 2011).

Here we attempt to validate ages or to use alternative ways to assign the specimen to age groups, as well as to address species growth on the basis of picarel sex change. Sex selection was also studied, and the presence of early maturing males (EMMs) was examined (Allsop and West, 2004a). Finally, the length and age at median (50%) female-to-male sex change were investigated to see whether they are as invariant as predicted by Charnov and Skúladóttir (2000) and supported by Allsop and West (2003a). We consider the present work innovative, since both these alternative ways of age validation, as well as the growth study of a protogynous species examined within the sex change framework, are seldom found in the literature.

Materials and methods

Samples of picarel were collected monthly with a beach seine in the Saronikos Gulf (Fig. 1) during the period from September 1998 through August 1999 (Table 1). Because of bad weather conditions in November and December, a chartered bottom trawler was used in-

Table 1

Data on sampling picarel (*Spicara smaris*) in the Saronikos Gulf off Greece from September 1998 through August 1999 with beach seine (SB) or otter bottom trawl (OTB).

Sampling month	Fishing gear	Number of fish collected[1]	Number of fish retained[2]	Number of otoliths removed
September 1998	SB	681	213	137
October 1998	SB	969	278	152
November 1998	OTB	613	348	144
December 1998	OTB	278	176	129
January 1999	SB	1163	429	181
February 1999	SB	726	372	201
March 1999	SB	272	120	107
April 1999	SB	325	180	116
May 1999	SB	259	118	93
June 1999	SB	625	345	151
July 1999	SB	293	186	163
August 1999	SB	254	160	120
Total:		6458	2925	1694

[1] The number of fish collected for measurement of total length.

[2] The number of fish retained in each 5-cm length class each month.

stead. The mesh size of the codend of the beach seine and trawler net between stretched knots was 8 and 20 mm, respectively. A total of 21 hauls were made in an effort to obtain as many representative samples as possible.

The unsorted picarel catch was placed in baskets on board. At the end of each haul, one basket was randomly selected and the total length (TL) of at least 200 individuals was measured to the nearest 0.5 cm. Ten fish from each 0.5-cm length class at each haul were retained. These fish were measured again for TL (to the nearest 0.1 cm), weighed (W, to the nearest 1.0 g) and sex was determined. After gross examination of the gonads, the fish were classified to maturity stages according to Nikolsky (1963). The number of specimens, by sex and maturity stage, was calculated on a monthly basis. From all the fish retained each month, both sagittae were removed from ten fish of each length class. However, only one (commonly the right sagitta) was thereafter analyzed. These otoliths were cleaned and kept dry.

The whole otoliths were examined while immersed in water under reflected light against a dark background, thus revealing alternating hyaline and opaque zones. The core of the otolith was opaque. Readings of hyaline zones (annuli) were made on the concave side and on both the posterior (postrostrum) and the anterior (rostrum) area of the otolith (Fig. 2). Development of the 1st annulus was detected by following the progression of the smaller-fish length group and the structure of the respective otoliths in successive monthly samples (Campana, 2001).

The total otolith diameter and diameter of the annuli were measured along the posterior–anterior axis under a microscope by using a micrometer scale (Fig. 2). The growth increments, annuli, used for age determination, should be "validated" (Beamish and McFarlane, 1983). Among the different methods for validating absolute age or periodicity of growth increment formation, those of marginal increment (MI) and otolith edge analysis are suitable for validation (Campana, 2001). These increments, if formed on a yearly basis, are represented by a sinusoidal curve when plotted against time. In particular, MI is well suited for determining the time of annulus formation (Campana, 2001). In the present work, both the percentages of otoliths with a hyaline or opaque zone on the edge and the MIs were studied monthly. The MI was defined as the width outside the last completed annulus, irrespective of the type of edge (opaque or hyaline) (Karlou-Riga, 2000). Therefore, the time when the value of MI next to each annulus was highest corresponded with the period of the next annulus formation. Monthly mean values of MI were compared by using one-way analysis of variance.

The time of annulus formation, as well as the date of capture, the otolith edge (opaque or hyaline), and the spawning period were used to assign the fish to the appropriate age group (ICSEAF, 1986; Panfili et al., 2002). Each otolith was then characterized either by the n^{th} incomplete annulus on the edge or the n^{th} complete and opaque zone on the edge. Length distributions of specimens classified according to otolith readings were constructed. Based on similarity indices, these distributions were clustered for the period from January to June (1st semester) and from July to December (2nd semester) separately. Whether the clusters derived corresponded with specimens of the same age groups, was then examined, according to age interpre-

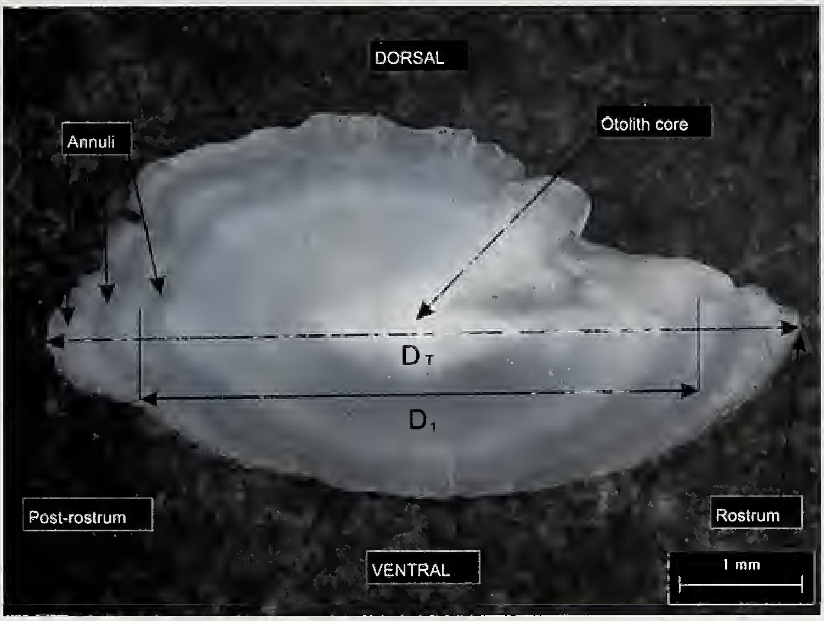

Figure 2

Concave side of the right otolith of a picarel (*Spicara smaris*) sampled in the Saronikos Gulf, Greece, in May 1999. D_T=total otolith diameter; D_1=diameter of first annulus.

tation criteria. The Bray and Curtis (1957) similarity index was used and data were square-root transformed.

Growth parameters were estimated by the classic von Bertalanffy growth function (VBGF):

$$L_t = L_\infty\,(1 - e^{-K(t-t_0)}), \tag{1}$$

where L_t = TL at age t;
L_∞ = the mean asymptotic TL;
K = the growth coefficient; and
t_0 = the theoretical age at TL zero.

A total of three different runs of the classic VBGF were tested: one including all individuals (sex determined and sex undetermined), one run for the combination (total) of males and females and one run for each sex to investigate possible differences in growth patterns between male and female picarel. Model parameters were estimated by using the nonlinear least squares method fitted to the mean observed lengths-at-age (age in monthly units). In addition, the seasonal (oscillating) VBGF (Pauly and Gaschutz[3]) was also implemented in order to investigate a discontinuous growth pattern:

$$L_t = L_\infty\left\{1 - exp - \left[K(t-t_0) - \left(\left(\tfrac{CK}{2\pi}\right)\sin(2\pi(t-t_S))\right)\right]\right\}, \tag{2}$$

where C = the amplitude of the growth oscillation; and
ts = "summer point," the beginning of the sinusoid growth oscillation with respect to t=0 and corresponds with the time of year when growth rate is highest and is related to the winter point (tw) by ts+0.5=tw.

In all cases residual diagnostic plots and histograms showed that models fitted the data appropriately. It should be noted that for many species from the Mediterranean Sea, the growth of young fish is very rapid (Caddy, 1989a, 1989b); therefore, the mean lengths-at-age have to be expressed over time intervals of less than 1 year, as was done in the present study. This approach forces the growth curve close to the origin and provides a better data fit. Assuming 1 April as a conventional birthdate, we then expressed age in months.

According to Allsop and West (2003a), length and age at sex change is the length or age at which 50% of the population are the second sex (male for protogynous fish, female for protandrous fish), and estimates of this value are based on the proportion of the number of males in relation to the number of males and females either per length or per age. Dichotomous sex data (0:female; 1:male) were modeled as a function of TL and age by using generalized linear models (GLM) with a binomial error distribution and a logit link. The analysis led to estimates of length and age at median (50%) female-to-male sex change (L_{50} and A_{50}, respectively). Standard errors for the L_{50} and A_{50} estimates were calculated by using the delta method.

---

[3] Pauly, D., and G. Gaschutz. 1979. A simple method for fitting oscillating length growth data, with a program for pocket calculators. ICES Council Meeting (C.M.) Documents 1979/G:24, 26 p.

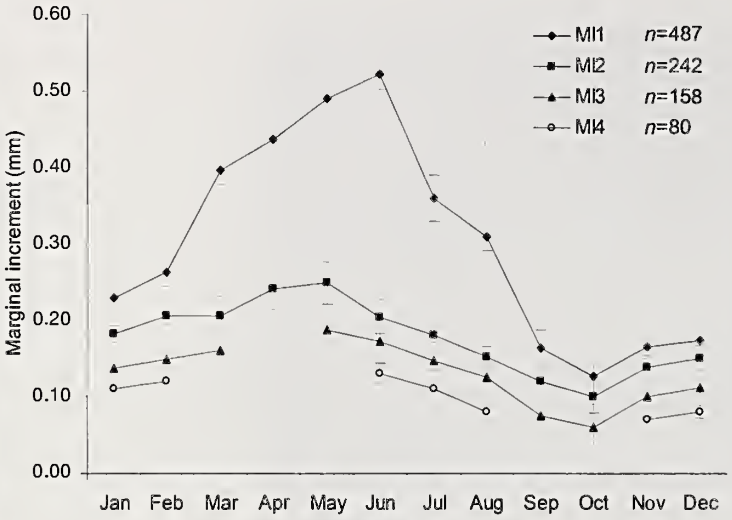

Figure 3

Monthly mean widths of otolith marginal increments next to the first (MI1), second (MI2), third (MI3), and fourth (MI4) annuli for picarel (*Spicara smaris*) collected during September 1998–August 1999 in the Saronikos Gulf, Greece. Bars indicate 2 standard errors of the mean.

The presence of EMMs was examined in an effort to determine whether the species is diandrous and, if so, to estimate the relative proportion of fish maturing directly or early into males. According to Allsop and West (2004a), the proportion of EMMs is calculated by using the logistic parameters derived from the number of males in each length class at the 5th percentile of the population length distribution according to the following equation:

$$\textit{Proportion male (sex ratio)} = \frac{e^{(a+bx)}}{1+e^{(a+bx)}}, \qquad (3)$$

where a = the intercept of the logistic regression;
b = the slope; and
x = the length at the 5th percentile.

According to Allsop and West (2004a), the sex ratio at the 5th percentile is chosen because it is sufficiently close to the lower end of the population length distribution, to ensure that the males present are EMMs and not the product of sex change and so as to minimize the error inherent in measuring and determining the sex of these smaller-size individuals.

Classic and oscillated VBGF curves were fitted to the data by using a script in the fsa package, vers. 0.8.20 (Ogle, 2018) of statistical software R, vers. 3.4.2 (R Core Team, 2017). Model diagnostics, including residual versus predicted plots and histograms were used for evaluating the goodness of fit of tested models. The linear correlation among study variables was examined by using the Pearson test. Additional statistical procedures were performed using Statgraphics Plus 5 software (Statgraphics Technologies, Inc., The Plains, VA). PRIMER 5 software (PRIMER-E, Auckland, New Zealand; Carr, 1997; Clarke and Gorley, 2001) was also used for obtaining the similarity index and for cluster analysis. All the statistical inferences were based on the 0.05-significance level.

Results

From a total of 6458 specimens collected, measuring 4.3 to 20.7 cm TL, 2925 fish were retained for further measurements, from which 1694 otoliths were removed for age determination (Table 1). In the present study, the maximum length ($L_{\max}$) of males and females was 20.7 and 19.7 cm TL, respectively. Specimens of undetermined sex ranged between 4.3 and 10.6 cm TL. Information on $L_{\max}$ values for picarel as drawn from the literature is given in the Supplementary Table.

Monthly length frequencies were constructed (Suppl. Fig. 1) to follow the progression of smaller fish modal lengths (4.5–8.0 cm TL) during the year, in order to examine annuli formation on the otoliths. The smaller specimens, which apparently belonged to the cohort of that year, were caught in July. The same cohort was followed in August, September, and October. The respective otoliths did not show any distinct hyaline zone (Suppl. Fig. 2A), which, however, started to be shown, with the progression of the same cohort, and in January samples. This hyaline margin increased progressively in successive months, and in some of the July otoliths, the hyaline zone, which was interpreted as the 1st annulus, appeared complete (Suppl. Fig. 2B). The successive hyaline zones were interpreted as annuli mainly on the basis of the gradual decrease of their width and their formation at progressively greater distances from the core (Suppl. Fig. 2C). It seems that the 4th, the 5th, and the 6th annuli appear very close to each other, and the contrast between the opaque and hyaline area is in general not strong. Despite this difficulty, the study of the otolith edge showed seasonality; the percentage of hyaline areas on the edge attained the highest value in June and the lowest in October (Suppl. Fig. 3). The oldest fish were found to have 6 annuli.

The MI widths next to the 1st (MI1), the 2nd (MI2), the 3rd (MI3), and the 4th (MI4) annuli showed a seasonal progression (one-way analysis of variance, $P<0.05$, MI1: df=486, MI2: df=241, MI3: df=157, MI4: df=79). The lowest values of MIs were found in October and the highest values during May–June, indicating that the annuli are completed between June and October (Fig. 3).

Table 2

Growth parameters of picarel (*Spicara smaris*) calculated by the different runs (classic, sex specific, and seasonal) of a von Bertalanffy growth function (VBGF) model for different subsets of individuals (all, males, and females): L_∞=the mean asymptotic total length; K=the growth coefficient; C=the amplitude of the growth oscillation; and ts or *summer point*=the beginning of the sinusoid growth oscillation with respect to t=0. Standard errors are given in parentheses. MSE=mean squared error; n=number of specimens in each subset. Lengths are total lengths.

VBGF	Data subset	L_∞ (cm)	K	t_0 (year)	C	t_s	MSE	n
Classic	All fish	19.91 (0.480)	0.512 (0.059)	−0.412 (0.145)			0.015	1694
	Males and females	19.93 (0.697)	0.433 (0.072)	−0.843 (0.265)			0.011	
Sex specific	Females	16.52 (0.339)	0.973 (0.158)	−0.040 (0.163)			0.009	951
	Males	20.29 (0.656)	0.455 (0.079)	−0.745 (0.288)				563
Seasonal	Females	16.95 (0.461)	0.757 (0.142)	−0.312 (0.251)	1.261 (0.569)	−0.457 (0.052)	0.018	951
	Males	20.94 (0.844)	0.379 (0.072)	−0.701 (0.179)	1.261 (0.569)	−0.572 (0.074)		563

Age interpretation criteria

Because the picarel spawning period lasts from February to June (Suppl. Fig. 4), the fish spawned during this period constituted one cohort. Given that the annuli are completed in the 2nd semester, specimens caught in the 1st semester with n annuli and an opaque zone on their otolith edge were assigned to the n+1 age group, whereas specimens with the n^{th} annulus on the otolith edge caught either in the 1st semester or the 2nd semester, were assigned to the n^{th} age group.

The following otolith readings were the most frequent: OP, H1, H1+OP, H2, H2+OP, H3, H3+OP, H4 and H4+OP, where OP and H correspond to opaque and hyaline edges respectively, and the number specifies the successive annulus. The clusters of the length distributions, classified according to their otolith readings, are shown in Figure 4. It was observed that the clusters corresponded with specimens of those age groups obtained according to age interpretation criteria.

Growth

The mean lengths at age showed a significant difference between sexes (t-test, n=39, P<0.05). Table 2 summarizes the VBGF parameters for the three versions of the model (classic, sex specific, and seasonal) and the various subsets investigated (all specimens and only specimens with identified sex). The growth curve that best fitted the data was the sex-specific VBGF (mean squared error [MSE]=0.009, see Table 2). Based on this curve, asymptotic length for females and males was 16.52 and 20.29 cm TL respectively (Fig. 5A). The two runs of the classic VBGF for all fish (Fig. 5B) and for only fish with identified sex gave similar estimates of L_∞ (all fish: 19.91 cm TL; for those with identified sex: 19.93 cm TL), similar K values (all fish: 0.512; for those with identified sex: 0.433) and quite different t_0 values (all fish: −0.412; for those with identified sex: −0.843). Residual diagnostic plots and histograms are

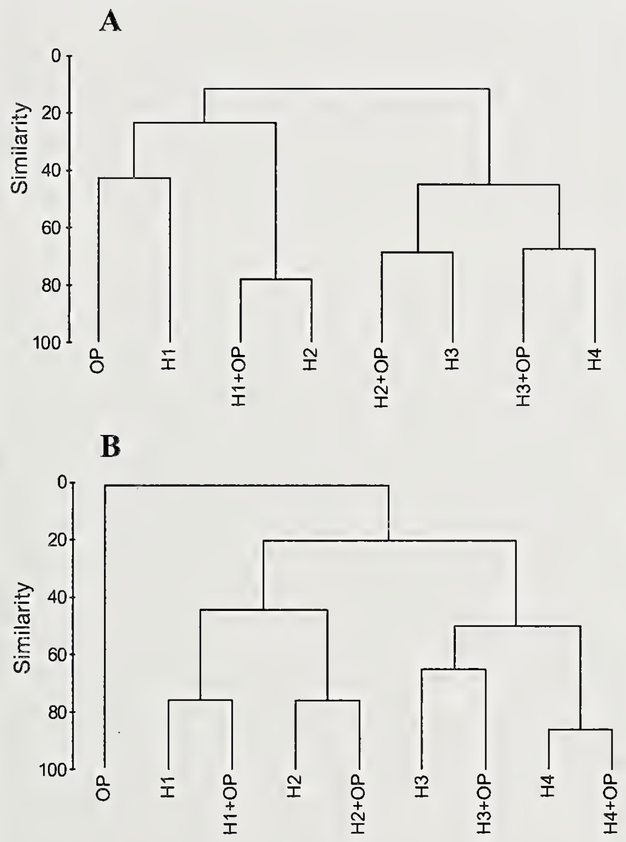

Figure 4

A cluster diagram of length-frequency distributions for specimens of picarel (*Spicara smaris*) collected during 1998–1999 in the Saronikos Gulf, Greece, classified according to results of otolith readings during the (**A**) first and (**B**) second semester. Clusters were formed according to the following criteria: no annulus (OP), first annulus on the edge (H1), first annulus that was completed and was opaque on the edge (H1+OP) and so on for H2, H2+OP, H3, H3+OP, H4, and H4+OP.

shown in Suppl. Fig. 5. The seasonal (oscillating) VBGF curve (Fig. 6) was also shown to fit data well (MSE=0.018), where the asymptotic length (L_∞=20.94 cm TL), was found very close to the L_{max} (20.7 cm TL). It is worth noting the high value of the C parameter (1.261), which clearly suggests a strong oscillating growth pattern with a prolonged no growth phase or a sustained period of no growth (Pauly and Gaschutz[3]).

In order to identify the season when change in growth occurs, or to examine the probable effect of sex change on the growth rate (Tsangridis and Filippousis, 1992; Vidalis and Tsimenidis, 1996), the observed mean lengths at age for each sex of picarel sampled were estimated during the life of the fish (Suppl. Fig. 6).

Examining the growth rate, it appears that males exhibit a higher growth rate than females, and a strong oscillating growth pattern is noticed during the 2nd, the 3rd, and the 4th year of life. More specifically, a decrease of the average length for each sex is marked from summer to autumn. During the life of the species, the difference in length between males and females was found to be positively correlated with age (Pearson test: n=34, P<0.05).

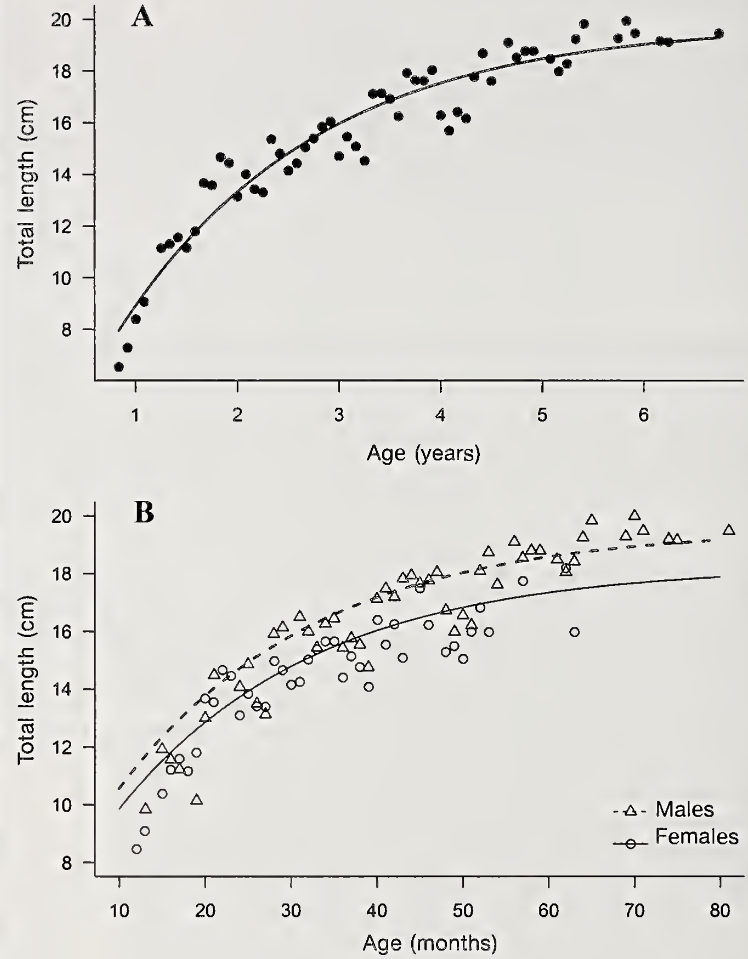

Figure 5

Von Bertalanffy growth function curves of picarel (*Spicara smaris*) collected during 1998–1999 in the Saronikos Gulf, Greece, based on ages determined from otoliths for (**A**) all fish (sex determined and sex undetermined) combined and (**B**) males and females separately.

Length and age at sex change and proportion of early maturing males

The proportion of males was found to be positively correlated with length (Pearson test: n=34, P<0.05) and with age (Pearson test: n=57, P<0.05), whereas the inverse occurred with the proportion of females. The coefficients of the binomial sex change model were a=−10.105 (P<0.01), b=0.654 (P<0.01) and the L_{50} was estimated as: L_{50}=15.34 cm TL (CI=15.17–15.51) (Fig. 7A). The length at sex change divided by the L_{max} of the individuals, was 0.74. Respectively, the coefficients obtained from the number of males in each length class were a= −4.711 (P<0.01), b=0.135 (P<0.01), and the A_{50} was 36.4 months (CI=35.21–37.63 months) or 3.0 years (Fig. 7B).

Using the logistic parameters obtained from the number of males in each length class at the 5th percentile of the population length distribution, we estimated the proportion of EMMs at 2.4%.

Discussion

Despite the weak contrast between the opaque and hyaline zones particularly after the 3rd annulus, the annuli of picarel were easily readable and show a normal growth pattern. The use of monthly samples during the first year of picarel life was essential to track completion of the 1st annulus.

The periodicity of annulus formation, shown by monthly examination of MIs, showed that these increments were true annuli. It should be noted that different marks can be occasionally laid down on whole otoliths, which are not age related but are due to events such as settlement, spawning, or maturity (Campana, 2001). However, those marks do not show the normal periodicity and structure of annuli as happens with true annuli. In the present work, the date of annuli completion, based on the MIs study, was estimated to occur after June, when the percentage of otoliths with a hyaline area on the edge was the highest (see Suppl. Fig 3).

The time of estimated annuli formation coincides with the end of spawning and is in general agreement

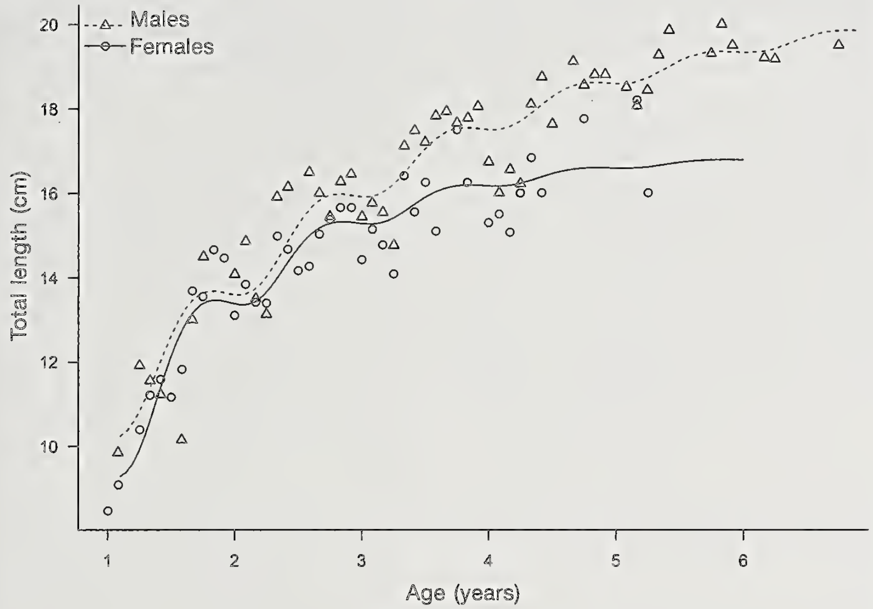

Figure 6

Seasonal (oscillating) von Bertalanffy growth function curve of female and male picarel (*Spicara smaris*) sampled in the Saronikos Gulf, Greece, during 1998–1999, based on ages determined from otoliths.

with the findings of Vidalis and Tsimenidis (1996), who also validated annulus completion by MI analysis. Denaxa et al. (2014), who determined picarel ages in Greek waters by means of otolith microstructure, reported that the first annulus is completed between January and April and formed between 180 (6 months) and 372 days (12.4 months) of life, which correspond to 8.63 and 14.3 cm TL respectively. The data of Denaxa et al. (2014) seem to be slightly lower than those of the present study, where the first annulus appears in otoliths from fish between 9.7 and 15.0 cm TL. Cluster analysis based on the similarity indices, and after we compared the length frequency distributions of fish classified according to their otolith readings, showed both the validity of the age interpretation criteria and an alternative way to assign the fish to age groups. It can be concluded that fish with similar lengths belong to the same age group, a relationship that many times in the past has been verified (Francis and Campana, 2004).

The application of the VBGF as a nonlinear approach to fitting length-at-age data is commonly used to describe fish growth, given that it is still the most useful tool for growth analysis despite the criticism of its use. As stated by Kimura (1980), rejection of the VBGF curve must ultimately be based on superior alternative curves or methods of analysis. In our work, we noticed good fitting (see Fig. 5), and the growth parameters were found to be very reasonable (L_∞ close enough to the L_{max} values observed, t_0 close enough to zero). The good fit of data in the present work is probably due to both a careful reading of annuli and the large number of specimens caught monthly. The mean observed lengths at ages 1, 2, 3, and 4 for sexes combined as reported by Tsangridis and Filippousis (1992) are in general agreement with those of the present study. The smaller lengths at age estimated by the VBGF as reported by Ismen (1995), Vidalis and Tsimenidis (1996), and Dulčiç et al. (2003), when compared to those of our study, are probably due to the interpretation of pre-annual (false) zone as the 1st annulus. Slight differences in lengths at age were also found between those in the present work and those in the work by Rizkalla (1997). It is noted, however, that lengths in Rizkalla (1997) were estimated with the back calculation method. It is worth noting that in both works (Vidalis and Tsimenidis, 1996; Rizkalla, 1997), differences in the growth rate between sexes (males become longer than females) were not observed.

An oscillating pattern in the growth of picarel was mentioned by Tsangridis and Filippousis (1992). In particular, they attribute the slowing down of growth rate to either maturity or sex change. In more detail, they observed only two oscillations related to two growth periods: one linked to a very fast female growth period (up to 15.0 cm TL) and the second linked to a male slow period (up to 19.0 cm TL). In the present study, the decrease in the observed average length for each sex is noticed from summer to autumn during the 2nd, 3rd, and 4th year of life and is most likely related to the

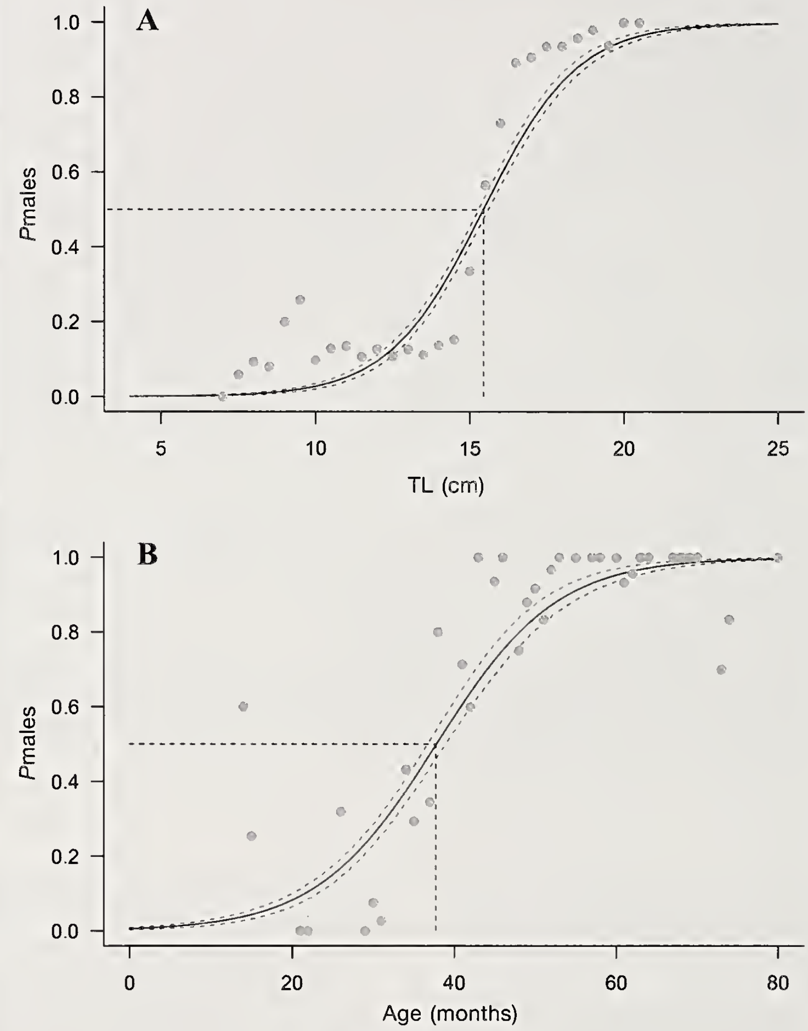

Figure 7

Fitted probability (*P*) of picarel (*Spicara smaris*) being male with (**A**) total length and (**B**) age and accompanying proportions of males per 0.5-cm and 1-month classes, respectively. The length at median (50%) female-to-male sex change was 15.34 cm in total length (TL). The age at median female-to-male sex change was 36.4 months. The solid line indicates the fitted curve, the dotted lines indicate the 95% confidence intervals, and the gray circles indicate the observed data.

sex change. The presence of juveniles (see also Suppl. Fig. 1), as well as the high temperature (19–25°C) which usually appears during this period (Suppl. Fig. 7), may play a role in the observed decrease in growth rate. It is noted however that Tsangridis and Filippousis (1994), who have tried a series of models for studying picarel growth, reported that the model that fitted best, showed that picarel growth changes when sex changes and the plotted curve also shows some kind of oscillation.

According to the literature (Salekhova, 1979; Tsangridis and Filippousis, 1992), sex change occurs after spawning, which is common in protogynous species (Provost et al., 2017). In the present study, the majority of spent females were observed from June through September (see Suppl. Fig. 4). A change in sex during nonbreeding periods is not surprising because this strategy is predicted to maximize seasonal reproductive output in individual fish as mentioned by Provost et al. (2017). In an attempt to explain this decrease of average length, we believe that during sex transition, the longest females at each age (1, 2, and 3 years) change into males. Considering that the mean lengths at age of males are greater than those of females, this inversion results in lower mean lengths at age for each sex. The selection of larger females for inversion into males supports the size-advantage model (Warner, 1988). This model is particularly effective in accounting for postmaturational protogynous sex change among teleosts in which a few large males can monopolize mating within the population (Francis and Barlow, 1993; Erisman et al., 2009).

The L_{50} (15.3 cm TL) of this study, which corresponds to an age of 3 years (A_{50}=3.0 years), is in general agreement with previous reports (Salekhova, 1979; Tsangridis and Filippousis, 1992; Dulčiç et al., 2003). It is noted, however, that initial maturation was observed at about one-half year old, or about 10 cm TL (Suppl. Figs. 4 and 6). According to the dimensionless theory (Charnov and Skúladóttir, 2000), the ratio of $L_{50}/L_{\max}$ is invariant. Allsop and West (2003a), who found support for this theory across 52 fish species, estimated the relative ratio at 0.80, a ratio that is related neither to the mating system nor to the presence of EMMs. When the same authors extended the list of species and estimated the same ratio for 77 species of fish, echinoderms, crustaceans, and molluscs, they found a value equal to 0.72 and concluded that the time when sex change occurs, is invariant for all animals (Allsop and West, 2003b). The same authors, on the other hand, agree that the invariant value of $L_{50}/L_{\max}$ corresponds to those species when the following criteria are met: 1) the species should be a unidirectional sex changer and 2) if it is diandrous, the proportion of EMMs should be low, ≤2% according to Allsop and West (2004b). In the case of picarel, the species is a unidirectional sex changer (the proportion of males is positively correlated with body length), whereas the proportion of EMMs, estimated at 2.4%, which is close enough to 2%, can be considered low. More specifically, Allsop and West (2004b) agree that the value of 2% EMMs is the upper limit for those species characterized as pure sex changers. The value of $L_{50}/L_{\max}$ estimated in this work (0.74), although is lower than the original estimated ratio ($L_{50}/L_{\max}$=0.80), is close enough to the value of 0.72 of the extended list of Allsop and West (2003b) and within the $L_{50}/L_{\max}$ range (from 0.62 to 0.84) estimated by Allsop and West (2003a) for 4 (other than picarel) species of the Sparidae family. Thus, the dimensionless theory could be potentially supported and it can be concluded that the animals change sex at a certain proportion of their $L_{\max}$. A number of studies, on the other hand, have implicated fishing pressure as a cause of decline in the size at sex change (Platten et al., 2002; Hamilton et al., 2007) and therefore it should be noted that sequential hermaphrodites are more sensitive to size-selective harvesting than separate-sex species (Hamilton et al., 2007).

According to the sex allocation theory (Charnov et al., 1978), the population is compensating for decreases in reproductive capacity. Picarel exhibit male parental care, where the males guard the eggs in their nest until time of hatching (Harmelin and Harmelin-Vivien, 1976). It seems that the picarel represents a rare example of a species that exhibits co-occurring protogynous sex change and parental care. Although this feature of synchronicity could reduce the potential reproductive rate of males and hence the selection for sex change (i.e, the selection of females undergoing a sex change) (Allsop and West, 2004a), it seems that for picarel, as for some labrids (Warner and Lejeune, 1985), the cost of minimal parental care is outweighed by the benefit of larger male size in attracting and spawning with multiple females. On the other hand, the production of EMMs, which depends on the structure of the mating system, increases with high population density. High densities destabilize the potential for mate monopolization and therefore selection for sex change (Allsop and West, 2004a). Preliminary results of stock assessment in the area (Karlou-Riga and Anastopoulou, 2005) showed that the picarel stock is under or lightly exploited (ratio of current spawning stock biomass to virgin stock biomass is about 80%). Therefore, high local population density is probably another potential factor, which could reduce the proportion of individuals undergoing a sex change and increase the proportion of EMMs. The findings of the present work most probably support the statement of Allsop and West (2004a), who suggested that the abundance of EMMs can be used as a measure of the amount of sex change taking place.

Acknowledgments

This work is a contribution to the "Management plans—Surveys in highly commercial fishing areas" Research Project, supported by the Hellenic Ministry of Rural Development and Food (Project Code 9686535). The authors wish to thank the staff of the Fisheries Laboratory of the Hellenic Ministry of Rural Development and Food, who collaborated on this project and in particular the three anonymous reviewers for critically reading the manuscript, providing insightful comments, and suggesting substantial improvements.

Literature cited

Allsop, D. J., and S. A. West.
2003a. Constant relative age and size at sex change for sequentially hermaphroditic fish. J. Evol. Biol. 16:921–929.
2003b. Changing sex at the same relative body size. Nature 425:783–784.
2004a. Sex allocation in the sex-changing marine goby, *Coryphopterus personatus*, on atoll-fringing reefs. Evol. Ecol. Res. 6:843–855.
2004b. Sex-ratio evolution in sex changing animals. Evolution 58:1019–1027.
Beamish, R. J., and G. A. McFarlane.
1983. The forgotten requirement for age validation in fisheries biology. Trans. Am. Fish. Soc. 112:735–743.
Bray, J. R., and J. T. Curtis.
1957. An ordination of the upland forest communities of southern Wisconsin. Ecol. Monogr. 27:325–349.
Caddy, J. F.
1989a. A research strategy in support of stock evaluation

of demersals in the Mediterranean Sea. *In* Report of the second technical consultation of the General Fisheries Council for the Mediterranean on stock assessment in the eastern Mediterranean; Athens, Greece, 28 March–1 April 1988. FAO Fish. Rep. 412 (M. Savini and J. F. Caddy, eds.), p. 116–127. FAO, Rome.

1989b. Comments on yield calculation presented at recent GFCM technical consultations on stock assessment. *In* Report of the second technical consultation of the General Fisheries Council for the Mediterranean on stock assessment in the eastern Mediterranean; Athens, Greece, 28 March–1 April 1988. FAO Fish. Rep. 412 (M. Savini and J. F. Caddy, eds.), p. 201–206. FAO, Rome.

Campana, S. E.
2001. Accuracy, precision and quality control in age determination, including a review of the use and abuse of age validation methods. J. Fish Biol. 59:197–242.

Carr, A.
1997. Primer user manual: Plymouth routines in multivariate ecological research, 42 p. Plymouth Marine Laboratory, Plymouth, UK.

Charnov, E. L., and U. Skúladóttir.
2000. Dimensionless invariants for the optimal size (age) of sex change. Evol. Ecol. Res. 2:1067–1071.

Charnov, E. L., D. W. Gotshall, and J. G. Robinson.
1978. Sex ratio: adaptive response to population fluctuation in pandalid shrimp. Science. 200:204–206.

Çiçek, E., and D. Avşar.
2010. Growth and mortality of *Spicara smaris* (Linnaeus, 1758) off Karatas Coast (Iskenderun Bay). Ecol. Life Sci. 5:126–134.

Clarke, K. R., and R. N. Gorley.
2001. PRIMER v5: user manual/tutorial, 91 p. PRIMER-E, Plymouth, UK.

DeMartini, E. E., A. R. Everson, and R. S. Nichols.
2011. Estimates of body sizes at maturation and at sex change, and the spawning seasonality and sex ratio of the endemic Hawaiian grouper (*Hyporthodus quernus*, F. Epinephelidae). Fish. Bull. 109:123–134.

Denaxa, M., P. Bekas, D. Tziertzidis, and Ch. Mytilineou.
2014. Preliminary study of juvenile picarel, *Spicara smaris* (Linnaeus 1758), growth from otolith microstructure. *In* HydroMedit 2014: 1st International Congress of Applied Ichthyology & Aquatic Environment; Volos, Greece, 13–15 November, p. 271–275.

Dulčiç, J., M. Bauchot, B. Grbec, and P. Cetinić.
2000. Age, growth and mortality of blotched picarel *Spicara maena* L. (Pisces: Centracanthidae) in the eastern central Adriatic. Fish. Res. 48:69–78.

Dulčiç, J., A. Pallaoro, P. Cetinić, M. Kraljević, A. Soldo, and I. Jardas.
2003. Age, growth and mortality of picarel, *Spicara smaris* L. (Pisces: Centracanthidae), from the eastern Adriatic (Croatian coast). J. Appl. Ichthyol. 19:10–14.

Erisman, B. E., M. T. Craig, and P. A. Hastings.
2009. A phylogenetic test of the size-advantage model: evolutionary changes in mating behavior influence the loss of sex change in a fish lineage. Am. Nat. 174:E83–E99.

Francis, R. C., and G. W. Barlow.
1993. Social control of primary sex differentiation in the Midas cichlid. Proc. Natl. Acad. Sci. U.S.A. 90:10673–10675.

Francis, R. I. C., and S. E. Campana.
2004. Inferring age from otolith measurements: a review and a new approach. Can. J. Fish. Aquat. Sci. 61:1269–1284.

Hamilton, S. L., J. E. Caselle, J. D. Standish, D. M. Schroeder, M. S. Love, J. A. Rosales-Casian, and O. Sosa-Nishizaki.
2007. Size-selective harvesting alters life histories of a temperate sex-changing fish. Ecol. Appl. 17:2268–2280.

Harmelin, J. G., and M. L. Harmelin-Vivien.
1976. Observations "in situ" des aires de ponte de *Spicara smaris* (L.) (Pisces, Perciformes, Centracanthidae) dans les eaux de Port-Cros. Trav. Sci. Parc Natl. Port-Cros 2:115–120.

ICSEAF (International Commission for the Southeast Atlantic Fisheries).
1986. Otolith interpretation guide: No. 2, Cape horse mackerel, 24 p. ICSEAF, Madrid, Spain.

Ismen, A.
1995. Growth, mortality and yield per recruit model of picarel (*Spicara smaris* L.) on the eastern Turkish Black Sea coast. Fish. Res. 22:299–308.

Karakulak, F. S., H. Erk, and B. Bilgin.
2006. Length–weight relationships for 47 coastal fish species from the northern Aegean Sea, Turkey. J. Appl. Ichthyol. 22:274–278.

Karlou-Riga, C.
2000. Otolith morphology and age and growth of *Trachurus mediterraneus* (Steindachner) in the eastern Mediterranean. Fish. Res. 46:69–82.

Karlou-Riga, C., and I. Anastopoulou.
2005. Stock assessment of picarel (*Spicara smaris*) exploited by trawlers and beach seiners in the Saronikos Gulf (GFCM–GSA 22). *In* Report of the seventh session of the General Fisheries Commission for the Mediterranean (GFCM) Sub-Committee for Stock Assessment (SCSA); Rome, Italy, 26–30 September, p. 5–6. General Fisheries Commission for the Mediterranean, Rome.

Karlou-Riga, C., A. Argirokastritis, and N. Vrantzas.
1997. Catch and effort of species caught by trawler and beach seiner in the Saronikos Gulf. *In* Proceedings of the 5th Hellenic Symposium on Oceanography and Fisheries, vol. 2; Kavala, Greece, 15–18 April, p. 25–28. National Centre for Marine Research, Athens, Greece.

Kimura, D. K.
1980. Likelihood methods for the Von Bertanlaffy growth curve. Fish. Bull. 77:765–776.

Mitcheson, Y. S. D., and M. Liu.
2008. Functional hermaphroditism in teleosts. Fish Fish. 9:1–43.

Mytilineou, C., and C. Papaconstantinou.
1991. Age and growth of *Spicara flexuosa* (Rafinesque, 1810) (Pisces, Centracanthidae) in the Patraikos Gulf (Greece). Sci. Mar. 55:483–490.

Mytilineou, C., C. Y. Politou, C. Papaconstantinou, S. Kavadas, G. D'Onghia, and L. Sion.
2005. Deep-water fish fauna in the eastern Ionian Sea. Belg. J. Zool. 135:229–233.

Nikolsky, G. V.
1963. The ecology of fishes, 351 p. Academic Press, London.

Ogle, D. H.
2018. FSA: fisheries stock analysis. R package vers. 0.8.20. [Available from website.]

Panfili, J., H. de Pontual, H. Troadec, and P. J. Wright (eds.).
2002. Manual of fish sclerochronology, 464 p. Ifremer-IRD coedition, Brest, France.

Papaconstantinou, C., A. Zenetos, V. Vassilopoulou, and G. Tserpes.
2007. State of Hellenic fisheries, 467 p. Hell. Cent. Mar. Res., Athens, Greece.

Platten, J. R., I. R. Tibbetts, and M. J. Sheaves.
2002. The influence of increased line-fishing mortality on the sex ratio and age of sex reversal of the venus tusk fish. J. Fish Biol. 60:301–318.

Provost, M. M., O. P. Jensen, and D. L. Berlinsky.
2017. Influence of size, age, and spawning season on sex change in black sea bass. Mar. Coast. Fish. 9:126–138.

R Core Team.
2017. R: a language and environment for statistical computing. R Foundation for Statistical Computing, Vienna, Austria. [Available from website, accessed October 2017.]

Ragonese, S., F. Fiorentino, G. Garofalo, M. Gristina, D. Levi, S. Gancitano, G.B. Giusto, P. Rizzo, and G. Sinacori.
2004. Distribution, abundance and biological features of picarel (*Spicara flexuosa*), Mediterranean (*Trachurus mediterraneus*) and Atlantic (*T. trachurus*) horse mackerel based on experimental bottom-trawl data (MEDITS, 1994–2002) in the Strait of Sicily. *In* Report of the MedSudMed expert consultation on small pelagic fishes: stock identification and oceanographic processes influencing their abundance and distribution; Salammbô, Tunisia, 1–3 October 2003. GCP/RER/010/ITA/MSM-TD-05. MedSudMed Tech. Doc. 5, p. 100–114. FAO MedSudMed, Mazara del Vallo, Italy.

Rizkalla, S. I.
1997. Age and growth studies of picarels (*Spicara flexuosa* and *Spicara smaris*) in the Egyptian Mediterranean waters. Oebalia 28:75–86.

Russell, B., D. Pollard, and K. E. Carpenter.
2015. *Spicara smaris*. The IUCN Red List of Threatened Species 2014. e.T170283A1308287. [Available from website.]

Salekhova, L. P.
1979. Picarels (*Spicara* spp.) in the Mediterranean Basin, 172 p. Kiev Academy of Science, Kiev, Ukraine.

Stergiou, K. I., D. K. Moutopoulos, and G. Krassas.
2004. Body size overlap in industrial and artisanal fisheries for five commercial fish species in the Mediterranean Sea. Sci. Mar. 68:179–188.

Stergiou, K. I., P. K. Karachle, A. C. Tsikliras, and E. Mamalakis.
2011. Shouting fishes: fishes from the Greek seas—biology, fisheries and management, 358 p. Patakis Publishers, Athens, Greece. [In Greek.]

Tsangridis, A., and N. Filippousis.
1989. Length-based approach to the estimation of growth and mortality parameters of *Spicara smaris* (L.) in the Saronikos Gulf, Greece and remarks on the application of the Beverton and Holt relative yield per recruit model. *In* Report of the second Technical Consultation of the General Fisheries Council for the Mediterranean on stock assessment in the eastern Mediterranean; Athens, Greece, 28 March–1 April 1988. FAO Fish. Rep. 412 (M. Savini, M., and J. F. Caddy, eds.), p. 94–107. FAO, Rome.
1991. Use of length-frequency data in the estimation of growth parameters of three Mediterranean fish species: bogue (*Boops boops* L.), picarel (*Spicara smaris* L.) and horse mackerel (*Trachurus trachurus* L.). Fish. Res. 12:283–297.
1992. Growth pattern of picarel, *Spicara smaris* (L.) (Centracanthidae), a protogynous species. Cybium 16:233–243.
1994. Analysis of two models for picarel (*Spicara smaris* L.) growth using Schnute's micro-simplex nonlinear estimation procedure. Fish. Res. 20:181–189.

Tsasitis, I., and C. Charilaou.
2016. Stock assessment form: *Spicara smaris*. General Fisheries Commission for the Mediterranean, Rome. [Available from website.]

Valle, C., J. T., Bayle, and A. A. Ramos.
2003. Weight–length relationships for selected fish species of the western Mediterranean Sea. J. Appl. Ichthyol. 19:261–262.

Vidalis, K., and N. Tsimenidis.
1996. Age determination and growth of picarel (*Spicara smaris*) from the Cretan continental shelf (Greece). Fish. Res. 28:395–421.

Vidalis, K., G. Markakis, and N. Tsimenides.
1997. Discrimination between populations of picarel (*Spicara smaris* L., 1758) in the Aegean Sea, using multivariate analysis of phenetic characters. Fish. Res. 30:191–197.

Warner, R. R.
1988. Sex change and the size-advantage model. Trends Ecol. Evol. 3:133–136.

Warner, R. R., and P. Lejeune.
1985. Sex change limited by paternal care: a test using four Mediterranean labrid fishes, genus *Symphodus*. Mar. Biol. 87:89–99.

Whitehead, P. J. P., M.-L. Bauchot, J.-C. Hureau, J. Nielsen, and E. Tortonese.
1986. Fishes of the north-eastern Atlantic and the Mediterranean, vol. 1, 510 p. UNESCO, Paris.

Zei, M.
1950. Typical sex-reversal in teleosts. Proc. Zool. Soc. Lond. 119:917–920.

Acknowledgment of reviewers

The editorial staff of *Fishery Bulletin* would like to acknowledge the scientists who reviewed manuscripts during 2017–2018. Their contributions have helped ensure the publication of quality science.

Kenneth Able
Alfonso Aguilar-Perera
Jeane Almeida
Michael Armstrong

Henry Bart Jr.
Ewann Berntson
Joseph Bizzarro
Katelyn Bosley
Richard Brill
Richard Brodeur
Stephen Brouwer
Joan Browder
Erin Burge

Matthew Campbell
John Carlson
Shannon Cass-Calay
Elizabeth Chilton
Toni Chute
Mark Collins
Christina Conrath
Kevin Craig

Toby Daly-Engel
Edward DeMartini
Emmanis Dorval
William Driggers III
J. Marcus Drymon
Cara Ewell Hodkin

Elizabeth Fairchild
Jessica Farley
Nathan Furey

Jin Gao
Audrey Geffen
James Gelsleichter
Daniel Gerdeaux
Anthony Gharrett
Gretchen Grammer
John Graves
Helga Guderley
Donald Gunderson
Jeff Guyon

L. Stanton Hales Jr.
Toshihide Hamazaki
Jon Hare
Rick Hart
Jason Hartog
Sean Hayes

Melissa Head
Mikko Heino
Michael Heithaus
Frank Hernandez Jr.
Eric Hoffmayer

Abua Ikem

Larry Jacobson
Thomas Jagielo
Gregory Jenkins
Donna Johnson

Christian Jones
Adrian Jordaan

Stefanos Kavadas
Aimee Keller
Bryan Keller
David Kerstetter
John Kocik

Tom Laidig
Erik Lang
Richard Langton
Michael Larkin
Robert Lauth
Rosângela Lessa
Kwang-Ming Liu
Nancy Lo
William Loftus
Luis Lucifora
Molly Lutcavage

John Manderson
Unai Markaida
Richard McBride
Stephen McIninch
Caleb McMahan
Antonio Medina
Richard Methot
Todd Miller
Muhammad Talib Kalhoro
Barbara Muhling
Bruce Mundy
John Musick
Michael Musyl

Lisa Natanson
Janet Nye

Costas Papaconstantinou

Thomas Peatman
Juan Pérez Jiménez
George Pess
Mark Peterson
Gregg Poulakis
Jessica Powell
Harold Pratt Jr.

Joseph Quattro

Sergio Ragonese
Rubén Roa-Ureta
Philip Roni
Anna Rossi

Courtney Saari
David Sampson
Kurt Schaefer
Zebulon Schobernd
Xiujuan Shan
Andrew Shelton
Robert Shipp
Michael Simpkins
Thomas Sminkey
Brian Smith
Dave Somerton
Brian Spence
Paul Spencer
Ingrid Spies
Daniel Stich
Jan Straley
Zhenming Su
Patrick Sullivan

Timothy Targett
Eric Taylor

Silva Uusi-Heikkilä

Jaap van der Meer

John Walter III
Yoshiro Watanabe
David Welch
Sabine Wintner
Catarina Wor
Bruce Wright
Mark Wuenschel

Mary Yoklavich

Mukti Zainuddin

Fishery Bulletin

Guidelines for authors

Contributions published in *Fishery Bulletin* describe original research in marine fishery science, fishery engineering and economics, as well as the areas of marine environmental and ecological sciences (including modeling). Preference will be given to manuscripts that examine processes and underlying patterns. Descriptive reports, surveys, and observational papers may occasionally be published but should appeal to an audience outside the locale in which the study was conducted.

Although all contributions are subject to peer review, responsibility for the contents of papers rests upon the authors and not on the editor or publisher. *Submission of an article implies that the article is original and is not being considered for publication elsewhere.*

All submissions are subject to a double-blind review to remove the identity of author and reviewer during the review process.

Plagiarism and double publication are considered serious breaches of publication ethics. To verify the originality of the research in papers and to identify possible previous publication, manuscripts may be screened with plagiarism-detection software.

Manuscripts must be written in English; authors whose native language is not English are strongly advised to have their manuscripts checked by English-speaking colleagues before submission.

Once a paper has been accepted for publication, online publication takes approximately 3 weeks.

There is no cost for publication in *Fishery Bulletin.*

Types of manuscripts accepted by the journal

Articles generally range from 20 to 30 double-spaced typed pages (12-point font) and describe an original contribution to fisheries science, engineering, or economics. Tables and figures are not included in this page count, but the number of figures should not exceed one figure for every four pages of text. Articles contain the following divisions: abstract, introduction, methods, results, and discussion.

Short contributions are generally less than 15 double spaced typed pages (12-point font) and, like articles, describe an original contribution to fisheries science. They follow the same format as that for articles: abstract, introduction, results, and discussion, but the results and discussion sections may be combined. They are distinguished from full articles in that they report a noteworthy new observation or discovery—such as the first report of a new species, a unique finding, condition, or event that expands our knowledge of fisheries science, engineering, or economics—and do not require a lengthy discussion.

Companion articles should be submitted together and are published together as a scientific contribution. Both articles should address a closely related topic and may be articles that result from a workshop or conference.

Review articles generally range from 40 to 60 double-spaced typed pages (12-point font) and address a timely topic that is relevant to all aspects of fisheries science. They should be forward thinking and address views or interpretations of information that encourage new avenues of research. They can be reviews based on the outcome from thematic workshops, or contributions by groups of authors who want to focus on a particular topic, or a contribution by an individual who chooses to review a research theme of broad interest to the fisheries science community. A review article will include an abstract, but the format of the article, per se, will be up to the author. Please contact the Scientific Editor to discuss your ideas regarding a review article before embarking on such a project.

Preparation of manuscript

Title page should include authors' full names, mailing addresses, and the senior author's e-mail address.

Abstract should be limited to 200 words (one-half typed page), state the main scope of the research, and emphasize the authors' conclusions and relevant findings. Do not review the methods of the study or list the contents of the paper. Because abstracts are circulated by abstracting agencies, it is important that they represent the research clearly and concisely.

General text must be typed in 12-point Times New Roman font throughout. A brief introduction should convey the broad significance of the paper; the remainder of the paper should be divided into the following sections: Materials and methods, Results, Discussion, and Acknowledgments. Headings within each section must be short, reflect a logical sequence, and follow the rules of subdivision (i.e., there can be no subdivision without at least two subheadings). The entire text should be intelligible to interdisciplinary readers; therefore, all acronyms, abbreviations, and technical terms should be written out in full the first time they are mentioned. Abbreviations should be used sparingly because they are not carried over to indexing databases and slow readability for those readers outside a discipline. They should never be used for the main subject (species, method) of a paper.

For general style, follow the U.S. *Government Printing Office Style Manual* (2008) [available at website] and *Scientific Style and Format: the CSE Manual for Authors, Editors, and Publishers* (2014, 8th ed.) published by the Council of Science Editors. For scientific nomenclature, use the current edition of the American Fisheries Society's *Common and Scientific Names of Fishes from the United States, Canada, and Mexico* and its companion volumes (*Decapod Crustaceans, Mollusks, Cnidaria and Ctenophora*, and *World Fishes Important to North Americans*). For species not found in the above mentioned AFS publications and for more recent changes in nomenclature, use the Integrated Taxonomic Information System (ITIS) (available at website), or, secondarily, the California Academy of Sciences *Catalog of Fishes* (available at website) for species names not included in ITIS. Common (vernacular) names of species should be lowercase. Citations must be given for the identification of specimens. For example, "Fishes were identified according to Collette and Klein-MacPhee (2002); sponges were identified according to Stone et al. (2011)."

Dates should be written as follows: 11 November 2000. Measurements should be expressed in metric units, e.g., 58 metric tons (t); if other units of measurement are used, please make this fact explicit to the reader. Use numerals, not words, to express whole and decimal numbers in the general text, tables, and figure captions (except at the beginning of a sentence). For example: We considered 3 hypotheses. We collected 7 samples in this location. Use American spelling. Refrain from using the shorthand slash (/), an ambiguous symbol, in the general text.

Cite all software, special equipment, and chemical solutions used in the study within parentheses in the general text: e.g., SAS, vers. 6.03 (SAS Inst., Inc., Cary, NC).

Word usage and grammar that may be useful are the following:

- *Aging*
  For our journal, the word *aging* is used to mean both age determination and the aging process (senescence). Authors should make clear which meaning is intended where ambiguity may arise.

- *Fish and fishes*
  The plural of the word fish (a collective noun that implies individuals without regard to species) is *fish*.
  Example: The *fish* were collected by trawl net.
  Example: The numbers of *fish* collected that season were less than the numbers from previous years.

  The plural for *fish species* is *fishes* (a contrived plural used by taxonomists to mean several or more *fish species*) or one can use *fish species* (which is preferred in this journal for clarity across disciplines).
  Example: The *fishes* of Puget Sound [biodiversity is implied] or
  Example: The *fish species* of Puget Sound [preferred plural for clarity across disciplines].

- *Crab and crabs, squid and squids, etc.*
  The plural of the word *crab* (i.e., many individuals without regard to species) is *crab*.
  Example: The crab were sorted by weight.
  Example: Many red king *crab* were dying [Many individuals of one species of crab.]

  The plural of *crab species* is *crabs* (a word used by taxonomists) or *crab species* (the latter is preferred in this journal for clarity).
  Example: These *crabs* were selected for treatment. [Different crab species are implied.]
  Example: These *crab species* were selected for treatment. [Preferred word choice for clarity of meaning.]
  Example: Snow *crabs* are found throughout the North Pacific Ocean and Bering Sea. [There are 2 species of snow crab and therefore the word *crabs* can be used here.]
  Example: *Two species* of snow *crab* are found throughout the North Pacific Ocean and Bering Sea. [Preferred usage for clarity.]
  Example: Three crabs were selected for treatment. [3 species of crab are implied.]
  Example: Three crab species were selected for treatment. [Preferred word choice for clarity.]

- *Fisherman and fisher*
  We use "fisherman" and "fishermen" in this journal not "fisher" and "fishers." One can always use crew member, vessel operator, and angler (the latter for recreational fishing).

- *The definite article with common names of species*
  When the singular common name of a species represents the entire class or group to which it belongs, use the definite article.
  Example: Only one species of the genus Salmo is found in the Atlantic Ocean—*the* Atlantic salmon (*Salmo salar*).
  Example: The sonic emissions of *the* bottlenose dolphin are complex.

  For plural common names, this rule does not apply.
  Example: Chinook salmon are found throughout the Pacific Ocean.
  Example: Bottlenose dolphins are found in temperate and tropical waters.

- *Sex*
  For the meaning of male and female, use the word *sex*, not *gender*. Do not write "fish were sexed." Write, "sex was determined."

- *Participles*
  As adjectives, participles must modify a specific noun or pronoun.
  Example: Using mark-recapture methods, these scientists determined the size of the population. [Correct. The participle *using* modifies the word *scientists*.]

Example: These scientists, based on the collected data, concluded that the mortality rate of these fish had increased. [Incorrect. The scientists were not based on the collected data.]

Example: These scientists concluded, on the basis of collected data, that the mortality rate of these fish had increased. [Correct. The offending participle has been eliminated and an adverbial phrase modifies the verb *concluded*.]

Equations and mathematical symbols should be set from a standard mathematical program (MathType or Equation Editor). Equations formatted in LaTex are not acceptable. For mathematical symbols in the general text (α, χ^2, π, $\pm$, etc.), use the symbols provided by the MS Word program and italicize all variables, except those variables represented by Greek letters. Do not use photo mode when creating these symbols in the general text and do NOT CUT and PASTE equations, letters, or symbols from a different software program.

Number equations (if there are more than 1) for future reference by scientists; place the number within parentheses at the end of the first line of the equation.

Literature cited section comprises published works and those accepted for publication (in press) in peer-reviewed journals. Follow the name and year system for citation format in the "Literature cited" section (that is to say, citations should be listed alphabetically by the authors' last names, and then by year if there is more than one citation by the same author. A list of abbreviations for citing journal names can be found at this website.

Authors are responsible for the accuracy and completeness of all citations. Literature citation format: Author (last name, followed by first-name initials). Year. Title of article. Abbreviated title of the journal in which it was published. Always include number of pages. For a sequence of citations in the general text, list chronologically: (Smith, 1932: Green. 1947; Smith and Jones, 1985).

Acknowledgments should be no more than 6 lines of text. Only those who have contributed in an outstanding way should be acknowledged by name. For recognition of other persons or groups, use a general term, such as "crew," "observers," "research coordinators," and do not include names with these terms.

Digital object identifier (doi) code ensures that a publication has a permanent location online. Doi code should be included at the end of citations of published literature. Authors are responsible for submitting accurate doi codes. Faulty codes will be deleted at the page-proof stage.

Footnotes are used for all documents that have not been formally peer reviewed and for observations and personal communications, but these types of references should be cited sparingly in manuscripts submitted to the journal.

All reference documents, administrative reports, internal reports, progress reports, project reports, contract reports, personal observations, personal communications, unpublished data, manuscripts in review, and council meeting notes are footnoted in 9 pt font and placed at the bottom of the page on which they are first cited. Footnote format is the same as that for formal literature citations. A link to the online source (e.g., [http://www/.......... , accessed July 2007.]), or the mailing address of the agency or department holding the document, should be provided so that readers may obtain a copy of the document.

Tables are often overused in scientific papers; it is seldom necessary to present all the data associated with a study. Tables should not be excessive in size and must be cited in numerical order in the text. Headings should be short but ample enough to allow the table to be intelligible on its own.

All abbreviations and unusual symbols must be explained in the table legend. Other incidental comments may be footnoted with italic numeral footnote markers. Use asterisks only to indicate significance in statistical data. Do not type table legends on a separate page; place them above the table data. *Do not submit tables in photo mode.*

- Note probability with a capital, italic P.
- Provide a zero before all decimal points for values less than one (e.g., 0.07).
- Round all values to 2 decimal points.
- Use a comma in numbers of five digits or more (e.g., 13,000 but 3000).

Figures must be cited in numerical order in the text. Graphics should aid in the comprehension of the text, but they should be limited to presenting patterns rather than raw data. Figures should not exceed one figure for every four pages of text and must be labeled with the number of the figure. Place labels **A, B, C,** etc. within the upper left area of graphs and photos. Avoid placing labels vertically.

Figure legends should explain all symbols and abbreviations seen in the figure and should be double-spaced on a separate page at the end of the manuscript.

Line art and halftone figures should be saved at a resolution of >600 dpi (dots per inch) and >300 dpi, respectively. Color is allowed in figures to show morphological differences among species (i.e., for species identification), to show stain reactions, to show gradations, (such as those of temperature and salinity within maps, and to distinguish between numerous lines and symbols in graphs. Figures approved for color should be saved in CMYK format.

All figures must be submitted as either pdf, tiff, or eps files.

- Capitalize the first letter of the first word in all labels within figures.

- Do not use overly large font sizes in maps and for axis labels in graphs.

- Do not use bold fonts or bold lines in figures.

- Do not place outline rules around graphs.

- Place a North arrow and label degrees latitude and longitude (e.g., 170°E) in all maps.

- Use symbols, shadings, or patterns (not clip art) in maps and graphs.

Supplementary materials that are considered essential, but are too large or impractical for inclusion in a paper (e.g., metadata, figures, tables, videos, websites), may be provided at the end of an article. These materials are subject to the editorial standards of the journal. A URL to the supplementary material and a brief explanation for including such material should be sent at the time of initial submission of the paper to the journal.

- **Metadata, figures, and tables** should be submitted in standard digital format (Word docx) and should be cited in the general text as (Suppl. Table, Suppl. Fig., etc.).

- **Websites** should be cited with a url in the general text.

- **Videos** must not be larger than 30 MB to allow a swift technical response for viewing the video. Authors should consider whether a short video uniquely captures what text alone cannot capture for the understanding of a process or behavior under examination in the article. Supply an online link to the location of the video.

Copyright law does not apply to *Fishery Bulletin,* which falls within the public domain. However, if an author reproduces any part of an article from *Fishery Bulletin*, reference to source is considered correct form (e.g., Source: Fish. Bull. 97:105).

Failure to follow these guidelines and failure to correspond with editors in a timely manner will delay publication of a manuscript.

Submission of manuscript

Submit manuscript online at the ScholarOne website. Commerce Department authors should submit papers under a completed NOAA Form 25-700. For further details on electronic submission, please contact the Associate Editor, Kathryn Dennis, at

kathryn.dennis@noaa.gov

When requested, the text and tables should be submitted in Word format. Figures should be sent as separate pdf, tiff, or eps files. Send a copy of figures in the original software if conversion to any of these formats yields a degraded version of the figure.

Questions? If you have questions regarding these guidelines, please contact the Managing Editor, Sharyn Matriotti, at

sharyn.matriotti@noaa.gov

Questions regarding manuscripts under review should be addressed to Kathryn Dennis, Associate Editor.

Fishery Bulletin

Subscription form

Superintendent of Documents **Publications** Order Form

*5178

☐ YES, please send me the following publications:

____ Subscriptions to *Fishery Bulletin*
for $32.00 per year ($44.80 foreign)

The total cost of my order is $ ________ . Prices include regular domestic postage and handling and are subject to change.

____
(Company or Personal Name) (Please type or print)

____
(Additional address/attention line)

____
(Street address)

____
(City, State, ZIP Code)

____
(Daytime phone including area code)

____
(Purchase Order No.)

Charge
your
order.
IT'S
EASY!

VISA

MasterCard

Please Choose Method of Payment:

☐ Check payable to the Superintendent of Documents
☐ GPO Deposit Account ☐☐☐☐☐☐☐–☐
☐ VISA or MasterCard Account
☐☐☐☐☐☐☐☐☐☐☐☐☐☐☐☐☐☐☐☐
☐☐☐☐ (Credit card expiration date)

**To fax
your orders
(202) 512-2104**

____
(Authorizing Signature)

Mail to: Superintendent of Documents
P.O. Box 979050, St. Louis, Missouri 63197
Tel. no. (U.S. callers): 866-512-1800
Tel. no. (International callers): 1-202-512-1800

***Thank you for
your order!***

Also available online at
http://bookstore.gpo.gov/actions/GetPublication.do?stocknumber=703-023-00000-2
email: ContactCenter@gpo.gov

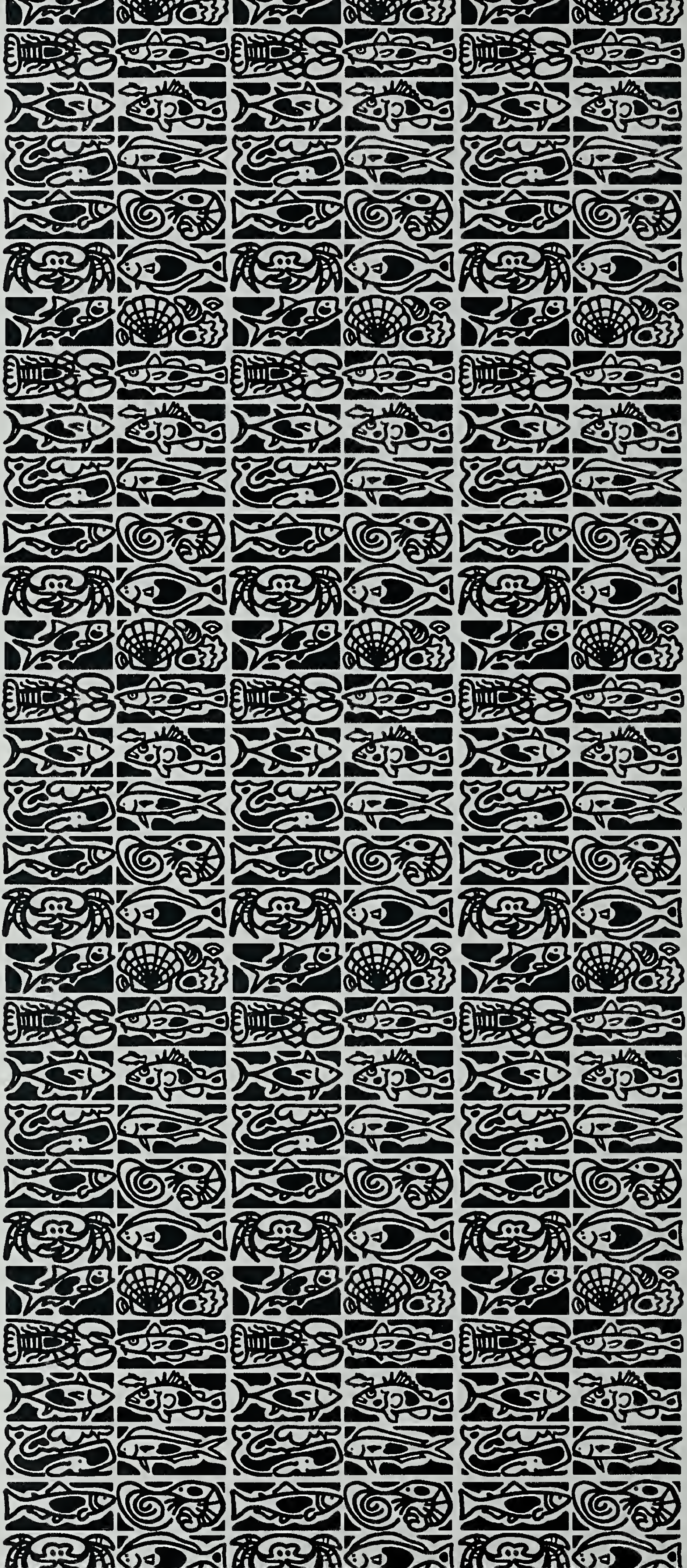

SMITHSONIAN LIBRARIES
3 9088 02004 2776